TOWARDS THE INVESTIGATION OF THE EFFECTS OF NITRATION ON THE ACTIVITY OF THE HUMAN P53 TUMOUR SUPPRESSOR PROTEIN

Nitration of the p53 Tumour Suppressor Protein

Roslina HUSAINI

submitted for the Degree
of Master of Philosophy

Department of Medical Biosciences

Faculty of Life Sciences

University of Bradford

2014

ABSTRACT

Roslina Husaini

Towards the Investigation of the Effects of Nitration on the Activity of the Human p53 Tumour Suppressor Protein.

Nitration of the p53 Tumour Suppressor Protein

Keywords: p53 tumour suppressor protein, nitration, oxidative stress, peroxynitrite, Western blotting

Upon responding to cellular stress, p53 protein becomes stabilised and acts as a transcription factor mainly resulting from phosphorylation and acetylation of the protein. Nitration of p53 protein is poorly characterised by comparison with phosphorylation and acetylation. The main aim of this work was to study the effects of nitration on p53 functional activities and on p53-MDM2 protein-protein interactions. Preliminary work was to characterise the nitration of p53 protein over-expressed in *E. coli* BL21(DE3) which was then purified by a series of column chromatography. GST-MDM2 protein along with control GST protein were also overexpressed in BL21 which were subsequently purified by a single step batch purification before subjected to nitration. Peroxynitrite, a nitrating agent used in this study, was generated *in vitro*. Preliminary nitration work was carried out using BSA as a model protein as it is easily nitrated owing to its high number of tyrosine residues (19 residues). The present results showed that p53 and GST-MDM2 proteins were hardly nitrated as no strong nitro-tyrosine signals were obtained. This might be due to these proteins, being overexpressed in *E. coli*, were not properly folded resulting in hidden/cryptic tyrosine residues of which making nitration difficult to achieve. Peroxynitrite was shown to have a degrading property, reducing protein levels of peroxynitrite-treated p53, GST-MDM2 and GST proteins. Immunoprecipitation studies of cancer cell lysates with different p53 status treated with peroxynitrite showed very weak signals of nitro-p53 protein in mutant p53 cells whereby no nitro-p53 protein signal in wild-type p53 MCF7 cells. In addition, NO donor GSNO-treated MCF7 cells showed weak nitro-p53 protein signals.

ACKNOWLEDGEMENTS

First and foremost, I would very much appreciate and are thankful to the Ministry of Science, Technology and Innovation (MOSTI) of Malaysia for giving me a scholarship, an opportunity of a lifetime, to pursue my MPhil in the Department of Medical Biosciences, University of Bradford, UK.

I would like to thank my principal supervisor, Dr Steven Picksley for his guidance, supervision and advice and more importantly his patience throughout the MPhil period. Not forgetting also his discussion and constructive comments on my report.

I also would like to thank my co-supervisors, Professor Khalid Naseem and Dr Martin Brinkworth for their support on my progress.

Special thanks to all my colleagues especially Maqsood Mansoor and also to technical staff including Jamie Fernley, Andy Reed, Lynne Keeble, Stephanie Atkins and the list goes on to help me whenever I need assistance.

Last but not least, my special thanks to my parents and other family members for their continuous support, encouragement, understanding and their constant prayers for my success.

TABLE OF CONTENTS

LIST OF FIGURES

LIST OF TABLES

ABBREVIATIONS

Akt	Protein kinase B
Ala	Alanine
ALDH4	Adehyde dehydrogenase 4
AMPK	Adenosine monophosphate-activated protein kinase
Ap	Ampicillin
Apo1	Apolipoprotein 1
APS	Ammonium persulfate
ARF-BP1	E3 ligase Arf-bp1
Arg	Arginine
Asn	Asparagine
Asp	Aspartic acid
atm	Ataxia Telangiectasia Mutated Kinase gene
ATM	Ataxia Telangiectasia Mutated Kinase protein
atr	Ataxia Telangiectasia Related Kinase gene
ATR	Ataxia Telangiectasia Related Kinase
BAK	BCL-2 antagonist killer
BAX	BCL-2 asociated X
BCL-2	B-cell lymphoma 2
BD	Basic domain
BH3-only proteins	Bcl-2 homology domain 3
BSA	Bovine Serum Albumin
CAK	Cdk-Activated Kinase
CBP	CREB Binding Protein
Cdc2	Cell division cycle 2

ABBREVIATIONS (continued)

CDKs	Cyclin Dependent Kinases
cDNA	Complementary DNA
CD95	Cluster of Differentiation 95
Chk1	Checkpoint kinase 1
Chk2	Checkpoint kinase 2
CKI	Casein Kinase I
CKII	Casein Kinase II
COP1	COP1 E3 ubiquitin-protein ligase
CRM1	Chromosomal region maintenance 1
Cys	Cysteine
DAXX	Death-Associated Protein 6
DBD	DNA Binding Domain
DEAE	Diethylaminoethyl
DNA	Deoxyribonucleic Acid
DNA-PK	DNA-dependent protein kinase
DTT	Dithiothreitol
DYRK-2	Dual specificity tyrosine-phosphorylation-regulated kinase 2
ECL	Enhanced Chemi-Luminescence
E. coli	*Escherichia coli*
EDTA	Ethylenediaminetetraacetic acid
EGFR	Epidermal growth factor receptor
ELISA	Enzyme-Linked Immunosorbent Assay
EMSA	Electrophoresis Mobility Shift Assay

ABBREVIATIONS (continued)

FAO	Fatty Acid Oxidation
Fas	CD95
FBXO11	F-box protein 11
FDXR	Ferredoxin Reductase
FPLC	Fast Protein Liquid Chromatography
Gadd45	Growth arrest and DNA damage inducible gene
GADD45	Growth Arrest and DNA Damage Inducible protein
GAMT	Guanidinoacetate methyltransferase
GLS2	Glutaminase 2
Glu	Glutamine
GLUT	Glucose transporter
GOF	Gain-of-function
GPX1	Glutathione peroxidase 1
GSNO	S-Nitrosoglutathione
GST	Glutathione S-transferase
HAUSP /USP7	Herpes virus-associated ubiquitin-specific protease/Ubiquitin-specific processing protease 7
HEPES	4-(2-Hydroethyl)-1-piperazineethanesulfonic acid hemisodium salt
HIPK2	Homeodomain-interacting protein kinase 2
HNO_3	Nitric acid
H_2O_2	Hydrogen Peroxide
HRP	Horse Radish Peroxidase
$I.C._{50}$	The half maximal inhibitory concentration
IGF-BP3	Insulin Growth Factor Binding Protein 3

ABBREVIATIONS (continued)

IGF2	Insuin-like growth factor 2
IgG	Immunoglobulin G
IPTG	Isopropyl-β-D-thiogalactopyranoside
IR	Ionising radiation
JNK	Jun N-terminal Kinase
KAT3B	Lysine acetyltransferase
Killer/DR5	TRAIL Death Receptor-5
KMT	Lysine methyltransferase family
KPi	Potassium Phosphate Buffer
LB	Luria-Bertani media
Lys	Lysine
MAPK	Mitogen-activated Protein Kinase
MCL-1	Myeloid cell leukemia sequence 1
mdm2	Mouse Double Minute gene
MDM2	Mouse Double Minute protein
MDR1	Mutidrug resistance 1
MEF	Mouse embryonic fibroblast
Met	Methionine
miR	MicroRNA
mRNA	Messenger RNA
MW	Molecular Weight
$NaNO_2$	Sodium Nitrite
NaOH	Sodium Hydroxide
NES	Nuclear Export Signal

ABBREVIATIONS (continued)

NF-κB	Nuclear factor--κB
NLS	Nuclear Localisation Signal
NMR	Nuclear Magnetic Resonance
NO	Nitric Oxide
NONOate	Diethylamine NONOate sodium salt
NOS	Nitric Oxide Synthase gene
NOS	Nitric Oxide Synthase protein
NOXA	Pro-apoptotic member of the Bcl-2 protein family
OD	Optical Density
OGG1	8-Oxoguanine DNA glycosylase
OXPHOS	Oxidative phosphorylation
p53AIP1	p53-regulated apoptosis-inducing protein 1
p53R2	p53-controlled ribonucleotide reductase
PAGE	Polyacrylamide Gel Electrophoresis
PARP	Poly (ADP-ribose) polymerase
PBS	Phosphate Buffered Saline
PBST	Phosphate Buffered Saline/ 0.2% Tween 20
PCAF	p300/CBP Associated Factor
PCNA	Proliferating Cell Nuclear Antigen
PERP	TP53 apoptosis effector
Phe	Phenylalanine
PIAS	Protein inhibitor of activated STAT
pig	p53 inducible gene
PIG3	p53 inducible protein 3

ABBREVIATIONS (continued)

PIG6	p53 inducible protein 6
Pin1	Prolyl isomerase 1
PI3K	Phosphatidylinositol 3-kinase
Pirh2	p53 induced RING-H2
PKC	Protein Kinase C
PKCdelta	Protein kinase C delta
PML	Promyelocytic leukaemia
PMSF	Phenyl-Methyl-Sulphonyl-Fluoride
PP1	Phosphoprotein phosphatase 1
PP2A	Protein phosphatase 2A
PRD	Proline Rich Domain
PRMT5	Protein Arginine N-methyl Transferase 5
Pro	Proline
PTEN	Phosphatase and tensin homolog
PTKs	Phosphotyrosine kinases
PTPs	Phosphotyrosine phosphatases
PUMA	p53 upregulated modulator of apoptosis
p38 MAPK	p38 mitogen-activated protein kinases
RanBP2	E3 SUMO-protein ligase
RB	Retinoblastoma Protein
RIPA buffer	Radio immunoprecipitation assay buffer
RNA	Ribonucleic acid
RNAse	Ribonuclease
RNS	Reactive nitrogen species

ABBREVIATIONS (continued)

ROS	Reactive oxygen species
RT-PCR	Reverse transcription polymerase chain reaction
SAM	Sterile-α-motif
SDS	Sodium Dodecyl Sulphate
Ser	Serine
SET7/9	Lysine methyltransferase
SIN-1	3-Morpholinosydnonimine
SIRT1	NAD-dependent deacetylase sirtuin-1
SMYD2	Protein-lysine N-methyltransferase
SNAP	S-Nitroso-N-acetylpenicillamine
STAT	Signal transducers and activators of transcription
SUMO-1	Small ubiquitin-like modifier protein 1
SV40	Simian Virus 40
TAD	Transactivation Domain
TAF	TBP-Associated Factor
TBP	TATA box Binding Protein
TD	Tetramerisation Domain
TEMED	N,N,N,N’-tetramethylenendiamine
TFIID	Transcription Factor II D
TFIIH	Transcription Factor II H
Thr	Threonine
TIGAR	TP53-inducible glycolysis and apoptosis regulator
TIP60/hMOF	Acetyltransferase family

ABBREVIATIONS (continued)

Topors	Topoisomerase I-binding RING finger protein
TRAIL	Tumour necrosis factor (TNF)-related apoptosis-inducing Ligand
Triton X-100	Octylphenol ethylene oxide condensate
tRNA	Transfer RNA
Trp	Tryptophan
Tween 20	Polyoxyethylene sorbitan monolaureate
Tyr	Tyrosine
Ubc9	SUMO-conjugating enzyme/SUMO-protein ligase
USP10	Ubiquitin-specific-processing protease 10
UV	Ultraviolet irradiation
WT	Wild type

CHAPTER 1

INTRODUCTION

Cancer is a genetic disease resulting from oncogene activation and/or inactivation of tumour suppressor genes. Furthermore, cancer is now appreciated to arise from epigenetic alterations that link environmental and dietary exposures and disease (Virani *et al*., 2012), however it is not the theme of this thesis. Changes in key genes, namely oncogenes and tumour suppressors, lead to the formation of cancer from a single progenitor cell. The most widely studied tumour suppressor gene in cancer is *p53*. p53's main role as a transcription factor transcribing its target genes upon exposure to cellular stresses is important for its tumour suppressor activities. p53 acts as a cellular gatekeeper to safeguard the integrity of the genome by preventing the propagation of cells with mutated DNA mainly through cell cycle arrest and/or apoptosis. This also led p53 to be coined as the Guardian of the Genome by Lane (1992). p53 has several other newer activities mainly its role in cellular metabolism, anti-oxidant defence and autophagy.

.

In normal cells, p53 regulates cell growth by controlling cell proliferation and cell death. The p53 tumour suppressor protein exerts anti-proliferative effects, including cell cycle arrest, repair of damaged DNA, and apoptosis in response to various types of cellular stress. These cellular functions of p53 protein are activated in response to cellular stress by enzymes that covalently modify p53 protein in direct response to DNA damage. Widely known post-translational modifications of p53 protein include phosphorylation, acetylation and ubiquitination and lesser characterised modifications include sumoylation, neddylation and methylation. It has emerged that p53 protein is also covalently modified by nitration (Calmels *et al*., 1997; Chazotte-Aubert *et al*., 2000). This thesis focuses on the nitration events of p53 protein and its impact on the p53 tumour suppressive activities.

1.1 The *p53* gene and its protein product

The *p53* gene was discovered over 30 years ago by the finding that its protein product p53 formed a complex with the large T-antigen in Simian Virus 40 (SV40) transformed cells (Lane & Crawford, 1979; Linzer & Levine, 1979). The gene was first thought to behave as an oncogene as evidenced by its ability to increase the plating efficiency in primary cultures transfected with *p53* cDNA (Jenkin *et al*., 1984) and transfection of *p53* in cooperation with the *ras* oncogene, could transform primary rat embryo fibroblasts (Eliyahu *et al*., 1984). However, it was later discovered that it is in fact a tumour suppressor gene, i.e., its activity stops the formation of tumours, as shown by Eliyahu *et al*. (1989) where the WT p53 protein has an anti-proliferative effect by blocking the ability of oncogenes, such as H-*ras*, to promote cancer. Further evidence that supports p53 as a tumour suppressor protein is by a study by Chen *et al.* (1990) which found that the transfection of the wild-type *p53* gene in human osteosarcoma cells lacking endogenous p53 stopped the neoplastic growth by reducing cell growth and division. cDNA clones of murine and human p53 were isolated in the early 1980's (Zakut-Houri *et al*., 1985). The *p53* gene is located on the short arm of Chromosome 17 (17p13.1) and spans 20 kb with 11 exons, the first of which is a non-coding exon (Oren *et al*., 1985). The gene encodes a protein of 393 amino acids with an apparent molecular weight of 53 kDa, hence the name. In normal cells, the p53 protein is located in the cell nucleus and is very labile. The p53 protein is maintained at very low levels or almost undetectable under normal conditions of cells and tissues and it has an extremely short half-life of around 20 minutes (reviewed in Levine, 1997). It coordinates cellular response to DNA damage and is a multi-functional protein. The p53 protein is activated in response to a number of cellular stresses, including DNA damage, hypoxia, ionizing radiation, oncogene activation, metabolic changes, viral infection, etc. The activation of p53 protein leads to the rapid elevation of p53 protein levels along with its increased half-life (Kastan *et al*., 1992; Lu and Lane, 1993; Zhan *et al*., 1993), due in part to increased mRNA translation (Fu *et al*., 1996), but mainly due to stabilisation of the protein by a post-translational mechanism (Maltzman and Czyzyk, 1984) and this also increases the ability of p53 to

bind DNA and mediate transcriptional activation (Kastan *et al.*, 1992). This then activates a number of genes whose products mainly trigger cell cycle arrest, or apoptosis. It is now known that p53 upregulates ~5000 genes and downregulates ~50 genes (Dr Picksley's personal communication). Figure 1.3 shows several p53 target genes. Cell cycle arrest and apoptosis are two discreet functions of p53 protein as a tumour suppressor, both in response to cellular stress (Kastan *et al*., 1991; Yonish-Rouach *et al*., 1991). When the extent of DNA damage is not severe, the p53 protein mediates cell cycle arrest during G1 to give cells time to repair their DNA before entry into S phase. Extensive, irrepairable DNA damage leads to programmed cell death, a process termed apoptosis. Activated p53 protein also mediates cellular senescence and differentiation depending on particular cellular conditions.

The *p53* gene is the most commonly mutated or lost gene in a wide range of human cancers (Hollstein *et al*., 1991). p53 mutation is normally a late event in carcinogenesis. More than half of all human cancers are found to have lesions in the *p53* gene which include cancers of the breast, cervix, colon, lung, liver, prostate, bladder, and the skin (Greenblatt *et al*, 1994; IARC p53 mutation database). The mutations are typically somatic missense mutations that result in aberrant p53 proteins with lost suppressor function and that promote cancer (Figure 1.1). Inactivated or mutated p53 protein results in the failure to cause suppression of aberrant cell growth, and results in the accumulation of cells with aberrant DNA, in turn results in tumour growth. This leads to genetic instability. It is now acknowledged that genome instability and mutation is an enabling characteristic of cancer cells (Hanahan and Weinberg, 2011). There is extensive debate as to whether such events are the cause or consequence of tumoriogenesis (as reviewed by Sieber *et al*., 2003).

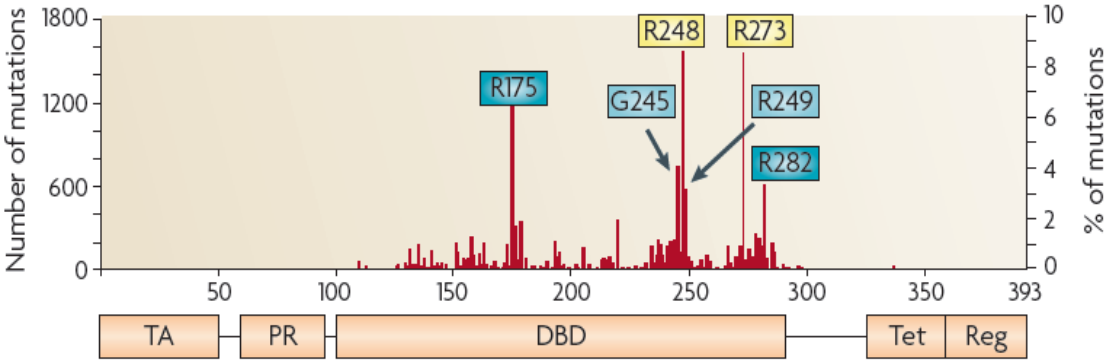

Figure 1.1. A diagram showing the distribution of mutations in the *p53* gene. The majority are missense mutations (70%) which are clustered in the DNA binding domain (80%) with mutation hotspots including R175, G245, R248, R249, R273 and R282. TA, transactivation domain; PR, proline rich domain; DBD, DNA binding domain; Tet, tetramerisation domain; Reg, C-terminal regulatory domain; R, Arginine; G, Glycine (adapted from Brown *et al*., 2009).

1.2 p53 Structure-Function

The p53 has been conserved in vertebrate species during evolution (reviewed by Soussi *et al*., 1987, 1990). The human p53 protein contains five major functional domains which are typical structural domains of a transcription factor. These are the N-terminal transcription activation domains TAD1 (amino acids 1-40) and TAD2 (amino acids 41-83), a proline rich region (amino acids 63-97) containing five repeats of the SH3 binding motif PXXP, the central sequence-specific DNA binding domain (amino acids 102-292) and the C-terminal region which includes both the oligomerisation or tetramerisation domain (amino acids 323-356) and the regulatory domain (amino acids 360-393). Figure 1.2 illustrates the structure of p53 protein with five main domains shown.

Figure 1.2. p53 structure with 5 major functional domains**;** N-terminal domain comprising of Transactivation domains TAD1 & TAD2, Proline rich domain, Central core DNA binding domain, and C-terminal domain comprising Tetramerisation and Regulatory domains. This figure also shows sequence homology between human p53 and mouse p53 and locations of mutation sites for TAD1 (L25Q; W26S mutations) and TAD2 (F53Q; F54S mutations) in the TAD mutant knock-in strains (adapted from Beiging and Attardi, 2011).

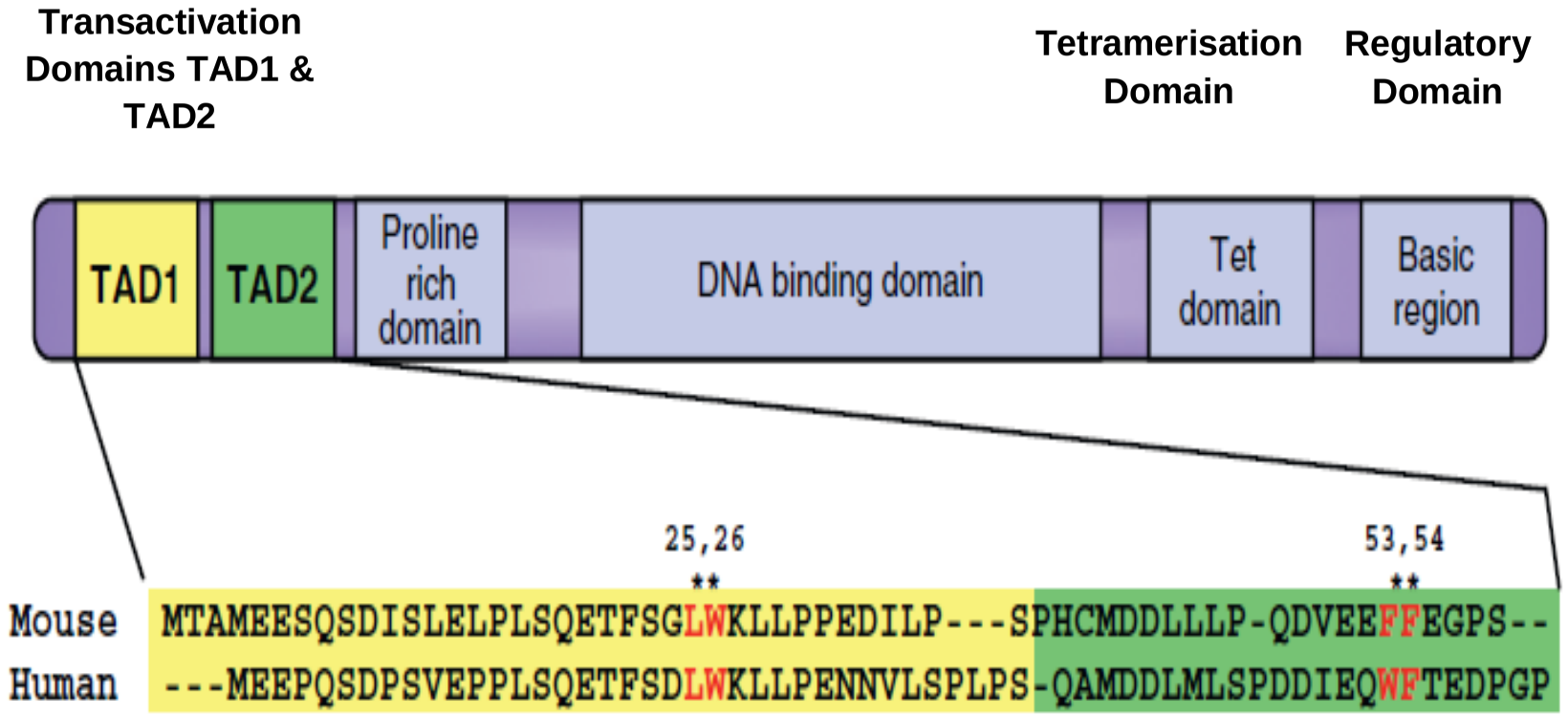

1.2.1 N-terminal region

The N-terminal region of p53 protein is a highly acidic region. It contains two Transactivation domains TAD1 (Met1-Met40) and TAD2 (Asp41-Pro83), both have a role in p53 activation and function independently (Candau *et al*., 1997; Anderson and Apella, 2010).). TAD1 has highly conserved residues Met1-Met40 and is mostly important for transactivation function. TAD1 binds with transcription factors TFIID, TFIIH, several TAFs, the coactivator histone acetyltransferase KAT3A/KAT3B, PCAF and MDM2 ubiquitin ligase (Anderson and Apella, 2010). Residues Glu17-Asn29 form an amphipathic helix which binds to a hydrophobic cleft in the MDM2 N-terminal domain (Kussie *et al.,* 1996). Residues Glu11-Leu26 acts as a nuclear export signal (Zhang and Xiong, 2001; Anderson and Apella, 2010). TAD1 allows p53 to recruit the basal transcriptional machinery in positively regulating gene expression, including TATA box binding protein (TBP) and TBP-associated factors (TAF) components of TFIID (Lu and Levine, 1995; Thut *et al*., 1995). TAD2 was found overlap with a proline-rich domain (PRD) (Asp61-Leu94). TAD2 is required for p53 stability, transactivation and transcription-independent apoptosis (Walker and Levine, 1996; Anderson and Apella, 2010).

TAD1 mutation termed $p53^{25,26}$ (L25Q; W26S mutations) show impaired transactivation of most known p53 target genes such as p21, Puma and Noxa. However, it retained the ability to induce certain p53 target genes such as Bax (Johnson *et al*., 2005; Brady *et al*., 2011; Bieging and Attardi, 2012). $p53^{25,26}$ could not induce G1 cell-cycle arrest or apoptosis in response to acute DNA damage signals. However, $p53^{25,26}$ can promote apoptosis in non-genotoxic-induced MEFs indicating that full p53 transactivation is not required for apoptosis in response to non-genotoxic stresses (Lozano and Zambetti, 2005). TAD2 mutation ($p53^{53,\ 54)}$ (F53Q; F54S mutations) alone do not affect p53 transactivation activity but mutation of both TADs ($p53^{25,\ 26,\ 53,\ 54}$) shows a gene expression profile similar to that of p53-null cells. The mutant p53 is ineffective in tumour suppression both *in vitro* and *in vivo* (Brady *et al*., 2011; Bieging and Attardi, 2012).

The N-terminal domain also contains a hydrophobic Proline-rich region (amino acids 63-97), which links the transcriptional activation domain with the central core. It consists of five copies of the sequence "PxxP" that is important in the apoptotic function of p53 (Sakamuro *et al*., 1997; Venot *et al*., 1998; Baptiste *et al*., 2002). Pro-apoptotic activity of p53 was lost when this Proline-rich region was deleted (Ozaki and Nakagawara, 2011).

1.2.2 Central core DNA binding domain

The central core region of the p53 protein (amino acids 102-292) is highly hydrophobic and contains highly conserved regions II-V. This domain contains the DNA binding domain that interacts with the target sequences in the genes undergoing transcriptional transactivation. An X-ray crystallography study by Cho and colleagues (Cho *et al*., 1994) of the complex containing the p53 core domain and DNA target sequence shows that the core domain structure contains a large β sandwich, made up of two anti-parallel β sheets containing four and five β-strands, respectively, which acts as a scaffold for three loop-based elements (L1, L2, L3) that interact directly with the DNA. The first loop L1 (LSH-loop sheet helix) binds to DNA within the major groove, the second loop L2 binds within the minor groove of DNA and the third loop L3 acts to stabilise L1. The L1 and L3 loops are connected by a zinc atom, which stabilises the overall structure.

This region is flexible and has low thermal and chemical stability and point mutations make it prone to aggregation, and tumour associated mutations destabilise the protein at body temperature (reviewed by Saha *et al*., 2015). The tetramerisation domain also has a role in maintaining stabilisation for the core domain (McCoy *et al*., 1997; Mateu and Fersht, 1998).

In normal cells, WT p53 acts as a latent sequence specific DNA transcription factor but upon exposure to cellular stress it becomes active as a transcription factor which transactivates target genes through the binding of the

core DNA binding domain to the p53 Response Elements (R.E.) of the genes. el-Deiry *et al* (1992) have identified that a consensus binding sequence or R.E. of human genomic fragments that can bind to the DNA binding domain of WT p53 protein *in vitro* contains two copies of a 10 base pair (bp) motif 5'-Pu.Pu.Pu.C.A/T.A/T.G.Py.Py.Py – 3' separated between 0 and 13 bp. One copy of the 10 bp motif is insufficient for binding and affinity for p53 protein will be lost if the motif alters (el-Deiry *et al*., 1992; Ozaki and Nakagawara, 2011).

1.2.3 C-terminal region

The carboxy-terminal region (residues 300-393) of the p53 protein is hydrophilic and rich in base residues. This domain consists of a flexible linker (amino acids 300-318) that connects the central core domain with the C-terminal region, a region responsible for oligomerisation (amino acids 323-356) and a regulatory domain (amino acids 363-393). The native p53 protein is a tetramer in solution and amino acid residues 323-356 are essential for oligomerisation of the protein (Kraiss *et al*., 1988). Tetramerisation is required for efficient transactivation *in vivo* and for p53-mediated tumour suppression (Pietenpol *et al*., 1994). The three dimensional structure of this region has been mapped from nuclear magnetic resonance (NMR) (Clore *et al*., 1994) and X-ray crystallography (Jeffrey *et al*., 1995). It forms a highly symmetrical tetramer where each monomer is composed of a turn, a β-strand, a second turn and an α-helix. Two monomer peptides form a dimer in which the α-helices and β-strands lie antiparallel and two dimers in turn interact through their α-helices to form four-helix tetramers. Since p53 interacts with DNA as a tetrameric protein, therefore mutant p53 proteins fail to bind a p53 consensus sequence. As a transcription factor, p53 must be localised to the nucleus, thus the C-terminal region also contains three nuclear localisation signals (NLS) for efficient nuclear access of p53. These NLSs are recognised by importin α/β complex (Fabbro and Henderson, 2003; Ozaki and Nakagawara, 2011) that regulate the subcellular localisation of the p53 protein. Mutations in NLS1 (amino acids 316-325) cause p53 protein to become located primarily in the cytoplasm, while alterations of NLS2 (amino acids 369-375) and NLS3 (amino acids 379-384)

result in both cytoplasmic and nuclear localisation (Dang and Lee, 1989; Shaulsky *et al*., 1990). p53 also contains Leu-rich nuclear export signal NES (amino acids 339-352) which is recognised by nuclear export machinery CRM1 (chromosomal region maintenance 1) (Fabbro and Henderson, 2003). NES is masked by tetramer formation of p53 which inhibits p53 nuclear export (Stommel *et al*., 1999). In contrast, monoubiquitination of C-terminal lysine residues of p53 by MDM2 disrupted p53 tetramer formation, thus exposed NES to CRM1 binding (Brooks *et al*. 2007; Ozaki and Nakagawara, 2011).

The extreme C-terminal domain (amino acids 363-393) acts as a negative regulator of p53 sequence specific DNA binding that may keep the tetramer poised in a state inactive for sequence-specific DNA binding (Hupp and Lane, 1994). This idea is further supported by a study showing that binding of p53 to the anti-p53 monoclonal antibody PAb421 (which recognises a C-terminal epitope) can activate specific DNA binding (Hupp *et al*., 1992; Hupp and Lane, 1995; Abarzua *et al*., 1996). It has also been shown that PAb421 is able to restore binding ability to some mutant p53 proteins *in vitro* (Hupp *et al*., 1993) and *in vivo* (Abarzua *et al*., 1995). Phosphorylation of this region by protein kinase C or Casein kinase II, association with DnaK protein (*E. coli* homologue of human Hsp70), or 14-3-3 protein induces the p53 tetramer to bind DNA sequence specifically with high affinity. It has been demonstrated that deletion of the C terminus results in constitutive sequence-specific DNA binding by p53 (Hupp *et al*., 1992), as does interaction of the C terminus nonspecifically with single-stranded DNA (Jayaraman and Prives, 1995; Kim and Deppert, 2006) or peptides derived from the C terminus (Hupp *et al*., 1995). The p53 C-terminus is able to form complexes with non-specific DNA targets such as mismatched DNA, double-strand breaks, (DSBs), single-stranded DNA (ssDNA) and Holliday junction structures (Okorokov and Orlova, 2009). The C-terminal domain was initially thought to negatively regulate the core DNA binding domain activity (Hupp and Lane, 1994; Anderson and Apella, 2010) but it was later shown to modulate the promoter activation efficiency through facilitating diffusion of p53 protein along DNA for searching for response elements (Liu *et al*., 2004; McKinney *et al*., 2004; Tafvizi *et al*., 2008;

Anderson and Apella, 2010). This region has been reported to bind with more than 50 proteins such as components of transcription apparatus and other transcription factors.

1.3 Tumour suppressor function of p53

p53 protein is said to act as tumour suppressor due to its ability to inhibit cell growth by inducing cell cycle arrest or apoptosis. Cell cycle arrest and apoptosis are two major tumour suppressive activities contributed by the ability of p53 to function as a transcription factor (reviewed by Bates and Vousden, 1996; Riley *et al*., 2008; Kruse and Gu, 2009; Meek, 2009). Many cellular genes which are transcriptional targets of p53 are divided into those contributing to activation of a cell cycle arrest and those mediating the apoptotic response (reviewed by Ko and Prives, 1996; Riley *et al*., 2008; Kruse and Gu, 2009). All tumour-derived p53 mutants producing proteins with reduced affinity for DNA strongly suggests that sequence-specific DNA binding activity of p53 protein is important as its function as a tumour suppressor (Pietenpol *et al*., 1994). A study by Chen *et al.* (1990) showed that the wild type p53 protein acts as tumour suppressor where the transfection of the wild-type p53 gene into human osteosarcoma cells lacking endogenous p53 abrogates the cells neoplasticity by reducing cell growth and division. p53 knock-out or p53-null mice show a high incidence of spontaneous tumours and enhanced susceptibility to carcinogen- and radiation-induced tumourigenesis but are viable and develop normally (Donehower *et al*., 1992). This indicates that p53 is not essential for cell growth and normal development, but is important in tumour suppression. In 1990, Malkin and colleagues demonstrated that some individuals with Li-Fraumeni syndrome that inherited germline mutations of p53, are at increased risk of developing a variety of cancers including soft tissue sarcoma and cancers of the bone, breast, brain and genito-urinary tract at an earlier age than usual. Some affected individuals carry a heterozygous p53 mutation in the germline, and tumours arise due to loss of the remaining wild-type allele in the tumour cells (Malkin *et al*., 1990). This phenomenon illustrates

the role of p53 in cancer susceptibility and tumour development and mirrors the phenotype of heterozygote +/- mice (except the cancer spectrum is different) (Lozano and Jackson, 2013; Muller and Vousden, 2013; Garcia and Attardi, 2014). Other than mediating cell cycle arrest and apoptosis upon responding to genotoxic and non-genotoxic stresses, p53 also involves in aging, senescence, metabolism, autophagy, cellular differentiation, anti-oxidant defence, angiogenesis, fertility, pigmentation and in regulating microRNA processing (Vousden and Lu, 2002). Figure 1.3 represents a schematic view of some upstream and downstream regulators of *p53*.

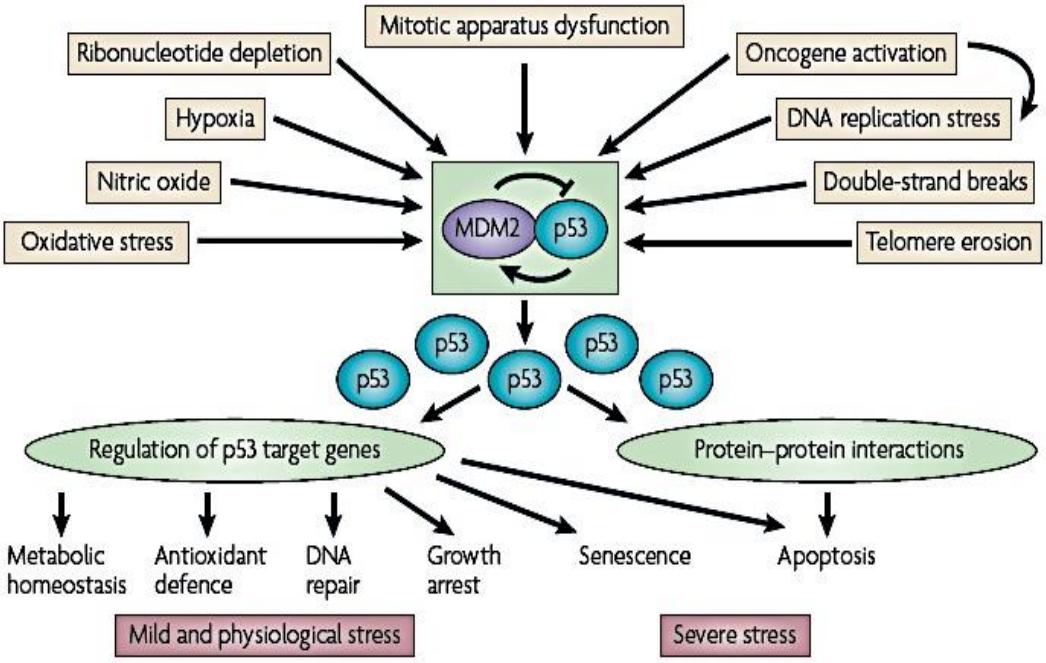

Figure 1.3. Schematic view of some upstream and downstream regulators of p53 (adapted from Levine & Oren, 2009).

1.4 p53 and the cellular response to DNA damage

The p53 protein has been implicated in the cellular response to DNA damage and in the maintenance of genomic integrity. p53 protein is activated in response to a wide range of cellular stresses including DNA damage, most probably in the form of double strand breaks induced by genotoxic agents

(Kastan *et al*., 1991; Lu and Lane, 1993; Riley *et al*., 2008; Meek, 2009) through strongly binding of the p53 C-terminal domain to strand breaks (Nelson and Kastan, 1994). Several forms of DNA damage that activate p53 protein include those generated by ionising radiation (IR), radiomemetic drugs, ultraviolet light (UV) and chemicals such as methane sulfonate. Under normal conditions, p53 protein levels are very low due to its extremely short half life (Kubbutat and Vousden, 1998). It also exists in an inactive state that is relatively inefficient at binding to DNA and activating transcription. Following DNA damage, ensuing p53 activation results in a rapid elevation in p53 protein levels due to its increased half-life and its ability to bind to DNA and transcriptional activation also increases (Maltzman and Czyzyk, 1984; Price and Calderwood, 1993; Riley *et al*., 2008; Kruse and Gu, 2009; Meek, 2009). p53 can either activate or repress its target genes depending on factors such as cofactors, spacer lengths, quarter site orientation, nucleosomes and post-translationally modified p53 protein (Riley *et al*., 2008). There are pathways leading to the activation of p53 by signals emanating from damaged DNA, with p53 integrating these signals and triggering a cascade of responses leading to either growth arrest and/or apoptosis. Other studies suggest that p53 protein may be involved in the repair machinery (Smith *et al*, 1994; Wang *et al*, 1995). For instance, Wang and colleagues (1994, 1995) have shown that p53 protein binds to and modulate the repair activity of the nucleotide excision repair (NER) factors XPB and XPD. Activated p53 induces genes responsible for promoting growth arrest, DNA repair or apoptosis, and represses genes stimulating growth or blocking apoptosis. It has been shown that DNA damage triggers a series of phosphorylation, dephosphorylation and acetylation events on the p53 polypeptide (reviewed by Giaccia and Kastan, 1998) which is to be discussed in further details under p53 post-translational modifications section. Figures 1.4 and 1.5 show a list of genes activated or repressed by active p53 and p53 tumour suppressive functions, respectively.

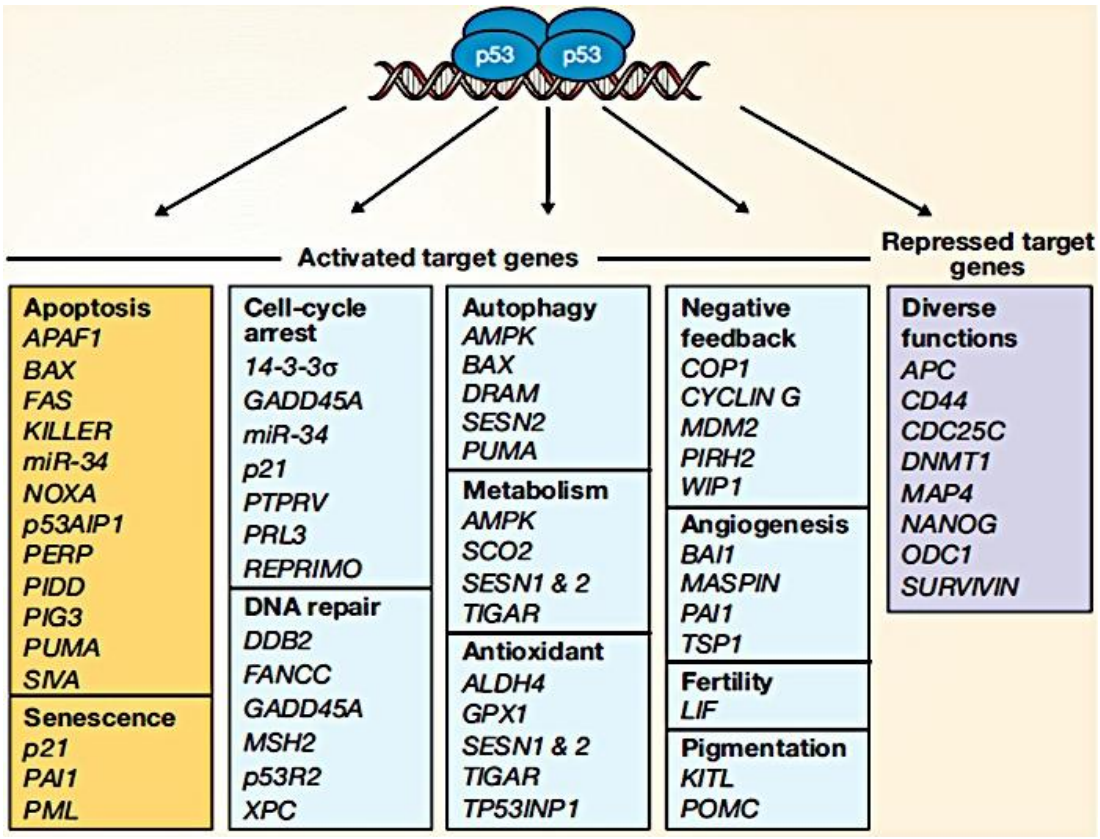

Figure 1.4. Numerous target genes involved in a variety of responses transcriptionally activated or repressed by active p53 protein in response to both genotoxic and non-genotoxic stresses (adapted from Brady and Attardi, 2010).

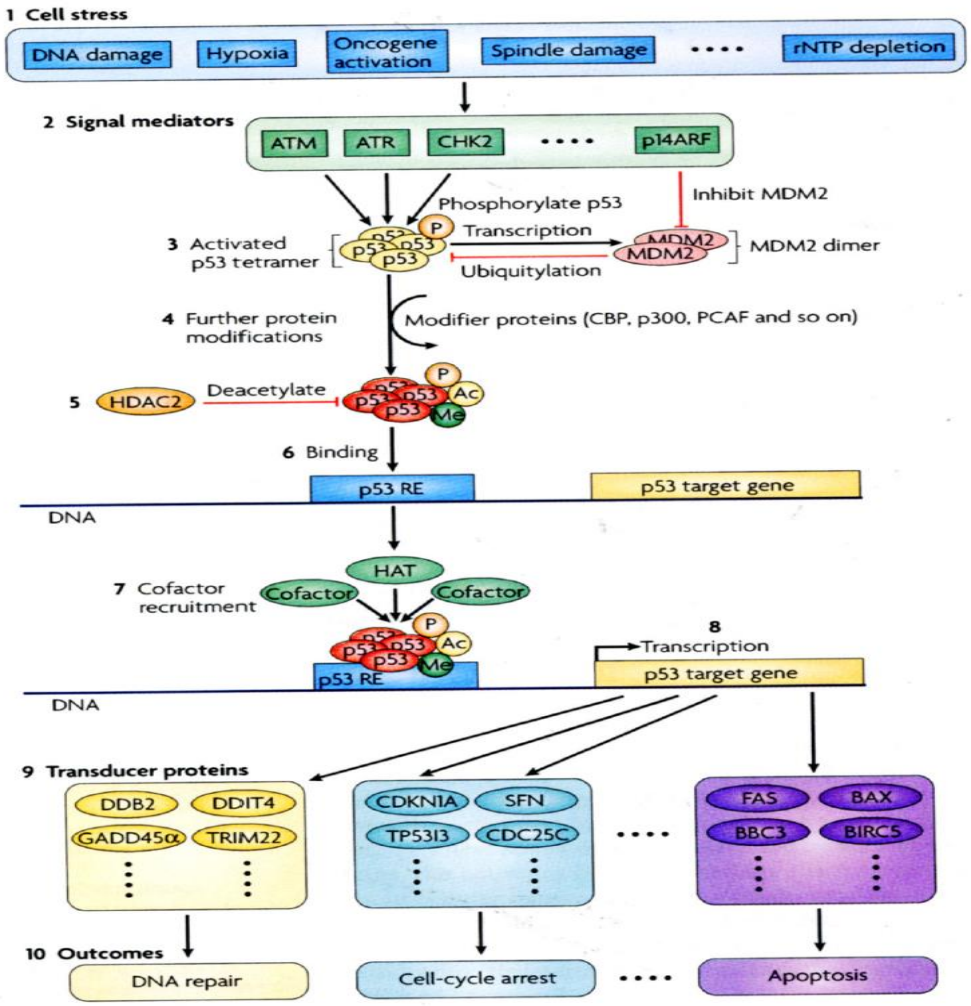

Figure 1.5. p53 activation and its tumour suppressive functions by upregulating genes involved in cell-cycle arrest, DNA repair or apoptosis depending on the contextual conditions of the cells. Step 1: Cells are subject to many types of stresses most of the time. Step 2: Signal mediator proteins upregulate p53 by phosphorylation or suppressing ubiquitylation by MDM2. Step 3: Both processes increase the half-life of p53 which quickly leads to higher levels of p53. Step 4: Moreover p53 can be modified by acetyltransferases (CBP, p300, PCAF) and methyltransferases (SET9) that accumulate p53 protein and increase its DNA binding. Step 5: The deacetylase HDAC2 can inhibit p53 binding to DNA by deacetylation. Step 6: The p53 tetramer binds to a p53 response element (RE) to promote transcription of its gene. Step 7: P53 also needs cofactors such as histone acetyltransferases (HATs) and TATA-binding protein-associated factors (TAFs). Step 8: In this example, p53 mediates transactivation of its target genes. Step 9: P53 protein mediates various genes which produce proteins involved in various functions. Step 10: The previously activated proteins can perform DNA repair, cell-cycle arrest, senescence and apoptosis. ATM, ataxia telangiectasia mutated; BAX, BCL2-associated X protein; BBC3, BCL2-binding component-3; BIRC5, survivin; CDKN1A, cyclin-dependent kinase inhibitor-1A; CHK2, checkpoint kinase-2; DDB2, damage-specific DNA-binding protein-2; DDIT4, DNA-damage-inducible transcript-4; FAS, TNF receptor subfamily, member 6; GADD45 , growth arrest and DNA-damage inducible; p14ARF; SFN, stratifin; TP53I3, tumour protein p53-inducible protein-3; TRIM22, tripartite motif containing-22 (adapted from Riley *et al*., 2008).

1.5 p53 and cell cycle arrest

Involvement of p53 in cell cycle arrest is important for maintaining the integrity of the genome and as a safeguard for the prevention and initiation of cancer formation by arresting cells with damaged DNA time to repair the abberant DNA before re-entering of the repaired cells to the proliferating pool of cells after the repair is complete. This is in order to make sure cells with damaged DNA do not propagate aberrant DNA to daughter cells. This normally involves not severe and repairable DNA damage.

Activation of p53 in many cell types leads to an arrest at G1 and G2-M phases of the cell cycle. Ionising irradiation produces p53-dependent transient arrest in G1 phase of the cell cycle in proliferating fibroblasts (Kastan *et al*., 1991). It is well established that wild-type p53 is required for the initiation of G1 arrest in response to ionising radiation (IR) because cell lines engineered to lack p53 activity show an attenuated response (Kuerbitz *et al*., 1992, Kessis *et al*., 1993). Furthermore, embryonic fibroblasts from p53-null mice lose the ability to G1 growth arrest in response to IR (Kastan *et al*., 1992).

Several genes have been shown to be involved in p53-dependent cell cycle arrest. Perhaps the most important gene that is critical in p53-mediated G1 growth arrest is $p21^{WAF1}$ (El-Deiry *et al*., 1993; Bartek and Lukas, 2003; Giono and Manfredi, 2006; Riley *et al*., 2008). It contains a p53-binding motif (p53 response element or in short R.E.) in its promoter and encodes a 21 kDa protein (p21). $p21^{WAF1}$ serves as a potent inhibitor of several cyclin dependent kinases (CDKs) complexes including cyclin E-CDK2 and cyclin A-CDK2 that are necessary for the G1-S transition. Two separate studies have shown that embryonic fibroblasts from p21-/- (null) mice are only partially defective in mediating G1 arrest following exposure to IR (Brugarolas *et al*., 1995; Deng *et al*., 1995), indicating another gene product transactivated by p53 responsible for a complete response.

p21 protein inhibits the activity of CDKs involved in the phosphorylation of the retinoblastoma (RB) protein. RB protein is hypophosphorylated during G1 where it binds and sequesters transcription factor E2F which is required for entry into S phase (Giaccia and Kastan, 1998; Sherr, 1998). Upon hyperphosophorylation of RB protein by G1 cyclin-dependent kinases, active E2F is released, which leads to the transcriptional activation of genes required for S phase progression (Giaccia and Kastan, 1998; Sherr, 1998). However, the inhibition of cyclin D-CDK4/6 complexes by p21 prevents the release of E2F which then causes the accumulation of unphosphorylated RB and subsequently results in G1 cell cycle arrest (Giaccia and Kastan, 1998; Sherr, 1998). Transient arrest of the cell cycle during G1 is to allow time for repair of damaged DNA, which might otherwise interfere with accurate DNA replication and for repair of lesions that might be perpetuated as mutations in cells entering S phase. p53 protein also binds to proliferating cell nuclear antigen (PCNA), a co-factor of DNA polymerase δ and a protein involved in both DNA replication and repair, and inhibits PCNA-dependent DNA replication but not DNA repair (Li *et al*., 1994; Waga *et al*., 1994).

The first p53-regulated gene identified to be involved in G1 cell cycle arrest was *gadd45* which is expressed in response to a variety of DNA-damaging agents including ionising radiation (Kastan *et al*., 1992; Zhan *et al*., 1994). *Gadd45* belongs to the *gadd* (growth arrest and DNA damage inducible) family of genes and has a response element in its third intron (Kastan *et al*., 1992). In gene transfer experiments, expression of GADD45 protein results in growth inhibition as measured by reduced ability of recipient cells to form colonies in culture. The GADD45 protein exerts its effect through binding to PCNA. The association results in inhibition of DNA replication while at the same time enhancing DNA repair (Smith *et al*., 1994).

p53 also mediates the G2/M transition by directly inhibiting Cdc2 function via repression of cyclin B1 from binding to Cdc2 (Taylor and Stark, 2001; Zilfou and Lowe, 2009). The *14-3-3* σ gene has been implicated in

mediating G2 arrest. This was shown by a study by Hermeking and colleagues (1997) where exposure of colorectal cancer cells to ionising radiation resulted in induction of *14-3-3 σ* gene, which then stimulated G2 arrest. 14-3-3σ is a negative cell cycle regulator and induces G2/M arrest in response to DNA damage in a p53-dependent manner (Hermeking, 1997; review in Ozaki and Nakagawara, 2011). Studies by Yang showed that 14-3-3σ abrogated MDM2-mediated degradation of p53 protein and p53 nuclear export (Yang, 2003). Other p53-target genes discovered to be involved in G2/M arrest in response to DNA damage are *Reprimo* (Ohki *et al*., 2000) and *p53R2* (Tanaka *et al*., 2000) (review in Ozaki and Nakagawara, 2011). Figure 1.6 depicts a shematic diagram for p53-mediated cell cycle arrest.

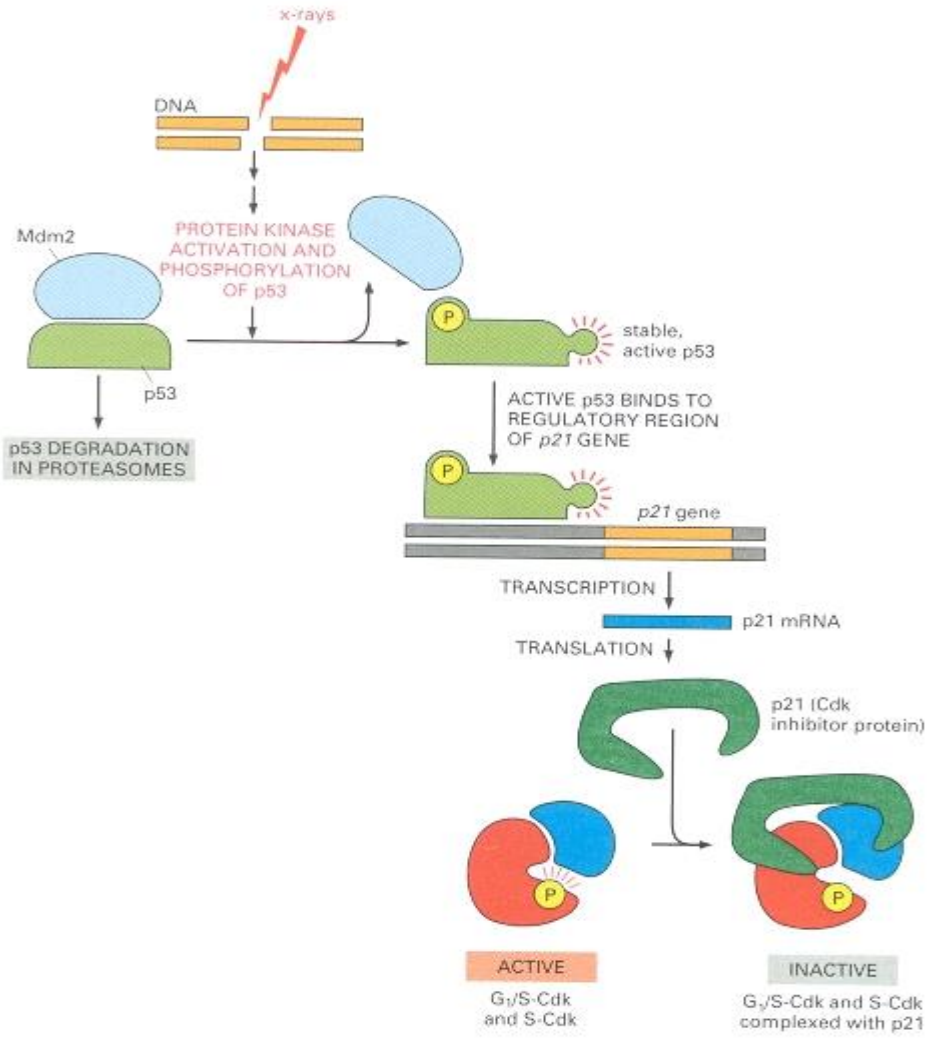

Figure 1.6. p53-mediated cell-cycle arrest upon response to DNA damage (adapted from Alberts *et al*., 2002).

1.6 p53-mediated apoptosis

Apoptosis is the ordered and rapid destruction of the cell without the involvement of inflammatory response (Schmitt *et al*., 2002; Taylor *et al*., 2008; reviewed in Meek, 2009). Apoptosis is characterised by morphological changes that include cell shrinkage, plasma membrane blebbing, nuclear condensation, DNA fragmentation and apoptotic vesicles (cell remnants). To exert its function as a tumour suppressor protein, p53 plays a role in apoptosis and inhibition of pro-survival signals as represented in Figure 1.7 below.

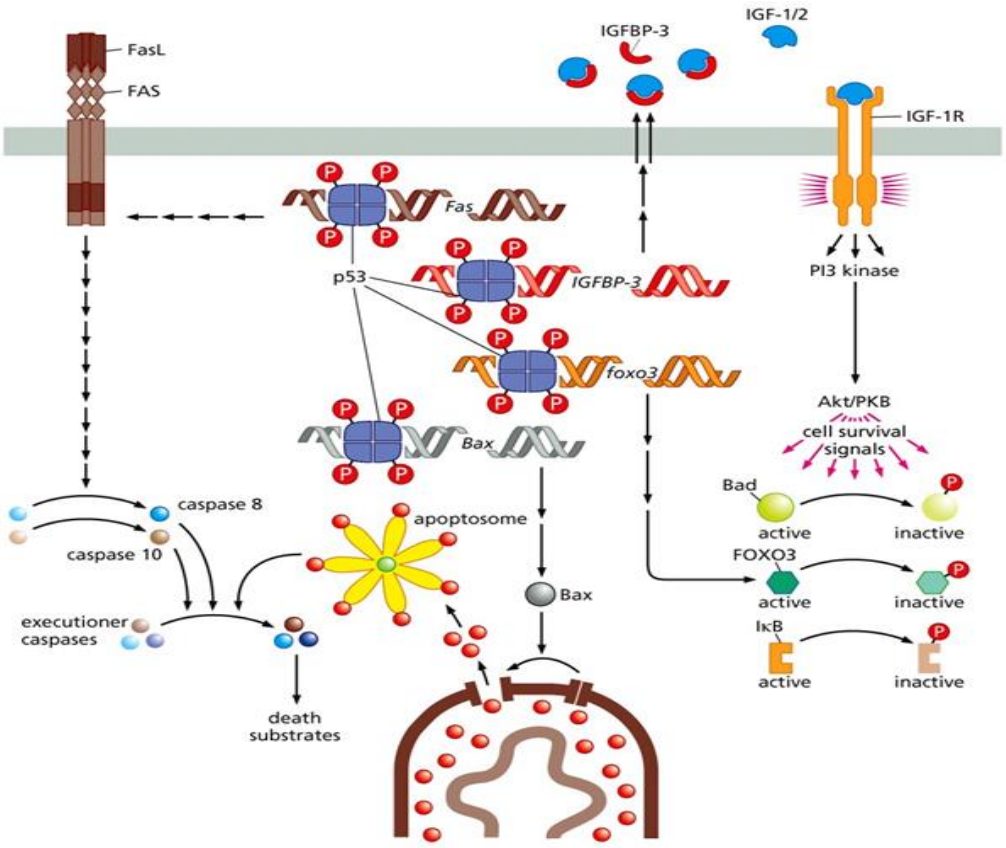

Figure 1.7. Regulation of apoptosis and inhibition of pro-survival signals. Once activated, p53 induces the expression of Bax which then induces the release of cytochrome c from the mitochondria resulting in the activation of a caspase cascade leading to apoptosis. In inhibiting pro-survival, p53 acts by inducing the expression of IGFBP-3 which binds to IGF-1/2, thus inhibits IGF-1/2 from binding to IGF-1R to inhibit the activation of survival proteins PI3k kinase and Akt/PKB (Weinberg Biology of Cancer, 2014).

p53-mediated apoptosis occurs when the DNA damage is too severe and irrepairable and it is induced to get rid of damaged cells from the replicative pools in order to eliminate malignant transformation. p53-mediated apoptosis most often involves mitochondrial dysfunction (review in Ozaki and Nakagawara, 2011). p53 protein was first identified as having a role in apoptosis by a study using a clone of the mouse myeloid cell line M1 lacking endogenous expression of p53. These cells were stably transfected with a temperature-sensitive p53 mutant (32^{o}C). Upon downshift to the permissive temperature, it was observed that transfectants underwent massive apoptotic cell death (Yonich-Rouach *et al*., 1991). Subsequent studies have shown that normal murine thymocytes and quiescent lymphocytes exposed to ionising radiation in culture underwent apoptosis whereas thymocytes of p53 null (knock-out) mice were severely deficient in their ability to undergo apoptosis in response to irradiation (Clarke *et al*., 1993; Lowe *et al*., 1993), a treatment that normally results in a marked increase in p53 protein levels (Maltzman and Czyzyk, 1984; Kastan *et al*., 1991).

p53 protein has been shown to mediate apoptosis in cells exposed to agents that either directly or indirectly cause DNA strand breakage. Its loss of function can contribute to tumourigenesis by allowing inappropriate cell survival. In response to DNA damage, p53 induces the expression of a variety of different genes involved in mediating an apoptotic response. The genes involved include *BAX*, the product of which antagonises the anti-apoptotic activity of Bcl-2 protein, insulin growth factor binding protein 3 (IGF-BP3) which inhibits the mitogenic activity of IGF receptor signalling and a series of p53-induced genes (*PIG* genes) that are assumed to encode proteins that could generate or response to oxidative stress. Other genes induced include *Killer/DR5, CD95 (Fas or Apo-1), p53AIP1(p53-regulated apoptosis-inducing protein 1), Perp* and BH3-only proteins *Noxa* and *PUMA* (Riley *et al*., 2008; Brady and Attardi, 2010) which are mostly members of pro-apoptotic Bcl-2 family (Green and Kroemer, 2009; review in Zilfou and Lowe, 2009). In contrast to all these genes, p53 protein down-regulates the *bcl-2* gene whose product acts as an anti-apoptotic agent (White, 1996). BAX was the first

identified pro-apoptotic protein from the Bcl-2 family member (Selvakumaran *et al*., 1994). It has a dominant negative effect against pro-survival Bcl-2. BAX protein promotes apoptosis by dysregulating the mitochondrial outer membrane permeability (MOMP) and inducing the release of cytochrome c to the cytosol from the mitochondrial intermembrane space, which in turn activates caspases culminating in the activation of a caspase cascade important in apoptosis (Green, 2006; review in Ozaki and Nakagawara, 2011). The *bax* gene itself has been shown to contain a p53 response element (R.E.) within its promoter region and to be upregulated in response to DNA damage and p53 (Miyashita and Reed, 1995). On top of this, p53 protein was also shown to repress the promoter of *Bcl-xl*, which has an anti-apoptotic activity, and survivin, which is important for cell growth and survival (Sugars *et al*., 2001; Hoffman *et al*., 2002). P53AIP1 was transcriptionally upregulated upon response to apoptotic stimuli by phosphorylated p53 Ser46. P53AIP1 promotes MOMP by directly interacting with Bcl-2 which then induces the release of cytochrome c from mitochondria (Matsuda et al., 2002; review in Ozaki and Nakagawara, 2011).

In response to stress stimuli, p53 mediates apoptosis through induction of Bcl-2 family members such as Bax (Miyashita *et al*., 1994), Bid (Sax *et al*., 2002), Puma (Nakano and Vousden, 2001) and Noxa (Oda *et al*., 2000). PUMA has been shown to mediate p53-dependent and –independent apoptosis *in vivo*. PUMA is located at mitochondria and like p53AIP1, it induces apoptosis by interacting with Bcl2 causing the release of cytochrome c leading to activation of a caspase cascade (Nakano and Vousden, 2001; review in Ozaki and Nakagawara, 2011). PUMA knockout mice showed complete deficiency in DNA damage-induced apoptosis, reminiscent as those observed in p53 knockout mice (Jeffers *et al*., 2003; Villunger *et al*., 2003; Yu and Zhang, 2003). BAX has been shown to be required for PUMA-mediated apoptosis, demonstrating that BAX action is downstream of PUMA (Yu, 2001; Jeffers et al., 2003; review in Ozaki and Nakagawara, 2011). PUMA is a key mediator of p53-dependent and –independent apoptosis *in vivo* (Yu and Zhang, 2003).

Separate studies by Haupt and colleagues (1995) and Chen and co-workers (1996) have demonstrated that mutant p53 which fail to activate transcription can still induce apoptosis. Furthermore, p53-dependent apoptosis can occur in the presence of inhibitors of transcription and translation (Caelles *et al*., 1994). The direct interaction of the extreme C-terminal region of p53 with the XPB and XPD DNA helicases has been shown to play a role in p53-dependent apoptosis (Wang *et al*., 1996). p53 protein is able to traffic the death receptor protein, Fas, to the cell surface, thereby sensitising cells to Fas-mediated apoptosis (Bennett *et al*., 1998). p53 has been linked to oncogene-induced apoptosis by oncogenes such as c-myc and Adenovirus EIA, particularly after serum depletion and this apoptosis is said to be p53-dependent. Loss of p53-mediated apoptosis resulted in the survival of oncogene expressing cells undergoing inappropriate cell growth carrying mutations and carcinogenic lesions (Lowe *et al*., 1994).

p53 also activates apoptotic protein activating factor-1 (APAF-1) which then associates with cytochrome c and pro-caspase 9 and thus forms apoptosome resulting in the initiation of a caspase cascade by promoting the cleavage of pro-caspase 9, the initiator caspase. The active caspase 9 then activates executioner pro-caspases 3 and 7 resulting in active caspases 3 and 7 which then mediate DNA fragmentation through cleaving the inhibitor of Caspase Activated DNase (ICAD) leading to activation of Caspase Activated DNase (CAD) which then cleaves the DNA into internucleosomal fragments of about 180 base pairs, the event of which is an important hallmark of apoptosis (review in Helton and Chen, 2007).

p53 protein is also able to induce apoptosis in a transcription-independent mechanism. Considerable evidence has accumulated to support this notion. In transcription-independent pathways of p53-mediated apoptosis, p53 localises to mitochondria and forms a complex with the anti-apoptotic proteins Bcl-2 and Bcl-XL to liberate BAX and BAK resulting in the release of cytochrome c which activates the caspase cascades (Sakahira *et al*., 1998; Mihara *et al*., 2003). In addition, it has been shown that a common p53

polymorphic variant R72 greatly promotes nuclear export to mitochondria and apoptosis (Dumont *et al*., 2003). A study by Chipuk *et al*. shows that p53 directly bound with BAX which enabled BAX to associate with mitochondria resulting in the release of cytochrome c from the mitochondria and subsequent induction of apoptosis (Chipuk *et al*., 2004). p53 interaction with BAK forming the p53-BAK complex inhibits BAK from interacting with the anti-apoptotic Bcl-2 family member Mcl1 (Leu *et al*., 2004).

Loss of p53-dependent apoptosis causes aggressive mouse brain tumourigenesis (Symonds *et al*., 1994; Bai and Zhu, 2006). Also found that mice harbouring the p53 R172P mutant develop a variety of tumours probably due to defect in p53-mediated apoptosis (Liu *et al*., 2004; Bai and Zhu, 2006). This indicates that p53-mediated apoptosis plays an important role in tumour suppression function of p53. p53 also mediates TRAIL-induced apoptosis upon responding to cellular stress via the extrinsic pathway or death receptor pathway through its upregulation of DR4/5 and caspase-8 (Zhao *et al*., 2012). Figure 1.8 below is a representative diagram showing p53-dependent TRAIL-induced apoptosis pathway.

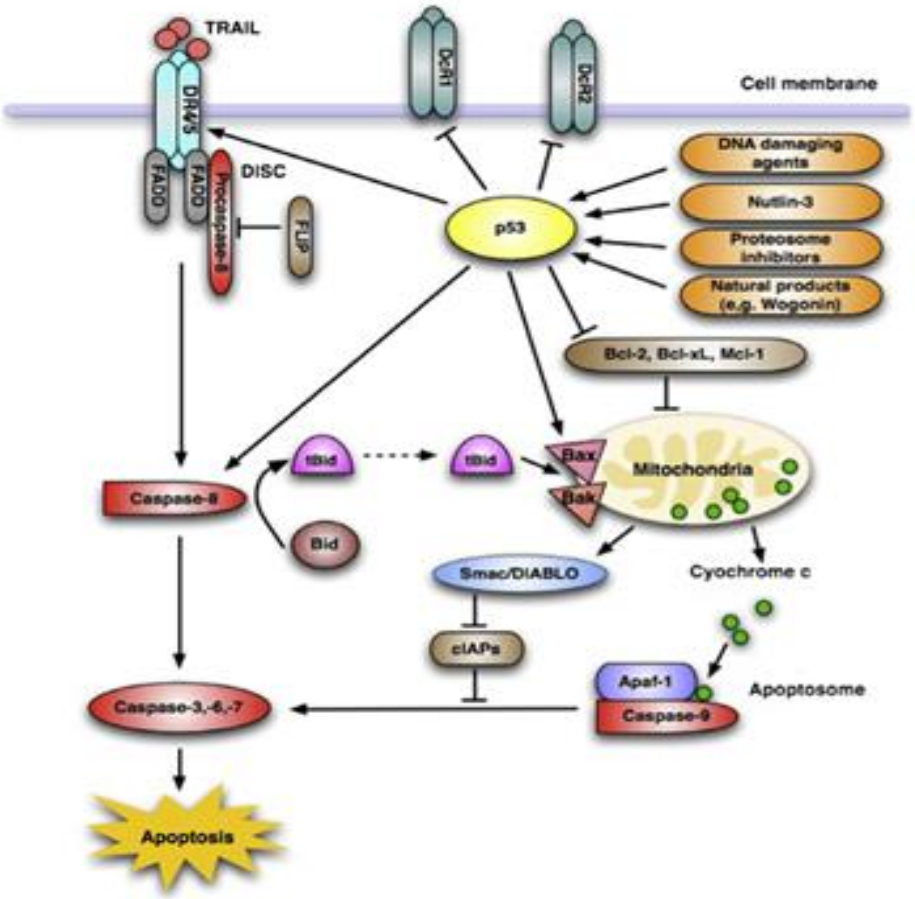

Figure 1.8. TRAIL-mediated signaling and p53-dependent TRAIL-induced apoptosis either the extrinsic pathway (through activation of caspase-8 and caspase-10) or the intrinsic/mitochondrial pathway (through activation of caspase-9). In response to cellular stress, p53 upregulate some pro-apoptotic genes and downregulate some anti-apoptotic genes to enhance the intrinsic pathway (adapted from Zhao *et al*., 2012).

1.7 p53 roles in senescence and aging

Senescence is a permanent growth arrest where the cells cannot re-enter the cell cycle (Rufini *et al*., 2013). Senescent cells are enlarged and flat, reduced replicative capacity and increased upregulation of p53, p21, p16, p27 and p15 (Kuilman *et al*., 2010; Romagosa *et al*., 2011). Both initiation and maintenance of senescence depend on p53. Senescence is important in both tumour suppression and organismal aging (Rufini *et al*., 2013). Senescence cells are unable to replicate DNA, thus resulting in permanent cell-cycle arrest (Zilfou

and Lowe, 2009). p53-induced senescence can eliminate tumour cells through the mediation of p21. “Eat me” or opsonisation signal of senescent cells triggers an innate immune response leading to phagocytosis and killing by macrophages to eliminate the tumour cells from the host (Suzuki and Matsubara, 2011). p53 family members p63 and p73 also involve in the regulation of senescence and aging (Rufini *et al*., 2013).

The decision to induce either growth arrest, senescence or apoptosis after p53 activation is determined by several large, highly complex and inter-dependent factors including the cell type, the types of cellular stress stimuli, the amount and severity of the stress, the presence or absence of survival factors in the extracellular environment, the p53-MDM2 autoregulatory feedback loop and the levels of p53 protein, promoter selectivity and response levels and duration. The absolute p53 protein levels and the presence of p53-binding proteins influence promoter selectivity (Khoo *et al*., 2014). Generally, cells with low levels of p53 protein will arrest in G1 and those with high levels will undergo apoptosis after a certain threshold is achieved (Chen *et al*., 1996; Wu and El-Diery, 1996; Kracikova *et al*., 2013; Khoo *et al*., 2014).

Other than functioning mainly in cell cycle arrest and apoptotic cell death, there is emerging evidence that p53 protein is also involved in cellular metabolism and autophagy, lysosome-mediated degradation of cellular components such as degradation of cytoplasms and organelles (Feng *et al*., 2005; Bensaad *et al*., 2006; Crighton *et al*., 2006; review in Helton and Chen, 2007; Ide *et al*., 2009; Meek, 2009), both atypical tumour suppressive mechanisms of p53 protein. While apoptosis is dependent on ATP-mediated caspase activation, autophagy induction may be an alternative to apoptosis in times when cellular energy levels are low following DNA damage (review in Helton and Chen, 2007). Autophagy is promoted during nutritional starvation to replace metabolic reserves and promote cell survival (Kroemer *et al*., 2010; Maddocks and Vousden, 2011). p53 has a dual role in autophagy, to either induce or inhibit autophagy (Crighton *et al*., 2006; Tasdemir *et al*., 2008; Yee *et*

al., 2009; Maddocks and Vousden, 2011). Figure 1.9 below shows senescence regulation by p53.

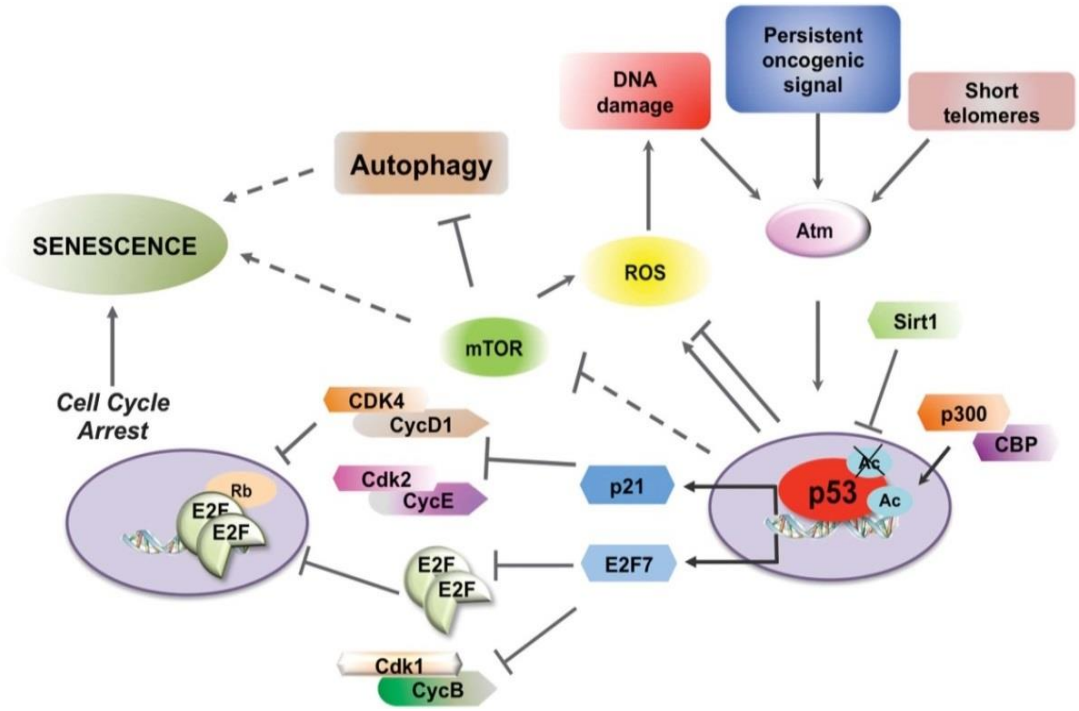

Figure 1.9. Regulation of senescence by p53. Several posttranslational modifications modulate p53 activity. Active p53 induces senescence and represses mitosis. p53 also controls other pathways such as ROS generation and mTOR. ROS, Reactive Oxygen Species (adapted from Rufini *et al*., 2013).

1.8 p53 roles in cellular metabolism

There is an emerging, novel role of p53 in regulation of cellular metabolism in physiology and diseases. p53 involves in a wide range of human physiology and pathologies including diabetes, dysfunctions of central nervous system and obesity. Metabolic alterations are a hallmark of tumour cells for continued growth, survival and proliferation (Maddocks and Vousden, 2011; Liang *et al*., 2013). Tumour cells uptake and utilise glucose at a much higher rate than normal cells thus produce excessive lactate while normal cells gain energy from mitochondrial oxidative phosphorylation. Most tumour cells primarily obtain their energy from aerobic glycolysis known as the Warburg effect (Warburg, 1956). p53 regulates mitochondrial oxidative phosphorylation

(OXPHOS), glycolysis, glutamine metabolism, lipid metabolism, antioxidant defense. Through this regulation p53 maintains the cellular metabolism homeostasis and redox balance thus contributing to tumour suppressor role of p53 (Maddocks and Vousden, 2011; Liang *et al*., 2013).

1.8.1 Mitochondrial oxidative phosphorylation (OXPHOS) and glucose metabolism (glycolysis)

p53 involves in maintaining mitochondrial integrity and promoting mitochondrial oxidative phosphorylation and glycolysis. Down-regulation or loss of p53 lead to reduction in mitochondrial oxidative phosphorylation and increased glycolysis in both *in vitro* cultured cells and *in vivo* mouse models (Matoba *et al*., 2006; Liang *et al*., 2013). On the contrary, p53 represses aerobic glycolysis by the regulation of glucose transportes and glycolytic enzymes. Reduction of glucose uptake by p53 is through downregulation of the expression of transporters 1 and 4 (GLUT1 and GLUT4) (Schwartzenberg-Bar-Yoseph *et al*., 2004) and indirect downregulation of glucose transporter 3 (GLUT3) through the negative regulation of NF-κB signalling (Vousden and Lane, 2007; Kawauchi *et al*., 2008). In summary, p53 induces mitochondrial oxidative phosphorylation and inhibits aerobic glycolysis, resulting in the deregulation of the Warburg effect through the differential expression of p53 target genes and various signaling pathways involved.

1.8.2 Glutamine metabolism (Glutaminolysis)

Rapidly growing tumour cells use glutamine for proteins and nucleotide synthesis and ATP generation. p53 plays an important role in glutaminolysis, a process by which glutamine is converted to glutamate by glutaminase. A further conversion of glutamate to α-ketoglutarate is used as an important substrate for the tricarboxyclic acid (TCA) to generate ATP in cells (Dang, 2010; Wang *et al*., 2010; Liang *et al*., 2013).

1.8.3 Lipid metabolism (lipid oxidation)

Under glucose starvation, p53 promotes fatty acid oxidation used to drive the TCA cycle to provide energy (ATP) to meet the cellular energy demands (Jensen, 2003). Promotion of fatty acid oxidation (FAO) by p53 is an alternative energy source as evidenced by starvation of mouse models expressing wildtype p53 showed increased FAO compared to p53-null mice. FAO occurs partly through the activation of guanidine acetate methyl transferase (GAMT) which in turn facilitates apoptosis instead of cell survival (Ide *et al*., 2009; Liang *et al*., 2013).

1.8.4 Antioxidant defense

In tumour cells, oxidative stress and accumulated reactive oxygen species (ROS) are important in tumourigenesis. Several studies have shown that reduction of the ROS levels and elicited anti-oxidant defense is part of mechanism by which p53 exerts its role in tumour suppression. Increased endogenous ROS levels in cells are the result of mitochondrial oxidative phosphorylation. A group of antioxidant genes transcriptionally induced by p53 include *sestrins 1* and *2*, *TIGAR, GPX1, ALDH4, GLS2* and *Parkin* in order to lower ROS levels and prevention of DNA damage (Budanov *et al*., 2004; Yoon *et al*., 2004; Bensaad *et al*., 2006; Hu *et al*., 2010; Zhang *et al*., 2011; Liang *et al*., 2013). On the contrary, p53 deficiency causes the elevated levels of intracellular ROS, which greatly enhances DNA oxidation and mutagenic rate in cells. Paradoxically to p53 role in antioxidant defense, in severe oxidative stress, the elevated ROS levels activate p53 to prooxidant function by transcriptionally up-regulating a group of antioxidant genes such as *PIG3, PIG6, FDXR, Bax* and *Puma* which can further increase intracellular ROS levels thus promote apoptosis and senescence in order to eliminate damaged cells in order to maintain genomic stability (Bensaad *et al*., 2006; Liang *et al*., 2013).

1.9 p53 mutation

The *p53* gene is mutated in over 50% of human cancers where most frequently missense mutation in one allele is accompanied by loss of the second allele with alterations in every region of the protein (Hollstein *et al*., 1991; Leroy *et al*, 2013). This ultimately leads to a complete loss of wild-type expression. Most p53 mutations in human tumours are missense mutations and most are single amino acid mutations/substitution clusters in the central DNA-binding domain with mutation hotspots at R175, G245, R248, R249, R273 and R282 (Greenblatt, 1994; Brosh and Rotter, 2009; Muller and Vousden, 2012), indicating that DNA-binding activity is mostly altered resulting in the changes in the transcription of p53 target genes. It is within this central part that more than 90% of the missense mutations in p53 are found. p53 mutations can be divided into two categories: i) structural mutants which cause unfolding of the p53 protein, ii) DNA-contact mutants which change amino acids important for DNA binding. p53 structural mutants dramatically affect the folding of the p53 protein in comparison to p53 DNA contact mutants. Both mutations interfere the binding of p53 to its response elements and result in the loss of the tumour suppressor functions of p53 (Cho *et al*., 1994; Sigal and Rotter, 2000; Muller and Vousden, 2012).

1.9.1 p53 mutation gain-of-function (GOF)

Different p53 hotspot mutants elicit different gain-of-function (GOF) phenotypes (contact mutant versus conformation mutant). p53 mutant displays GOF activities by exerting carcinogenesis (Liu *et al*., 2010; Muller and Vousden, 2012; Garcia and Attardi, 2014). The changes in p53 structural stability may be crucial for the acquired gain of function phenotypes. Mutant p53 exerts a dominant-negative regulation/effects towards wildtype p53. Mutant p53 also acquires novel oncogenic properties/functions such that it promotes genomic instability, survival, proliferation, invasion and metastasis. Mutant p53 gains tumour-promoting functions where it shows oncogenic properties in the absence of wtp53 (Muller and Vousden, 2012; Jackson and Lozano, 2013;

Garcia and Attardi, 2014). Figure 1.10 depicts the oncogenic phenotypes associated with p53 mutant gain-of function activities.

Mutant p53 binds and inhibits the tumour suppressor activities of p53 family members p63 and p73. p53 structural mutants have high binding affinity to p63 and p73 compared to p53 contact mutants. Both mutants inhibit p63 and/or p73 by promoting invasion and metastasis or apoptosis inhibition. Mice heterozygous for p63 and p73 ($p63^{+/-}$ and $p73^{+/-}$) develop spontaneous metastatic tumours reminiscent in mice with mutant p53 suggesting that mutant p53 inhibits p63/p73 (Muller and Vousden, 2012; Garcia and Attardi, 2014). Mutp53 deregulates the tumour suppressing functions of TAp63/TAp73 and promotes the oncogenic activities of ΔNp63/ΔNp73. ΔNp63 and ΔNp73 are both pro-survival and anti-apoptotic. While TA forms of both p63 and p73 have tumour suppressive activities, their ΔN variants are likely to be oncogenic (Lee *et al*., 2006; Ravni *et al*., 2010; Wilhelm *et al*., 2010). Mutant p53 invasive capabilities is mainly mediated by inhibition of p63 and/or p73 (Adorno *et al.,* 2009; Muller *et al.,* 2009). Mutant p53 sequesters both p63 and p73 from their target genes thus represents a potential molecular mechanism underlying inactivation of p63 and p73 in cells harbouring mutant p53 (Flores *et al*., 2002; Strano *et al*., 2003; Strano *et al*., 2007). Inhibition of mutant p53-p73 interaction by small peptides sensitise mutant p53-expressing cells to genotoxic drugs whereas such peptides show no effects on cells expressing wtp53 or null-p53 (Di Agostino *et al*., 2008; Oren and Rotter, 2009). p73 knockdown causes cancer cells to become chemoresistant and elimination of mutant p53 sensitises cancer cells to chemotherapeutic agents (Strano *et al*., 2003; Strano *et al*., 2007). This suggests that mutant p53-p73 complex causes chemoresistant of tumours with mutant p53 compared to wt-p53 bearing tumours.

Mutant p53s cannot recognise wt-p53 consensus sequence but still serve as oncogenic transcription factors. Genome-wide expression profile study shows that mutant p53 regulates a set of genes mediating oncogenic activities (O'Farrell *et al*., 2004; Scian *et al*., 2004; Strano *et al*., 2007). Mutant p53 can

either directly bind to undefined DNA consensus or physically interact with other proteins to function as a bona fide transcription factor. While wt p53 transcribes genes to induce apoptosis and inhibit tumourigenesis, mutant p53 suppresses CD95 (Fas/APO-1) gene expression implicated in apoptotic responses. Mutant p53 proteins are phosphorylated and acetylated at sites that stabilise wt p53, thus facilitates the accumulation of dysfunctional mutant p53 in the nucleus of tumour cells (Bai and Zhu, 2006). Mutant p53 can transcribe genes involved in growth and survival. Some mutant p53 selectively bind to promoters of p53 target genes such as p21 and MDM2 but not promoters of proapoptotic genes such as bax and PIG3 (Pan and Haines, 2000; Bai and Zhu, 2006). This results in mutant p53 to induce cel cycle arrest just like wt p53 but defective in mediating apoptosis (Friedlander *et al*., 1996; Ludwig *et al*., 1996; Bai and Zhu, 2006).

Studies on mutant p53 isoforms transfected into p53-null cell lines indicate that cells with mutant p53 GOF feature became resistant to the killing effects of various anticancer agents while the knockdown of endogenous mutant p53 sensitised the cells to killing by such agents (Oren and Rotter, 2009). siRNA-mediated knockdown of endogenous mutant p53 in cancer cells rendered cells more susceptible to apoptosis by anticancer agents (Vikhanskaya *et al*., 2007), also *in vivo* setting (Bossi *et al*., 2006). Overexpressed mutant p53 increased cell proliferation, increased tumour aggressiveness and enhanced metastasis which are among the hallmarks of mutant p53 GOF in mouse models. Mutant p53 can increase cell migration and invasion in *in vitro* assay (Adorno *et al*., 2009; Oren and Rotter, 2009; Wang *et al*., 2009). Mutant p53 knockdown in mouse models shows that tumours were less vascularised implicating p53 regulation of angiogenesis (Bossi *et al*., 2008). Mutant p53 knockin mice developed aggressive, metastatic tumours compared to p53-null counterparts (p53 knockout mice) (Lang *et al*., 2004; Olive *et al*., 2004; Oren and Rotter, 2009). Microarray analysis showed overexpression of mutant p53 isoforms can exert gene expression involved in pro-proliferative or antiapoptotic proteins including multidrug resistant gene 1 (MDR1), PCNA, EGFR, c-myc and IGF2. On the other hand, the mutant p53

isoforms also repress the transcription of other genes such as *CD95/Fas/AApo1, caspase-3, p21, GADD45 and PTEN* (Vikhanskaya *et al*., 2007). Mutant p53 interacts with transcription factors, modulate both positive and negative transcriptional output (Oren and Rotter, 2009). Mutant p53 also regulates microRNAs thus altering the stability of various microRNA target transcripts such as miR-130b, miR-155 and miR-205, each of which involves in invasive and metastatic pathways (Dong *et al*., 2012; Neilsen *et al*., 2012; Tucci *et al*., 2012).

Mutant p53s gain new functions to drive tumour cell migration, invasion and metastasis. The Slug/Snail and Twist family of transcription factors are master regulators of the epithelial-mesenchymal transition (EMT) (Shiota *et al*., 2008; Muller *et al*., 2011) by opposing p53 function, indicating p53 prevents a transcriptional program of EMT. p53 expression promotes MDM2-mediated degradation of Slug, thus enhances E-cadherin expression (Wang *et al*., 2006). Loss of E-cadherin commonly occurs in cancer which is able to drive metastasis in animal models (Derksen *et al*., 2006). Athough p53 mutation mostly in the DNA binding domain, mutant p53 still promotes promoter activity via the N-terminal transactivation domain. It has been shown that mutant p53 inhibition of apoptosis is abrogated by abolition of its N-terminal trasactivation domain (Muller *et al*., 2011). p63 knockdown enhances the expression of genes involved in motility, invasion and metastasis (Barbieri *et al*., 2006; Gu *et al*., 2008). Mutant p53 regulates Sharp-1 and Cyclin G2. Suppression of Sharp-1 or Cyclin G2 mimicked mutant p53 to induce cell migration and reduced Sharp-1 and Cyclin G2 expression resulted in poor prognosis and recurrence in breast cancer. TAp63 modulates Dicer to prevent metastasis (Sue *et al*., 2010). miRNA processing is down-regulated in many cancers (Lu *et al*., 2005; Kumar *et al*., 2009). Reduced levels of Dicer can promote tumourigenesis and invasion and are associated with a poor prognosis (Kumar *et al*., 2009; Sue *et al*., 2010). Decreased Dicer levels increased PKB/Akt activation suggesting that it acts on the same pathway as mutant p53 and p63 to induce invasion (Han *et al*., 2010; Muller *et al*., 2011).

Dong *et al*. found that over-expressed mutant p53-R175H enhanced cell migration and invasion of human endometrial cancer cells and activated epidermal growth factor receptor (EGFR/phosphatidylinositol 3-kinase (PI3K)/Akt pathway. However, upon knockdown of mutant p53-R175H the reverse occurred (Dong *et al*., 2009). Mutant p53 promotes cell growth via inhibition of AMP-activated protein kinase (AMPK) activation. Mutant p53 downregulation increases AMPK activation under energy stress. AMPK acts a an energy sensor and tumour suppressor. Inhibition of AMPK activation is revealed as an important mechanism of mutant p53 gain of function properties (Zhou *et al*., 2014).

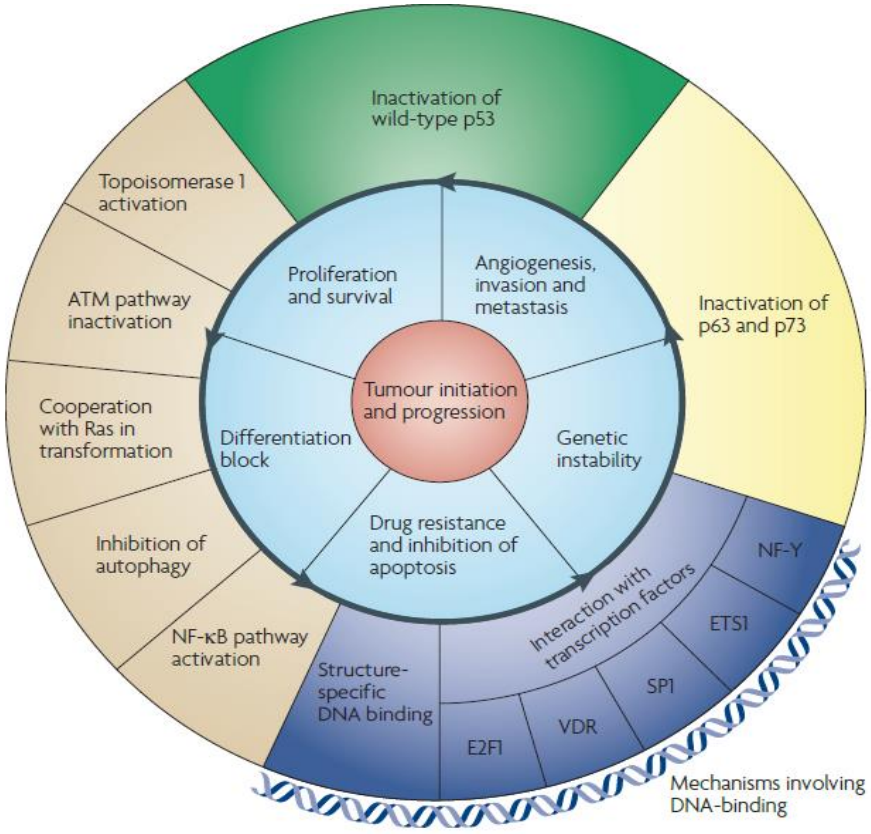

Figure 1.10. The inner light blue circle represents the oncogenic phenotypes associated with the mutant p53 proteins activities. The outer circle represents the key mechanistic properties that mutant p53 adopts to contribute to the phenotypes listed in the inner circle. Most of the phenotypic effects can be attributed to almost each of the mechanistic properties; therefore the inner blue circle can be rotated freely. Image adapted from Brosh and Rotter (2009).

1.10 Post-translational modifications of p53 protein

p53 is activated in response to both genotoxic and non-genotoxic stresses, however, the patterns of p53 post-translational modifications (PTMs) and the activation or repression of p53 target genes are quite distinct, thus their cellular outcomes are different. This also potentially affects numerous protein interactions with p53 protein (Anderson and Apella, 2010). Post-translational modifications of p53 protein are crucial for stabilisation (by escape from constitutive, proteosome-dependent degradation) and transcriptional activation (by conversion from 'latent' into 'active' form) of the protein where over 60 sites of 363 residues of the human p53 protein have been reported to be post-translationally modified (reviewed in Apella and Anderson, 2000 and 2001; Anderson and Apella, 2010; Nguyen *et al*., 2014) (see Figure 1.11). Figure 1.12 shows a diagram summarising posttranslational modifications to p53 in response to genotoxic and non-genotoxic stress.

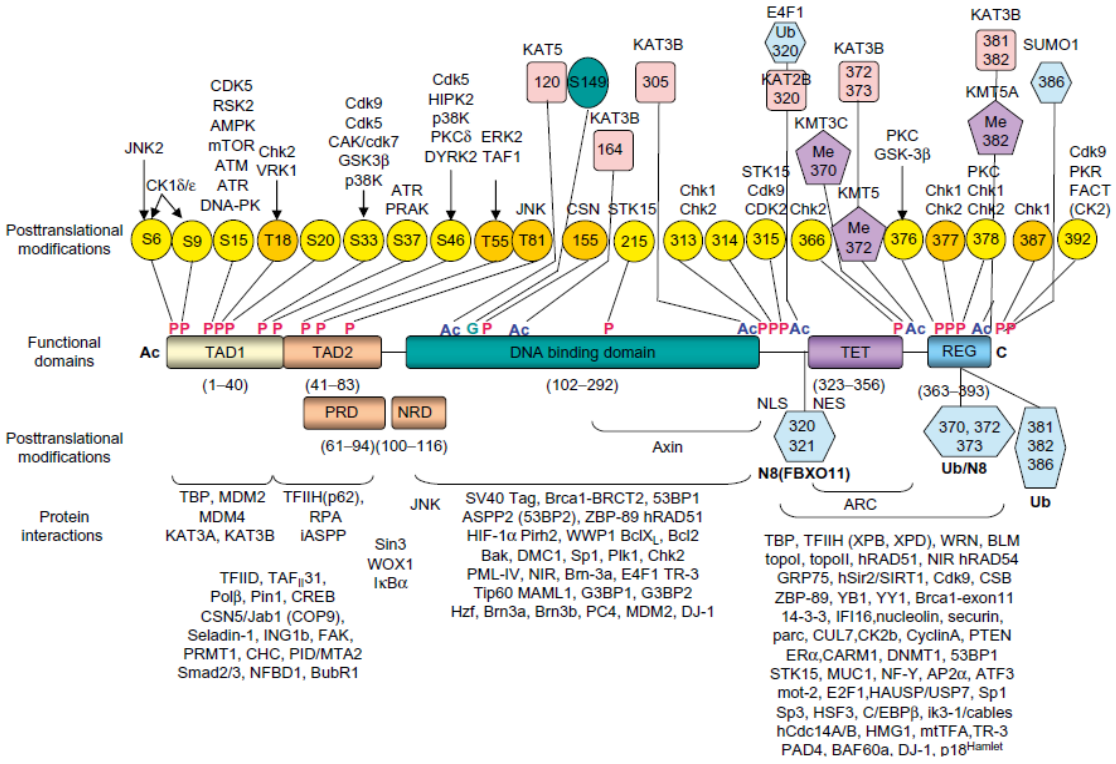

Figure 1.11. A schematic diagram showing p53 main domains, posttranslational modification sites and proteins that interact with human p53. Posttranslational modification sites (P, phosphorylation; Ac, acetylation; G, glycosylation; Me, methylation, N8, neddylation; Ub, ubiquination) are indicated together with enzymes that can accomplish the modifications *in vitro*. (adapted from Anderson and Apella, 2010).

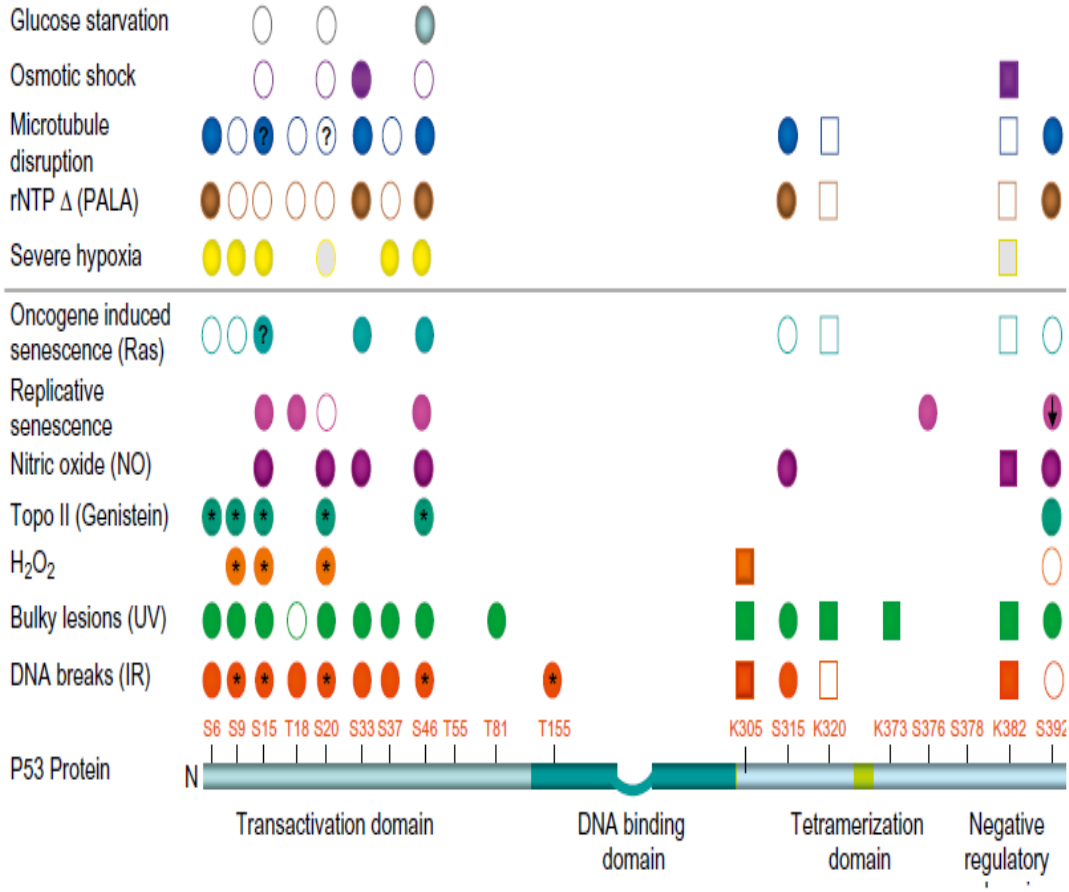

Figure 1.12. Posttranslational modifications to p53 in response to genotoxic and non-genotoxic stress. The bar at the bottom represents the human 393 amino acid p53 polypeptide; functional regions are indicated. Selected posttranslational modification sites (Figure 1.12) are indicated above the bar; S, serine; T, threonine; K, lysine. Filled circles (phosphorylation) or squares (acetylation) indicate modification in response to the indicated stress (left); open symbols (or light gray) indicate no change in modification in response to stress. No symbol indicates the site has not been examined. An "*" denotes ATM dependent phosphorylations; a "?" indicates conflicting literature reports; a down arrow indicates treatment induced a decrease in site modification (adapted from Anderson and Apella, 2010).

It is now clear that full cell-specific transcription responses in response to cellular stresses require a rich cascade of post-translational modifications of p53 protein (as reviewed in Anderson and Appella, 2010), which ultimately determine the cell fate. Exposure of cells to a wide range of genotoxic and non-genotoxic stresses such as ionising radiation (IR), ultraviolet irradiation (UV),

oncogene activation, nucleotide depletion or hypoxia results in transient stabilisation of the p53 protein, causes its accumulation in the nucleus, and activates it as a transcription factor (reviewed in Prives and Hall, 1999; Apella and Anderson, 2000; Anderson and Apella, 2010). It has been proposed that different stress signals lead to different types of p53 protein modifications and consequently the transcriptional programme of p53 (Riley *et al*., 2008), for details see Figure 1.12. Activation of p53 mainly leads to either growth arrest at the G1/S or G2/M transitions of the cell cycle or apoptosis. p53 stabilisation, nuclear accumulation and activation or in short, the regulation of p53 activity, involve a variety of post-translational modifications, mostly by phosphorylation and acetylation. Other types of post-translational modifications of p53 protein include sumoylation, ubiquitination and to a lesser extent glycosylation and ribosylation (Meek and Anderson, 2009). Another post-translational modification on p53 protein is neddylation (Xirodimas *et al*., 2004), see Figure 1.11 and Table 1.1 for details. Overall, these modifications serve to regulate p53 protein by affecting its DNA binding, degradation, localisation, oligomerisation and association with cellular factors such as co-activators or negative regulators (reviewed in Liu and Kulesz-Martin, 2001; Meek and Anderson, 2009). However, this thesis will only focus on the two most common types of p53 post-translational modifications phosphorylation and acetylation, briefly mention on other p53 PTMs and mainly to study p53 nitration. To date, nitration sites of p53 protein in the form of nitrotyrosine have not been mapped and nitration can either activate or inactivate p53 protein.

1.10.1 Phosphorylation of p53 protein

p53 protein has been identified as a substrate for many different kinases that phosphorylate it at several sites mainly within the N-terminal and C-terminal regulatory domain *in vitro*. The kinase signalling to p53 protein includes casein kinase 1 and 2, CHK1 and 2, ATM (ataxia telangiectasia mutated), ATR (ATM/Rad3 related kinase), JNK (c-jun N-terminal kinase) and DNA-PK (DNA-dependent protein kinase) (Jayaraman and Prives, 1999). Phosphorylation on

p53 protein has been studied intensively and these studies have been greatly facilitated by the availability of phosphoserine and phosphothreonine antibodies on phosphorylated-modified p53 protein (reviewed in Apella and Anderson, 2001; Anderson and Apella, 2010). Seven serines (Ser6, 9, 15, 20, 33, 37, 46) and two threonines (Thr18 and 81) in the N-terminal transactivation domain of human p53 are phosphorylated and dephosphorylated in response to DNA damage stimuli such as ionizing radiation or UV light. In unstressed cells, Thr55 is constitutively phosphorylated but dephosphorylated after DNA damage (Anderson and Apella, 2010).

MDM2 protein is a key negative regulator of p53 protein stability and activities in normal cells. Disruption of the interaction of p53 protein with MDM2 protein prevents ubiquitin-mediated degradation of p53 protein. Increased p53 stability occurs through multi-site phosphorylation of both p53 and MDM2 proteins (review in Appella and Anderson, 2001; Meek, 2004; Anderson and Apella, 2010). Studies by Shieh and colleagues have shown that phosphorylation of serines 15 and 37 of p53 protein *in vitro* by DNA-PK disrupts the interaction of p53 protein with MDM2 protein, leads to p53 protein stability and accumulation in the nucleus and also disrupts MDM2-mediated inhibition of p53-dependent transcription (Shieh *et al*., 1997; Shmueli and Oren, 2007; Meek and Anderson, 2009; Nguyen *et al*., 2014). To further support this notion, it was shown that substitution of serine-15 with glutamic acid gives rise to increased p53 stability (Ashcroft *et al*., 1999). Serine-15 phosphorylation has also been shown to enhance the interaction of p53 protein with transcriptional co-activators CBP and PCAF (Lambert *et al*., 1998; Sakaguchi *et al*., 1998; Liu *et al*., 1999). Ser15 phosphorylation acts as a nucleation event to stimulate modifications of other sites by phosphorylation and acetylation (Meek and Anderson, 2009). Furthermore, serine-20 has been shown to be phosphorylated in response to DNA damage and interestingly, it resides in the region of p53 that binds to MDM2 (Picksley *et al*., 1994). Phosphorylation of serine-20 by checkpoint kinase 1 (Chk1) and Chk2 in response to IR can lead to abrogation of the p53-MDM2 interaction (Hirao *et al*., 2000).

p300 and CBP have dual role in p53 regulation. Both act as transcriptional activator proteins and also ubiquitinate p53 for MDM2 degradation (Grossman *et al*., 1998 & 2003). Several studies showed that phosphorylation of p53 amino terminal sites including Ser15, Thr18 and Ser20 augments p53 association with p300/CBP and stimulate p53 transcriptional activities (Lambert *et al*., 1998; Dumaz and Meek, 1999; Dornan *et al*., 2003; Finlan and Hupp, 2004; Meek and Anderson, 2009). Furthermore, phosphorylation of these residues blocked MDM2 binding to p53 and decreased p53 turnover (Shieh *et al*., 1997; Bottger *et al*., 1999; Craig *et al*., 1999; Dumaz *et al*., 1999; Schon *et al*., 2002). Thr18 phosphorylation enhances the inhibition of p53 binding to MDM2 compared to other residues (Ser15, -20, -33, -37, -46, -55). However phosphorylation of all seven amino-terminal residues inhibits MDM2 binding by four fold higher than Thr18 phosphorylation alone (Teufel *et al*., 2009).

Phosphorylation of serine-46 has been implicated in the activation of p53-mediated apoptotic response (D'Orazi *et al*., 2002; Saito *et al*., 2002; Nguyen *et al*., 2014). Phosphorylation of Threonine-81 by c-Jun N-terminal kinase (JNK) has been shown to result in p53 stabilisation (Buschmann *et al*., 2001(b)). It has been reported that serine-315 and serine-392 phosphorylation may be responsible for the regulation of the oligomerisation of p53 protein and thus its sequence-specific DNA binding (Wang and Prives, 1995; Sakaguchi *et al*., 1997). DNA damaged-induce phosphorylation of p53 protein has been reported to cause propyl isomerase Pin1 to bind to p53 protein and enhance p53 DNA binding and transcriptional activity (Zacchi *et al*., 2002; Zheng *et al*., 2002; Nguyen *et al*., 2013).

Phosphorylation of the p53 C-terminal regulatory domain by CKII, PKC or Cdks has been shown to activate sequence-specific DNA binding of p53 *in vitro* (Hupp *et al*., 1992; Hupp and Lane, 1994; Wang and Prives, 1995). Upon exposure to UV light, phosphorylation at S392 activates specific DNA binding activity through the p53 tetramer stabilisation (Matsumoto *et al*., 2006). S389A (human S392A) mutation in knock-in mice showed unaffected p53 stability but

were predisposed to UV-induced skin cancer (Johnson *et al*., 2006), also altered induction of p53 target genes in comparison to wild-type mice (Bruins *et al*., 2007 & 2008). It is reported that S392 hyper-phosphorylation correlates with poor prognosis, advanced tumour stage and tumour grade (Matsumoto *et al*., 2004(a) & (b), Bar *et al*., 2009). All of the studies mentioned above have led to the conclusion that each phosphorylation of p53 protein is a key mechanism responsible for activation and regulation of its tumour suppressor function in response to cellular stress in a tissue- and promoter-specific manner (reviewed in Dai and Gu, 2010). However, p53 phosphorylation is dispensable on its induction by the ARF pathway or in response to small molecules inducers such as Nutins (Meek and Anderson, 2009).

Several studies on *Tp53* knock-in mouse models on individual or combination sites of p53 phosphorylation had been conducted by several groups have provided valuable information about modulation of p53 functions (Menendez *et al*., 2009; Nguyen *et al*., 2014). These include single mutation, a change of serine to alanine, at the N-terminal domain $Trp53^{S18A/S18A}$, $Trp^{S23A/S23A}$, double homozygous mutation $Trp53^{S18A/S18A;S23A/S23A}$ and at the C-terminal domain such as p53 knockin mutant S312A and S389A. Humanise p53 mouse model was also created (*hupki*) with human p53 Ser46 modification. Overall, mice with some p53 PTM site mutations showed low survival rates and increased spontaneous tumour formation. However, none of these mutations had such a severe impact as compared to the $Trp53^{-/-}$ mutation (Nguyen *et al*., 2014).

p53 protein activity may also be regulated by being dephosphorylated in response to DNA damage. Waterman *et al* (1998) have shown that p53 is ATM-dependent dephosphorylated on serine-376 in response to IR (Waterman *et al*., 1998). This dephosphorylation event induces the interaction of p53 with 14-3-3 proteins resulting in activation of its sequence-specific DNA binding potential. Thr55 and Ser376 were shown to be dephosphorylated upon DNA damage induced by ionising radiation, indicating that dephosphorylation also activates p53 (Bai and Zhu, 2006).

1.10.2 Acetylation of p53 protein

The histone acetyltransferase (HATs), CREB-binding protein (CBP) and p300 can co-activate numerous transcription factors, including p53 protein (Gu and Roeder, 1997). p53 protein is covalently modified by acetylation at multiple lysine residues namely lysine-370, 371, 372, 381, 382 and 386 of the carboxy-terminal regulatory domain by CBP/p300 and, to a lesser extent, lysine-320, which is located within the main nuclear localisation signal of p53, by p300/CBP associated factor (PCAF) (Sakaguchi *et al*., 1998). Both CBP/p300 and PCAF possess intrinsic HATs activity and therefore can acetylate human p53 protein by adding one or more acetyl groups to the stated lysine sites. Acetylation of these residues has been found to enhance sequence-specific DNA binding of wild-type p53 protein, possibly by inhibiting p53's non-sequence-specific DNA-binding activity, (Anderson *et al*., 1997) and therefore transcriptional activity, possibly as a result of an acetylation-induced conformational change of the C-terminus, thus increasing p53 DNA binding capacity (Gu and Roeder, 1997; Sakaguchi *et al*., 1998). The acetylation of lysine residues in the carboxy-terminal of p53 protein, which also targets for ubiquitination, results in the inhibition of p53 degradation. Notably, prior phosphorylation of p53 on serine-33 and/or serine-37 (Sakaguchi *et al*., 1998) has been implicated in recruiting CBP/p300 to p53 and thereby controlling p53 acetylation *in vitro*. This therefore leads to the possibility that a combination of phosphorylation and acetylation events on p53 protein is collectively responsible for its activation in response to genotoxic stresses. Modifications of p53 protein are therefore highly complex and inter-dependent.

Lysine residues K120 (Sykes *et al*., 2006; Tang *et al*., 2006) and K164 (Tang *et al*., 2008) in the DNA binding domain of p53 protein are two recently discovered acetylation sites. K120 acetylation is indispensable for induction of genes involved in apoptosis but not in cell cycle arrest. (Sykes *et al*., 2006; Tang *et al*., 2006). K120 acetylation has been shown for p53 to dissociate BAK from MCL-1 at mitochondria (Sykes *et al*., 2009). It is likely that K120 acetylation might be involved in transcription-dependent and transcription-

independent mechanisms of p53-mediated apoptosis (review in Dai and Gu, 2010). While K120 acetylation involved in the activation of pro-apoptotic genes, K164 acetylation is important for the activation of most p53 target genes (Tang *et al*., 2008). Mutations of K (lysine) to R (arginine) in K120, K164 and the six C-terminal lysine residues completely abolishes p53-induced cell cycle arrest and apoptosis (Tang *et al*., 2008), indicating that acetylation is indispensable for the activation of p53 protein as a tumour suppressor (review in Dai and Gu, 2010).

K320 in the tetramerisation domain in p53 protein is acetylated by PCAF (Kruse and Gu, 2008) which then mediates the activation of p21 (Knights *et al*., 2006). K317R (human K320R) mutation in p53 gene in mice enhanced p53-mediated apoptosis upon irradiation (Chao *et al*., 2006), suggesting the inhibition of p53 apoptotic activities by K320 acetylation upon exposure to DNA damage (review in Dai and Gu, 2010).

The C-terminal lysine acetylation sites of p53 protein are essential for ubiquitination and subsequent degradation of p53 by MDM2. MDM2 might suppress p53 acetylation by p300 by forming a complex with p300 and p53 protein (Kobet *et al*., 2000). Acetylation of these residues is therefore thought to contribute to p53 stabilisation by impairing ubiquitination.

Tumour suppressor promyelocytic leukaemia (PML) protein has also been shown to induce p53 acetylation at lysine-382 through the formation of a trimeric p53-PML-CBP complex (Pearson *et al*., 2000). Overexpression of PML relocalises p53 protein into nuclear bodies and induces phosphorylation and acetylation of p53 protein, thereby enhancing its transcriptional activity (Fogal *et al*., 2000; Guo *et al*., 2000; Pearson *et al*., 2000).

Histone deacetylase complexes (HDACs) are often associated with co-repressor complexes and can exert their repressive effects on both histone and non-histone proteins by removing an acetyl group resulting in deacetylation of the proteins (Smith, 2002). Even though the influence of HDAC activity on p53

function and the general role of p53 deacetylation is not clear, deacetylation probably provides a quick acting mechanism to stop p53 function once transcription activation of target genes is no longer needed. This therefore leads to the restoration of the steady-state level of p53 target genes which is crucial for cellular homeostasis. De-acetylation of p53 protein could also play an important step in the MDM2-mediated degradation of p53 protein by promoting its ubiquitination and subsequently degradation (Ito *et al*., 2002; reviewed in Brooks and Gu, 2003; Kruse and Gu, 2009) but this inhibitory effect can be abrogated by the tumour suppressor $p19^{ARF}$, suggesting that acetylation also plays an important role in the p53-MDM2-$p19^{ARF}$ feed back loop (Ito *et al*., 2001; Bai and Zhu, 2006).

1.10.3 Other post-translational modifications of p53 protein

Sumoylation of p53 protein is another type of p53 post-translational modification where p53 protein is modified in response to DNA damage by a small ubiquitin-like modifier protein 1 (SUMO-1) which conjugates p53 protein at lysine-386 (Gostissa *et al*., 1999). Although SUMO modification does not regulate p53 stability, this modification enhances p53's transcriptional activity (Gostissa *et al*., 1999, Rodriguez *et al.*, 1999, Muller *et al*., 2000). It is still under intense debate as to whether sumoylation activates or inactivates p53 protein activity (Chen & Chen, 2003; reviewed in Liu and Shuai, 2008). Several other modifications of p53 protein namely methylation (Chuikov *et al*., 2004), glycosylation (Shaw *et al*., 1996) and ribosylation by poly (ADP-ribose) polymerase (PARP) might affect both protein stability and protein function (Vaziri *et al*., 1997; Kumari *et al*., 1998, Wang *et al*., 1998; Simbulan-Rosenthal *et al*., 1999).

A finding by Xirodimas and colleagues has shown that p53 transactivation might be repressed by neddylation promoted by MDM2 (Xirodimas *et al*., 2004). In this process, the C-terminal glycine residue of the ubiquitin-like protein NEDD8 can be covalently linked to lysine-370, lysine-372

and/or lysine-373 of p53 protein (Xirodimas *et al*., 2004). These lysine residues are also targeted by ubiquitination. A question is still raised whether p53-specific de-neddylation pathways exist, or whether neddylation competes with acetylation or enhances ubiquitination (reviewed in Bode and Dong, 2004). Moreover, NEDD8 ulimate buster 1 (NUB1), a non-covalent interactor of the ubiquitin-like molecule Ubl NEDD8, has been shown to cooperate with the NEDD8 and ubiquitin pathways in controlling p53 localisation and function, notably resulting in the cytoplasmic localisation and loss of p53 transcriptional activity (Liu and Xirodimas, 2010). NUB1 exerts its effects on p53 largely dependent on NEDDylation and MDM2, also through the co-operation of NEDD8 with ubiquitin by decreasing p53 NEDDylation and promoting p53 ubiquitination.

Lysine and arginine residues in p53 protein are potential targets for methylation. Arginine methylation is targeted only by Protein Arginine N-methyl Transferase 5 (PRMT5) at R333, R335 and R337 (Jansson *et al*., 2008; Scoumanne and Chen, 2008). On the other hand, lysine methylation is better understood of which three Lysine Methyl Transferase (KMTs) are responsible for mono-methylating p53 protein and at least two KMTs for demethylating it. p53 lysine methylation can result in either activating or repressing the p53 activity depending on the site of modification and the number of attached methyl groups (review in Dai and Gu, 2010). K372 is mono-methylated by SET7/9 (also known as KMT7) and this activates the transactivation activity of p53 target genes (Chuikov *et al*., 2004). K382-mono-methylation by SET (KMT5A) and SMYD2 (KMT3C)-mediated K370 mono-methylation inhibit p53 transcriptional activities (Huang *et al*., 2006; Shi *et al*., 2007) while G9A (KMT1C) and G9A-like protein (KMT1D) di-methylate p53 at K373 which suppresses p53-mediated apoptosis (Huang *et al*., 2010). Overall, these findings clearly show that p53 function is regulated at least in part by the interplay between methylation and demethylation of the protein together with the crosstalk with other well characterised p53 modifications principally by phosphorylation and acetylation and to a lesser extent by ubiquitination, sumoylation and neddylation.

In summary, protein posttranslational modifications are usually reversible due to the available enzymes which can convert phosphorylation (by kinases) to dephosphorylation (by phosphatases), acetylation (by acetyl-transferases) to deacetylation (by de-acetylase), ubiquitination (ubiquitin ligases) to deubiquitination (by de-ubiquitinases) and methylation (by methyltransferases) to de-methylation (by de-methylases). The involvement of the actions of these opposite enzymes thus results in setting thresholds and re-setting activation for p53 to exert its main function as a tumour suppressive protein and to restore p53 normal levels after cellular stresses dissipate (Anderson and Appella, 2010). Table 1.1 below summarises the post-translational modification events of human p53 protein.

Table 1.1: Covalent modifications of human p53 protein

Amino acid	Modification	Putative enzymes involved	References
Serine-6, Serine-9	Phosphorylation	CKI	Milne *et al*., 1992; Knippschild *et al*., 1997; Higashimoto *et al*., 2000
Serine-15	Phosphorylation	DNA-PK, ATM, ATR, Chk1, AMPK	Shieh *et al*., 1997; Canman *et al*., 1998; Khanna et al., 1998; Tibbetts *et al*., 1999; Goudelock *et al*., 2003; Jones *et al*., 2005
Threonine-18	Phosphorylation	CKI	Sakaguchi *et al*., 2000
Serine-20	Phosphorylation	Chk2, Plk3	Chehab *et al*., 2000; Xie *et al*., 2001; Craig *et al*., 2003
Serine-33	Phosphorylation	CAK	Ko *et al*., 1997
Serine-37	Phosphorylation	DNA-PK, ATR, JNK	Shieh *et al*., 1997; Canman *et al*., 1998
Serine-46	Phosphorylation	p38 MAPK, HIPK2, PKCdelta, DYRK-2	Bulavin *et al*., 1999; D'Orazi *et al*., 2002; Perfettini *et al*., 2005; Yoshida *et al*., 2006; Taira *et al*., 2007
Threonine-55	Constitutive Phosphorylation	TAF1	Gatti *et al*., 2000; Li *et al*., 2004
Threonine-81	Phosphorylation	JNK	Ronai, the 10th p53 Workshop. 2000, California, USA.
Serine-149 Threonine-150, Threonine-155	Phosphorylation	COP9 signalosome (CSN)-associated kinase	Bech-Otschir *et al*., 2001
Serine-313	Phosphorylation	Chk1, Chk2	Anderson and Apella, 2010
Serine-314	Phosphorylation	Chk1, Chk2	Anderson and Apella, 2010
Serine-315	Phosphorylation	cdk	Wang and Prives, 1995
Serine-366	Phosphorylation	Chk2	Anderson and Apella, 2010

Serine-371 Serine-376 Serine-378	Constitutive Phosphorylation	PKC, TFIIH	Milne *et al*., 1994; Delphin *et al*., 1997
Serine-392	Phosphorylation	CKII, p38 MAPK	Herrmann *et al*., 1991; Keller *et al*., 2001
Serine-15 Serine-376, Threonine-55	Dephosphorylation	PP1, PP2A	Lu *et al*., 2007
Lysine-120	Acetylation	TIP60/hMOF	Sykes *et al*., 2006
Lysine-164	Acetylation	CBP/p300	Tang *et al*., 2006
Lysine-320	Acetylation	PCAF	Liu *et al*., 1999
Lysine-370, Lysine-372, Lysine-373, Lysine-381, Lysine-382, Lysine-386	Acetylation	p300/CBP, KAT3B	Gu and Roeder, 1997; Sakaguchi *et al*., 1998; Liu *et al*., 1999; Ivanov *et al*., 2007
Lysine-373 Lysine-382	Deacetylation	SIRT1	Luo *et al*., 2000; Michishita *et al*., 2005,
Lysine-370, Lysine-372, Lysine-382	Methylation	KMT3, KMT5, KMT5A	Ivanov *et al*., 2007; Shi *et al*., 2007; Kurash *et al*., 2008
Lysine-386	Sumoylation	PIASy, Topors	Bischof *et al*., 2006; Stehmeier *et al*., 2009
Lysine-320, Lysine-321	Neddylation	FBXO11	Abida *et al*., 2007
Lysine-370, Lysine-372, Lysine-373	Neddylation	MDM2	Xirodimas *et al*., 2004
C-terminal lysine residues	Ubiquitination	MDM2, Pirh2, COP1, ARF-BP1	Rodriguez *et al*., 2000; Leng *et al*., 2003; Harris and Levine, 2005
C-terminal lysine residues	Deubiquitination	HAUSP (USP7), USP10	Li *et al*., 2004; Brooks *et al*., 2007; Yuan *et al*., 2010

1.11 The *p53* gene family

Two p53 family members, p63 and p73, were discovered in 1997 (Kaghad *et al*., 1997; Yang *et al*., 1998; review in Bourdon, 2007(a) & (b)). The *p53* gene family members *p53, p63* and *p73* are involved in development, differentiation and cellular response to stress (review in Bourdon, 2007(a) & (b)). These p53 family members are not functionally redundant as individual knockout mice showed they have different phenotypes, thus, they have their own unique functions. *p53* gene encodes 9 protein isoforms, 6 protein isoforms by *p63* gene and at least 29 protein isoforms by *p73* gene. These protein isoforms arise due to multiple splicing sites, alternative internal promoter usage and alternative translation initiation (review in Murray-Zmijewski *et al*., 2006). The high level of sequence homology in the DNA binding domain among p53 protein family members allows p63 and p73 to bind to p53 responsive elements and transactivate genes responsible for cell cycle arrest and apoptosis. The p53 family members p53, p63 and p73 functions are regulated by subcellular localisation, post-translational modifications and regulatory proteins, however, little is known about p63 and p73 post-translational modifications (Melino *et al*., 2003).

1.11.1 p53 isoforms

Some evidence shows that p53 isoforms exist in human normal and cancerous cells. Since 1985, there is accumulating evidence showing that p53 exists in shorter forms which are derived due to various mechanisms, such as alternative internal promoter, alternative mRNA splicing, proteolytic cleavage, autodegradation, and internal translation initiation. 9 different p53 isoforms have been discovered which are abnormally expressed in tumour tissues in comparison to normal cells (Bourdon *et al*., 2005). The p53 isoforms are p53, p53β, p53γ, Δ133p53, Δ133p53β, Δ133p53γ, Δ40p53, Δ40p53β and Δ40p53γ. p53 gene is transcribed from two distinct sites upstream of exon 1 and from an internal promoter in intron 4. These alternative promoter expression results in N-terminally truncated p53 protein at codon 133 (Δ133 p53). Alternatively,

spliced intron 9 produces 3 isoforms, p53, p53β and p53γ, of which the p53β and p53γ isoforms are without the oligomerisation domain. The 9 isoforms that the human p53 gene encodes are due to the intron 9 alternative splicing and the alternative promoter usage in intron 4 (p53, p53β, p53γ, Δ133p53, Δ133p53β and Δ133p53γ) and also due to the intron 9 alternative splicing and alternative translation initiation or intron 2 alternative splicing (Figure 1.13) (Bourdon *et al*., 2005; review in Bourdon, 2007(a) & (b)).

These p53 isoforms likely coordinate with full length wild-type p53 function as a tumour suppressor. Studies on the potential roles of the various isoforms are still lacking and current knowledge is controversial. However, these variants were reported to either enhance the tumour suppressor activity of wild-type p53 or in contrast, inhibit the transactivation and suppressive functions via dominant-negative effect, and in short these isoforms can function as an activator or a repressor. The abnormal p53 isoform expression could deregulate the p53 response to stress stimuli making further genetic damage to cells thereby leading to tumour initiation and progression (Murray- Zmijewski *et al*., 2006). p53 isoforms have distinct biochemical activities such that co-transfection of p53 and p53β slightly enhanced p53-mediated apoptosis while co-transfection of p53 and Δ133p53 strongly blocked p53-mediated apoptosis in a dose-dependent manner (Bourdon *et al*., 2005; Murray-Zmijewski *et al*., 2006; Khoury and Bourdon, 2010). On the other hand, Δ40p53 isoform acts in a dominant negative manner towards wtp53 by inhibiting both p53 transcriptional transactivation and p53-mediated apoptosis (Ghosh *et al*., 2004; Murray-Zmijewski *et al*., 2006). It is suggested that p53 isoforms can modulate p53 transcriptional transactivation activities. Each p53 isoform possibly has distinct biological and biochemical activities independent of full length p53, suggesting the involvement of p53 in a wide range of biological functions such as cell cycle arrest, apoptosis, differentiaton, replication, and DNA repair (Murray-Zmijewski *et al*., 2006). p53 isoforms similar in structure and functions to those of p63 and p73. They have a conserved DNA-binding domain and vary in their N- and C-terminal regions (Courtois *et al*., 2004). The abnormal and differential expression of p53 isoforms in different types of cancer suggest that

they disrupt the normal p53 response and contribute to tumourigenesis. Thus, this might explain why it is difficult in many clinical studies to link p53 status to prognosis and cancer treatment (review in Khoury and Bourdon, 2010).

1.11.2 p53 family members (p63 & p73) & their isoforms

p63 and *p73* are two members of the p53 family which were discovered in late 1990s (Kaghad *et al*., 1997; Yang *et al*., 1998). *p63* and *p73* genes are rarely mutated in human cancers, however, *p73* is lost in neuroblastomas and T-cell lymphoma. This indicates that both *p63* and *p73* are not classical tumour suppressor genes as *p53* is. They share significant homology with p53, though, they are structurally similar to each other than to p53. p63 and p73 show similarity with the TAD, the DBD and the TD of p53 (Schmale and Bamberger, 1997; Scoumanne *et al*., 2005). The basic domain (BD) is only present in p53 but not in p63 and p73 and certain p63 and p73 isoforms, but not p53, have the sterile-α motif (SAM) domain. Thus, they also induce p53 target genes involved in cell cycle arrest and apoptosis (Scoumanne *et al*., 2005). p63-/- (Mills *et al*., 1999; Yang *et al*., 1999) and p73-/- (Yang *et al*., 2000) knockout mice were not cancer prone but showed epidermal and neuronal defects in development (review in Melino *et al*., 2003) as compared to p53-/- null mice which developed normally but were tumour prone (Donehower *et al*., 1992 & 1995; Scoumanne *et al*., 2005) but it was recently demonstrated that p63 and p73 have a role in tumour suppression since mice heterozygous for p63 and p73 were susceptible to tumour formation (Flores *et al*., 2005). Thus, the p53 family members show both common as well as distinct functions. Like p53, p63 and p73 give rise to multiple isoforms with distinct functions due to alternative promoter utilisation and alternative mRNA splicing (Marin & Kaelin, 2000).

Both p63 and p73, like p53, can form homo-oligomers, bind to DNA to transcribe p53-target genes and mediate apoptosis (Jost *et al*., 1997, Osada *et al*., 1998, Yang *et al*., 1998). p53, p63 and p73 activate the expression of many common genes, such as p21 and Bax. Like p53, p63 and p73 are mostly

located in the nucleus and contain NLS and NES sequences. Similar to p53, p73 might undergo ubiquitination in the nucleus and be exported to the cytoplasm for degradation by the 26S proteasome pathway. N-terminally truncated (ΔN) forms of p63 and p73 that lack the TA domain act as dominant negative inhibitors of the TA isoforms and p53 where TA is pro-apoptotic while ΔN is anti-apoptotic.

1.11.2.1 p63 and its isoforms

p63 has 6 different isoforms (TAp63α, TAp63β, TAp63γ, ΔNp63α, ΔNp63β and ΔNp63γ). ΔNp63 isoforms lack transactivation domain found in TAp63 isoforms. At least 3 alternatively spliced C-terminal isoforms (α, β and γ) are expressed by human and mouse *p63* genes which can also be transcribed by promoter in the intron 3. While TA isoforms are formed in the upstream promoter in exon-1, the N-terminal truncated p63 isoforms (ΔNp63) are alternatively spliced by promoter in intron 3 (Figure 1.14).

p63 isoforms bind DNA through p53RE and p63RE leading to upregulation of target genes involved in differentiation, cell-cycle arrest or apoptosis (Murray-Zmijewski *et al*., 2006; Bourdon 2007(a) & (b); Stiewe 2007). p63 is important for epidermal morphogenesis and limb development. p63-null mice are fatal after birth and show malformations in the limb and failure in the skin and other epidermal tissues development (Mills *et al*., 1999; review in Bourdon, 2007(a) & (b)). However, p63 role in cancer is still elusive. Paradoxically, Flores *et al*. (2005) have shown that p63+/- mice were shown to be cancer-prone while Keyes *at al*. (2005) demonstrated that p63+/- mice show premature aging without any sign of cancer growth.

1.11.2.2 p73 and its isoforms

p73 gene expresses at least 35 mRNA variants which theorytically give rise to 29 different p73 protein isoforms, however, only 14 isoforms have so far been described (review in Khoury and Bourdon, 2010). The *p73* gene can be

alternatively transcribed by promoter in the intron 3, where at least 7 isoforms arise from alternative C-terminal splicing (such as α, β, γ, δ, ε, ζ, η) and at least 4 from alternative N-terminal splicing, each with different transactivation domain (TA, Ex2, Ex2/3 and ΔN). (Figure 1.15). p73 isoforms specifically bind DNA through p53RE and p73RE leading to trancription of target genes which either induce cell cycle arrest or apoptosis (Murray-Zmijewski *et al*., 2006; review in Bourdon, 2007(a) & (b); Stiewe, 2007). Mice null for all the p73 isoforms exhibited defects in development but did not susceptible to cancer (Yang *et al*., 2000; review in Bourdon 2007(a) & (b)).

p73 isoforms are differentially expressed in a wide range of tumours compared to normal tissues (review in Murray-Zmijewski *et al*., 2006). ΔNp73 isoforms overexpression has been linked to be a poor prognostic marker in patients with neuroblastoma and is important for tumour survival by inactivating the apoptotic activities of p53 and TAp73 (Casciano *et al*., 2002; Murray-Zmijewski *et al*., 2006). ΔNp73 isoforms have been shown to activate specific target genes not induced by TAp73 isoforms (Liu *et al*., 2004).

1.11.3 The interplay between the p53 family members

The interplay between the p53 family members p53, p63 and p73 and their isoforms might play a role in carcinogenesis (Deyoung and Ellisen, 2007; Mochado-Silva *et al*., 2010). p53 response to stress is dependent on the dynamics of the p53/p63/p73 isoforms and the ratio between these isoforms determine cell fate (Strano *et al*., 2000; Lang *et al*., 2004; Olive *et al*., 2004; Murray-Zmijewski *et al*., 2006). The interplay of the p53/p63/p73 family members and their isoforms involves direct and indirect protein-protein interactions, the regulation of the same target gene promoter as well as each other's promoters (review in Murray-Zmijewski *et al*., 2006). TAp63 and TAp73 recognise p53RE thus activate genes involved in cell cycle arrest and apoptosis. TAp63/TAp73 isoforms are tumour suppressive and these two isoforms are inactivated by ΔNp63/ΔNp73 isoforms which are dominant-negative inhibitors of the p53 family members by either competition of DNA

binding sites or by direct protein-protein interactions. p53 mutants are capable of binding and inactivating p73 isoforms thus abrogate the TAp73 apoptotic function (Strano *et al*., 2000; Lang *et al*., 2004; Olive *et al*., 2004; Murray-Zmijewski, 2006). It is assumed that the presence/absence as well as the ratio of p53 isoforms determine cell fate. The interplay between p53/p63/p73 isoforms is important to our understanding of the transformation of normal cells to tumour formation (Machado-Silva *et al*., 2010).

(a) Human *p53* gene structure

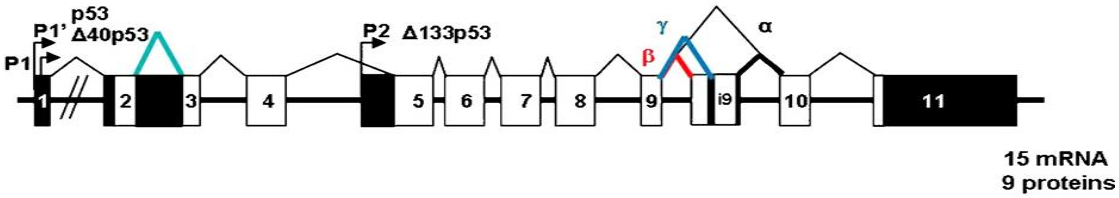

(b) p53 protein isoforms

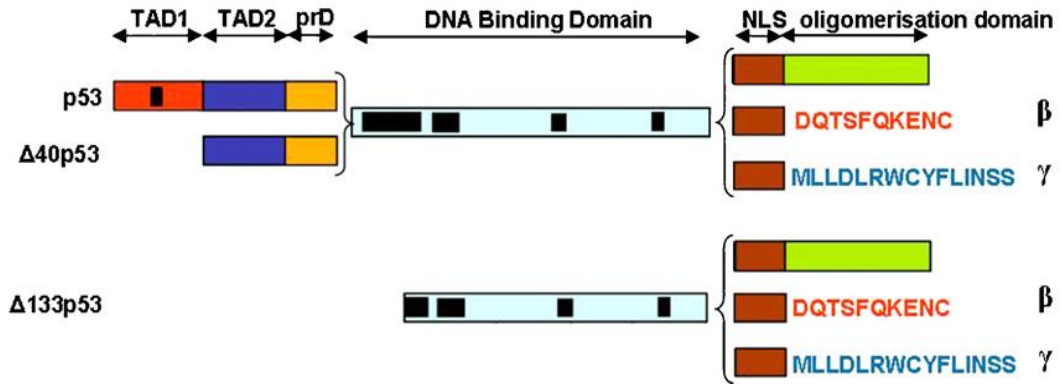

Figure 1.13. (a) Human *p53* gene: Alternative splicing (α, β, γ) and alternative promoters (P1, P1' and P2) and (b) its isoforms (9 isoforms altogether**;** p53, p53β, p53γ, Δ133p53, Δ133p53β, Δ133p53γ, Δ40p53, Δ40p53β and Δ40p53γ) (adapted from Machado-Silva *et al*., 2010).

(a) Human *p63* gene structure

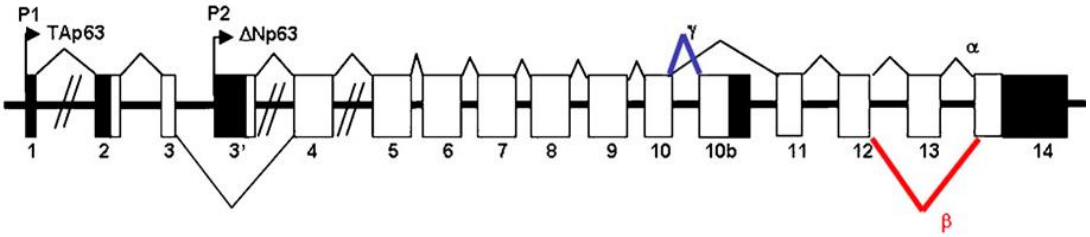

(b) p63 protein isoforms

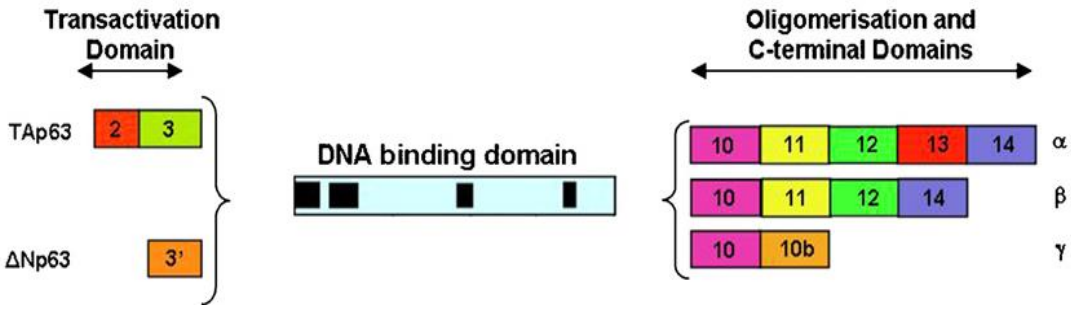

Figure 1.14. (a) Human *p63* gene: Alternative splicing (α, β, γ) and alternative promoters (P1 and P2) and (b) its isoforms (6 isoforms altogether; TAp63α, TAp63β, TAp63γ, ΔNp63α, ΔNp63β and ΔNp63γ) (adapted from Machado-Silva *et al*., 2010).

(a) Human *p73* gene structure

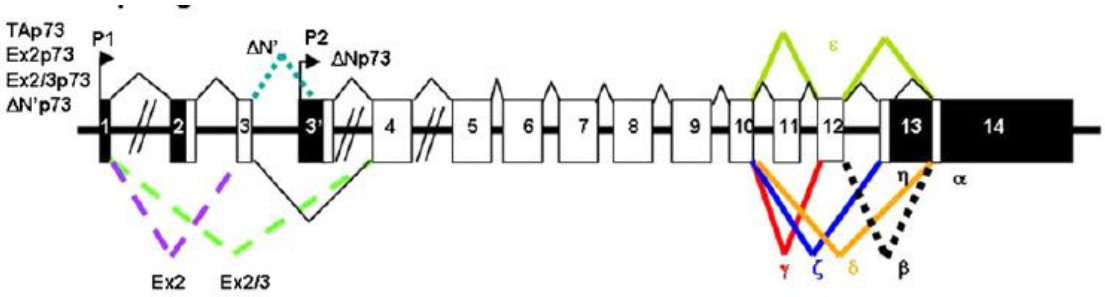

(b) p73 protein isoforms

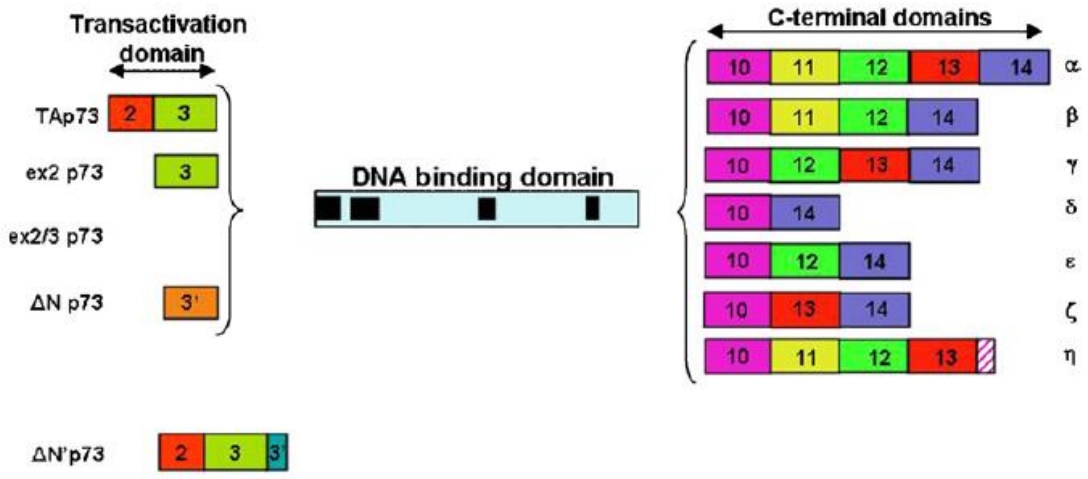

Figure 1.15. (a) Human *p73* gene: Alternative splicing (α, β, γ, ζ, Δ, ε, η) and alternative promoters (P1 and P2) and (b) its isoforms (29 isoforms altogether) (adapted from Machado-Silva *et al*., 2010).

1.12 MDM2

1.12.1 The MDM2 oncogene and oncoprotein

The *mdm2* oncogene was first discovered as an amplified gene on a murine double- minute chromosome in a spontaneously transformed Balb/c 3T3DM mouse cell line (Cahilly-Snyder *et al*., 1987). The murine *mdm2* gene is located at chromosome 10, region C1-C3, while its human homologue known as *hdm2* gene is located at chromosome locus 12q13-15, a region that is frequently amplified in over 30% of human sarcomas (Oliner *et al*., 1992). In this context both mouse and human gene and protein are referred to as *mdm2* and MDM2, respectively. The *mdm2* gene encodes at least five MDM2-related polypeptides (p90-95, p85, p76, p74, p57-58) within cultured mouse cells (Olson *et al*., 1993), presumably due to alternative splice variants of *mdm2* and/or post-translationally modified forms. As shown in Figure 1.16, MDM2 protein consists of a p53 binding domain at the N-terminus (aa 1-220), a nuclear localisation signal (NLS) (aa 181-185), a nuclear export signal (NES) (aa 197-211), a central acidic domain (aa 223-274) and C-terminal zinc finger (aa 305-322) and RING (really interesting new gene) finger domains (aa 438-478).

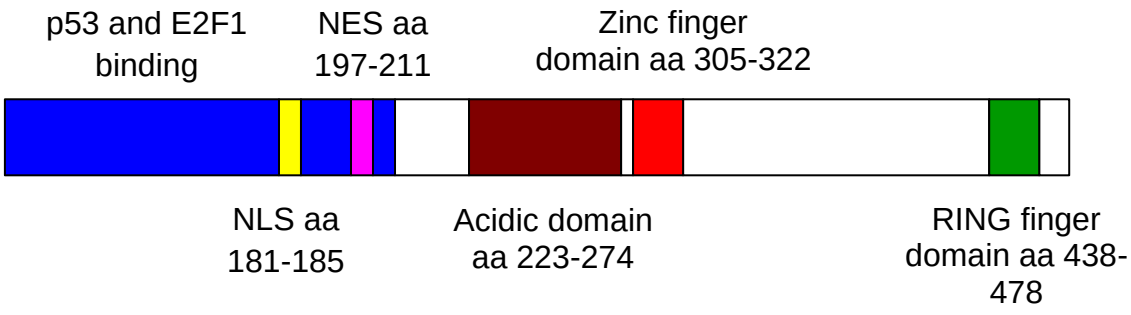

Figure 1.16. Structure of human MDM2 protein. NLS, Nuclear localisation signal; NES, Nuclear export signal (adapted from Picksley *et al*., 2001).

The N-terminal p53 binding of MDM2 protein has been demonstrated to be involved in protein-protein interactions. The central acidic domain has been shown to interact with the ribosomal L5 protein where the ribosomal L5 protein can form complexes with MDM2 and MDM2-p53 protein complex. Both MDM2-L5 and MDM2-L5-p53 protein complexes can bind 5SRNA (Marechal *et* al., 1994). The MDM2 protein also contains a nuclear localisation signal and a nuclear export signal. The nuclear export signal is believed to be involved in the nucleocytoplasmic shuttling of MDM2 protein from the nucleus to the cytoplasm, required for efficient cytoplasmic MDM2-targeted p53 degradation (Roth *et al*., 1998). Nuclear export was proposed to be mediated through a short lysine-rich sequence present in MDM2, similar to the NES of the Rev protein from the human immunodeficiency virus (Roth *et al*., 1998). The Ring finger domain may mediate both protein-protein and protein-nucleic acid interactions (Elenbaas *et al*., 1996) and is critical for MDM2 E3 ligase activity (Fang *et al*., 2000). MDM2 is typically a very short-lived protein, whose rapid degradation is due to autoubiquitin-dependent proteolysis. Thus, the E3 ligase activity of MDM2 is not only important for the regulation of cellular p53 protein levels but also for the regulation of MDM2 levels.

The MDM2 oncogene is amplified or overexpressed in a number of human tumours and it has been suggested that MDM2 levels are associated with poor prognosis in these tumours (review in Momand, 1998). In combination of a p53 mutation, the prognosis is far worse than either event alone (Cordon-Cardo *et al*., 1994; Wurl *et al*., 1998). In general, human cancer cell lines or tumour tissues with MDM2 gene amplifications often have wt p53 protein, suggesting an inactivation of p53 by MDM2 (review in Momand, 1998; Wade *et al*., 2013).

1.12.2 The p53-MDM2 autoregulatory interaction

MDM2 is the main E3 ubiquitin ligase that ubiquitinates p53 (Yang and Li, 2004). Other ubiquitin ligases that target p53 for ubiquitination and degradation include COP1, Pirh2, Topors, Synoviolin and ARF-BP1 (Brook and Gu, 2006;

Anderson and Apella, 2010). MDM2 protein is a negative regulator of p53 protein activity. This is strongly shown by the evidence that the *mdm2* null genotype results in embryonic lethality but is rescued in mice null for p53 gene (Jones *et al*., 1995; de Oca Luna *et al*., 1996) suggesting that the principle function of MDM2 protein is to regulate p53 protein function. Lack of MDM2 causes cell death, mainly by p53-mediated apoptosis.

Crystallographic analysis showed that the N-terminus of p53 protein formed an amphipathic helix with Phe^{19}, Trp^{23} and Leu^{26} buried deep into a deep hydrophobic cleft formed by the N-terminus of MDM2 protein (Figure 1.17) (Kussie *et al*., 1996). Interaction between the MDM2 and p53 proteins has been shown to inhibit p53 protein from recruiting the transcriptional machinery, thereby inactivating the ability of p53 protein to act as a transcription factor (Momand *et al*., 1992; Oliner *et al*., 1993).

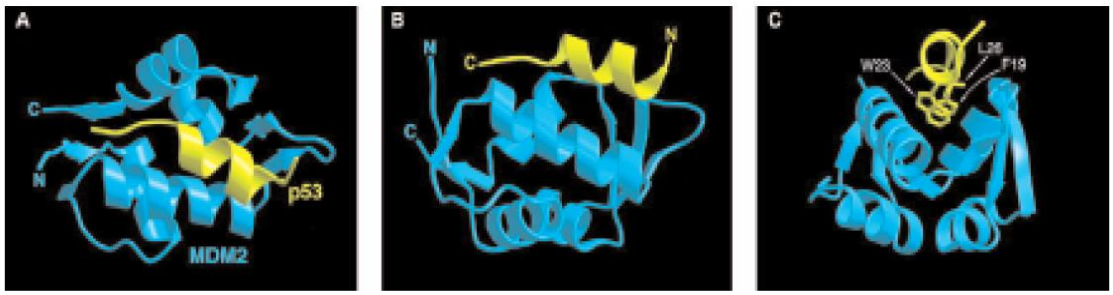

Figure 1.17. p53-MDM2 protein-protein interactions. p53 protein is shown in yellow while MDM2 protein in blue. Amino acid residues F19, W23 and L26 of the p53 protein are buried deep into a hydrophobic cleft of the MDM2 N-terminus. F, Phenylalanine; W, Tryptophan; L, Leucine (adapted from Kussie *et al*., 1996).

MDM2 binds to p53 protein preferentially when p53 protein is present as a tetramer (Marston *et al*., 1995). This is to ensure that, under normal conditions and without DNA damage insults, MDM2 will not cause a complete elimination of cellular p53, and p53 (and MDM2) will remain at basal level (reviewed in Zhang and Wang, 2000). MDM2 acts on p53 in two ways. Firstly, by binding to p53 transactivation domain TAD1, thus masking p53 from its

transcriptional machinery leading to inhibition of p53 to transcribe its target genes. Secondly, MDM2 acts as an E3 ubiquitin ligase to ubiquitinate p53 and translocate p53 from the nucleus to the cytoplasm in a RING domain-dependent manner, thus subjecting p53 for proteosomal degradation (Shadfan *et al*., 2012). The C-terminal part of p53 as well as the oligomerisation domain was shown to be important for MDM2-targeted degradation (Kubbutat *et al*., 1998). This might be due to the presence of multiple lysine residues, which serve as sites for MDM2-directed ubiquitination (Kubbutat *et al*., 1998). Change of cysteine to alanine (C462A) in the knockin mutation of the MDM2 RING finger shows that the physical interaction between MDM2 and p53 is not sufficient to regulate p53 but is co-modulated by MDMX, the MDM2 family member (Anderson and Apella, 2010). p53 activation involves uncoupling it from its main negative regulators, MDM2 and MDM2 homologue MDMX (Marine *et al.*, 2007). Inhibition and/or degradation of MDM2 and MDMX is needed for a rapid accumulation of p53 protein and its activation as transcription factor (review in Toledo and Wahl, 2006; Meek, 2009). In addition, a small reduction in MDM2 can significantly increase p53 activity (Brown *et al*., 2009; Khoury *et al*., 2011).

p53 protein degradation is mediated by the ubiquitin-proteosome pathway which involves a system of enzymes that conjugate multiple ubiquitin chains to lysines in the targeted protein. Polyubiquitinated proteins are then degraded by the 26S proteosome. More importantly, MDM2 protein functions as the E3 ligase that ubiquitinates p53 protein for proteosome degradation (Honda *et al*., 1997; Michael and Oren, 2003). p53 ubiquitination may serve not only as a degradation tag, but also as a subcellular relocalisation tag. After p53 mono-ubiquitination by MDM2, p300 can catalyse poly-ubiquitination of mono-ubiquitinated p53 and promote p53-protein degradation (Grossman *et al*., 2003). Li and colleagues reported that the different levels of MDM2 protein mediate either mono-ubiquitination of p53 protein resulting from low levels of MDM2 protein or poly-ubiquitination of p53 protein due to higher levels of MDM2 protein (Li *et al*., 2003), possibly indicating that MDM2 protein levels determines a ubiquitination switch (review in Wahl *et al*., 2005). Indeed, p53

mono-ubiquitination leads to subcellular localisation but not degradation through nuclear export of p53 protein, while p53 poly-ubiquitination leads to p53 proteosomal degradation having a chain of at least four ubiquitins attached (Li *et al*., 2003; Wahl *et al*., 2005). The ubiquitination of p53 on C-terminal lysines may alter the conformation of that region, in a manner that exposes the C-terminally located NES and thus, allows its efficient recognition by the nuclear export machinery (reviewed in Michael and Oren, 2003). It is believed that optimal p53 protein ubiquitination relates to p53 oligomerisation. The oligomerisation domain of p53 protein was found to be important for MDM2 binding and degradation (Kubbutat *et al*., 1998). The Ring finger domain, the N-terminal p53-binding domain as well as the central acidic domain of MDM2 are required for efficient p53 degradation (reviewed in Kubbutat *et al*, 1999; Argentini *et al*., 2001). Several p53 C-terminal lysine residues involved in acetylation are also subjected to MDM2-mediated ubiquitination (Lee and Gu, 2010; Pei *et al*., 2012). When these residues become acetylated in responding to cellular stress, p53 becomes stable and active because acetylation of p53 prevents it from being ubiquitinated and degraded by MDM2 (Pei *et al*., 2012).

The SUMO-1 protein inhibits MDM2 self-ubiquitination and increases the ubiquitin-ligase activity of MDM2 protein. DNA damage inhibits the activity of the SUMO-1 protein, thus indirectly stabilising p53 protein (Buschmann *et al*., 2000). The ubiquitin ligase activity of MDM2 can be inhibited by the binding of another tumour suppressor protein, $p14^{ARF}$ ($p19^{ARF}$ in mice), to the Ring finger domain of MDM2 which contains the E3 ligase activity and importantly is distinct from the p53 binding site (Honda and Yasuda, 1999). $p14^{ARF}$ is a direct inhibitor of the E3 ligase activity of MDM2 protein. $p14^{ARF}$ also sequesters MDM2 into the nucleolus, thus preventing nuclear export of p53 protein and in turn its degradation (Tao and Levine, 1999; Weber *et al*., 1999; Hu *et al*., 2012). Sequestration requires the combined nucleolar localisation signals (NoLS) of both ARF and MDM2 (Honda and Yasuda, 1999; Lohrum *et al*., 2000). The major consequence of MDM2-ARF interaction lies in the stabilisation and increased levels of transcriptionally active p53 protein in the nucleoplasm (Honda and Yasuda, 1999). A $p14^{ARF}$ –p53-MDM2 regulatory

loop exists since $p14^{ARF}$ stabilises p53 protein and elevated p53 protein in turn down-regulates $p14^{ARF}$ protein expression (Gu and Kruse, 2009).

Inhibition of cell growth and marked cell death are often observed in the absence of p53 regulation by MDM2, further emphasising the importance of the p53-MDM2 auto-regulatory loop in the control of cell growth and death (review in Alarcon-Vargas and Ronai, 2002). Figure 1.18 below summarises the control of cellular p53 protein levels by the p53-MDM2 negative autoregulatory feedback loop.

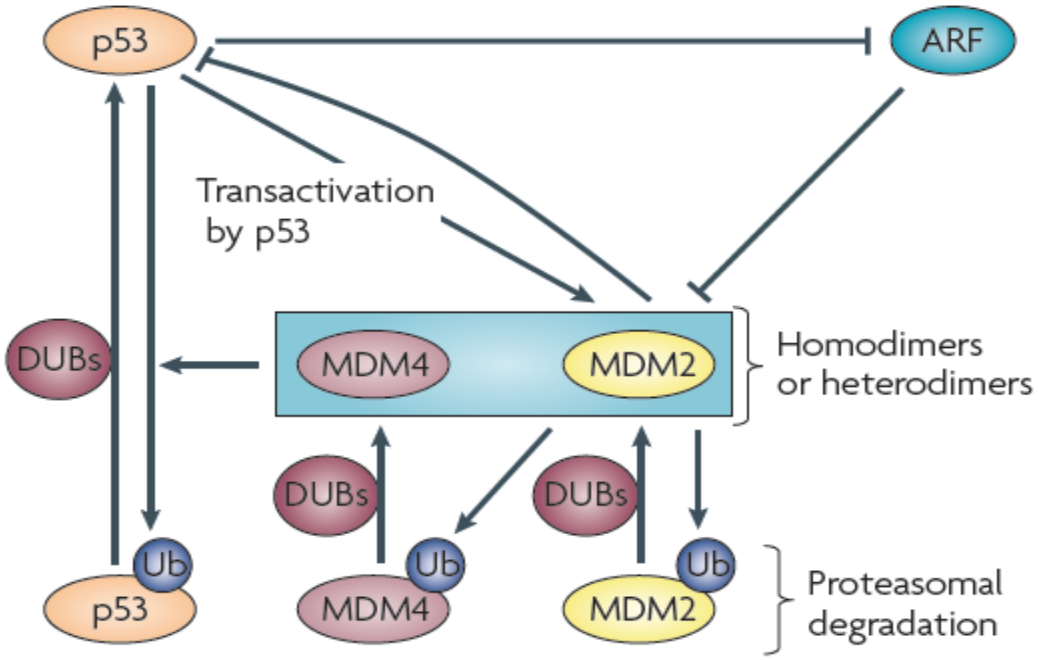

Figure 1.18. p53-MDM2 negative autoregulatory feedback loop controlling the p53 cellular protein levels. Ub, ubiquitin; DUBs, deubiquitinations (adapted from Brown *et al*., 2009).

1.12.3 Post-translational modifications of MDM2

Post-translational modifications can prevent the interaction between MDM2 and p53 proteins. It was shown that phosphorylation of serine 15 and/or serine 20 of p53 protein in response to DNA damage can disrupt its interaction with

MDM2 (Unger *et al*., 1999) and as a consequence p53 protein levels increase by preventing MDM2 from targeting p53 protein for cytoplasmic degradation.

MDM2 is also a phosphoprotein, hence its interaction with p53 may be regulated through phosphorylation not only of p53 as mentioned above but also of MDM2 protein itself (Barak and Oren, 1992; Momand *et al*., 1992). MDM2 protein has many putative phosphorylation sites for various protein kinases, with most of the modification sites clustered within the p53-binding domain and the central acidic domain (Hay and Meek, 2000). To date, the kinases implicated in MDM2 phosphorylation are DNA-dependent protein kinase (DNA-PK), ataxia telangiectasia-mutated kinase (ATM), mitogen-activated kinase (MAPK), AKT, p38 and cyclin-dependent kinases 1 and 2 (CDK1 and CDK2) (Mayo *et al*., 1997; Maya *et al*., 2001; Zhang *et al*., 2001; Zhu *et al*., 2002). Importantly, *in vitro* phosphorylation of MDM2 by DNA-PK abrogates its interaction with p53 protein (Mayo *et al*., 1997). MDM2 entry into the nucleus is dependent on its phosphorylation by the phosphatidylinositol 3-kinase (PI3K)/AKT kinases (Mayo and Donner, 2001; Gottlieb *et al*., 2002). AKT phosphorylation of MDM2 at Ser166 and Ser186 results in the translocation of MDM2 from the cytoplasm to the nucleus where it ubiquitinates p53 protein and mediates its degradation (Mayo *et al*., 2002; review in Meek 2004) while abrogation of the PI3K/Akt pathway by overexpression of PTEN and PI3K inhibitor LY294002 and withdrawal of survival signalling inhibits phosphorylation of these residues and blocks MDM2 entry into the nucleus. PTEN tumour suppressor gene product inactivates AKT but mutated PTEN can constitutively increase MDM2 activity in tumour cells (Mayo *et al*., 2002; review in Meek 2004). Ser166/186 phosphorylation of MDM2 also abrogates the interaction between MDM2 and its negative regulator ARF. The induction of MDM2 by the PI3K/Akt pathway results in increased p53 turnover, inhibition of p53 transcriptional activities and inhibition of p53-mediated apoptosis (Mayo and Donner, 2001; Zhou *et al*., 2001; Mayo *et al*., 2002; Ogawara *et al*., 2002). Thr216 phosphorylation of MDM2 reduces the MDM2-p53 interaction and augments the MDM2-ARF association. Ser17 phosphorylation of MDM2 disrupts MDM2-p53 protein-protein interactions. However, S17A mutant of

MDM2 effectively inhibited p53-mediated transactivation. Thr216 phosphorylation thus synergises with Ser17 phosphorylation to maximise p53 induction (review in Meek and Knippschild, 2003).

Phosphorylated MDM2 inhibits p53 degradation (review in Meek and Knippschild, 2003; Meek, 2004). MDM2 phosphorylated at serine 395 by ATM inhibits MDM2-mediated degradation of p53 protein. MDM2 serine 395 phosphorylation blocks nuclear export of p53 protein by MDM2 protein and increases p53 stability. Dephosphorylation of this residue does not interfere with MDM2-mediated ubiquitination of p53 protein but abolishes p53 degradation. Phosphorylated MDM2 at serines 386, 395, 425 and 428 and at threonine 419 cooperatively stabilise p53 protein by preventing its poly-ubiquitination. Likewise, MDM2 phosphorylation at serine 407 by ATR inhibits p53 nuclear export. In response to DNA damage, ATM activates downstream c-Abl kinase by direct phosphorylation, which then phosphorylates MDM2 at tyrosines 276 and 394 (Goldberg *et al*., 2002; Dias *et al*., 2006). Phosphorylation of MDM2 at tyrosine 276 increases MDM2 binding to its negative regulator ARF which protects p53 protein by re-localisation of MDM2 to the nucleolus (Dias *et al*., 2006; Waning *et al*., 2010). Ser267 of murine MDM2 (Ser269 in human MDM2) was mainly phosphorylated by CK2 while Ser258 was a minor CK2 target (Hjerrild *et al*., 2001). Phosphorylated Ser267 by CK2 occurs physiologically which regulates p53 turnover by MDM2.

Upon DNA damage, ATM is activated and phosphorylates MDM2 at Ser394 (human Ser395) resulting in inactivation of MDM2 ubiquitin ligase activity, thus increases p53 levels and tumour suppressive activities by inducing apoptosis, thereby inhibiting tumour formation in mouse models (Gannon *et al*., 2012; Li and Wahl; 2012). It is evident that phosphorylated MDM2 Ser394 regulates the amplitude and duration of the response to DNA damage at least in mice. Mouse knockin model of substitution of S394A (serine to alanine) which cannot be phosphorylated by ATM in response to DNA damage stimuli by ionising radiation/ irradiation (IR) causes MDM2 to ubiquitinate p53 leading its export to the cytoplasm and degradation in

proteasome and also inactivation of p53 tumour suppressive functions (cell cycle arrest, apoptosis). However, knockin mutant S394D (serine to aspartic acid) mice, mimicking constitutively phosphorylated serine, proved to be viable and showed inhibition of p53 nuclear export and degradation. These two mice models demonstrate that phosphorylation status of MDM2 Ser394 impact p53 protein levels and its tumour suppressive functions in response to DNA damage *in vivo* (Gannon *et al*., 2012; Li and Wahl; 2012).

Dephosphorylation of some or all of these residues (Ser240, 242, 260, 262) reduces MDM2-mediated degradation of p53 protein and consequently promotes p53 accumulation (review in Meek and Knippschild, 2003). Wip1, a phosphatase, dephosphorylates MDM2 at Ser395 and MDMX at Ser403, increasing their stability thus inactivating p53 tumour suppressive activities (Lu *et al*., 2008; Zhang *et al*., 2009; Pei *et al*., 2012).

MDM2 was sumoylated at Lys136, 146, 182 and 185 *in vivo* by Sumo E3 ligases Ubc9, PIAS1 and PIASxβ and by these enzymes and RanBP2 *in vitro*. ARF has been shown to stimulate MDM2 sumoylation (Xirodimas *et al*., 2002) as ARF blocks the ubiquitination of p53 by MDM2. Mutant Ubc9 protein results in inhibition of MDM2 sumoylation in a dominant negative manner, leading to increased MDM2 ubiquitination and decreased p53 ubiquitination thus favours p53 accumulation. UV radiation has been shown to inhibit MDM2 interaction with Ubc9 and subsequent loss of MDM2 sumoylation (Buschmann *et al*., 2001(a); review in Meek and Knippschild, 2003). HAUSP (USP7), a deubiquitinase, deubiquitinates p53 as well as MDM2 and MDMX, resulting in their stability (Kruse and Gu, 2009; Brady and Attardi, 2010; Wang and Jiang, 2012). The protein DAXX regulates HAUSP-mediated MDM2 deubiquitination (Tang *et al*., 2006; Kruse and Gu, 2009). Figure 1.19 depicts important post-translational events of Mdm2 protein. Thus, in a nutshell, posttranslational modifications to both p53 protein and MDM2 protein can influence the stabilisation and activation of the p53 pathway.

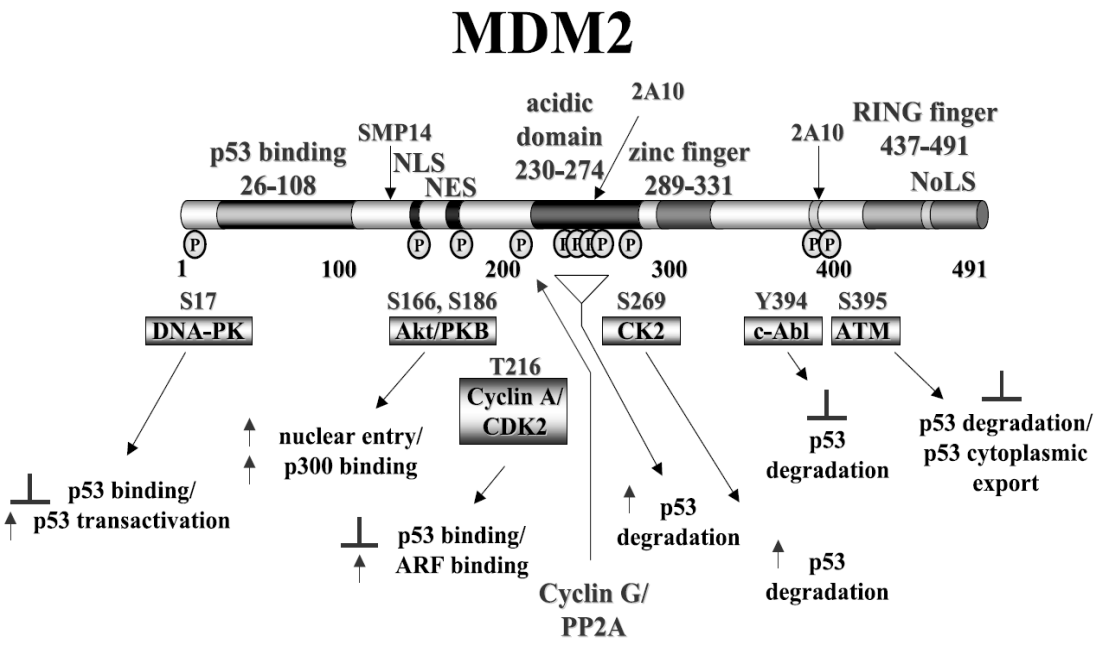

Figure 1.19. Posttranslational modification events of MDM2 protein. NLS, Nuclear localisation signal; NES, Nuclear export signal (adapted from Meek and Knippschild, 2003).

1.12.4 p53-MDM2 inhibitors

Nutlin is the first non-peptidic molecule that interrupts the p53-MDM2 binding. Nutlin induces apoptosis via p53 transcription-dependent and transcription-independent mechanisms (Vassilev *et al*., 2004; Khoo *et al*., 2014). Other drugs such as MI-219 (Shangary *et al*., 2008), RG7388 (Ding *et al*., 2013) and MI-888 (Zhao *et al*., 2013) result in tumour regression in xenograft model of human cancer cells with wildtype p53. These drugs induced p53 accumulation and apoptosis (Khoo *et al*., 2014). RG7112, the second-generation nutlin, potently killed cancer cells. It also promoted cell cycle arrest and apoptosis in human tumour xenograft (Tovar *et al*., 2013).

1.13 MDMX (MDM4), an MDM2 homologue

A structural analogue of MDM2 called MDMX, also known as MDM4, was first discovered by Shvarts and colleagues in 1996 (Shvarts *et al*., 1996), however, it is much less characterised in comparison to MDM2. p53 is postulated to be

constitutively active, meaning it inherently binds to DNA but is repressed by its major negative regulators MDM2 and MDMX complex (Kruse and Gu, 2009; Zilfou and Lowe, 2009). MDMX, like MDM2, binds to p53 protein via its N terminus thus inhibits p53-mediated transcription activation *in vitro* (Shvarts *et al*., 1996; Finch *et al*., 2002). However, MDMX itself is not an E3 ligase, nor does it have nuclear localisation and export signals, thus it does not mediate degradation of p53 protein and it depends on MDM2 for nucleocytoplasmic shuttling (Shvarts *et al*., 1996; Finch *et al*., 2002; Pei *et al*., 2012; Shadfan *et al*., 2012). In contrast to MDM2, MDMX is not a p53 target gene but it is an essential negative regulator of p53 like MDM2 (Marine *et al*., 2007). MDMX mainly functions to regulate p53 transcriptional activity instead of p53 protein levels since it is not an ubiquitin ligase itself, therefore it cannot ubiquitinate p53 and target p53 for proteosomal degradation (Toledo *et al*., 2006). Sharp *et al.* (1999) have shown that MDMX interferes with MDM2-mediated degradation of p53 protein resulting in increased levels of p53 protein (Jackson and Berberich, 2000). MDMX also prevents MDM2 degradation and translocation of p53 protein to the cytoplasm by MDM2 (Stad *et al*., 2000 & 2001). In the absence of MDMX, MDM2 is relatively ineffective in down-regulating p53 protein due to its extremely short half-life (Gu *et al*., 2002). However, at appropriate ratio between MDMX and MDM2, MDMX renders MDM2 protein sufficiently stable to function at its optimal potential for p53 degradation by interacting through their RING finger domains (Tanimura *et al*., 1999; Gu *et al*., 2002; Wang and Jiang, 2012). Heterodimerisation between MDM2 and MDMX through their Ring finger domains stimulate the ubiquitin ligase activity of MDM2 (Kawai *et al*., 2007). These findings show the mutual interplay between MDM2 and MDMX to achieve maximal inhibition of p53 protein and are consistent with the studies on deletion of either gene eliciting embryonic lethality, although occurring later in embryogenesis in *Mdmx*$^{-/-}$ mice than in *Mdm2*$^{-/-}$ mice, thus showing their distinct activities (Review in Wahl *et al*., 2005; Brady and Attardi, 2010). p53^{QS} knockin mutant mice were unable to interact with both MDM2 and MDMX and this might be the reason for the embryonic lethality reminiscent to MDM2 null mice resulting from uncontrolled p53-mediated apoptosis (Johnson *et al*., 2005; Kruse and Gu, 2009). The relative level of MDM2 and MDMX determines p53

stability and activity (Pei *et al*., 2012). Figure 1.20 below shows a comparison between MDM2 and MDMX protein structures.

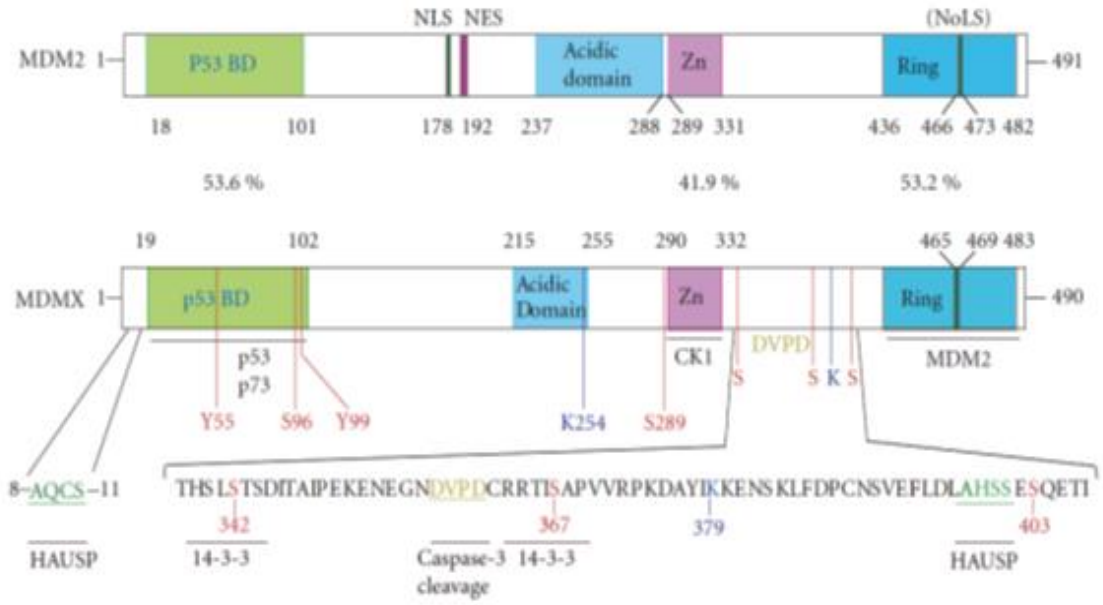

Figure 1.20. A schematic diagram showing MDMX protein structure in comparison with MDM2 protein (adapted from Lenos and Jochemsen, 2011).

MDMX is either amplified or overexpressed in numerous tumours and tumour-derived cell lines, where it coexists with elevated levels of wt p53 (Ramos *et al*., 2001; Pei *et al*., 2012). It has also been shown that MDMX overexpression stabilises and increases both p53 and MDM2 proteins levels (Sharp *et al*., 1999; Stad *et al*., 2000). Importantly, *mdmx* knock-out in mice leads to p53-dependent embryonic lethality (Parant *et al*., 2001). However, the mdmx null phenotype is completely rescued by deletion of the p53 gene, thereby resembling some of the major characteristics of MDM2 (Parant *et al*., 2001). Similar to p53, MDMX is ubiquitinated and degraded by MDM2 in stress conditions (Tang *et al*., 2006). Like MDM2, MDMX is also phosphorylated at multiple sites in DNA damage response but their impact on MDMX regulation remains to be determined (Meek & Hupp, 2010; Waning *et al*., 2010). Figure 1.21 below shows important phosphorylation events of MDM2 and MDMX

proteins. To summarise, MDM2 and MDMX protein levels and their interactions with p53 are in part important determinant for p53 activity (Toledo and Wahl, 2006; Fu *et al*., 2012).

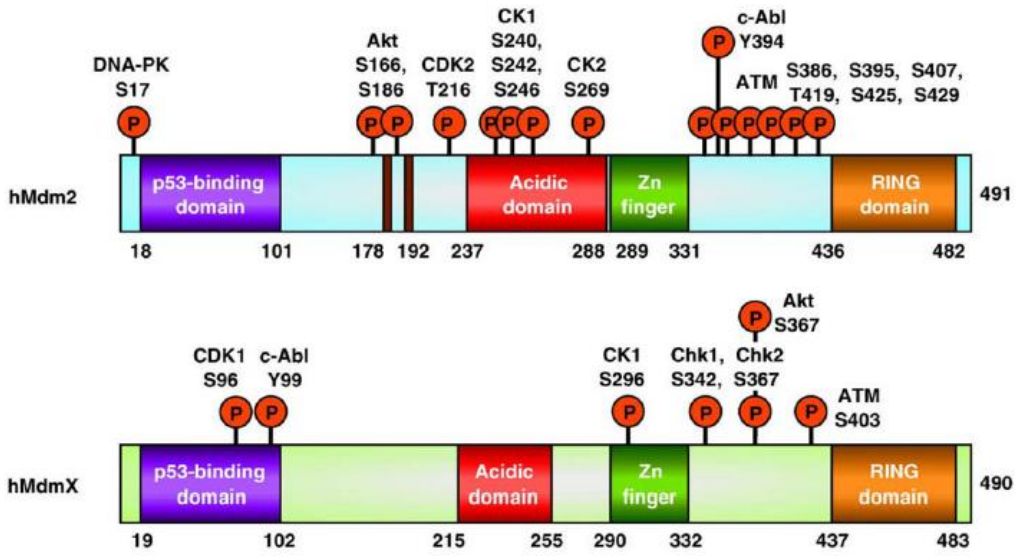

Figure 1.21. Phosphorylation events of MDM2 and MDMX proteins (adapted from Wade *et al*., 2010).

1.14 Protein nitration

Having discussed the well characterised modifications of p53 protein (phosphorylation and acetylation), this section will now discuss a modification type poorly characterised for p53 protein i.e. protein nitration. Protein nitration is a covalent post-translational protein modification resulting from the reaction of proteins with nitrating agents. The nitrating agents attack phenol groups on protein to produce nitrophenol. Nitrotyrosine has been the most well characterised amino acid due to the availability of nitrotyrosine antibodies which are not species-specific and also due to a historical role of phosphotyrosine in signal transduction. Tryptophan and phenylalanine are also nitrated but are poorly characterised. Figure 1.22 shows the location of tyrosine (Y), tryptophan (W) and phenylalanine (F) in a p53 amino acid sequence while

Figure 1.23 shows the positions of tyrosine (Y), tryptophan (W) and phenylalanine (F) in the p53 main domains. Following are examples of a precursor of nitrating agent nitric oxide and one commonly known and most important nitrating agent peroxynitrite.

1.14.1 Precursor of nitrating agents

Nitric Oxide ($NO^{\bullet}$)

Nitric oxide ($NO^{\bullet}$) is one of several free radicals ubiquitous in our body which are generated by normal physiological process, including aerobic metabolism and inflammatory responses, to kill tumour cells and to eliminate invading bacteria or parasites (reviewed by Hussain *et al*, 2003). Free radicals have been shown to cause DNA damage, and protein structural and functional modifications (reviewed by Wiseman and Halliwell, 1996). $NO^{\bullet}$ is a small hydrophobic molecule and freely permeable to cell membranes without through channels or receptors where there is no barrier between $NO^{\bullet}$ and membranes (Muntane and De la Mata, 2010).

Figure 1.22. Location of tyrosine (Y), tryptophan (W) and phenylalanine (F) in a p53 amino acid sequence.

MEEPQSDPSVEPPLSQETFSDLWKLLPENNVLSPLPSQAMDDLMLSPDDIEQWFTED

PGPDEAPRMPEAAPRVAPAPAAPTPAAPAPAPSWPLSSSVPSQKTYQGSYGFRLGFL

HSGTAKSVTCTYSPALNKMFCQLAKTCPVQLWVDSTPPPGTRVRAMAIYKQSQHMTE

VVRRCPHHERCSDSDGLAPPQHLIRVEGNLRVEYLDDRNTFRHSVVVPYEPPEVGSD

CTTIHYNYMCNSSCMGGMNRRPILTIITLEDSSGNLLGRNSFEVRVCACPGRDRRTE

EENLRKKGEPHHELPPGSTKRALPNNTSSSPQPKKKPLDGEYFTLQIRGRERFEMFR

ELNEALELKDAQAGKEPGGSRAHSSHLKSKKGQSTSRHKKLMFKTEGPDSD

Figure 1.23. Positions of tyrosine (Y), tryptophan (W) and phenylalanine (F) in p53 main domains.

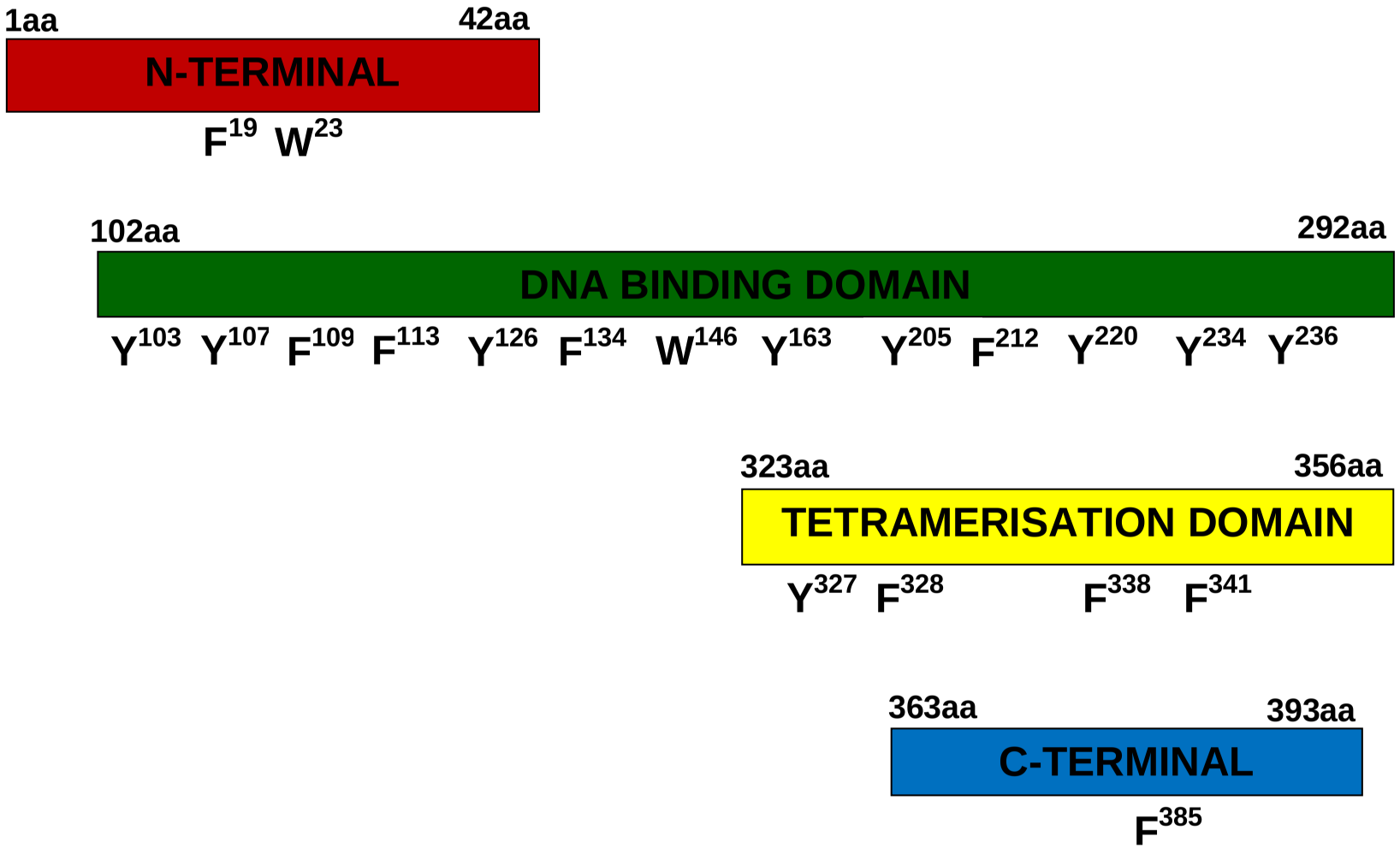

$NO^{\bullet}$ is a physiological intracellular and intercellular messenger that is produced by several kinds of cells, including endothelial cells, nerve cells, and macrophages (Bredt and Snyder, 1994). $NO^{\bullet}$ serves as a key signalling molecule virtually in every physiological process in the human body (review in Choudhari, 2013). In 1987, $NO^{\bullet}$ was identified as the endothelium-derived relaxing factor (EDRF) that increases blood flow and decreases blood pressure through vasodilatation of blood vessels as well as being important in platelet inhibition (Ignarro *et al*., 1987; Palmer *et al*., 1987; Muntane and De la Mata, 2010). $NO^{\bullet}$ also acts as a neurotransmitter in certain types of nerves. $NO^{\bullet}$ is also an important component of host-defense and innate immunity against invading microorganisms. $NO^{\bullet}$ is enzymatically generated *in vivo* from the amino acid L-arginine by a family of enzymes called $NO^{\bullet}$ synthases (NOS) which metabolise arginine into citrulline with the formation of $NO^{\bullet}$. Oxygen and NADPH are necessary cofactors in this process (Muntane and De la Mata, 2010). $NO^{\bullet}$ is widely and actively synthesised, thereby virtually every type of mammalian cell is under the influence of $NO^{\bullet}$ (reviewed in Schmidt and Walter, 1994). Figure 1.24 shows a schematic diagram which simplifies the *in vivo* generation of $NO^{\bullet}$.

Figure 1.24. *In vivo* Generation of Nitric Oxide ($NO^{\bullet}$).

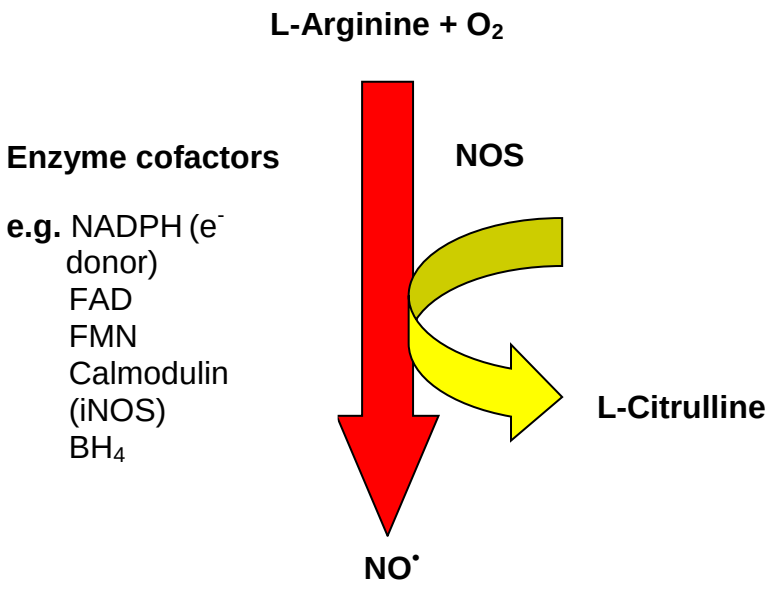

Two functional classes of the NOS are constitutive and inducible forms. In human and mouse, 3 different genes, namely nNOS (NOS1), eNOS (NOS3) and iNOS (NOS2), named according to their activity or the tissue type in which they were first described, encode for $NO^{\bullet}$ synthases isolated from neurons, endothelial cells and inducible NOS isoforms, respectively (Leon *et al*., 2008; Muntane and De la Mata, 2010). nNOS and eNOS isoforms are constitutively expressed and dependent on elevated concentrations of calcium and calmodulin for activity (Nathan and Xie, 1994; Muntane and De la Mata, 2010). The inducible NOS (iNOS) isoforms are generally independent of increases in calcium concentrations and can produce consistent, high concentrations of $NO^{\bullet}$ upon exposure with cytokines and lipopolysaccharide (Nathan and Xie, 1994; Hussain and Harris, 2007; Muntane and De la Mata, 2010). iNOS produces prolonged and at much higher concentrations of $NO^{\bullet}$ in the cell compared to the other two isoforms.

$NO^{\bullet}$ takes part in diverse biological signalling such as cell-mediated immune responses, cytotoxicity, regulation of cell death (apoptosis), cell motility, vasodilation and neurotransmission (Moncada *et al.,* 1991; Leon *et al*., 2008). $NO^{\bullet}$ is a highly reactive free radical species as it has an unpaired electron and participates in many chemical reactions. It is lipophilic and neutrally charged in vertebrates that allows it to diffuse freely in and out of cell membranes thousands of times a second and is able to diffuse of more than several hundred microns (Lancaster, 1994). $NO^{\bullet}$ has a very short biological half-life of a few seconds (1-10 s in biological fluids) and can interact with many molecules resulting in it is rapidly utilised close to where it is synthesised. $NO^{\bullet}$ reactions with a number of targets such as haem groups, cysteine residues and iron and zinc clusters help to explain the wide range of roles it plays. $NO^{\bullet}$ can activate p53, which acts as anti-carcinogenic agent, or it can be mutagenic and increase cancer risk, implicating it in carcinogenesis (Goodman *et al*., 2004). $NO^{\bullet}$, as a mediator of inflammation, was also shown by Hussain *et al* (2004) to suppress tumourigenesis where lymphomas developed more rapidly in p53-/-NOS2-/- or p53-/-NOS2+/- mice than in p53-/-NOS2+/+ mice. In addition, sarcomas and lymphomas developed faster in p53+/-NOS2-/- or p53+/-

NOS2+/- than in p53+/-NOS2+/+ mice. Thus, $NO^{\bullet}$ has a double-edged role where it plays both beneficial and detrimental roles (Schmidt *et al*, 1992) depending on its concentration, its chemical fate, the microenvironment and the rate and location of its production (Mayer and Hemmens, 1997). It has been demonstrated that lower concentrations of $NO^{\bullet}$ stimulates growth and is anti-apoptotic while higher levels induce cell cycle arrest, senescence and/or apoptosis (reviewed in Thomas *et al*., 2008).

1.14.2 Cytotoxic effects of $NO^{\bullet}$

$NO^{\bullet}$ oxidation products rather than $NO^{\bullet}$ itself most likely mediate its cytotoxic effects. Thus, $NO^{\bullet}$ does not directly attack DNA instead it is due to its oxidation derivatives such nitrogen oxide and dinitrogen trioxide (Wink *et al*., 2005). Activated macrophages which produce both $NO^{\bullet}$ and superoxide inactivate mitochondria in tumour cells through the action of peroxynitrite formed from the reaction of these two free radicals (Radi *et al*., 1994). The rate constant between reaction of $NO^{\bullet}$ and superoxide to produce peroxynitrite is 6.7×10^{9} M^{-1}. s^{-1} The rate of superoxide reacting with antioxidant superoxide dismutase (SOD) is ~2×10^{9} M^{-1}. s^{-1}. (Huie and Padmaja, 1993). This shows that $NO^{\bullet}$ reacts with superoxide faster than SOD reacts with superoxide indicating that $NO^{\bullet}$ outcompetes endogenous SOD for superoxide.

The detrimental effects of $NO^{\bullet}$ in diseases are mostly mediated by peroxynitrite (review in Pacher *et al*., 2007), produced through diffusion-limited reaction between $NO^{\bullet}$ and superoxide radicals. 5-10 nM $NO^{\bullet}$ will activate guanylate cyclase to produce cGMP which then activates cGMP-dependent kinases in the target tissue which controls intracellular calcium levels to modulate various processes in the target tissues (review in Pacher *et al*., 2007). Excessive and upregulated $NO^{\bullet}$ synthesis can cause pathophysiological conditions such as cancer (review in Choudhari *et al.*, 2013) but downregulation also can cause Cardiovascular disease (CVD).

$NO^{\bullet}$ is cytostatic and/or cytotoxic to tumour cells. $NO^{\bullet}$ produced from macrophages, Kupffer cells, natural killer cells and endothelial cells acts to kill tumour cells i.e. showing tumouricidal activity (Li *et al*., 1991; Lechner *et al*., 2005). $NO^{\bullet}$ can either inhibit (cytostatic/cytotoxic or tumouricidal effects) or stimulate (tumour promoting effects by promoting tumour growth and proliferation) carcinogenesis. When cancer has occurred, $NO^{\bullet}$ seems to be pro-tumoural rather than anti-tumoural because cancer cells cannot achieve $NO^{\bullet}$ concentrations sufficient to cause tumour cell cytotoxicity (review in Korde-Choudhari *et al*., 2012; review in Choudhari *et al*., 2013).

1.14.3 Nitric oxide ($NO^{\bullet}$) role in apoptosis

$NO^{\bullet}$-mediated apoptosis depends on the dose of $NO^{\bullet}$ and the type of cells used. $NO^{\bullet}$ has been shown to be able to both induce apoptosis for instance by activating p53 and to protect from apoptosis in different cell types. $NO^{\bullet}$ was reported to be a potent activator of p53 protein. p53 accumulation and activation by $NO^{\bullet}$ is reported through $NO^{\bullet}$-induced down-regulation of MDM2 protein which is accompanied by a corresponding reduction in the rate of p53 ubiquitination which precedes the rise in p53 protein (Wang *et al*., 2002). Wang *et al* (2003) have shown that $NO^{\bullet}$ promotes p53 nuclear retention and inhibits MDM2-mediated p53 nuclear export. $NO^{\bullet}$ induces phosphorylation of p53 on serine 15 resulting in increased p53 stability and its nuclear accumulation due to attenuated nuclear-cytoplasmic shuttling and failure of ubiquitin-mediated degradation of phosphorylated p53 protein (Schneiderhan *et al*., 2003; Lee *et al*., 2006). It was found that $NO^{\bullet}$ markedly enhances the ability of ionising radiation to elicit apoptotic killing of neuroblastoma cells expressing cytoplasmic wild-type p53 (Wang *et al*., 2003). These findings imply that $NO^{\bullet}$ can sensitise tumour cells to p53-dependent apoptosis. Thus, $NO^{\bullet}$ donors may potentially increase the effectiveness of chemotherapy or radiotherapy for treatment of all types of cancer in general. The followings are some descriptions of the involvement of $NO^{\bullet}$ and peroxynitrite in apoptosis in other pathological conditions in the human body.

In Parkinsons disease, $NO^{\bullet}$ donor SNP in SN4741 dopaminergic neuron cells nitrated and activated protein kinase C (PKC)-δ which then phosphorylated p53 at Ser-15 resulting in the increased p53 protein stability leading to $NO^{\bullet}$-induced apoptosis (Lee *et al*., 2006). In RAW 264.7 macrophages, $NO^{\bullet}$ induced apoptosis through upregulation of mitochondrial manganese superoxide dismutase (MnSOD; SOD2) and down-regulation of cytosolic copper zinc superoxide dismutase (CuZnSOD; SOD1) at both mRNA and protein levels. Down-regulation of CuZnSOD resulted in $NO^{\bullet}$ cytotoxicity and CuZnSOD over-expression inhibited macrophage from apoptosis mediated by $NO^{\bullet}$ cytotoxicity (Brockhaus and Brune, 1999).

In Type 1 diabetes mellitus (T1DM), proinflammatory cytokines such as tumour necrosis factor alpha (TNF-α) and interferon gamma (IFN-γ), produced by activated lymphocytes and macrophages, activate iNOS expression in β cells resulting in increased $NO^{\bullet}$ levels and induction of apoptosis (Eizirik *et al*., 1996; review in Quitana-Lopez *et al*., 2013). Mechanisms of $NO^{\bullet}$-mediated β-cell apoptosis involve DNA damage by $NO^{\bullet}$ oxidative derivatives leading to DNA strand breaks which then activate p53 resulting in the induction of pro-apoptotic effector genes such as the Bcl-2 family of proteins BAX, NOXA, PUMA and FAS, caspases and cytochrome (review in Quitana-Lopez *et al*., 2013). It has been demonstrated that $NO^{\bullet}$ shows an anti-apoptotic effect at low concentration in several systems, including β cells (Sata *et al*., 2000; Ozaki *et al*., 2002; Dash *et al*., 2003).

Both exogenously supplied ($NO^{\bullet}$ donors) and endogenously produced $NO^{\bullet}$ (iNOS induction) induce apoptosis in megakaryocytes. Treatment with peroxynitrite also promotes apoptosis in these cells (Battinelli and Loscalzo, 2000). Stably transfected human *Bcl-2* inhibits apoptosis after exposing RAW 264.7 macrophages with $NO^{\bullet}$ donors such as S-nitrosoglutathione (GSNO) and spermine-NO whereas these $NO^{\bullet}$ donors induce internucleosomal DNA cleavage in a dose-dependent manner in parental RAW 264.7 and neomycin control-transfected cells. iNOS expression via response to lipopolysaccharide

and interferon-γ also induce apoptosis in parental RAW 264.7 and neo controls within 24 hr incubation (Mebmer *et al*., 1996).

Cytokine IL-1β-induced iNOS expression stimulates $NO^{\bullet}$-dependent apoptosis in cardiac fibroblasts resulting from DNA damage and through p53-dependent apoptotic pathway. IL-1β induces iNOS expression and $NO^{\bullet}$ generation is associated with increased expression of p53 and Bax, enhanced caspase-3 activity and induction of apoptotic cell death (Tian *et al*., 2002).

1.14.4 The nitrating agent Peroxynitrite

Peroxynitrite ($ONOO^-$) is a strong cytotoxic oxidant and nitrating species which is formed by the extremely rapid, diffusion-limited reaction between two parent free radicals, $NO^{\bullet}$ and superoxide anion ($O_2^{\bullet -}$) (Pacher *et al*., 2007; Szabo *et al*., 2007; Jones, 2012). While the sources of $NO^{\bullet}$ are mainly from the various isoforms of NOS, $O_2^{\bullet -}$ is mainly formed from the mitochondrial electron transport chain, NADPH oxidase and xanthine oxidase (review in Liaudet *et al*., 2009). The intermediate product peroxynitrous acid (peroxynitrite conjugate acid) then easily decomposes at physiological pH to the highly reactive and toxic hydroxyl radical ($HO^{\bullet}$) and nitrogen dioxide ($NO_2^{\bullet}$) (Beckman *et al*, 1990) as shown in the following equations:

$NO^{\bullet} + O_2^{\bullet -} \longrightarrow ONOO^-$ (peroxynitrite)
$ONOO^- + H^+ \longrightarrow ONOOH$ (peroxynitrous acid)
$ONOOH \longrightarrow HO^{\bullet} + NO_2^{\bullet}$

Peroxynitrite has a relatively short half-life of around 10 ms but despite this it can easily crosses biological membranes and interact with target molecules within one or two cell diameters (Pacher *et al*., 2007; Szabo *et al*., 2007: review in Liaudet *et al*., 2009). Peroxynitrite has been associated with both deleterious and beneficial effects (Moro *et al*, 1994; Vinten-Johansen, 2000). Peroxynitrite plays important roles in virtually all diseases affecting

humans (review in Pacher *et al*., 2007). The physiological effects of peroxynitrite are dependent on the environment in which the anion is present and also on its concentrations (Mallozzi *et al*., 1997; Ronson *et al*., 1999; Ma *et al*., 2000). In comparison to $NO^{\bullet}$, peroxynitrite is toxic to cells, killing *E. coli* at micromolar concentrations (Zhu *et al*, 1992). Peroxynitrite can cause oxidative damage to protein, lipid and DNA, mainly resulting in structural and functional inactivation of these molecules leading to dysfunction of multiple cellular processes (Pacher *et al*., 2007; Szabo *et al*., 2007: review in Liaudet *et al*., 2009). Peroxynitrite can react with DNA by attacking both deoxyribose and by direct oxidation of purines and pyrimidines which consequently result in DNA damage (Salgo *et al*, 1995). Peroxynitrite can damage DNA through modifications in nucleobases by modifying guanine to 8-nitroguanine, modification in sugar-phosphate backbone resulting in DNA strand breaks and inactivation of DNA repair enzyme (Burney *et al*., 1999; Niles *et al*., 2006).

Peroxynitrite levels are low in normal physiological conditions controlled by endogenous antioxidant defences (Radi *et al*., 2002(a) & 2002(b)). A moderate flux of prolonged peroxynitrite production will result in oxidative damage to host cellular constituents which in turn can result in the dysfunction of critical cellular processes, dysregulation of cell signalling pathways and mediation of cell death via both apoptosis and necrosis (Schroeder *et al*., 2001). Thus, peroxynitrite plays a role in the development of many pathological processes *in vivo*. Peroxynitrite generated under inflammatory conditions can inactivate NOS by oxidatively modifying its haem group (Huhmer et al., 1997) which contributes to a negative feedback regulation between these two molecules. Ischiropoulos *et al* (1992) have found that peroxynitrite nitrates the ortho positions of tyrosine residues on proteins to form nitrotyrosine. Nitrotyrosine has been found in human pathologies (Kaur and Halliwell, 1994) and is a useful marker for peroxynitrite formation *in vivo*. Peroxynitrite may change protein structure and function by tyrosine nitration of the protein. Inactivation of proteins will lead to impaired cell signal transduction and loss of normal physiological functions which are two main aspects of peroxynitrite-mediated cytotoxicity. Proteomic analyses have shown that nitration is a highly

selective process and specific to certain tyrosine residues in a small number of proteins. It has been shown that tyrosine nitration is found in at least 50 human diseases and more than 80 in animal models of diseases (Greenarce and Ischiropoulos, 2001). Tyrosine nitration is associated with significant loss of function. For instance, mitochondrial Mn-SOD lost its enzyme activity upon nitration, the first protein found to be nitrated *in vivo*. Nitration of a single tyrosine residue (Tyr-34) causes complete enzyme inactivation (MacMillan-Crow and Thompson, 1999).

1.14.5 Peroxynitrite and apoptosis

Peroxynitrite activates apoptotic program through permeabilisation of mitochondria outer membrane (MOMP), which depends on the cell type and experimental conditions. This apoptotic program is initiated by the efflux of a variety of proapoptotic signalling molecules which promote apoptosis via both caspase-dependent and caspase-independent mechanisms (review in Pacher *et al*., 2007). MOMP is triggered by pore formation within the outer membrane by pro-apoptotic proteins (e.g. Bax, Bak and Bid) which are inhibited by anti-apoptotic Bcl-2 and Bcl-XL proteins or by mitochondrial permeability transition (MPT) (review in Armstrong, 2006). Other than directly targeting mitochondria, peroxynitrite modulates various cell signalling processes such as MAPKs (mitogen-activated protein kinases) and Akt (protein kinase B). It has been shown *in vitro* that peroxynitrite activates MAPKs resulting in apoptosis but on the other hand it significantly inhibits Akt, a serine-threonine protein kinase which functions to promote survival or limit apoptosis in various stress conditions including oxidative stress (Martindale and Holbrook, 2002). Peroxynitrite inactivates Akt through nitration and inactivation of PI3K (phosphatidylinositol 3-kinase) which is upstream of Akt (Hellberg *et al*., 1998; El-Remessy *et al*., 2005; review in Parcher *et al*., 2007). However, an increased level of active Akt masks the pro-apoptotic effects of peroxynitrite (El-Remessy *et al*., 2005; Shacka *et al*., 2006). Thus, there is a link between Akt inhibition and apoptosis in such experimental conditions.

1.14.6 Peroxynitrite in phosphotyrosine and nitrotyrosine signalling

Protein nitration by peroxynitrite results in inhibition of cell signalling processes dependent on tyrosine phosphorylation (Shi *et al*., 2007; Leon *et al*., 2008; Singh and Gupta, 2011), however, in other instances, peroxynitrite also promotes phosphotyrosine signaling. Peroxynitrite nitration of tyrosine residue can impair cell signalling relying on tyrosine phosphorylation and tyrosine nitration is capable of blocking downstream signalling *in vitro*. The dysregulation of tyrosine phosphorylation by peroxynitrite may affect various crucial cellular functions. Paradox to inhibition of phosphotyrosine-dependent signalling, peroxynitrite has been shown to activate phosphotyrosine-dependent signalling in various cell types. For instance, peroxynitrite strongly activates MAPK family members, consequences from the upstream activation of various protein-tyrosine kinases, which further supports a positive tyrosine phosphorylation by peroxynitrite. (Pacher *et al*, 2007). The up-regulation of phosphotyrosine signalling by peroxynitrite at a relatively low concentration is transient and reversible, which is typical in any signalling processes. A higher concentration of peroxynitrite leads to irreversible nitrotyrosine formation and downregulation of phosphotyrosine signalling indicating that nitration and phosphorylation processes compete at high concentrations of peroxynitrite. Up-regulated phosphotyrosine signalling can be either due to inhibited phosphotyrosine phosphatases (PTPs) or activated phosphotyrosine kinases (PTKs). Peroxynitrite has been shown to regulate these two events (review in Pacher *et al*., 2007).

1.15 Relationships between nitric oxide/peroxynitrite, inflammatory processes and carcinogenesis

An imbalance between production in reactive oxygen species (ROS) and their elimination by anti-oxidant mechanisms leads to oxidative stress. Sustained oxidative stress significantly damages important biomolecules, cell structure and functions and may induce mutation and neoplastic initiation (Fang *et al*., 2009; Khandrika *et al*., 2009; Reuter *et al*., 2010). Oxidative stress has been

linked to carcinogenesis by increasing DNA mutation and DNA damage, inactivation of DNA repair enzymes, genomic instability and cell proliferation (Figure 1.25). Persistent oxidative or nitrosative stresses can result in chronic inflammation which ultimately lead to most chronic diseases such as cancer, diabetes, cardiovascular, pulmonary and neurological diseases (Visconti & Grieco, 2009; Reuter *et al*., 2010).

Chronic infection and inflammation have long been known as risk factors for human cancers at various sites (reviewed by Ohshima and Bartsch, 1994), for instance, Hepatitis B virus infection and hepatocellular carcinoma; and chronic inflammatory bowel disease and colon carcinoma. The cytotoxic effect of $NO^{\bullet}$ has been attributed to its reactive nitrogen species such as peroxynitrite. Reactive nitrogen and oxygen species generated in inflamed tissues can cause injury to target cells and also damage DNA. $NO^{\bullet}$ and its derivatives can react directly with various enzymes and proteins to either activate or inhibit their function by reacting with their thiol groups (Li *et al*., 1997; Mohr *et al*., 1999), oxidizing SH groups, complexing with metal ions, or by reacting with tyrosine residues (reviewed by Henry *et al*., 1993). Overproduction of $NO^{\bullet}$ and its derivatives over a long period of time in inflamed tissues play a role in the multistage process of carcinogenesis (reviewed by Tamir and Tannenbaum, 1996; Muntane and De la Mata, 2010). eNOS is expressed in various cancers such as cervical, breast and central nervous system and the resulting $NO^{\bullet}$ is implicated in different cancer-related events including cell cycle, apoptosis, angiogenesis, invasion and metastasis (Ying and Hofseth, 2007; review in Choudhari *et al*., 2013). $NO^{\bullet}$ can act dichotomously either as tumour promoting or tumoricidal dependent on its timing, location, concentrations, the cell type, the redox state and the duration of exposure (review in Choudhari *et al*., 2013).

In the pathophysiology of inflammation, proinflammatory cytokines produced will induce iNOS expression resulting in an increased $NO^{\bullet}$ production. This $NO^{\bullet}$ is toxic to the cells by, i) oxidatively modifying nucleobases, mostly guanine resulting in 8-oxoguanine, ii) nitrating guanine to form 8-nitroguanine, iii) inactivating DNA repair enzymes e.g. OGG1, and iv)

inhibiting p53 through tyrosine nitration. As $NO^{\bullet}$ levels are increased in mitochondria during inflammation, superoxide levels are also increased within the mitochondrial matrix resulting in an increased in peroxynitrite levels. Peroxynitrite then nitrates and inhibits Mn-SOD, thus inhibits the breakdown of superoxide produced in mitochondria which in turn results in increased peroxynitrite formation (MacMillan-Crow and Thompson, 1999; review in Pacher *et al*., 2007). Peroxynitrite inhibits most electron transport chain components through mechanisms such as oxidation of cysteine residue, nitration of tyrosine and damage of iron sulphur centres (Radi *et al*., 2002(a) & (b)). Peroxynitrite also has genotoxic potential, where prolonged peroxynitrite-oxidative and -nitrative stress in cell cultures and purified DNA mimicking inflammatory conditions/chronic infections, can increase the risk of cancer, consequently leading to cancer development. Similar to $NO^{\bullet}$, peroxynitrite can cause oxidative DNA damage and formation of DNA strand breaks.

1.16 Nitration of p53 protein and the cellular response to genotoxic stress

Nitration of tyrosine residues in various proteins and enzymes has been associated with inactivation of their functions. Several studies have shown that tyrosine nitration is a selective process as not all proteins and not all tyrosine residues of a protein are nitrated *in vivo* (Gow *et al*., 1996; Leon *et al*., 2008). Protein 3-nitrotyrosine has been found in a number of human and animal models of diseases (reviewed by Ischiropoulos, 1998). Nitrotyrosine (NTYR) is present in a variety of human tissues with significantly high levels in diverse human diseases such as Alzhemier's disease (Good *et al*., 1996) and inflammatory bowel disease (Singer *et al*., 1996) as well as in animal models of diseases such as liver and skin carcinogenesis (Robertson *et al*., 1996; Ahn *et al*., 1999).

p53 protein nitration is not extensively studied and to date there are only a few relevant studies concerning p53 nitration (25 articles on current PubMed search). Here are some of the landmark findings of the studies carried out by

independent groups of investigators. Forrester *et al* (1996) and Chazotte-Aubert *et al* (2000) have suggested that p53 functions may be regulated post-translationally by tyrosine nitration, thus indicating the existence of a close interaction between $NO^{\bullet}$ and p53. It has been shown that p53 accumulates in cells incubated with $NO^{\bullet}$-releasing compounds (Forrester *et al*., 1996; Calmels *et al*., 1997; Hofseth *et al*., 2003) which cause DNA damage. p53 protein is also post-translationally modified upon exposure to $NO^{\bullet}$ resulting in the inhibition of cellular growth (Hofseth *et al*., 2003; reviewed in Hussain *et al*., 2003). In human gliomas, p53 is nitrated at Tyr327 within the tetramerisation domain, promoting p53 oligomerisation, nuclear accumulation and transcriptional activation without p53 Ser15 phosphorylation (Cobbs *et al*., 2001; Yakovlev *et al*., 2010). p53 is also transcriptionally inactivated in human glioblastoma cells upon exposure to nitric oxide donor 3-morpholinosyndonimine-1 (SIN-1) (Cobbs *et al*., 2003; Kim *et al*., 2011). On the other hand, overexpression of WT p53 transcriptionally transrepresses iNOS mRNA expression through inhibition of the iNOS promoter. These data are consistent with the hypothesis of a negative feedback loop in which $NO^{\bullet}$-induced DNA damage induces wild-type (WT) p53 accumulation and subsequent down-regulation of $NO^{\bullet}$ synthesis through p53-mediated transrepression of NOS2 gene expression through inhibition of NOS2 promoter. (Forrester *et al*., 1996; Ambs *et al*., 1997) (Figure 1.25).

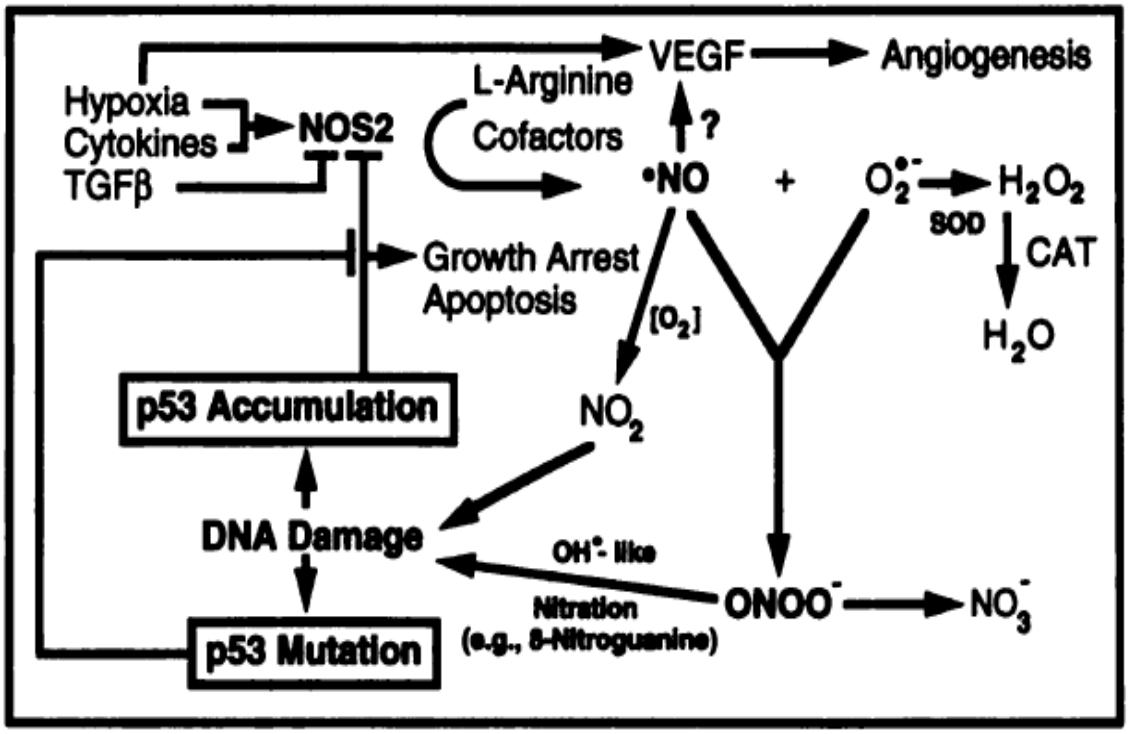

Figure 1.25. Negative feedback loop between p53 and NO• (adapted from Ambs *et al*., 1997).

NO• has also been shown to induce the accumulation and activation of p53 protein through downregulation of MDM2 protein resulting in reduced p53 ubiquitination by MDM2 protein. However, prolonged exposure to NO• resulted in the increased levels of MDM2 protein owing to the upregulation the *mdm2* gene by active p53 protein resulting in the reduced level of p53 protein due to MDM2-mediated degradation of the p53 protein (Wang *et al*., 2002; Muntane and De la Mata, 2010). In addition, S-nitrosylation of cysteine 77 residue of MDM2 by NO inhibits MDM2 binding to p53 protein and this reaction is reversible (Schonhoff *et al*., 2002; Kim *et al*., 2011). This clearly shows that MDM2 plays a central role in the p53 and NO• signalling pathways (Figure 1.26).

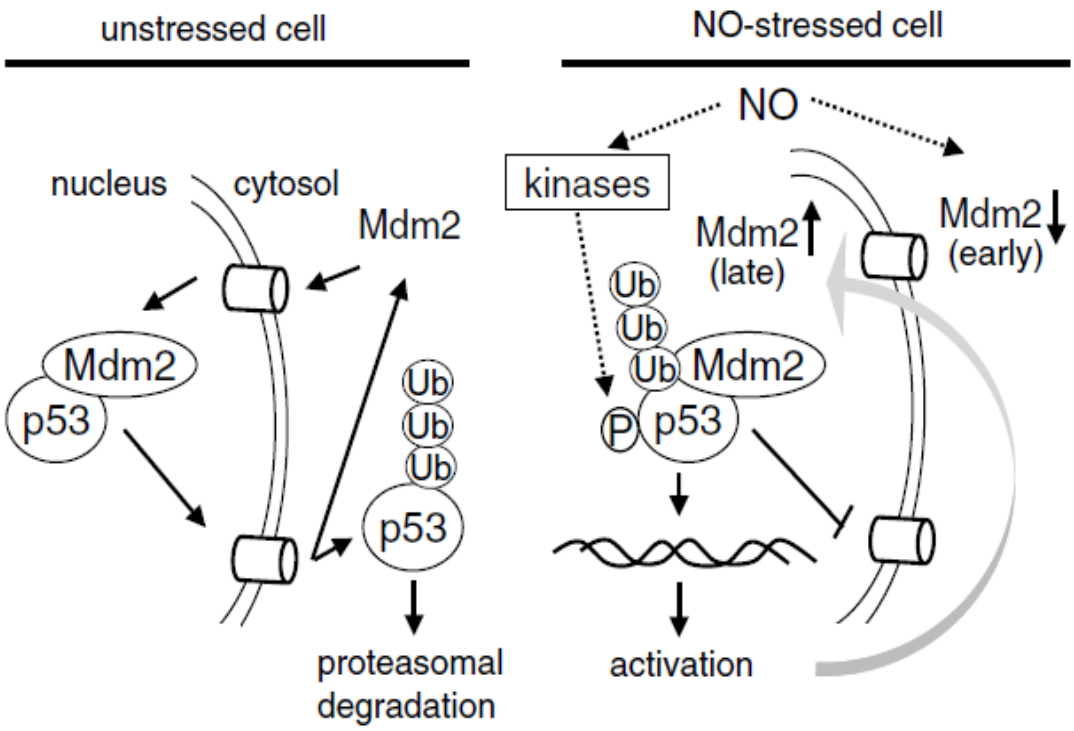

Figure 1.26. Nuclear accumulation of p53 protein in NO-stressed cells in comparison to its low levels in unstressed cells (adapted from Brune, 2003).

Calmels *et al* (1997) have shown that high levels of $NO^{\bullet}$ cause profound structural changes of p53 from a wild type to a mutant conformation with loss of DNA binding activity and subsequently impairing its tumour suppressor functions. These could be due to a direct reaction of $NO^{\bullet}$ with the zinc atom in p53 protein or from oxidation of cysteine residues (Calmels *et al*., 1997). Chazotte-Aubert *et al.* (2000) have demonstrated that incubation of MCF-7 cells, expressing WT p53 protein, with an $NO^{\bullet}$ donor results in nitration of tyrosine residues in p53 protein, which has been suggested to be a possible mechanism that could contribute to p53 functional impairment by $NO^{\bullet}$. However, p53 protein isolated from control cells has been shown only to contain low levels of nitrotyrosine. Thus, there is a possibility that p53 functions are partly regulated by nitration of its tyrosine residues by $NO^{\bullet}$ and its derivatives (Chazotte-Aubert *et al*., 2000) but the evidence is weak. The

possibility that these effects are due to nitration of tryptophan and phenylalanine residues have not yet been explored. In another study by Hofseth *et al.* (2003), they found that p53 protein was post-translationally modified by $NO^{\bullet}$ from donor drugs, leading to an increase in p53 transcriptional targets such an MDM2, p21(WAF1) and an increased expression of pro-apoptotic proteins such as Bax together with a down-regulation of Bcl-2 and a G(2)M cell cycle checkpoint. They also found that inducible $NO^{\bullet}$ synthase protein levels were positively correlated with p53 serine 15 phosphorylation levels. This proves a pivotal role of $NO^{\bullet}$ in the induction of cellular stress and in the activation of a p53 response pathway by genotoxic stress.

AIMS AND OBJECTIVES OF THE STUDY

This project is initiated a few aims and objectives as stated below:

1) In this thesis, we ask whether nitration of p53, a less common form of post-translational modification, will result in stabilisation of the p53 protein just like in phosphorylation and acetylation?

2) Before starting to embark on the nitration of p53 protein, the optimal conditions for nitration has to be determined using BSA since it is highly pure and easily nitrated as it contains 19 tyrosine residues. So a preliminary study is to make a lot of p53 protein both soluble and insoluble from the pT7.7Hup53 construct expressed in *E. coli* expression system BL21(DE3) strain. Both forms of p53 protein will be purified by a series of purification systems. The purified p53 protein will then be nitrated with different doses of nitrating agent peroxynitrite and the levels of nitrated p53 and total p53 proteins will be determined by Western blotting.

3) GST-MDM2 fusion protein (a.a 1 to 188) from the pGEX-2T-MDM2 construct along with its control protein GST from the pGEX-2T construct are to be expressed in *E. coli* expression system BL21 strain followed by a single-step purification. The purified GST-MDM2 protein is to be nitrated with peroxynitrite at different doses to see nitration effects on its stability and on the protein-protein interactions of GST-MDM2 protein with p53 protein.

4) *In vitro* nitration of the MCF-7 cell line harbouring wild-type *p53* gene with NO donor GSNO will be examined to see whether nitration induces stability of wild-type p53 protein.

5) *In vitro* nitration of mutant p53 protein in the PANC-1 cell lysates will be carried out. This cell line facilitates the analysis of nitrated p53 protein since it is abundant in mutant p53 protein.

6) Cell lysates from various cell lines with different p53 status, such as HCT116 p53+/+ (wt-p53), HCT116 p53-/- (null-53), PANC-1 (mut-p53) and SW620 (mut-p53), will either be directly nitrated with peroxynitrite before being immunoprecipitated for p53 protein by anti-p53 antibody or first be immunoprecipitated for p53 protein before being nitrated with peroxynitrite in order to determine nitration effects on nitro-p53 protein levels and also on total p53 protein levels.

CHAPTER 2

MATERIALS AND METHODS

2.1 General reagents

All reagents for microbiological media (e.g. agar, yeast extract and tryptone) were obtained from Oxoid, Ltd, Basingstoke U.K. General laboratory chemicals were obtained from Sigma, Fissons plc and BDH, unless stated to the contrary.

2.2 Microbiological media

The following descriptions were for preparing a litre of the stated media.

i. Luria-Bertani (LB) Media

LB media contained 10 g of bacto-tryptone, 5 g of bacto-yeast extract, 10 g of NaCl and was adjusted to pH 7.0 using 5 M NaOH and then sterilised by autoclaving. Solid LB agar contained the same ingredients supplemented with 20 g of agar. Where required LB media was supplemented with filter sterilised ampicillin to a final concentration of 50 µg/ml.

2.3 Buffers

i. Phosphate Buffered Saline (PBS)

1 litre PBS was prepared by dissolving 8.0 g of NaCl, 0.2 g of KCl, 1.44 g of Na_2HPO_4 and 0.24 g of KH_2PO_4 in distilled water and the pH was adjusted to 7.4 with 0.1 M HCl and then sterilised by autoclaving.

2.4 Bacterial strains

The bacterial strains used in this work are shown in Table 2.1, and with the exception of strain BL21 and derivatives thereof, are all derived from *Escherichia coli* K12. The *E. coli* strain BL21 was derived from *Escherichia coli* strain B. Where *E. coli* strains have been used to over-express human proteins, prior approval was obtained from the local Genetically Manipulation Safety Committee at the University of Bradford, and the regulatory body notified.

Table 2.1: *E. coli* bacterial strains used in this work

Strain	Genotype	Source
BL21	F^- *ompT* *hsdS*$_B$ ($r_B^- m_B^-$) *gal* *dcm*	Studier & Moffat, 1986.
BL21(DE3)	*hsdS* gal (*λc*I*ts*857 *ind*1 Sam7 *nin*5 *lac*UV5-T7 *gene 1*	Studier & Moffat, 1986.
BL21(DE3) Star	F^-*ompT* *hsdS*$_B$ (r_B^- m_B^-) *gal dcm* *rne*131 (DE3)	Invitrogen.
DH5	*sup*E44 *hsdR*17 *recA*1 *endA*1 *gyrA*96 *thi*-1 *relA*1	Meselson and Yuan 1968; Hanahan 1983
DH5α	*sup*E44 *Δlac* U169 (*ø*80*lacZ* *Δ*M150 *hsdR*17 *recA*1 *endA*1 *gyrA*96 *thi*-1 *relA*1	Hanahan 1983; Bethesda Research Laboratories.

Two host *E. coli* strains namely BL21(DE3) and BL21(DE3)Star were used in the over-expression of p53 protein. These two genetic backgrounds are deficient in both *lon* and *ompT* proteases, thus proteins are not degraded by these proteases. BL21(DE3)Star has additional feature where it is also RNAse E deficient, designed to increase protein expression by preventing RNA from being degraded. The two host *E. coli* strains are λDE3 bacteriophage lysogens of the BL21 strain that carry the gene for the T7 RNA polymerase, under the control of the isopropyl β-D-thiogalactopyranoside (IPTG)-inducible promoter P_{tac}.

2.5 Plasmid vectors and derivatives

Below is a list of plasmids used in this work.

Table 2.2: Plasmids used in this work

Plasmid	Characteristic	Source
pT7.7	Amp^R, a MCS under the regulation of a T7 promoter.	Tabor and Richardson, 1985; Studier *et al*., Methods of Enzymology (1990).
pT7.7Hup53	Amp^R, with the human p53 gene under the regulation of a T7 promoter.	Midgley *et al*., J. Cell Science (1992).
pGEX-2T	Amp^R, a MCS under the regulation of a P_{tac} promoter.	Pharmacia
pGEX-2T-MDM2	Amp^R, with the human N-terminal MDM2 (a.a. 1-188) gene under the regulation of a P_{tac} promoter.	Bottger *et al*., Oncogene (1996); Bottger *et al*., J. Mol. Biol. (1997).

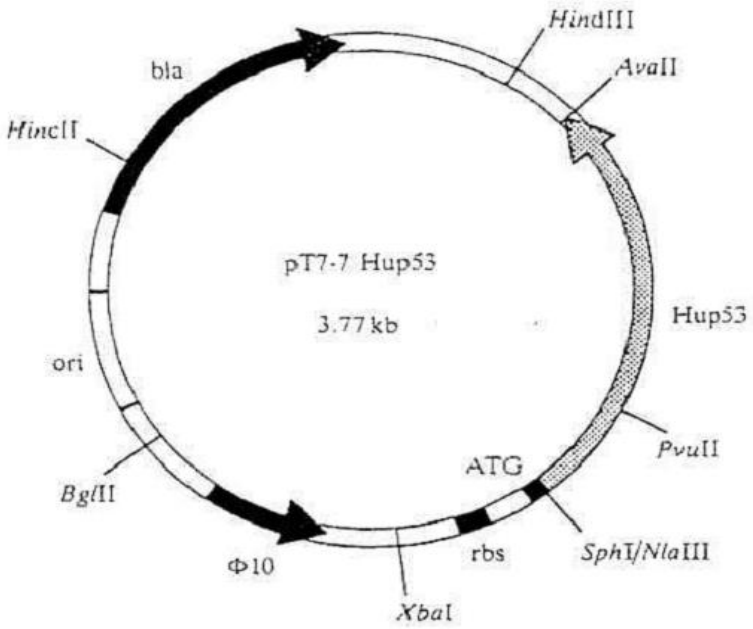

Figure 2.1. Map showing the pT7.7 plasmid with an inserted full length human *p53* gene (Midgley *et al*., 1992).

2.6 Purification of plasmid DNA

Plasmid DNA was purified using the alkaline lysis method of Birnboim and Doly (1979) and Ish-Horowicz and Burke (1981) in the form of Qiagen mini-kits to prepare plasmid DNA from 10 ml overnight cultures. 1.5 ml of culture was transferred into 2 separate sterile microcentrifuge tubes and the cells were pelleted by centrifugation at 13,000 rpm for 2 minutes in a benchtop MSE micro-centrifuge at room temperature, and the supernatants were then discarded. The cell pellets were resuspended with 250 µl Buffer P1 (100 µg/ml RNase, 50 mM Tris-HCl, 10 mM EDTA, pH 8.0) and following resuspension 250 µl of Buffer P2 (200 mM NaOH, 1% w/v SDS) was added and the tube inverted 4-6 times to gently mix the two solutions until the solution became viscous and slightly clear. 350 µl of Buffer N3 (5.6 M KAc, pH 4.8) was the added and the tubes were again inverted several times to mix. At this point, a cloudy precipitate was noticed which was followed by centrifugation for 10 minutes at 13,000 rpm at room temperature in a benchtop micro-centrifuge. A compact white pellet was formed. The supernatants were then applied to 2 separate QIAprep spin columns and centrifuged at 13,000 rpm for 30-60 seconds at room temperature in a benchtop micro-centrifuge. The flow-through was discarded. The columns were then washed by adding 0.75 ml Buffer PE (1.0 M NaCl, 50 mM MOPS, 15% v/v ethanol, pH 7.0) and centrifuged as before for 30-60 seconds. The flow-through was discarded again and the columns were centrifuged for an additional 1 minute to remove residual wash buffer. The QIAprep columns were then placed in 2 autoclaved 1.5 ml micro-centrifuge tubes. To elute DNA, 5 µl Buffer EB (10 mM Tris-HCl, pH 8.5) was added to the centre of each QIAprep spin column, let stand for 1 minute and finally centrifuged for 1 minute at 13,000 rpm at room temperature in a benchtop micro-centrifuge.

2.7 DNA transformation using Calcium chloride ($CaCl_2$)

2.7.1 Preparation of competent cells

A single colony was inoculated into 5 ml of sterile LB medium in two 15 ml Falcon tubes. One Falcon tube with 5 ml of un-inoculated LB medium was

used as negative control. The cultures were grown overnight at 37^{o}C with moderate shaking at 180 rpm in an orbital shaker. 100 µl of each overnight culture was inoculated into 10 ml of fresh LB medium in 2 separate sterile 50 ml Falcon tubes. They were grown at 37^{o}C with moderate shaking at 180 rpm in an orbital shaker until an OD_{600nm} of 0.3 to 0.4 (mid-log phase). The cells were then centrifuged for 5 min at 5000 rpm at 4^{o}C. The supernatants were decanted and each pellet was re-suspended in 5 ml ice cold 0.1 M $CaCl_2$ solution. The mixtures were held on ice for 20 min and then centrifuged again as before. The supernatants were discarded and each pellet was re-suspended in 2.5 ml ice cold 0.1 M $CaCl_2$. The re-suspended pellets were kept on ice for 10 min and followed by centrifugation at 5000 rpm for 5 min at 4^{o}C. Finally, the pellets were re-suspended in 1 ml ice-cold 0.1 M $CaCl_2$ solution.

2.7.2 Transformation of competent cells

200 µl competent cells were transferred into 2 separate 1.5 ml sterile Eppendorf tubes followed by addition of 5 µl plasmid DNA. The tubes were inverted gently to mix, and then placed on ice for 30 min. To facilitate the uptake of plasmid DNA, the cultures were heat shocked at 42^{o}C for 45 sec, followed by incubation on ice water for 5 min. 1 ml of LB medium was added to each tube and then incubated 45 min at 37^{o}C with shaking at 180 rpm in an orbital shaker to allow expression of β-lactamase. 200 µl of cells were plated on selective LB agar plates supplemented with 50 µg/ml of ampicillin. Another aliquot of cells were also plated on LB plates without ampicillin to demonstrate cell viability. The cells were then spread evenly on the agar plates using sterile spreaders. The plates were left to dry for a few minutes, inverted and then incubated overnight at 37^{o}C.

2.8 Small scale expression of p53 protein

Overnight cultures of pT7.7Hup53 transformed strains were prepared by inoculating 5 ml of LB broth supplemented with 50 µg/ml of ampicillin, in separate sterile 15 ml Falcon tubes with a colony of each strain from their

respective selection agar plates. The cultures for each transformed strain were prepared in duplicates. One 15 ml Falcon tube containing 5 ml of un-inoculated LB broth supplemented with 50 µg/ml ampicillin served as a negative control. The next day, 20 ml of ampicillin selective LB broth was then inoculated with 200 µl of each overnight culture in separate sterile 50 ml Falcon tubes. The cultures were grown to early mid-log phase (OD_{600nm} 0.15-0.20) at 37^{o}C at 180 rpm in a shaking incubator and growth was monitored every 30 min. Once the OD_{600nm} of the culture was within 0.15-0.20, isopropyl β-D-thiogalactopyranoside (IPTG) was added to the final concentration of 1 mM to one of each pair of the cultures. The other tubes where no IPTG was added served as negative controls. The growth was continued to 4 hours with growth monitored at 30 min time points. At each time point 1 ml of culture was removed and OD_{600nm} reading was taken. The cells were pelleted by centrifugation at 13,000 rpm for 2 min at room temperature in a micro-centrifuge. The supernatants were discarded and the pellets were then re-suspended in 100 µl of 2x SDS gel-loading buffer (50 mM Tris-HCl, pH 6.8, 2% w/v SDS, 0.1% w/v bromophenol blue, 10% v/v glycerol) and 100 mM dithiothreitol (DTT) which was added fresh. Cells were then stored at -20 ^{o}C for future use.

2.9 Analysis of p53 expression

p53 protein expression was analysed by two methods namely SDS-PAGE and Western Blot as described below.

2.9.1 SDS-PAGE of protein samples

The electrophoresis analysis of protein was carried out in a one-dimensional SDS-Polyacrylamide gel Bio-Rad Mini Protean II vertical slab apparatus which was assembled according to the manufacturer's instructions. Table 2.3 shows the concentration of acrylamide to be used according to the size of the desired protein. Since p53 protein falls within 16-68 kDa, therefore we used 10% acrylamide to prepare resolving gels throughout this work.

Table 2.3: Concentrations of acrylamide and its corresponding linear range of separation on SDS-polyacrylamide gels (adapted from Molecular Cloning by Sambrook, 1989)

Acrylamide[a] concentration (%)	Linear range of separation (kDa)
15	12-43
10	16-68
7.5	36-94
5.0	57-212

[a]Molar ratio of bisacrylamide:acrylamide is 1:29

Tables 2.4 and 2.5 below are recipes for preparing 10% resolving and 5% stacking gels, respectively:

Table 2.4: Solutions for preparing 10% resolving gels for Tris-glycine SDS-polyacrylamide gel electrophoresis (adapted from Molecular Cloning by Sambrook, 1989)

Solution components	Component volumes (ml) per gel mold volume of:			
	5 ml	10 ml	15 ml	20 ml
H_2O	2.6	5.3	7.9	10.6
30% (v/v) acrylamide mix	1.0	2.0	3.0	4.0
1.5 M Tris (pH 8.8)	1.3	2.5	3.8	5.0
10% (w/v) SDS	0.05	0.1	0.15	0.2
10% (w/v) ammonium persulfate (APS)	0.05	0.1	0.15	0.2
TEMED (density 0.775 g/ml)	0.004	0.008	0.012	0.016

Table 2.5: Solutions for preparing 5% stacking gels for Tris-glycine SDS-polyacrylamide gel electrophoresis (adapted from Molecular Cloning by Sambrook, 1989)

Solution components	Component volumes (ml) per gel mold volume of:			
	1 ml	2 ml	3 ml	4 ml
H_2O	0.68	1.4	2.1	2.7
30% (v/v) acrylamide mix	0.17	0.33	0.5	0.67
1.0 M Tris (pH 6.8)	0.13	0.25	0.38	0.5
10% (w/v) SDS	0.01	0.02	0.03	0.04
10% (w/v) ammonium persulfate (APS)	0.01	0.02	0.03	0.04
TEMED (density 0.775 g/ml)	0.001	0.002	0.003	0.004

Upon preparation of the samples they were loaded directly onto an SDS-PAGE gel or stored at -20^{o}C. Stored samples were thawed to room temperature and later sonicated three times for approximately 10 seconds each on ice at maximum amplitude (using a MSE 150 Watt Ultrasonic Disintegrator - MK2) to degrade chromosomal DNA. Samples were then boiled for 5 min. 20 µl of each sample and 10 µl of a pre-stained protein molecular weight marker (MBI Fermentas, Sunderland, UK) were loaded onto a polyacrylamide gel consisting of a 10% w/v resolving gel and a 5% w/v stacking gel. The gel was run at 90 V for about 2 hours in Tris-Glycine running buffer (25 mM Tris, 250 mM glycine, 0.1% w/v SDS) at pH 8.3.

For protein bands visualisation, the gel was first incubated in Destain I (50% v/v methanol, 10% v/v acetic acid in distilled water) for approximately 10 minutes and the protein bands were stained with Coomassie Blue (50% v/v methanol, 10% v/v acetic acid and 0.2% w/v Coomassie Brilliant Blue R-250, Sigma, in distilled water) for about 10 minutes. Following this the gel was destained overnight with Destain II (7.5% v/v methanol, 10% v/v acetic acid in distilled water).

2.9.2 Western Blotting

Samples were run on a 10% w/v resolving gel and a 5% w/v stacking gel as 2.9.1 above. The gel was removed and briefly soaked in transfer buffer (39 mM glycine, 48 mM Tris base, 0.037% w/v SDS and 20% v/v methanol) before being placed onto a nitrocellulose membrane, which were then sandwiched with a Whatmann 3MM filter paper and absorbent sponges on either side. The proteins were transferred using an electro-transfer apparatus (BioRad), at 90 V in transfer buffer for about 3 hours.

After several trials, the following optimal conditions were obtained for immuno-detection of the p53 proteins. Following protein transfer, the membrane was removed from the transfer apparatus and incubated in blocking buffer solution (5% w/v non-fat dry milk powder in PBS/0.2% v/v

Tween 20) for 1 hour at room temperature with gentle agitation to block non-specific binding to the membrane. The membrane was then washed 3 times, 5 minutes each in PBS/0.2% v/v Tween 20. It was then incubated with the stated primary mouse monoclonal antibody at 1:1000 dilution in 1% w/v bovine serum albumin (BSA, Sigma) dissolved in PBS/0.2% v/v Tween 20 overnight at 4^{o}C. The unbound primary antibody was removed by washing 3 times, 5 min each with PBST solution with constant shaking. A secondary horseradish peroxidase (HRP) conjugated rabbit anti-mouse IgG antibody (1:1000 dilution) (DAKO, Ely, UK) prepared in 1% w/v BSA in PBS buffer was added and left for at least 1 hour at room temperature. Three further washes of 5 minutes each were carried out using PBST with continuous shaking. The membrane was then immersed in 1:1 mix of ECL solutions I (1 ml of 250 mM luminol in DMSO, 0.44 ml of 90 mM p-coumaric acid in DMSO, 10 ml of 1M Tris-HCl pH 8.5 in 100 ml total volume) and ECL solution II (64 µl of 30 % v/v H_2O_2, 10 ml of Tris-HCl pH 8.5 in 100 ml total volume) sufficient to cover the membrane surface for 1 minute, and then blotted to remove excess solution before being wrapped in cling film. The membrane was then exposed to Kodak X-ray film for a defined period of time in the dark, and then developed before a final wash by immersion in water.

2.10 Large scale expression and solubilisation of human p53

A 10 ml of overnight culture was used to inoculate 1 litre of LB broth supplemented with 50 µg/ml of ampicillin. The culture was incubated at 37^{o}C with shaking at 180 rpm until its OD_{600nm} reached 0.15 - 1.2 (early mid-log phase). IPTG was added to a final concentration of 1 mM and growth was continued with aeration for a further 4 hours. Cells were harvested by centrifugation at 8000 rpm for 10 minutes at 4^{o}C in a Beckmann Avanti J25 centrifuge in JLA 10,500 rotor. The pellet of induced cells was re-suspended twice in 20 ml ice-cold 50 mM Tris-HCl pH 8.0 and was finally resuspended in 0.66 ml/g of cells of lysis buffer (10% w/v sucrose, 50 mM Tris-HCl pH 8.0) and stored at -80^{o}C until further use.

After thawing at 25^{o}C, 15 µl of 10 mg/ml lysozyme and 20 µl of 5 M NaCl per ml of cells was added to the cells, mixed gently and kept on ice for 45 minutes. The cells were warmed at 37^{o}C for 1 minute, the tube rolled gently and then returned to ice-water. The cells were sonicated 3 times at maximum amplitude on ice for approximately 30 seconds each until the cells became less viscous. The insoluble proteins including p53 were pelleted by centrifugation at 10,000 rpm at 4^{o}C for 10 minutes. At this stage, the supernatant which was assumed to contain 2% soluble p53 protein could be kept for further analysis. The pellet was then re-suspended in 5 ml of lysis buffer (50 mM Tris HCl pH 8.0, 2 mM EDTA, 10 mM NaCl, 1 mM PMSF, 0.5% v/v Triton-X100) and repelleted. The wash was repeated two times in order to obtain a firm pellet. The protein was solubilised in 5 ml of: 5 M guanidine hydrochloride, 50 mM Tris-HCl pH 8.0, 0.005% v/v Tween 80 by mixing gently by a rotating wheel at 4^{o}C (in a cold room) for 5 hours. The remaining insoluble material was pelleted as before. The supernatant was rapidly diluted to a final concentration of 1 M guanidine hydrochloride (20 mls of a mixture of 50 mM Tris-HCl pH 8.0, 0.005% v/v Tween 80, 2 mM reduced glutathione and 0.02 mM oxidised glutathione) and was mixed for a further 12-18 hours. Protein was then dialysed at 4^{o}C against 800 ml of the following buffers for at least 5 hours each:

i) 50 mM Tris-HCl pH 8.0, 300 mM NaCl, 0.005% v/v Tween 80
ii) 50 mM Tris-HCl pH 8.0, 250 mM NaCl, 0.005% v/v Tween 80
iii) 50 mM Tris-HCl pH 8.0, 200 mM NaCl, 0.005% v/v Tween 80
iv) 50 mM Tris-HCl pH 8.0, 150 mM NaCl, 0.005% v/v Tween 80

Any insoluble or precipitated protein was pelleted at 10,000 rpm for 20 minutes at 4 ^{o}C. 100 µl of the supernatant (dialysed protein) was taken and the same volume of 2x gel loading dye was added supplemented with 1/10 volume of DTT which was freshly added and kept at -20 ^{o}C before checking the protein purity on a SDS-PAGE gel. 10% v/v glycerol was added to the remaining dialysed protein and kept at -80^{o}C for future purification.

2.11 Purification of p53 protein dialysate

Several purification techniques were carried out in order get optimal conditions for purification in order to produce about 5 mg of purified p53 protein.

2.11.1 Purification of human p53 protein by ion-exchange chromatography by stepwise gradient

5 ml of dialysed human p53 protein from 2.10 above which was stored at -80^{o}C, was thawed and purified by ion-exchange chromatography (DEAE). 5 ml of DEAE-Sepharose was poured into a 25 ml empty column (manual purification process through gravity) and was equilibrated with Buffer A (50 mM Tris-HCl pH 8.0, 10% v/v glycerol, 0.1 mM EDTA, 1 mM DTT, 1 mM benzamidine, 0.1% v/v Triton-X100, 0.5 mM PMSF). The p53 protein was first diluted with 2 volumes of buffer A so that the final concentration of NaCl was 50mM. The diluted p53 lysate was then loaded onto the column in buffer A containing 50mM NaCl. 10 mls fractions of flow through (pre-washed) were collected. The washing step was followed where buffer A was loaded onto the column to remove unbound proteins and 10 ml fractions were again collected. After washing the column with buffer A, bound proteins were eluted from the column by a salt gradient ranging from 50 mM to 500 mM NaCl (in a step-wise manner). 1.5 ml fractions were collected and then analysed by a 10% (w/v) SDS-PAGE gel.

i. p53 concentration by TCA precipitation

To 900 µl of sample, 10 µl of 100% TCA to a final concentration of 10% v/v was added and left 30 minutes on ice. The mixture was pelleted by centrifugation at 13,000 rpm for 10 minutes and the supernatant was removed. The pellet was re-centrifuged, the supernatant discarded, and all traces of TCA were removed, followed by washing with absolute alcohol. A centrifugation was repeated as before and the pellet was drained and the alcohol was allowed to evaporate. 50 µl 1x SDS gel loading buffer was added. In case a yellow colour was obtained, the sample was neutralised

with 1 M Tris-HCl, pH 8.0 unadjusted until the dye turned blue. The proteins were then assayed by a 10% w/v SDS-PAGE gel.

2.11.2 Purification of human p53 protein by affinity chromatography

5 ml dialysed protein from pooled pellet from 6 litre cultures was subjected to heparin purification. The sample was first dialysed against 800 ml of Buffer B (10% v/v glycerol, 25 mM HEPES pH 8.0, 0.1 mM EDTA, 0.1 mM EGTA, 0.1% v/v Triton X-100, 5 mM DTT, 1 mM benzamidine, 0.5 mM PMSF) overnight at 4^{o}C in a cold room. A 1 ml Hi-Trap-Heparin Sepharose (Pharmacia Biotech Inc.) column was equilibrated with 20 ml buffer B. The dialysed lysate containing p53 was first diluted with Buffer B containing 50 mM NaCl and loaded onto the column by a pump connecting the sample and the column via a tubing. 1 ml fractions of flow-through was collected. The column was washed with 20 ml buffer B to remove unbound proteins and 1 ml fractions were collected. Bound proteins including p53 protein were then eluted from the column by a stepwise elution with buffer B containing NaCl ranging from 0.05 M to 1.00 M. To be precise, six different concentrations of NaCl were used as follows: 50 mM, 100 mM, 200 mM, 300 mM, 500 mM and finally 1 M. The flow rate was 0.5 ml/min, and 1 ml eluted fractions were collected. The fractions were then analysed by a 10% w/v SDS-PAGE gel.

2.11.3 Purification of human p53 protein by phosphocellulose, P-11 (Whatman)

Selected fractions containing enriched p53 proteins in 2.11.2 above were pooled together and applied to a phosphocellulose, P-11 (Whatman), column. The phosphocellulose (resin) (5 ml) was first activated by incubating it with 10 column volumes (50 ml) 0.5 M NaOH which was stirred for a while and then let to stand for 10 minutes, then with 10 column volumes 0.5 M HCl and followed by washes in 0.1 M HEPES, pH 8.0. The column was washed with buffer B containing 1 M NaCl and then equilibrated in Buffer B containing 50 mM NaCl. The pooled fractions were applied to the equilibrated phosphocellulose column. The column was washed with Buffer

B to remove unbound proteins. The bound proteins were eluted from the column by a salt gradient (step elution) ranging from 0.05 M to 1.0 M NaCl at a flow rate of 0.5 ml/min and 1.5 ml fractions were collected. To be precise, six different concentrations of NaCl were used as follows: 50 mM, 100 mM, 300 mM, 500 mM, 800 mM and finally 1 M. The proteins were then assayed by a 10% (w/v) SDS-PAGE gel.

2.11.4 Purification and concentration of p53 protein by ultracentrifugation

All the sample was loaded into 2 ml Centricon-30 (microcentrifuge filter, NMWL: 30 kDa, Millipore). The sample in the centricon was first centrifuged at 2,000 rpm for 10 minutes at 4^{o}C. Centrifugation was repeated and concentrated by TCA precipitation as described previously. 1 ml of buffer B was added to the sample and repeatedly centrifuged as before until the volume reached the indicated level. Concentrated p53 protein (retentate) was then collected by transferring it into a 15 ml falcon tube. The two collected fractions, i.e. flow-through and retentate, were assayed by a 10% w/v SDS-PAGE gel. The retentate was stored at -20^{o}C until required.

2.12 *In vitro* Generation of Peroxynitrite

Sodium nitrite (1.2 M $NaNO_2$) was placed in one 30 ml syringe and nitric acid (1 M HNO_3)/ 0.26% H_2O_2 in the other. Both the syringes were connected via a T-junction tubing. The syringes were pressed simultaneously with even pressure and the mixture was passed into a beaker containing 10 ml of 1.5 M NaOH. Below are the chemical equations for *in vitro* generation of peroxynitrite:

$$H_2O_2 + HNO_2 \longrightarrow ONOOH + H_2O \quad (1)$$

$$ONOOH + OH^- \longrightarrow ONOO^- + H_2O \quad (2)$$

(Pryor and Sequadrito, 1995; Saha *et al*., 1998)

The reaction was quenched by NaOH (reaction 2) where peroxynitrite is more stable in alkaline solution. Excess H_2O_2 was removed by passing the mixture down onto a manganese oxide placed in a funnel lined with filter paper until effervescence had ceased. The peroxynitrite solution was then scanned from 200-400 nm using a multi-wavelength scanning spectrophotometer. Absorbance readings of the peroxynitrite solution at 302 nm were taken in triplicate and the peroxynitrite concentration was measured using the formula below:

$$[\text{Peroxynitrite}] = (\text{Optical Density}_{302nm} / 1.67 \times 10^3 \times \text{Dilution Factor}) \text{ M}$$

The peroxynitrite solution was either used directly or aliquoted and kept at -80°C for approximately 6 months. The aliquoted peroxynitrite solution was only thawed once and the optical density was measured each time the thawed peroxynitrite was used for nitration work.

2.13 Nitration methods for proteins

2.13.1 Two nitration methods

2 nitration methods were employed namely an aggregometer set at 37°C at maximum speed (1200 rpm), and vortexing and a rocking water bath set at 37°C at 200 rpm to determine the best method for nitration by nitrating 2 mg/ml free fatty-acid bovine serum albumin (BSA) (a common nitration standard protein) dissolved in PBS, pH 7.4 with increasing concentrations of peroxynitrite ranging from 10 µM to 1 mM.

2.13.1.1 Aggregometer set at 37°C at 1200 rpm

100 µl of 2 mg/ml fatty acid-free BSA was first incubated for 10 min in an aggregometer set at 37°C at 1200 rpm. Peroxynitrite was then added slowly and the mixture was allowed to incubate for a further 15 minutes.

2.13.1.2 Vortexing and rocking water bath set at 37°C at 200 rpm

100 µl of 2 mg/ml fatty acid-free BSA was first incubated for 10 min in a rocking water bath set at 37°C at 200 rpm. With constant and vigorous vortexing of the BSA, peroxynitrite was added directly and slowly to the BSA. The mixture was then incubated for a further 15 min in a rocking water bath set at 37°C at 200 rpm.

2.13.2 Nitration of human p53, GST and GST-MDM2 proteins

The proteins were nitrated with increasing concentrations of peroxynitrite (0, 10 µM, 50 µM, 100 µM, 300 µM and 500 µM) using a vortex and rocking water bath method as described above in Section 2.13.1.2 for BSA.

2.14 Western blot for nitration of proteins

2 different anti-nitrotyrosine antibodies were used to determine the one which gave a better signal (Table 2.6). Blots with untreated and 100 µM peroxynitrite treated BSA were also incubated with a variety of secondary anti-mouse antibodies.

Table 2.6: Antibodies used in western blot optimisation for nitration

Primary anti-nitrotyrosine used	Secondary antibody used
Anti-nitrotyrosine mouse monoclonal IgG, Clone 16A (Upstate Biotechnology)	Rabbit anti-mouse monoclonal antibody IgG HRP conjugated (DAKO Cytomation)
	Anti-rabbit IgG HRP conjugated (Cell Signalling)
	Goat anti-rabbit IgG HRP conjugated (Amersham Biosciences)
Rabbit polyclonal anti-nitrotyrosine IgG (Sigma)	Sheep anti-rabbit IgG HRP conjugated (Serotec)
	Swine anti-rabbit IgG HRP conjugated (DAKO Cytomation)

Titration study of rabbit polyclonal anti-nitrotyrosine IgG (Sigma) was also carried out at 1:1000, 1:1500, 1:2000, 1:3000 and 1:5000 dilution. Protein transfer was carried out using 2 different membranes namely PVDF transfer membrane (Amersham Biosciences, 0.45 µm) and nitrocellulose (BDH Laboratory Supplies, 0.2 µm). The evaluations of different blocking conditions were also carried out. This was carried out by making one large well loaded with 100 µl of 1 mg/ml BSA dissolved in PBS in a 10% w/v SDS-PAGE gel. After electrophoretic transfer, 2 blots with the same amount of BSA loaded were cut into 5 strips each and then incubated the blocking buffer below. One set of 5 strips were incubated with an anti-mouse monoclonal IgG HRP-conjugated alone in each blocking buffer used and the other set was incubated with an anti-rabbit polyclonal IgG HRP-conjugated alone in each blocking buffer used. Tables 2.7 and 2.8 below show the optimisation of blocking conditions and optimised Western blot conditions for nitration studies, respectively.

Table 2.7: Blocking conditions used for optimisation of western blot for nitration (adapted from Antibody Manual by Harlow & Lane with slight modifications)

Blocking Buffer	Composition
Blotto	5% (w/v) non-fat dry milk (Marvel) in PBS
Blotto/Tween	5% (w/v) non-fat dry milk (Marvel) & 0.4% (v/v) Tween 20 in PBS
Tween	0.4% (v/v) Tween 20 in PBS
BSA	3% (w/v) BSA in PBS
Horse Serum	10% (v/v) horse serum in PBS

Table 2.8: Optimised Western blot conditions for nitration studies (adapted from Dr Picksley's lab protocol with slight modifications)

Steps	Details
1. Blocking	5% non-fat dry milk (Marvel), 0.4% Tween 20 in PBS for 1 hr.
2. Washes	3 changes of PBS, 10 min each
3. Primary antibody	1:1000 dilution in 2% Marvel/0.2% Tween 20 in PBS for 1 hr.
4. Washes	3 changes in PBS/0.2% Tween 20, 10 min each.
5. Secondary antibody	1:1000 dilution in 2% Marvel/0.2% Tween 20 in PBS for 1 hr.
6. Washes	5 changes (~ 5 mins each) with 2% skimmed milk Marvel, 0.2% Tween 20 in PBS and lastly transfer in PBS with 2 changes for ~ 2 mins each to rinse out the skimmed milk Marvel.

2.15 Purification of soluble p53 protein using an FPLC system

The supernatant obtained from large scale expression of p53 protein as mentioned in 2.10 was diluted 4-fold by the addition of buffer C [10% (v/v) glycerol, 25 mM HEPES (pH 7.6), 0.1 mM EDTA, and 2 mM dithiothreitol (DTT)] followed by the addition of $MgCl_2$ to 5 mM. This lysate was loaded 1 column volume per hour onto a 5 ml prepacked heparin Sepharose column that had been equilibrated in buffer C containing 50 mM KCl. After washing the column with 2 column volumes of buffer C containing 50 mM KCl, a 20 column volume linear gradient was performed at 1-2 column volumes/hour in buffer C from 0.05 to 1.0 M KCl. Fractions were assayed for p53 protein by immuno-blot analysis using the DO-1 antibody. p53 protein derived from this step was concentrated using Centricon-30 and applied to Pharmacia Superose 12 column equilibrated in 10% (v/v) glycerol, 25 mM HEPES (pH7.6), 0.5 M KCl, 0.1 mM EDTA, 0.1% Triton X-100, and 5 mM DTT. The column was pre-calibrated with prestained gel filtration molecular weight markers consisting of Cytochrome c (12.4 kDa), Carbonic Anhydrase (29 kDa), Bovine Serum Albumin (66 kDa), Alcohol Dehydrogenase (150 kDa) (Sigma) to determine the void volume of Blue Dextran (2000 kDa) and the elution volumes of other protein markers. The mobility (V_e/V_o) of each protein band was determined as the ratio of distance moved by each protein band to distance moves by tracking dye Blue Dextran. The gel filtration standard

curve was then generated by plotting the logarithm of the molecular weight against the mobility.

Selected fractions obtained were then subjected to SDS gel electrophoresis and Western blot probed with DO-1 to detect possible active soluble p53 protein. Attempted nitration of soluble p53 protein was carried out with increasing concentrations of peroxynitrite (0, 10 µM, 50 µM, 100 µM, 300 µM and 500 µM) using a vortex and rocking water bath method as previously described in Section 2.13.

2.16 Determination of protein concentration - Bradford Assay

Protein concentration was determined by Bradford Assay which involves the addition of an acidic dye to a protein solution. Several dilutions of standard protein (BSA) (1 mg/ml stock) ranging from 0 to 20 µg were prepared. 0.8 ml of standards and protein sample in distilled water were pipetted in a plastic cuvette. 0.2 ml of Dye Reagent Concentrate (Bio-Rad) was then added and mixed several times by gentle inversion. The samples were incubated at room temperature for at least 5 minutes. After incubation period the absorbance at OD_{595nm} was measured versus reagent blank. Using the standard curve the test protein concentration was calculated. Table 2.9 below shows the protein quantitation setup for Bradford Assay.

Table 2.9: Preparation of Bradford Assay using standard protein BSA. BSA amounts ranging from 0 to 20 µg was added to distilled water and Bradford Assay dye was added to the mixtures. After incubation, the mixtures were measured at 595 nm and a BSA standard curve was plotted.

Tube number	1 mg/ml Standard BSA (µl)	BSA (µg)	Distilled water (µl)	Bradford reagent dye (µl)
1	0	0	800	200
2	5	5	795	200
3	10	10	790	200
4	15	15	785	200
5	20	20	780	200

1 mg/ml stock of standard protein BSA was prepared by dissolving 1 mg of BSA in 1 ml of distilled water.

The components in the table above were mixed in 1.5 ml microcentrifuge tubes and briefly vortexed and incubated for at least 5 min at room temperature. The mixtures were then transferred into plastic cuvettes and then readings at 595_{nm} were taken using a spectrophotometer.

2.17 Cell culture and cell extract preparation

A panel of cancer cell lines were used in the nitration study. These include: the MCF7 breast cancer cell line (wt p53), the PANC-1 pancreatic cancer cell line (mutant p53), SW620 colorectal cancer cell line (mutant p53) and the HCT116 colorectal cancer cell line (null or wt p53). SW620 and HCT116 cells were used by Dart *et al.* (2004) to study the role of p53 in chemotherapeutic responses to selected anti-cancer drugs. Dart *et al.* found that the status of p53 protein in SW620 is mutant, non-functional, shows positive nuclear staining and p53 band present on Western blot. HCT116 shows negative p53 staining, no band present on Western blot, p53 is wild type and functional. In the meanwhile, HCT116 $p53^{-/-}$ shows negative staining, no band present on Western blot, null p53 status and function. These cells were grown in T25 or T75 flasks in DMEM medium (Biosera) supplemented with 100 U/ml penicillin and 100 µg/ml streptomycin, 2 mM L-glutamine and 10% (v/v) foetal bovine serum (FBS) until 80% confluent. MCF7 cells were priorly treated with 500 ng/ml Actinomycin D for 24 hrs to induce the expression of wt p53 protein (as employed by Cobbs *et al*., 2001) as and when needed before the cell lysates were treated with peroxynitrite. The cell lysates were used in order to directly nitrate p53 protein. For NO donor S-Nitrosoglutathione (GSNO) (Sigma) treatment, MCF7 cells which were used as a model cell, were grown to ~80% confluent and incubated with 0.5 mM or 1.0 mM GSNO for a duration of 4 hrs before being harvested. Below is a molecular structure of GSNO:

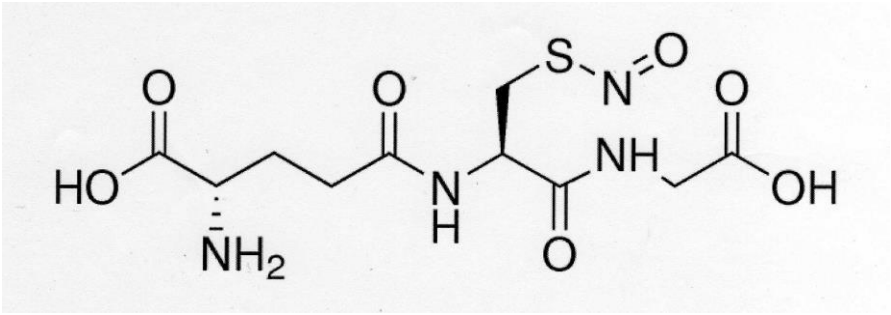

Figure 2.2. GSNO Molecular Structure (taken from Sigma Aldrich)

In order to harvest the cells, they were first washed with PBS before adding trypsin-EDTA and after the cells fully detached from the flask, complete growth medium was added which inactivated the trypsin due to the presence of serum. The cells were then pelleted by a low speed centrifugation at 1000 rpm for 5 min. Some of the cells were left in the flask and grown in a 5% (v/v) CO_2 incubator at 37°C for further growth. The cell pellets were lysed by incubating in NET buffer [150 mM NaCl, 5 mM EDTA pH 8.0, 50 mM Tris-HCl pH 8.0, 1% (v/v) Igepal supplemented with protease inhibitors cocktail (Roche)] for 30 minutes on ice, with occasional gentle mixing. Cell extracts were collected by centrifugation at 13000 rpm for 30 minutes at 4^oC. The supernatant was immediately transferred to a fresh micro-centrifuge tube and used directly while the pellet was discarded. The supernatant was pre-cleared of non-specifically reacting material by incubating it with protein G Sepharose bead slurry for 30 min on ice with occasional mixing. Protein G Sepharose was prepared by washing the beads twice with PBS and restored to 50% (v/v) slurry with PBS. The sample was then centrifuged for 30 sec in a microcentrifuge at 13,000 rpm to remove non-specifically reacting material and the supernatant was transferred to a fresh tube for use in immunoprecipitation assay. The protein concentration of the cell lysate was determined by performing Bradford assay. The cell lysates were nitrated with increasing concentrations of peroxynitrite (0, 10 µM, 50 µM, 100 µM, 300 µM and 500 µM) using a vortex and rocking water bath method as previously described in Section 2.13.1.2.

2.18 Immunoprecipitation

The pre-cleared cell extract (100 µg) was incubated with 1 µl of either anti-nitrotyrosine monoclonal antibody or anti-p53 polyclonal (CM-1) antibody on ice for 60 min. 20 µl of protein G Sepharose bead slurry was then added and mixed in a rotating wheel for 15 minutes. The immune complexes bound to the beads were pelleted by centrifugation for 30 sec in a micro-centrifuge tube at 13000 rpm and then the supernatant was removed. The beads were then washed four times with 200 µl of NET buffer [150 mM NaCl, 5 mM EDTA pH 8.0, 50 mM Tris-HCl pH 8.0, 1% (v/v) Igepal supplemented with protease inhibitors cocktail (Roche)] containing 0.5 M NaCl. The washing step involved pelleting by centrifugation, the removal of supernatant and the addition of fresh buffer. The pellet was then resuspended in 50 µl of 2X SDS loading dye with freshly added DTT to a final concentration of 100 nM, boiled for 5 min to dissociate the immuno-complexes from the beads. The proteins were fractionated on an SDS-polyacrylamide gel and then followed by western blotting.

2.19 GST and GST-MDM2 proteins

2.19.1 Expression of GST and GST-MDM2 proteins

Overnight cultures of pGEX-2T or pGEX-2T-MDM2 transformed strains were prepared by inoculating 5 ml LB broth supplemented with 50 µg/ml ampicillin in 15 ml Falcon tubes with a colony of each strain from their respective selection agar plates. A 10 ml of overnight culture was used to inoculate 1 litre of LB broth (1:100 dilution) supplemented with 50 µg/ml of ampicillin. The culture was incubated at 37^{o}C with shaking at 180 rpm until its OD_{600nm} reached ~0.8 (late log phase). IPTG was added to a final concentration of 1 mM and growth was continued with aeration for a further 4 hours. Cells were harvested by centrifugation at 8000 rpm for 10 minutes at 4^{o}C in a Beckmann Avanti J25 centrifuge in JLA 10,500 rotor. The supernatant was discarded and the pellet drained and placed on ice. The pellet was then completely suspended in 50 µl of ice-cold 1 X PBS per ml of culture. The suspended cells were disrupted using a sonicator (MSE 150 Watt Ultrasonic Disintegrator MK2) on ice in short bursts at maximum amplitude. An aliquot

of the sonicate was saved for analysis by SDS-PAGE gel electrophoresis. 20% (v/v) Triton X-100 was added to a final concentration of 1% (v/v). A protease inhibitor dissolved in distilled water was also added to the suspension. The mixture was gently mixed for 30 min to aid in solubilisation of the fusion protein. The suspension was centrifuged at 10,000 rpm for 10 min at 4^{o}C. The supernatant was then transferred to a fresh container. Aliquots of the supernatant and the cell debris pellet were saved for analysis by SDS-PAGE.

2.19.2 Purification of GST and GST-MDM2 proteins

2.19.2.1 Preparation of a 50% Glutathione Sepharose 4B slurry

Glutathione Sepharose 4B (Amersham Biosciences) was used for batch purification of glutathione S-transferase (GST) or recombinant fusion GST-MDM2 using the pGEX expression vector. A 50% (w/v) slurry was produced from approximately a 75% (w/v) slurry as supplied by the manufacturers. 1.33 ml of the original Glutathione Sepharose 4B slurry per ml of bed volume was dispensed. One ml of drained gel was capable of binding at least 8 mg of recombinant GST. The gel was sedimented by centrifugation at 500 rpm for 5 min and the supernatant was carefully decanted. The Glutathione Sepharose 4B was then washed with 10 ml of cold 1 X PBS per 1.33 ml of the original slurry of Glutathione Sepharose 4B dispensed and inverted to mix. The gel was sedimented by centrifugation at 500 rpm for 5 min and the supernatant decanted. 1 ml of 1 X PBS was added to each 1.33 ml of the original slurry which produced a 50% (w/v) slurry.

2.19.3 Batch purification of GST and GST-MDM2 proteins

2.19.3.1 Binding

2 ml of a 50% v/v slurry of Glutathione Sepharose 4B equilibrated with 1 X PBS was added to each 100 ml bacterial sonicate as described earlier. The

mixture was incubated with gentle agitation at room temperature for 30 min. The suspension was then centrifuged at 500 rpm for 5 min to sediment the gel and the supernatant was removed. The Glutathione Sepharose 4B pellet was washed with 10 bed volumes of 1 X PBS. The suspension was centrifuged in a 4 X 750 ml MSE Windshield rotor at 500 rpm for 5 min to sediment the gel and the wash discarded. The wash was repeated twice for a total of three washes.

2.19.3.2 Elution

1.0 ml of glutathione elution buffer (0.154 g of reduced glutathione dissolved in 50 ml of 50 mM Tris-HCl, pH 8.0) was added per ml of bed volume of Glutathione Sepharose 4B. The suspension was mixed gently to resuspend the gel and incubated at room temperature for 10 min to liberate the fusion protein from the gel. The mixture was centrifuged at 500 rpm for 5 min to sediment the gel. The supernatant was then removed and transferred to a fresh centrifuge tube. Elution and centrifugation steps were repeated twice more. Finally the three eluates were pooled, after confirming they all contained the GST or GST fusion protein.

RESULTS CHAPTER 3

The aim of this work was to investigate the effects of nitration on p53 function, therefore, to start off, a significant amount of pure p53 protein was needed for this study. In order to do this human p53 protein was first overexpressed in small scale in two *E. coli* strains BL21(DE3) and BL21(DE3) Star transformed with pT7-7Hup53, a plasmid encoding a full length human p53 gene which was originally constructed by Midgley *et al* (1992). The optimum conditions for the human p53 protein expression were then to be determined and the human p53 protein expression levels between the two *E. coli* strains were compared before a large scale expression of p53 protein was carried out.

3.1 Small scale expression of p53 protein

The two competent strains as prepared in Materials and Methods (Section 2.7.1) were transformed either with pT7.7 Hup53 or a pT7.7 plasmid alone (Section 2.7.2). Each culture was split into two, one was grown until OD_{600nm} of 0.15 to 0.20 (early mid-log phase) prior to the addition of isopropyl β-D-thiogalactopyranoside (IPTG) to a final concentration of 1 mM to induce the expression of p53 protein and the other one was left uninduced to act as a control for induction. Transformed BL21(DE3) and BL21(DE3) Star strains with pT7.7 plasmids alone were only induced with IPTG and served as negative controls to monitor specific expression of p53 protein from the pT7.7Hup53 expression construct. Figure 3.1 shows IPTG-induced *E. coli* strain BL21(DE3) containing a pT7.7 plasmid alone. In Figure 3.1, no bands corresponding to p53 protein can be seen as expected as no p53 gene was present in the plasmid vector, thus, no p53 protein was produced. Figure 3.2 shows IPTG induction of human p53 protein from BL21(DE3) with a pT7.7Hup53 construct where bands corresponding to p53 protein can be seen with modest increased band intensity over time. A gel photograph of non-induced BL21(DE3) strain containing a pT7.7Hup53 construct (Figure 3.3) shows that bands corresponding to p53 protein can be seen with

increased band intensity over time. This indicates that p53 protein was expressed in the non-induced BL21(DE3)/pT7.7Hup53 culture. The possible reason for this event is due to a leaky P_{tac} promoter where even without IPTG being added the promoter was initiated to transcribe T7 polymerase gene with concomitant p53 protein expression (Dubendoff and Studier, 1991). Induced BL21(DE3) containing a pT7.7 plasmid alone is a more appropriate control as no bands corresponding to p53 protein were observed as expected. The same observation can be seen in the other *E. coli* strain i.e. BL21(DE3) Star (data not shown), as in BL21(DE3) above. These observations confirm that the two non-induced *E. coli* strains transformed with a pT7.7Hup53 construct constitutively produced T7 RNA polymerase which therefore resulted in a basal expression of p53 protein and made the induction of p53 protein expression less pronounced. This issue will be addressed in greater detail in the Discussion section.

The optical density at λ=600nm of the induced and non-inducedcultures of each sample was measured during the induction process and are shown in Figure 3.4. The optical density of the induced culture of both *E. coli* strains was less than that for the non-induced culture. This is more likely due to the domination of cellular transcription of T7 RNA polymerase was more of the problem which resulted in the retardation of the growth of the host cells (Studier *et al*., 1990). To confirm that p53 protein was expressed in both non-induced BL21(DE3) and BL21(DE3) Star transformed with pT7-7Hup53 constructs, the transformation process for the two strains was repeated and small scale cultures of the strains were grown as before (i.e. OD_{600nm} of 0.15-0.2, 37^{o}C at 180 rpm). Each culture was then split into two, one was induced with IPTG at OD_{600nm} of 0.15-0.2 and the other one was left non-induced. Both Figures 3.5 and 3.6 show that p53 protein was expressed in both non-induced transformed strains where p53 protein was expressed as early as at 120 min time point in BL21(DE3) cells (Figure 3.5, Lane 3) whereas p53 protein was only expressed at 240 min time point in BL21(DE3) Star cells (Figure 3.6, Lane 6). Since only two time points were taken, i.e. 120 min and 240 min, these show that there is a difference in the start of the expression in the two non-induced strains. These figures show that in the two induced

strains, stronger p53 bands were seen at 240 min time point compared to 120 min time point. Thus, the optimal time for the growth of the strains after IPTG induction is at least for 240 min (i.e. 4 hours), giving enough time for accumulation of target protein (Studier *et al*, 1990) which is evident by the earlier induction profile (Figure 3.2).

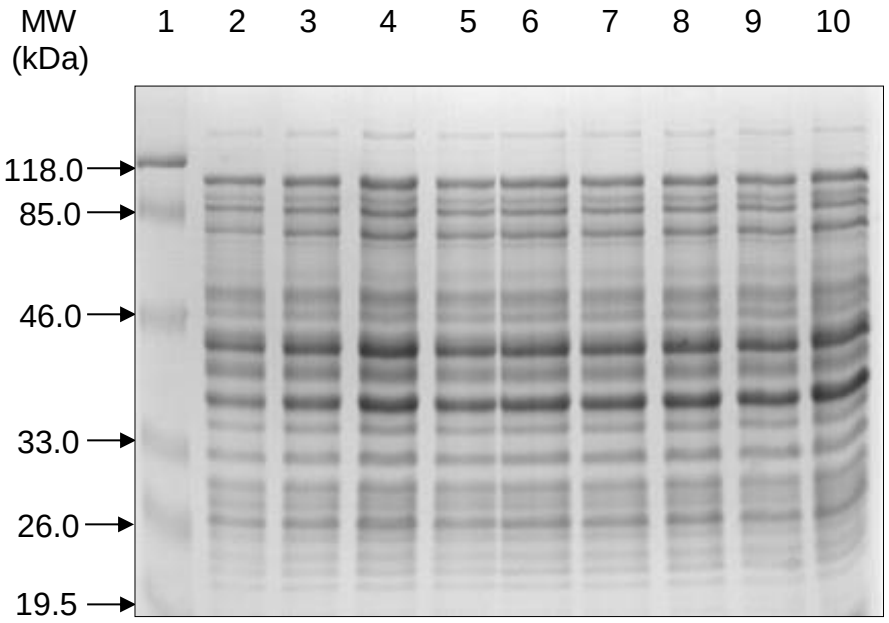

Figure 3.1. A 10% SDS-PAGE gel showing IPTG induced *E.coli* strain BL21(DE3) containing a pT7.7 plasmid alone to act as a negative control for expression of p53 protein.

Lane 1 – prestained protein molecular weight markers (Fermentas)

Lane 2 – induced cells at 0 min

Lane 3 – induced cells at 30 min

Lane 4 – induced cells at 60 min

Lane 5 – induced cells at 90 min

Lane 6 – induced cells at 120 min

Lane 7 – induced cells at 150 min

Lane 8 – induced cells at 180 min

Lane 9 – induced cells at 210 min

Lane 10 – induced cells at 240 min

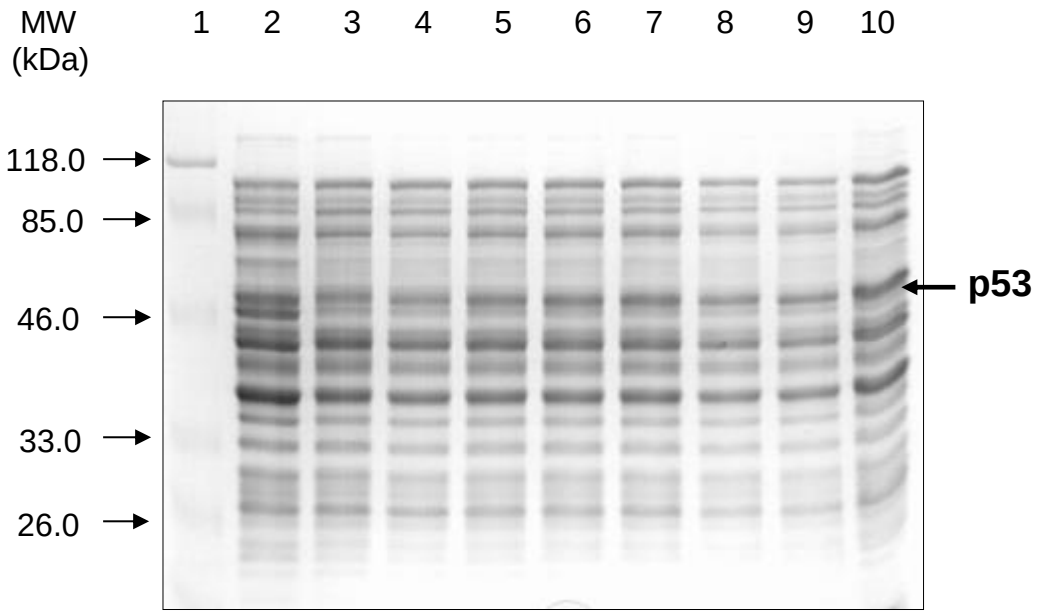

Figure 3.2. A 10% SDS-PAGE gel showing IPTG induction of the expression of human p53 protein from *E. coli* strain BL21(DE3) containing a pT7.7Hup53 plasmid. The position of p53 protein is indicated.

Lane 1 - prestained protein molecular weight markers (Fermentas)

Lane 2 - non-induced cells at 240 min (negative control)

Lane 3 - induced cells at 30 min

Lane 4 - induced cells at 60 min

Lane 5 - induced cells at 90 min

Lane 6 - induced cells at 120 min

Lane 7 - induced cells at 150 min

Lane 8 - induced cells at 180 min

Lane 9 - induced cells at 210 min

Lane 10 - induced cells at 240 min

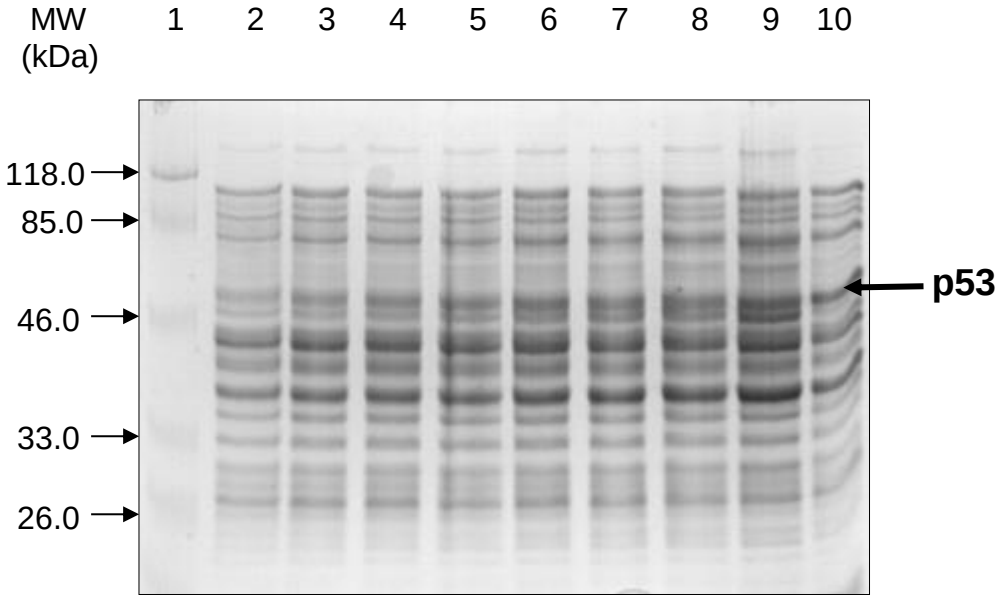

Figure 3.3. A 10% SDS-PAGE gel showing non-induced *E. coli* strain BL21(DE3) containing pT7.7Hup53 plasmid.

Lane 1 – prestained protein molecular weight markers (Fermentas)

Lane 2 – non-induced cells at 30 min

Lane 3 – non-induced cells at 60 min

Lane 4 – non-induced cells at 90 min

Lane 5 – non-induced cells at 120 min

Lane 6 – non-induced cells at 150 min

Lane 7 – non-induced cells at 180 min

Lane 8 – non-induced cells at 210 min

Lane 9 – non-induced cells at 240 min

Lane 10 – induced cells at 240 min (positive control)

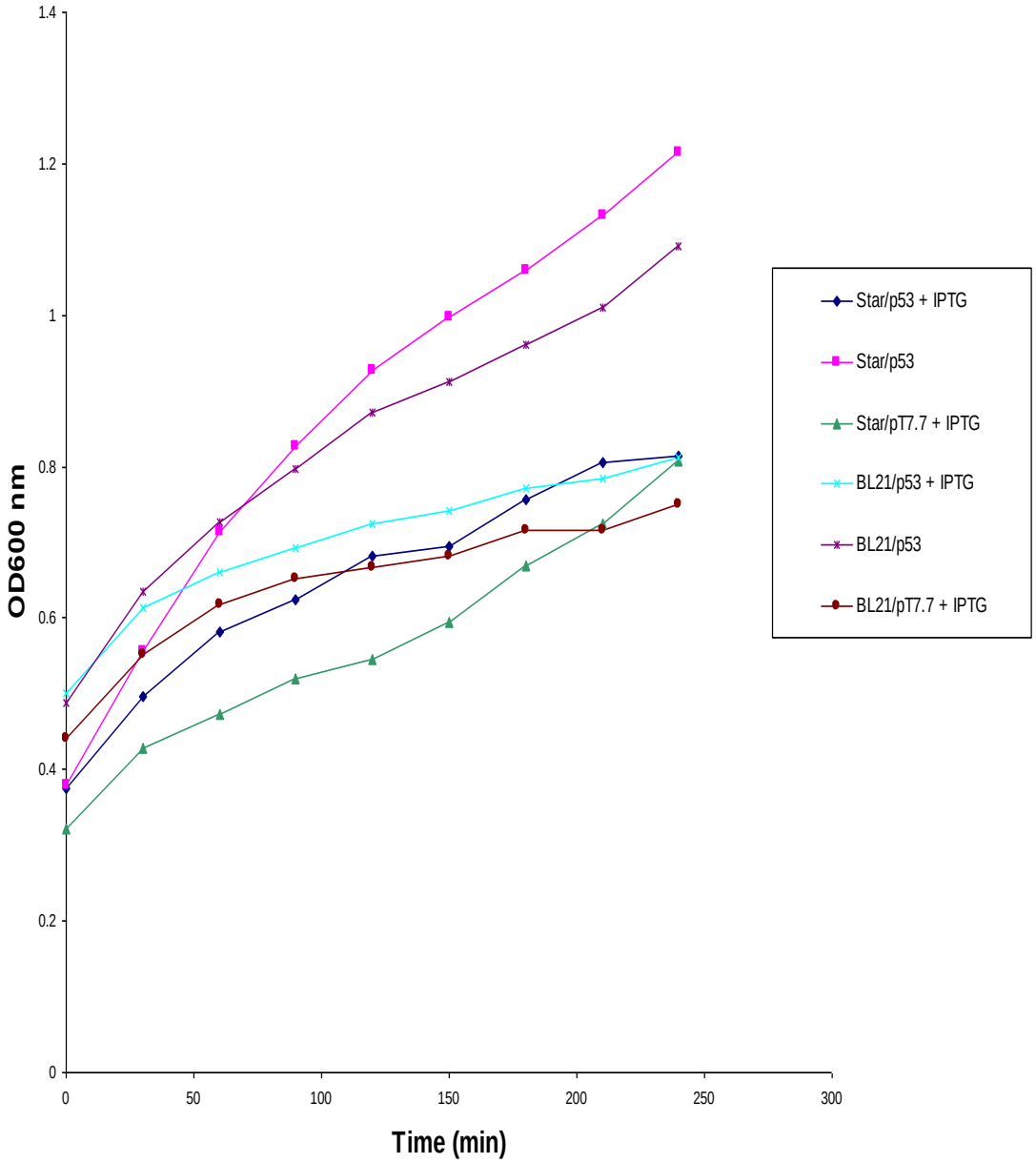

Figure 3.4. Growth curves of IPTG induced and non-induced *E. coli* strains BL21(DE3) and BL21(DE3) Star. The bacterial cultures were taken every 30 min and measured at OD_{600nm}.

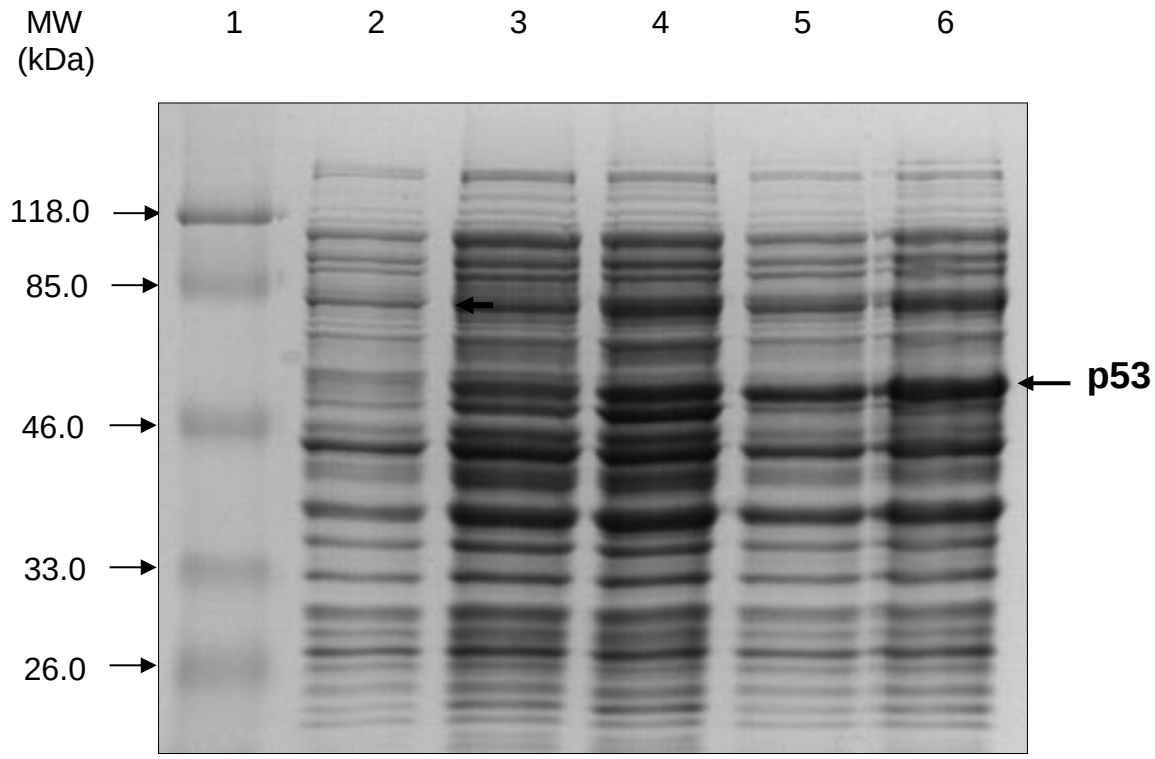

Figure 3.5. A 10% SDS PAGE gel showing induced and non-induced *E. coli* strain BL21(DE3) containing a pT7.7Hup53 construct.

Lane 1 – prestained protein molecular weight markers (Fermentas)

Lane 2 – sample at 0 min

Lane 3 – non-induced cells at 120 min

Lane 4 – non-induced cells at 240 min

Lane 5 – induced cells at 120 min

Lane 6 – induced cells at 240 min

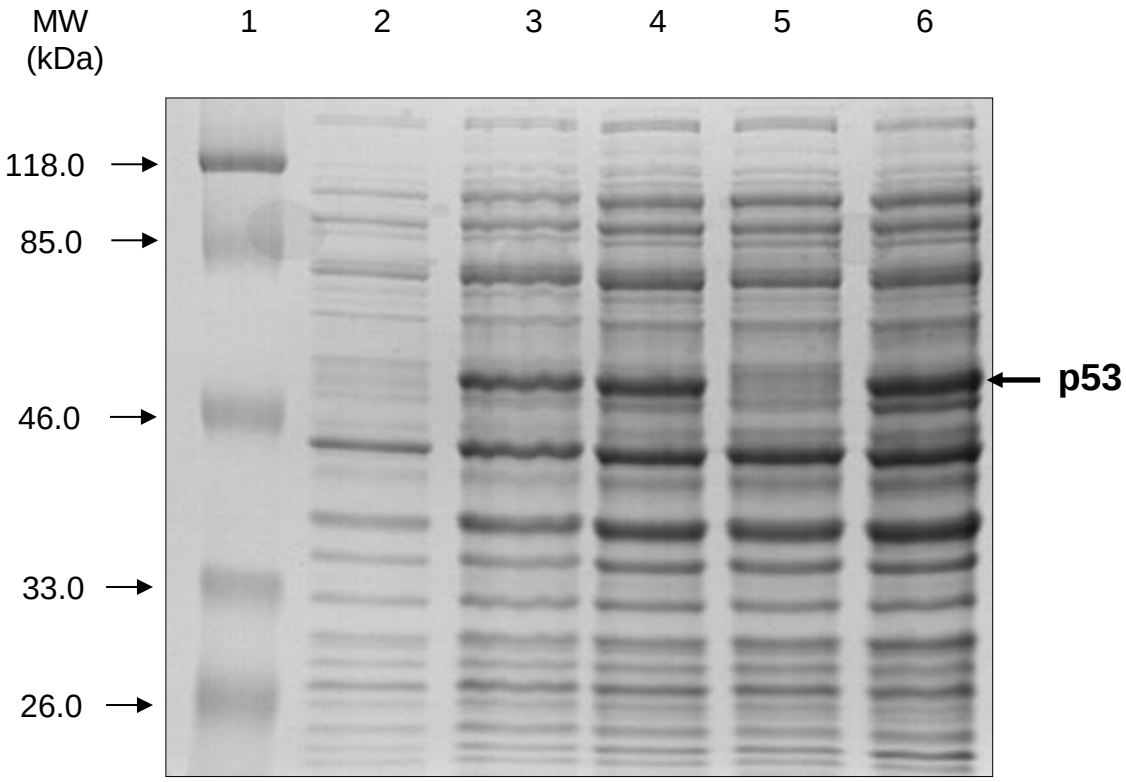

Figure 3.6. A 10% SDS PAGE gel showing induced and non-induced *E. coli* strain BL21(DE3) Star containing a pT7.7Hup53 construct.

Lane 1 – prestained protein molecular weight markers (Fermentas)

Lane 2 – sample at 0 min

Lane 3 – induced cells at 120 min

Lane 4 – induced cells at 240 min

Lane 5 – non-induced cells at 120 min

Lane 6 – non-induced cells at 240 min

3.2 Western Blotting

Western blotting was then carried out to confirm the band observed was the presence of p53 protein. After several trials, finally optimum conditions for western blotting were determined as described in the Materials and Methods Section. The data in Figure 3.7 further confirms that the two induced strains with the plasmid vector pT7.7 alone show no expression of p53 protein which is expected since no human p53 gene was inserted in the plasmid and therefore no p53 protein was expected to be produced (Figure 3.7, Lanes 2 and 3). Thus, these are good to be used as negative controls for expression of p53 protein. However, the two strains transformed with pT7-7Hup53 constructs expressed p53 protein even though they were not at all induced by IPTG (Figure 3.7, Lanes 4 and 7). From Figure 3.7 also we can notice that p53 protein was greatly expressed in both the induced strains at 240 min (Lanes 6 and 9). p53 degradation products can also be seen in Figure 3.7 with greater intensities especially in both the transformed strains induced at 240 min since DO-1 can detect not just full length p53 protein but also other forms of p53 protein.

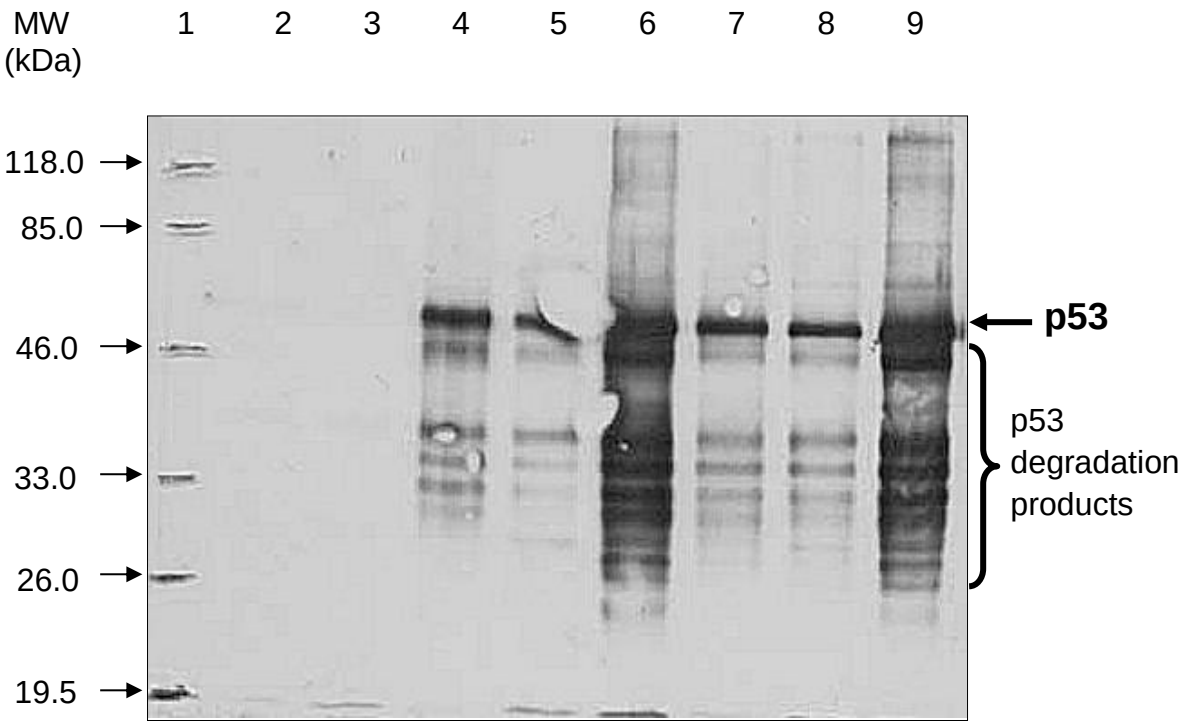

Figure 3.7. A Western blot analysis of non-induced and induced *E. coli* strains BL21(DE3) and BL21(DE3) Star containing pT7.7Hup53 constructs compared to induced strains transformed only with plasmid alone to act as negative controls. The primary antibody was anti-p53 mouse monoclonal antibody DO-1 and the secondary antibody used for detection was rabbit anti-mouse antibody conjugated with HRP.

Lane 1 – prestained protein molecular weight markers (Fermentas)

Lane 2 – BL21(DE3) pT7.7 induced at 240 min

Lane 3 – BL21(DE3) Star pT7.7 induced at 240 min

Lane 4 – BL21(DE3) pT7.7Hup53 non-induced at 240 min

Lane 5 – BL21(DE3) pT7.7Hup53 induced at 0 min

Lane 6 – BL21(DE3) pT7.7Hup53 induced at 240 min

Lane 7 – BL21(DE3) Star pT7.7Hup53 non-induced at 240 min

Lane 8 – BL21(DE3) Star pT7.7Hup53 induced at 0 min

Lane 9 – BL21(DE3) Star pT7.7Hup53 induced at 240 min

3.3 Large scale expression of human p53 protein

Given the conditions for the induction of p53 protein (final IPTG concentration of 1 mM, incubation time of 240 min after induction, incubation temperature of 37^{o}C with vigorous shaking at 180 rpm), our next step was to proceed with a large scale expression of p53 protein as described in 'Materials and Methods'(Section 2.10). In brief, the cell pellet was lysed and the inclusion bodies where 98% of human p53 protein present (Hupp *et al*., 1992) were solubilised in denaturant, 5 mM guanidine-hydrochloride, and subsequently dialysed in buffers with decreasing NaCl concentration where renaturation of p53 protein took place and finally native form of the protein was obtained. A flow chart showing purification steps of p53 protein is shown below.

Figure 3.8. Flow chart of steps involved in purification of p53 protein

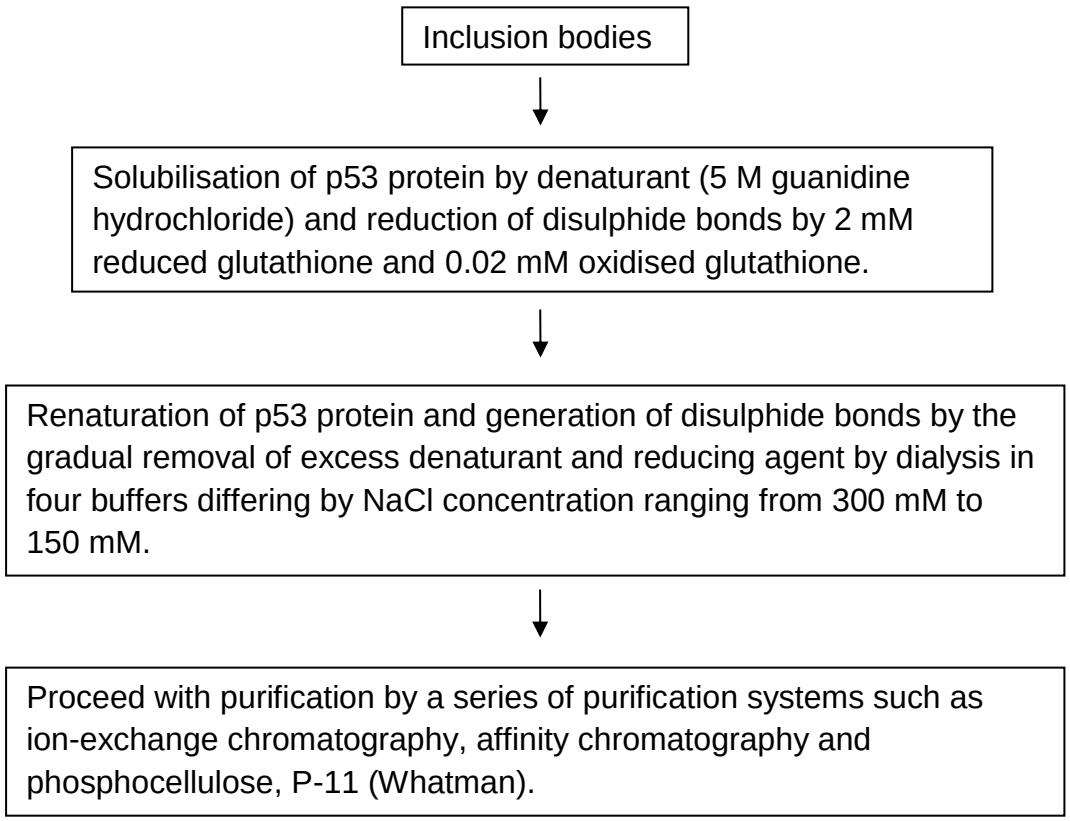

Figure 3.9 shows dialysed p53 protein loaded at different volumes, the higher the volume loaded the more stronger the p53 protein band seen which was the major component of protein expressed by *E. coli.* However, no further checks were carried out to determine if p53 was successfully isolated following dialysis.

3.4 Purification of p53 protein

Purification of p53 protein was first carried out with a 1 ml Hi-Trap-Heparin Sepharose column where a stepwise gradient elution was employed with buffer B with NaCl concentration ranging from 50 mM to 1 M. In this procedure, 1.5 ml fractions were collected which include flowthrough (pre-washed), wash and eluted fractions as shown in Figures 3.10(a) and (b). In Figure 3.10(a) we can see proteins in the flowthroughs (Lanes 4 and 5) indicating that some proteins including p53 protein were not bound to the column. The reason might be due to the p53 protein was not properly bound to the column due to improper folding of the protein. Since most contaminating proteins passed through the column as shown in Lane 5, Figure 3.10(a), therefore not many contaminating proteins present in the wash and the eluted fractions since little left which were previously weakly bound to the column. In Figure 3.10(b), Lanes 8 and 9, enriched p53 protein but with several minor low molecular weight contaminating proteins or p53 degradation products can be seen.

The next purification step was then carried out by pooling together eluted fractions (Els) 30 to 37 as shown in Lanes 8 and 9 in Figure 3.10(b) and then subjected the pooled fractions to further purification by phosphocellulose P-11 which is described in details in ‘Materials and Methods’ (Section 2.11.3). 1.5 ml fractions were also collected which included flowthroughs, wash and eluted fractions. Figure 3.11(b), Lane 8, shows a quite faint p53 protein band still with few low molecular weight contaminating proteins or p53 degradation products. The eluted fractions from Lane 8 (Figure 3.11(b)), i.e. eluted fractions 34 to 36, were concentrated by centricon and also TCA precipitation. Faint protein bands were obtained with two low molecular

weight contaminating proteins or p53 degradation products still present which can be clearly seen in TCA precipitation sample (data not shown). Protein quantitation was carried out but the levels were below level of detection of the Bradford Assay used which was not ideal to do the nitration work. While relatively pure p53 protein had been obtained, it was worth revisiting the induction conditions.

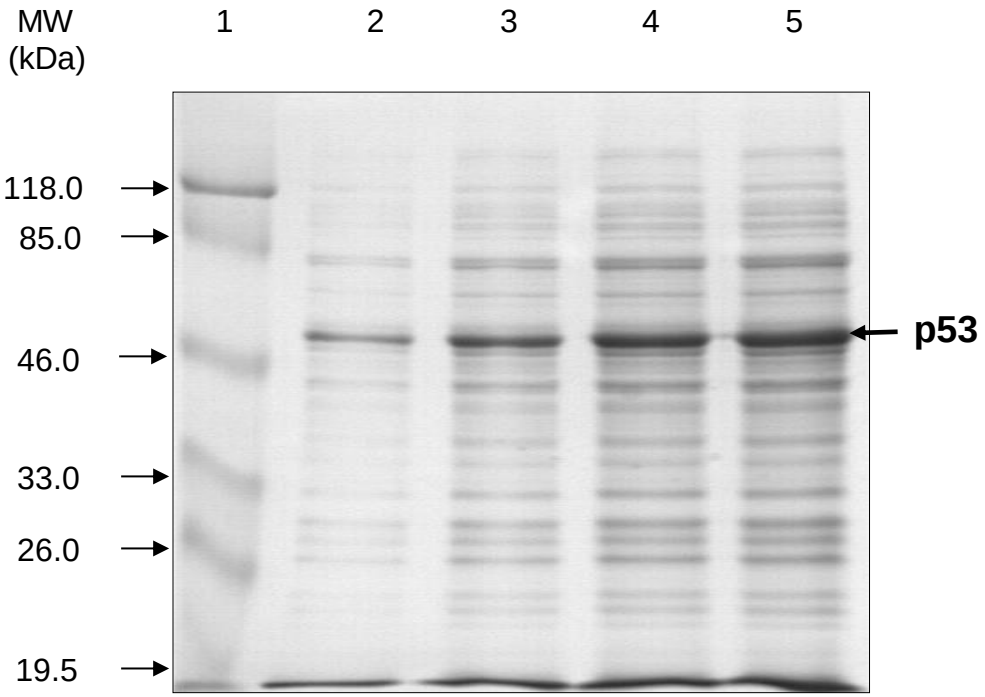

Figure 3.9. A 10% SDS-PAGE gel showing different volume loaded of dialysed p53.

Lane 1 – prestained molecular weight markers (Fermentas)

Lane 2 – 5 µl sample

Lane 3 – 10 µl sample

Lane 4 – 15 µl sample

Lane 5 – 20 µl sample

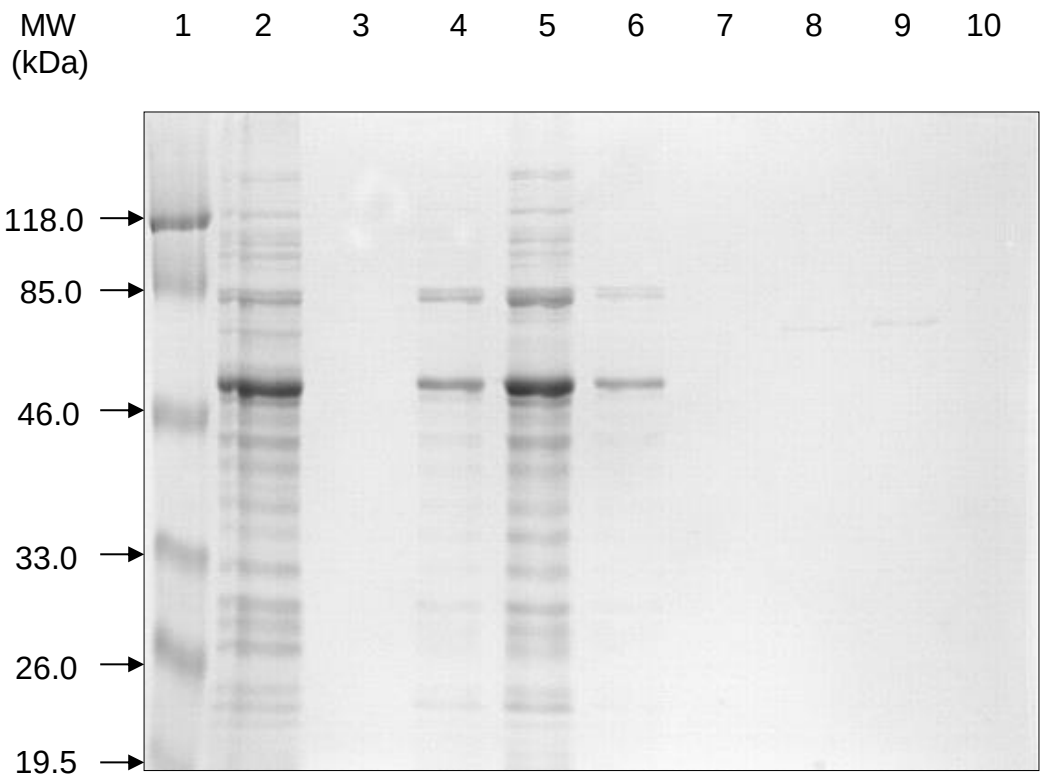

Figure 3.10(a). A 10% SDS PAGE gel showing fractions purified from a stepwise gradient elution on Hi-Trap Heparin Sepharose column.

Lane 1 – prestained protein molecular weight markers (Fermentas)

Lane 2 – non-purified p53

Lane 3 – Flowthrough 1-2

Lane 4 – Flowthrough 3-4

Lane 5 – Flowthrough 5

Lane 6 – Wash 1

Lane 7 – Wash 2

Lane 8 – Eluted #1-3

Lane 9 – Eluted #4-6

Lane 10 – Eluted #7-9

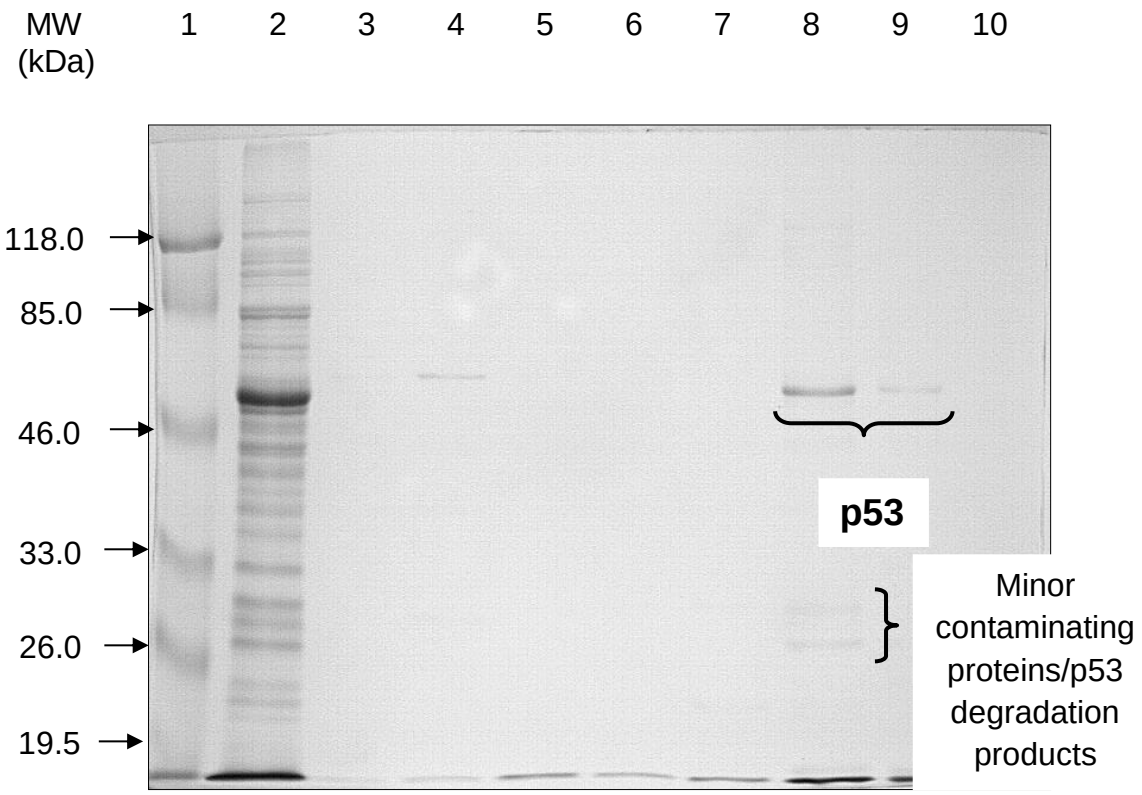

Figure 3.10(b). A 10% SDS PAGE gel showing fractions purified from a stepwise gradient elution on Hi-Trap Heparin Sepharose column.

Lane 1 – prestained protein molecular weight markers (Fermentas)

Lane 2 – non-purified p53

Lane 3 – Eluted # 10-13

Lane 4 – Eluted #14-17

Lane 5 – Eluted #18-21

Lane 6 – Eluted #22-25

Lane 7 – Eluted #26-29

Lane 8 – Eluted #30-33

Lane 9 – Eluted #34-37

Lane 10 – Eluted #38-41

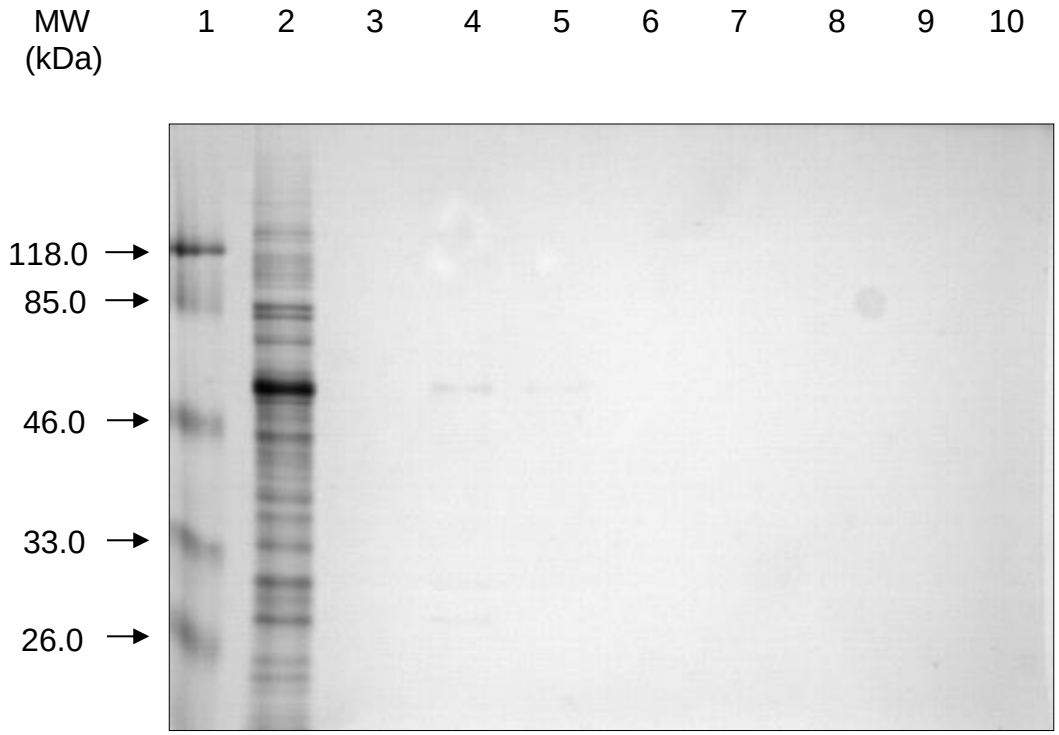

Figure 3.11(a). A 10% SDS PAGE gel showing fractions purified from a stepwise gradient elution on a Phosphocellulose P-11 column.

Lane 1 – prestained protein molecular weight markers (Fermentas)

Lane 2 – non-purified p53

Lane 3 – Flowthrough 1-4

Lane 4 – Flowthrough 5-8

Lane 5 – Wash 1

Lane 6 – Wash 2

Lane 7 – Eluted #1-4

Lane 8 – Eluted #5-8

Lane 9 – Eluted #9-12

Lane 10 – Eluted #13-16

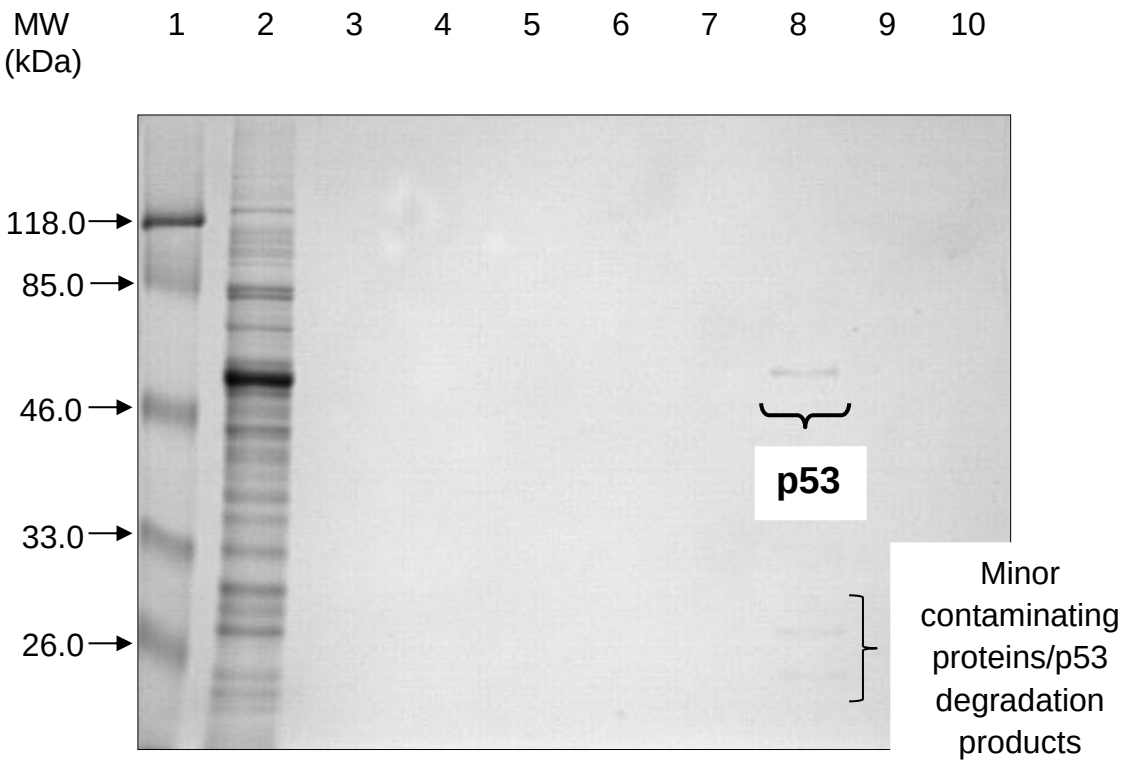

Figure 3.11(b). A 10% SDS PAGE gel showing fractions purified from a stepwise gradient elution on a Phosphocellulose P-11 column.

Lane 1 – prestained protein molecular weight markers (Fermentas)

Lane 2 – non-purified p53

Lane 3 – Eluted #17-20

Lane 4 – Eluted #21-24

Lane 5 – Eluted #25-27

Lane 6 – Eluted # 28-30

Lane 7 – Eluted #31-33

Lane 8 – Eluted #34-36

Lane 9 – Eluted #37-39

Lane 10 - Eluted #40-41

3.5 Optimisation of the p53 expression conditions

Small scale expression of p53 protein was repeated initially using freshly transformed E. coli strains BL21(DE3) pT7.7Hup53 in order to re-optimise the p53 expression conditions so that substantial amount of p53 protein would be obtained. Four OD_{600nm} values for induction start points were chosen this time around namely ~0.2, ~0.8, ~0.9 and ~1.0 at which 1 mM IPTG was added and the cultures were grown for 4 hr and then left to grow overnight. 1.5 ml of cells were harvested at 4 hr, centrifuged at 13,000 rpm for 2 min, the pellet was resuspended in 100 µl 2x SDS gel loading dye, sonicated 1x for 10 sec on ice at maximum amplitude, boiled for 5 min and 10 µl sample volume loaded onto a 10% SDS-PAGE gel. Finally 1.5 ml of cells were again harvested after overnight growth and then treated as before. From Figures 3.12(a) and (b) no obvious difference can be seen in the expression levels of p53 protein at OD_{600nm} of ~0.8, ~0.9 and ~1.0 that were grown for 4 hr. The growth between 4 hr and overnight at these ODs also show no obvious difference in the p53 protein expression levels. Thus, the growth duration for at least 4 hr after IPTG induction is sufficient to get substantial amount of p53 protein as determined earlier. Therefore, in the next step of p53 protein re-optimisation conditions, the growth duration for 4 hr after induction was followed.

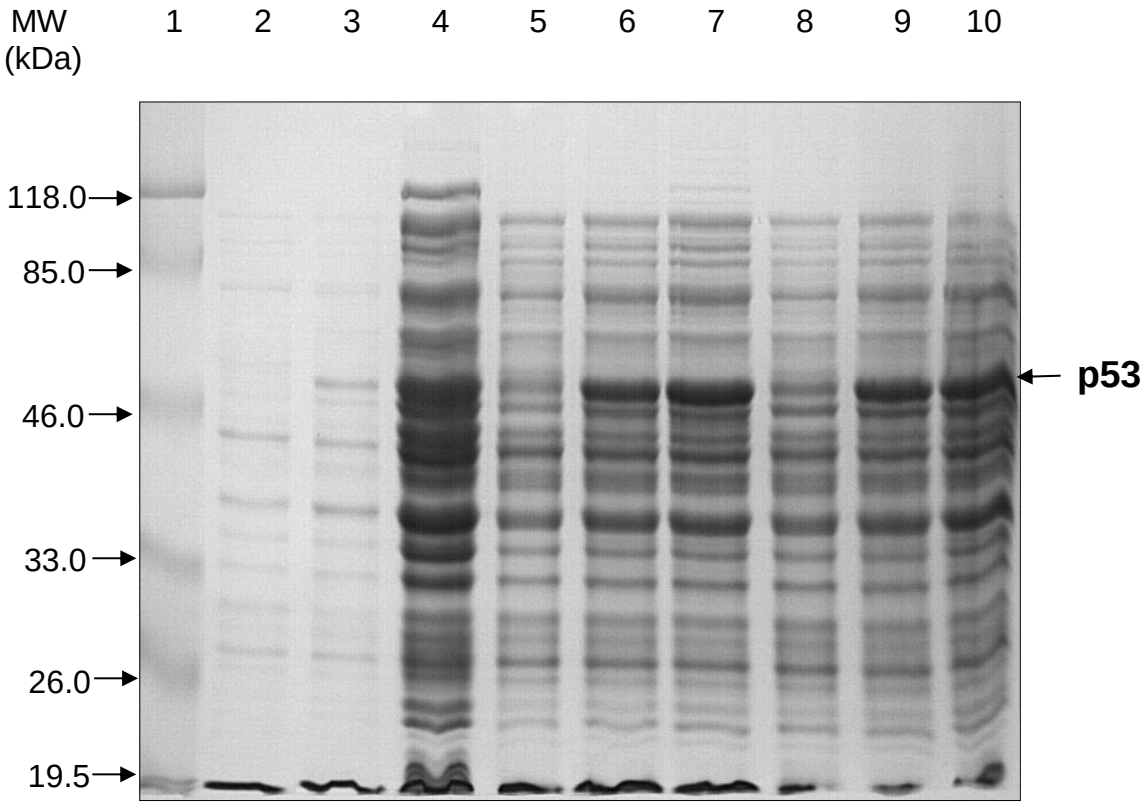

Figure 3.12(a). A 10% SDS PAGE gel showing optimisation of p53 protein expression in *E. coli* strain BL21(DE3) containing a pT7.7Hup53 construct.

Lane 1 – prestained protein molecular weight markers (Fermentas)

Lane 2 – induced cells at OD_{600nm} ~ 0.2 (0 min)

Lane 3 – induced cells at OD_{600nm} ~ 0.2 (4 hr)

Lane 4 – induced cells at OD_{600nm} ~ 0.2 (O/N)

Lane 5 – induced cells at OD_{600nm} ~ 0.8 (0 min)

Lane 6 – induced cells at OD_{600nm} ~ 0.8 (4 hr)

Lane 7 – induced cells at OD_{600nm} ~ 0.8 (O/N)

Lane 8 – induced cells at OD_{600nm} ~ 0.9 (0 min)

Lane 9 – induced cells at OD_{600nm} ~ 0.9 (4 hr)

Lane 10 – induced cells at OD_{600nm} ~ 0.9 (O/N)

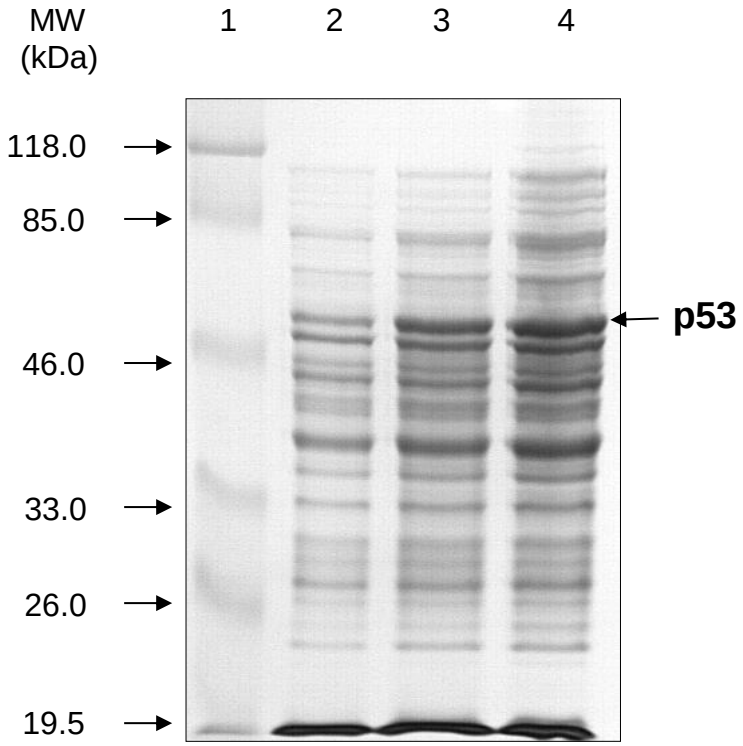

Figure 3.12(b). A 10% SDS PAGE gel showing optimisation of p53 expression in *E. coli* strain BL21(DE3) containing a pT7.7Hup53 construct.

Lane 1 – prestained protein molecular weight markers (Fermentas)

Lane 2 – induced cells at OD_{600nm} ~ 1.0 (0 min)

Lane 3 – induced cells at OD_{600nm} ~ 1.0 (4 hr)

Lane 4 – induced cells at OD_{600nm} ~ 1.0 (O/N)

E. coli strains BL21(DE3) and BL21(DE3) Star transformed with pT7.7Hup53 were cultured and grown to OD_{600nm} of ~0.2, ~0.4, ~0.6 and ~0.8 (OD_{600nm} ranging from early mid-log to late log phases) before 1 mM IPTG was added and left to grow for a further 4 hr. From Figure 3.13(b), we can see that p53 protein from transformed BL21(DE3) was best expressed after induction at OD_{600nm} of ~0.8 (Lane 7) and the best expression level of p53 protein in transformed BL21(DE3) Star was also after induction at OD_{600nm} of ~0.8 (Lane 9). However, there was no significant difference between the level of expression of p53 protein between BL21(DE3) Star and BL21(DE3). It has been reported that the presence of mutation of the gene encoding RNAse E (*rne*131) in BL21(DE3)Star increases the expression of heterologous protein due to increased mRNA stability (Invitrogen). Since no major differences in the expression levels of p53 protein between the two transformed strains, thus, mRNA stability is not an issue here, but rather codon usage bias which is discussed in details in the Discussion Section.

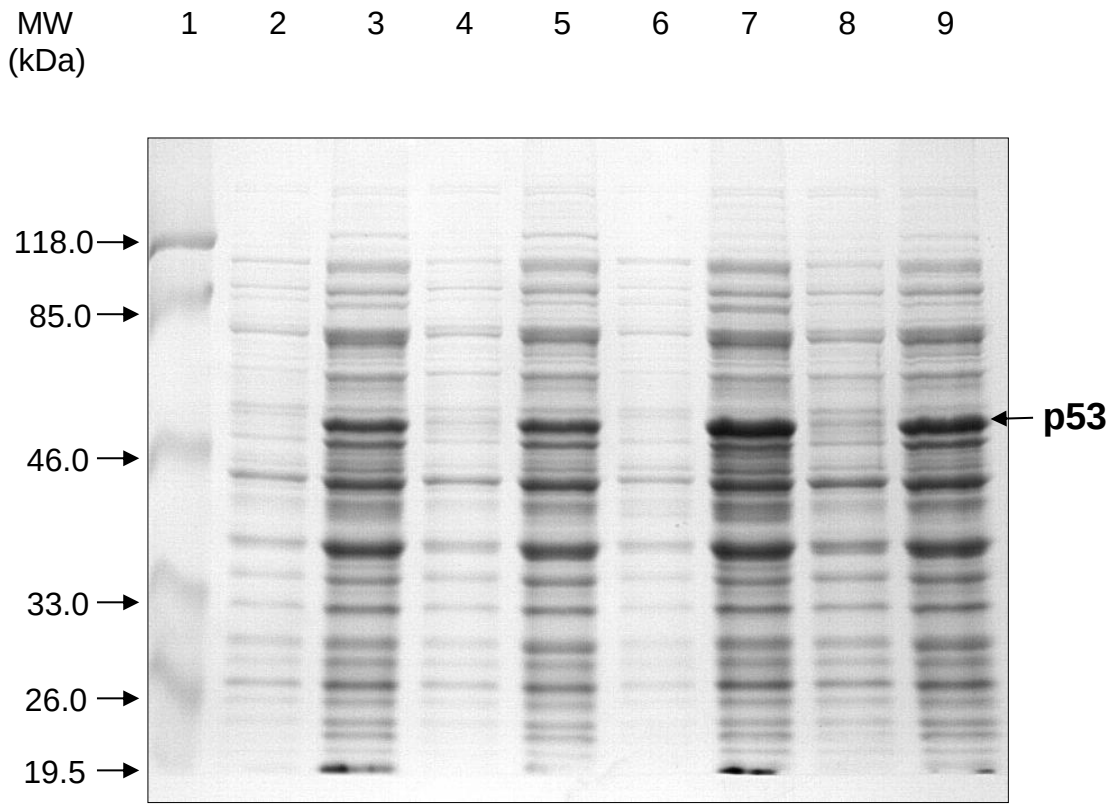

Figure 3.13(a). A 10% SDS PAGE gel showing optimisation of p53 expression in *E. coli* strains BL21(DE3) and BL21(DE3) Star both carrying pT7.7Hup53 constructs.

Lane 1 – prestained protein molecular weight markers (Fermentas)

Lane 2 – induced BL21(DE3) cells at OD_{600nm} ~ 0.2 (0 min)

Lane 3 – induced BL21(DE3) cells at OD_{600nm} ~ 0.2 (4 hr)

Lane 4 – induced BL21(DE3) Star cells at OD_{600nm} ~ 0.2 (0 min)

Lane 5 – induced BL21(DE3) Star cells at OD_{600nm} ~ 0.2 (4 hr)

Lane 6 – induced BL21(DE3) cells at OD_{600nm} ~ 0.4 (0 min)

Lane 7 – induced BL21(DE3) cells at OD_{600nm} ~ 0.4 (4 hr)

Lane 8 – induced BL21(DE3) Star cells at OD_{600nm} ~ 0.4 (0 min)

Lane 9 – induced BL21(DE3) Star cells at OD_{600nm} ~ 0.4 (4 hr)

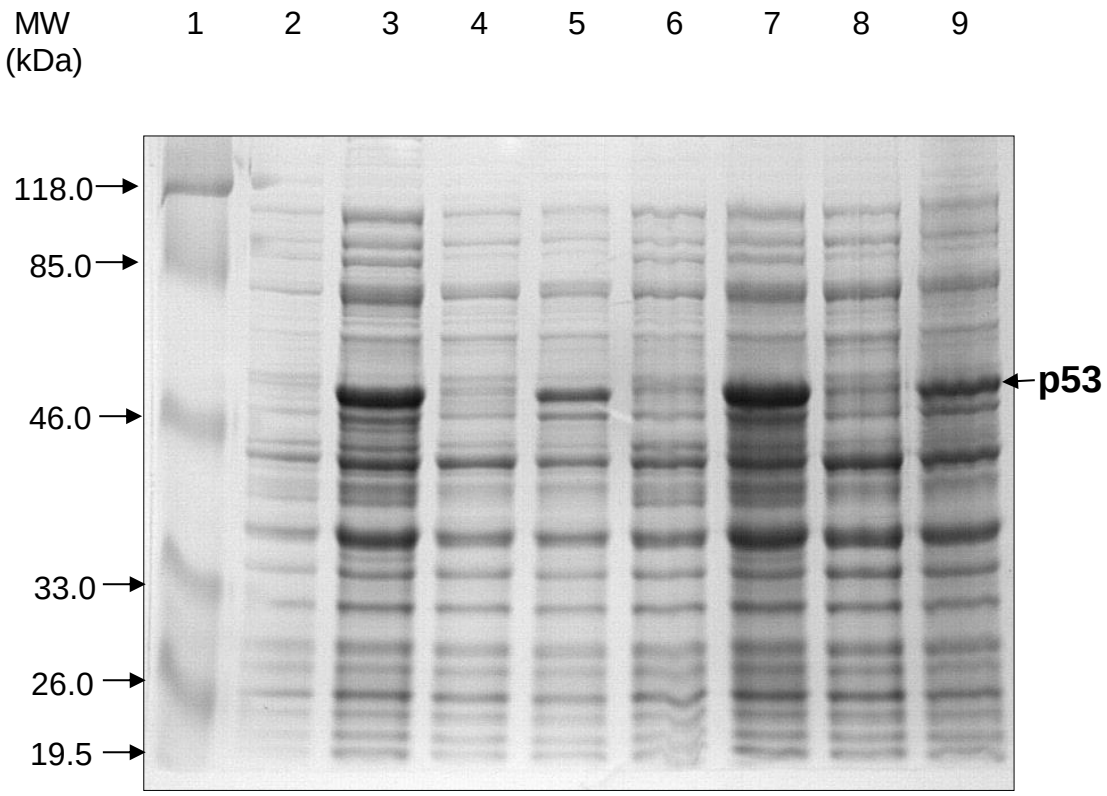

Figure 3.13(b). A 10% SDS PAGE gel showing optimisation of p53 expression in *E. coli* strains BL21(DE3) and BL21(DE3) Star both carrying pT7.7Hup53 constructs.

Lane 1 – prestained protein molecular weight markers (Fermentas)

Lane 2 – induced BL21(DE3) cells at OD_{600nm} ~ 0.6 (0 min)

Lane 3 – induced BL21(DE3) cells at OD_{600nm} ~ 0.6 (4 hr)

Lane 4 – induced BL21(DE3) Star cells at OD_{600nm} ~ 0.6 (0 min)

Lane 5 – induced BL21(DE3) Star cells at OD_{600nm} ~ 0.6 (4 hr)

Lane 6 – induced BL21(DE3) cells at OD_{600nm} ~ 0.8 (0 min)

Lane 7 – induced BL21(DE3) cells at OD_{600nm} ~ 0.8 (4 hr)

Lane 8 – induced BL21(DE3) Star cells at OD_{600nm} ~ 0.8 (0 min)

Lane 9 – induced BL21(DE3) Star cells at OD_{600nm} ~ 0.8 (4 hr)

Finally, the optimum conditions for the expression of p53 protein were determined as follows: pT7.7Hup53 transformed cells were grown at 37^{o}C with vigorous shaking (180 rpm) to OD_{600nm}=0.8-1.0 (late log phase) where bacteria grow at exponential phase giving rise to high yield of bacteria (Scope, 1982) which in turn express more p53 protein upon induction by IPTG, then 1 mM IPTG added to induce p53 protein expression and left to grow for at least 4 hr. Table 3.1 below is a summary of optimal conditions for expression of recombinant p53 protein in BL21(DE3):

Table 3.1: Optimised expression conditions for recombinant p53 protein in *E.coli* BL21(DE3)

Growth temperature	**IPTG concentration**	**Induction OD_{600nm}**	**Duration of growth after addition of IPTG**
37˚C at vigorous shaking at 180 rpm in an orbital shaker	1 mM	0.8-1.0 (late log phase)	At least 4 hrs or let to grow overnight

Figures 3.14 and 3.15 show induction profiles of large scale expression of p53 protein in BL21(DE3) pT7.7Hup53 and BL21(DE3) Star pT7.7Hup53, respectively where cells were harvested every 30 min and assayed by a 10% SDS-PAGE gel. From Figures 3.14 and 3.15, p53 protein expression levels in both BL21(DE3) and BL21(DE3) Star show no major difference. These two induction profiles confirm the previous results (Figures 3.13). Also seen are clear induction of p53 protein though not formally compared with uninduced. More importantly, much more p53 protein was produced at these optimum conditions and subsequently we expected to get more purified p53 protein for the nitration study.

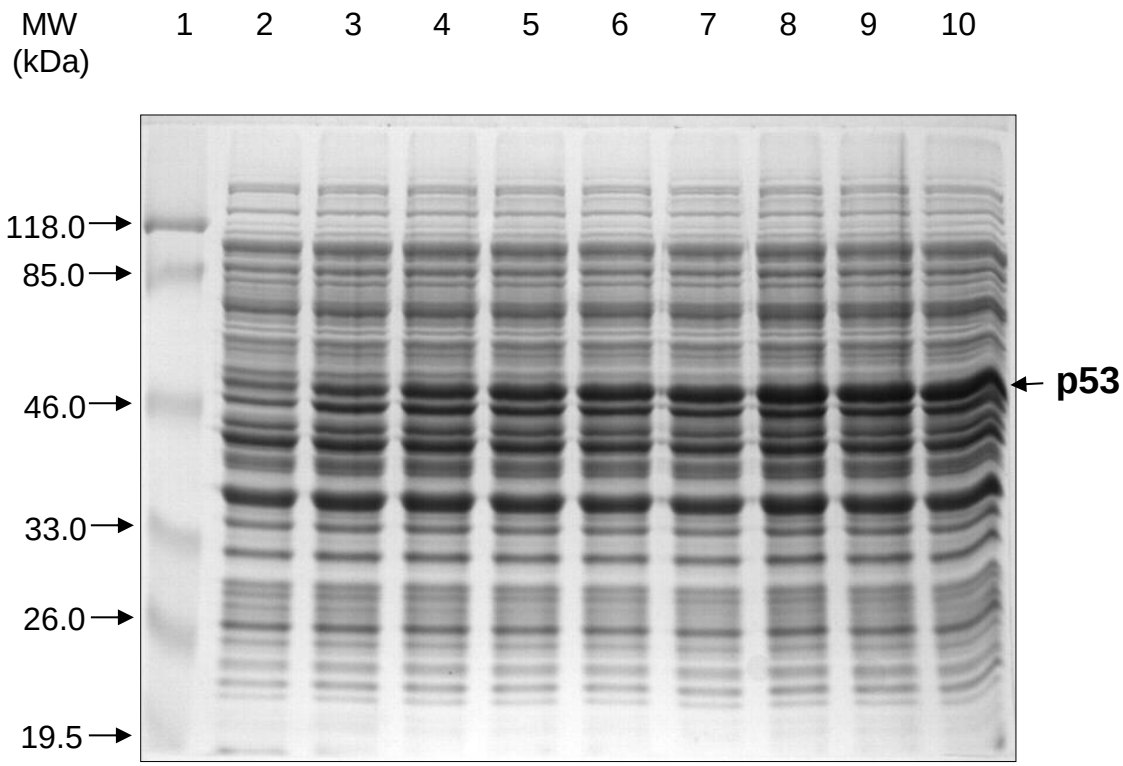

Figure 3.14. A 10% SDS PAGE gel showing a large scale expression of p53 protein induced at OD_{600nm} =0.8-1.0 in *E. coli* strain BL21(DE3) containing a pT7.7Hup53 construct.

Lane 1 – prestained protein molecular weight markers (Fermentas)

Lane 2 – induced cells at 0 min

Lane 3 – induced cells at 30 min

Lane 4 – induced cells at 60 min

Lane 5 – induced cells at 90 min

Lane 6 – induced cells at 120 min

Lane 7 – induced cells at 150 min

Lane 8 – induced cells at 180 min

Lane 9 – induced cells at 210 min

Lane 10 – induced cells at 240 min

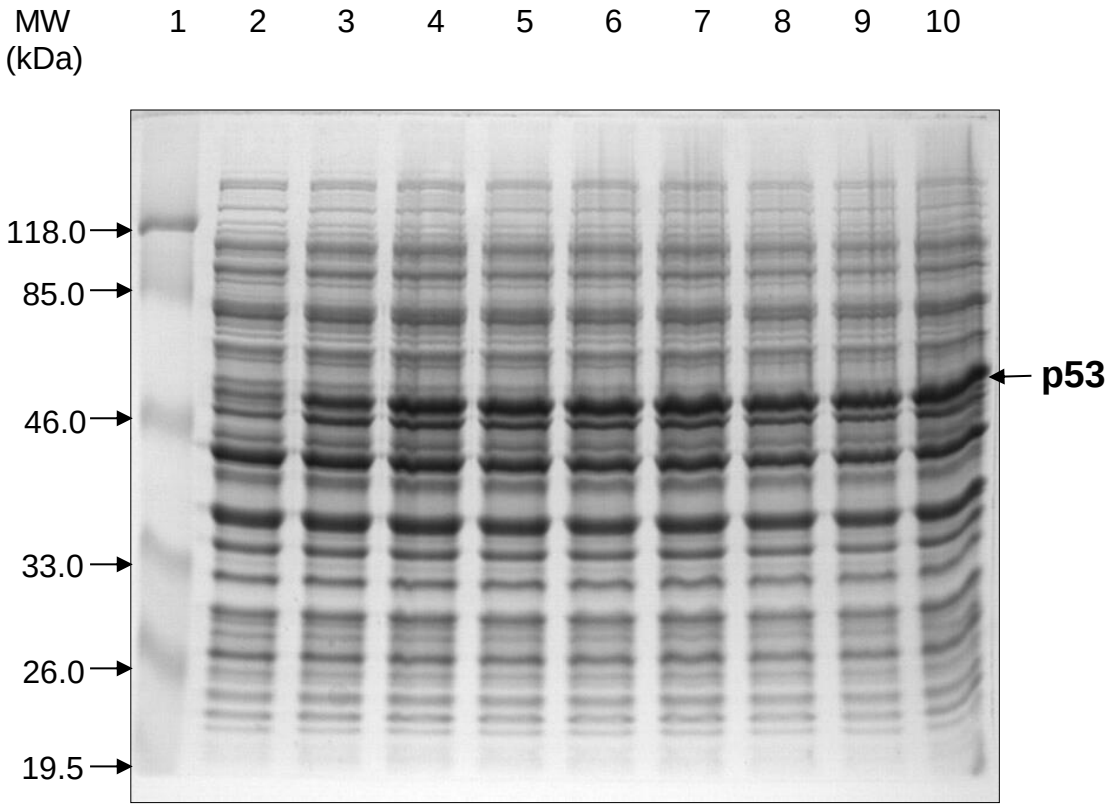

Figure 3.15. A 10% SDS PAGE gel showing a large scale expression of p53 protein induced at OD_{600nm} =0.8-1.0 in *E. coli* strain BL21(DE3) Star containing a pT7.7Hup53 construct.

Lane 1 – prestained protein molecular weight markers (Fermentas)

Lane 2 – induced cells at 0 min

Lane 3 – induced cells at 30 min

Lane 4 – induced cells at 60 min

Lane 5 – induced cells at 90 min

Lane 6 – induced cells at 120 min

Lane 7 – induced cells at 150 min

Lane 8 – induced cells at 180 min

Lane 9 – induced cells at 210 min

Lane 10 – induced cells at 240 min

Large scale p53 protein production using BL21(DE3) transformed with pT7-7Hup53 was then carried out. 12 litres of cultures of BL21(DE3) pT7.7Hup53 were grown until OD_{600n} of 0.8-1.0 prior to the addition of 1 mM IPTG and the cell pellets were re-suspended in 10% sucrose in 50 mM Tris HCl (pH 8.0) and frozen down at -80^{o}C until the cells were lysed, subjected to dialysis and subsequent purification.

3.6 Discussion

A small scale optimisation of the expression of proteins from expression plasmid containing the gene of interest in bacterial expression strains need to be determined before cultivating the bacterial cells in a large scale. The optimisation involved includes determination of which bacterial strain expresses the protein better, the concentration of inducer used such as IPTG and the optimal duration of the induction, the optical density at the start of induction and the optimal temperature for the growth of bacteria as temperature will affect the solubility of the protein. When the optimal conditions of protein expression is determined, a large scale production of the protein can be carried out.

p53 protein is expressed as inclusion bodies at about 98% of the total p53 protein whereas soluble p53 is expressed in the remaining 2% of the total p53 protein. This section mainly purified resolubilised p53 protein from inclusion bodies using a series of column purifications. The inclusion bodies were first resolubilised followed by dialysis for refolding before subjected to purification. The main problem with refolding of p53 protein from resolubilsed p53 protein is that some fractions of the protein were not properly folded causing the partially folded p53 proteins passed through the column as a flowthrough due to their inefficiency in binding to the column. This results in the loss of p53 protein and a low yield of pure p53 protein. Indeed, the conformation of purified p53 protein fractions can be determined by conformation-specific p53 antibodies such as PAb1620 which specifically

recognises the wild-type or native conformation and PAb240 which is specific for the mutant or denatured conformation (Santa Cruz).

In order to get the most expression levels of p53 protein, it is worth trying to express and compare the p53 protein in different bacterial expression strains with improved properties such as BL21(DE3)pLysS, which carry both DE3 lysogen and the plasmid pLysS. pLyS expresses T7 lysozyme to induce the basal expression of target gene through inhibition of T7 RNA polymerase (Novagen). Another strain worth trying is Lemo21(DE3), which is a derivative of BL21(DE3) with tunable T7 expression especially for proteins prone to insoluble expression (New England Biolab, 2013-2014 Catalogue and Technical Reference).

.

RESULTS CHAPTER 4

Both the soluble and insoluble forms of p53 protein were isolated and then separately subjected to a series of purification steps as described by Midgley *et al*. (1992) and Hupp *et al*. (1992). The resolubilised material was to look at nitration sites that might intrinsically be nitrated in the p53 protein, but might not be exposed in the native and active protein. Soluble p53 protein which was considered properly folded and active was to be used to study the effect of nitration on the functional activities of p53 protein such as in DNA-binding assay (EMSA) and in the study of protein-protein interactions between p53 and MDM2 proteins. We also isolated the N-terminus of MDM2 protein as a GST-MDM2 expression construct (a.a. 1-188) (Bottger *et al*., 1996) and a control GST protein from a pGEX-2T construct (Pharmacia) which were subsequently purified to obtain pure proteins to be used in nitration work.

4.1 Preparation of p53 protein

As detailed in the Materials & Methods (Sections 2.10-2.11 & 2.15), the human p53 protein was expressed as soluble (~2%) (in the supernatant of the cell lysate) and insoluble (~98%) (in the pellet of the cell lysate) of the total p53 protein (Hupp *et al*., 1992). The two forms of human p53 protein were purified separately as detailed in the Methods section.

4.1.1 Purification of resolubilised p53 protein

In order to do preliminary nitration work, we needed a large amount of p53 protein to work with which could be easily obtained from resolubilised p53 protein comprising of ~98% from the total p53 protein produced (Hupp *et al*., 1992). Preliminary work included whether p53 protein was easily nitrated at tyrosine residues at varying concentrations of nitrating agent peroxynitrite and to determine the effects of nitration on the stability and levels of p53 protein.

Resolubilised p53 protein expressed in *E. coli* BL21(DE3) strain was purified, according to Hupp *et al*. (1992), from a gradient elution (50 mM to 1 M NaCl in Buffer B) on a 5 ml Hi-Trap Heparin Sepharose column (1.6 cm X 2.5 cm) (Amersham Biosciences) that had been priorly equilibrated with buffer B containing 50 mM NaCl using an FPLC system at a flowrate of 0.5 ml/min where 5 ml fractions were collected in a total of 14 fractions. As can be seen in Fig. 4.1, the resolubilised p53 extract contained high levels of p53 protein (Lane 2, Fig. 4.1(a) and (b)) together with contaminating bacterial proteins. 14 fractions were collected altogether where fractions 1 and 2 were flowthroughs, fractions 3 and 4 were washes with 50 mM NaCl in Buffer B and fractions 5 to 14 were eluted fractions. The absence of the strong p53 band in the fractions 1-4 suggested that renatured p53 protein has bound and in flowthrough fraction 2 (Lane 4, Fig. 4.1(a)), many unbound proteins passed through the column where the protein profile looks similar to wash fraction 3 (Lane 5, Fig. 4.1(a)), leaving behind a few other unbound proteins in wash fraction 4 when passed through the column (Lane 6). In eluted fractions 5 to 14, all other bacterial contaminating proteins were eluted in eluted fractions 5 to 9 and the p53 protein only appeared in eluted fractions 10 to 12 with several other host contaminating proteins, both bigger and smaller sizes than p53 protein. The last two eluted fractions 13 and 14 (Lanes 7-8, Fig. 4.1(b)) did not seem to contain any p53 proteins but had a few low molecular weight proteins which could be p53 degradation products and/or bacterial contaminating proteins. These results were further confirmed by Western blot analyses (Fig. 4.2). As can be seen in Fig. 4.2(a), there were very little p53 proteins with its degradation products throughout flowthrough fractions to eluted fractions 8 (Lanes 3-10, Fig. 4.2(a)). Looking at SDS-PAGE protein profile in Fig. 4.1(b) and its corresponding western blot in Fig. 4.2(b), most of p53 proteins were eluted in fractions 9-14 where all these fractions contained p53 degradation products (sizes lower than p53 protein) as well as p53 non-reducible high molecular weight aggregates (Fig. 4.2(b), Lanes 3-6). If looked closely at, there were high mwt aggregates above 118 kDa marker in Fig. 4.2(b), Lane 2, as well as in Lanes 3-6, which was very much expected as not all the p53 protein had been completely solubilised. Eluted fractions 9-14 purified from Hi-Trap Heparin Sepharose which were

enriched with p53 proteins (Fig. 4.2(b), Lanes 3-8) were pooled together and then were further purified on a Phospocellulose P11 column (Whatman) as done (see Materials & Methods, Section 2.11.3) and described previously by Hupp *et al*. (1992). However, we could not detect any purified resolubilised

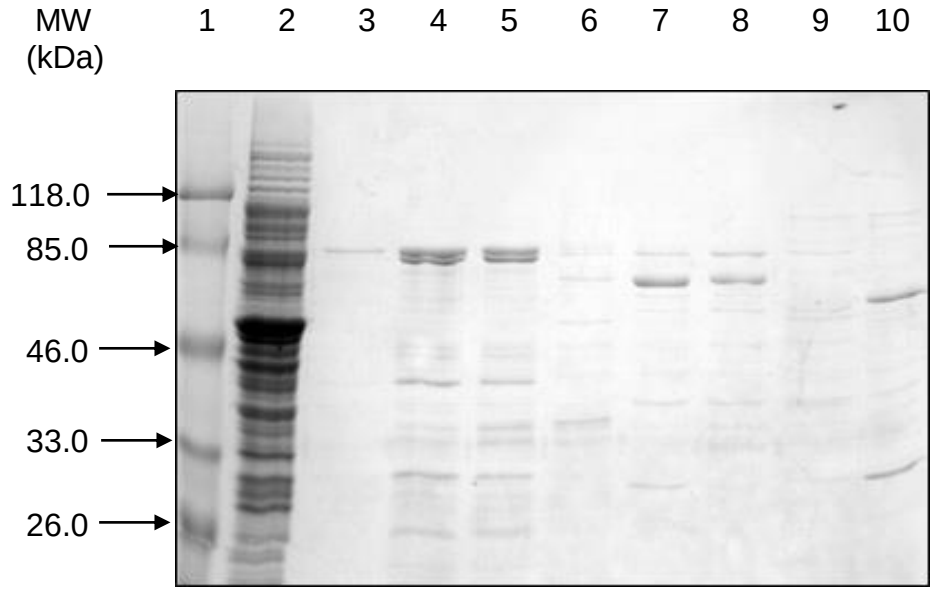

Figure 4.1(a). A 10% SDS PAGE gel showing purification profile of resolubilised p53 protein expressed in *E. coli* BL21(DE3) purified from a gradient elution (50 mM to 1 M NaCl in Buffer B) on a 5 ml Hi-Trap Heparin Sepharose column (1.65 cm X 2.5 cm)(Amersham Biosciences) using an FPLC system. 5 ml fractions were collected. The gel was stained with Coomassie Blue staining.

Lane 1 - prestained protein molecular weight markers (Fermentas)

Lane 2 - resolubilised p53 extract

Lane 3 - fraction 1
Lane 4 - fraction 2
} Flowthrough

Lane 5 - fraction 3
Lane 6 - fraction 4
} Washes with 50 mM NaCl in Buffer B

Lane 7 - fraction 5

Lane 8 - fraction 6

Lane 9 - fraction 7

Lane 10 - fraction 8

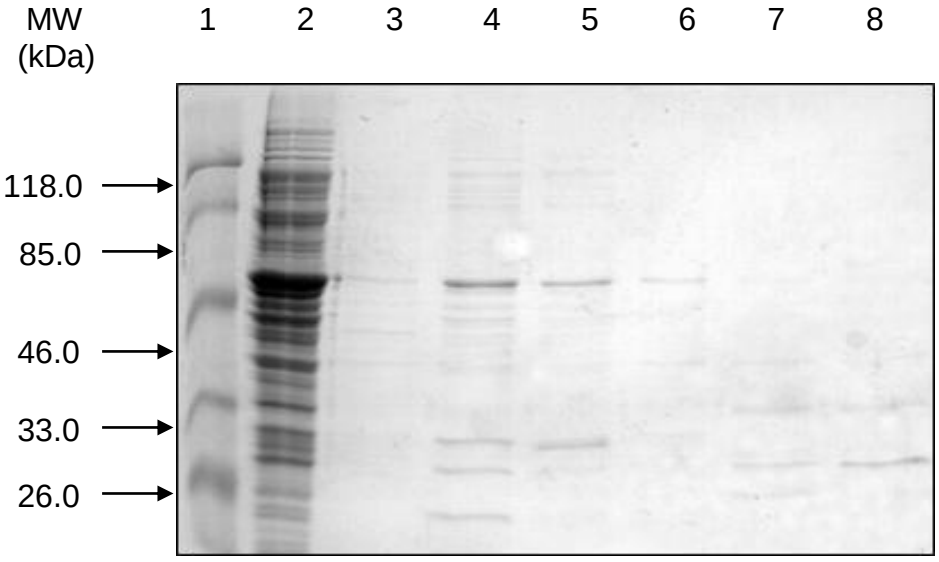

Figure 4.1(b). A 10% SDS PAGE gel showing purification profile of resolubilised p53 protein expressed in *E. coli* BL21(DE3) purified from a gradient elution (50 mM to 1 M NaCl in Buffer B) on a 5 ml Hi-Trap Heparin Sepharose column (1.65 cm X 2.5 cm) (Amersham Biosciences) using an FPLC system. 5 ml fractions were collected. The gel was stained with Coomassie Blue staining.

Lane 1 - prestained protein molecular weight markers (Fermentas)

Lane 2 - resolubilised p53 extract

Lane 3 - fraction 9

Lane 4 - fraction 10

Lane 5 - fraction 11

Lane 6 - fraction 12

Lane 7 - fraction 13

Lane 8 - fraction 14

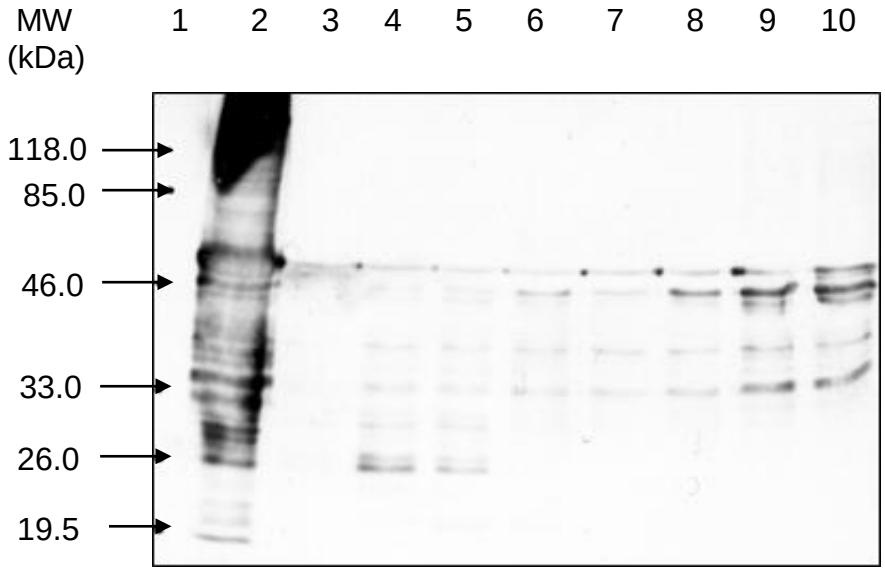

Figure 4.2(a). Western blot analysis showing purification profile of resolubilised p53 protein expressed in *E. coli* BL21(DE3) purified from a gradient elution (50 mM to 1 M NaCl in Buffer B) on a 5 ml Hi-Trap Heparin Sepharose column (1.65 cm X 2.5 cm) (Amersham Biosciences) using an FPLC system. 5 ml fractions were collected. The primary antibody used was mouse monoclonal anti-p53 (DO-1) and the secondary antibody was rabbit anti-mouse HRP conjugated polyclonal antibody (DAKO Cytomation).

Lane 1 - prestained protein molecular weight markers (Fermentas)

Lane 2 - resolubilised p53 extract

Lane 3 - fraction 1
Lane 4 - fraction 2
} Flowthrough

Lane 5 - fraction 3
Lane 6 - fraction 4
} Washes with 50 mM NaCl in Buffer B

Lane 7 - fraction 5

Lane 8 - fraction 6

Lane 9 - fraction 7

Lane 10 - fraction 8

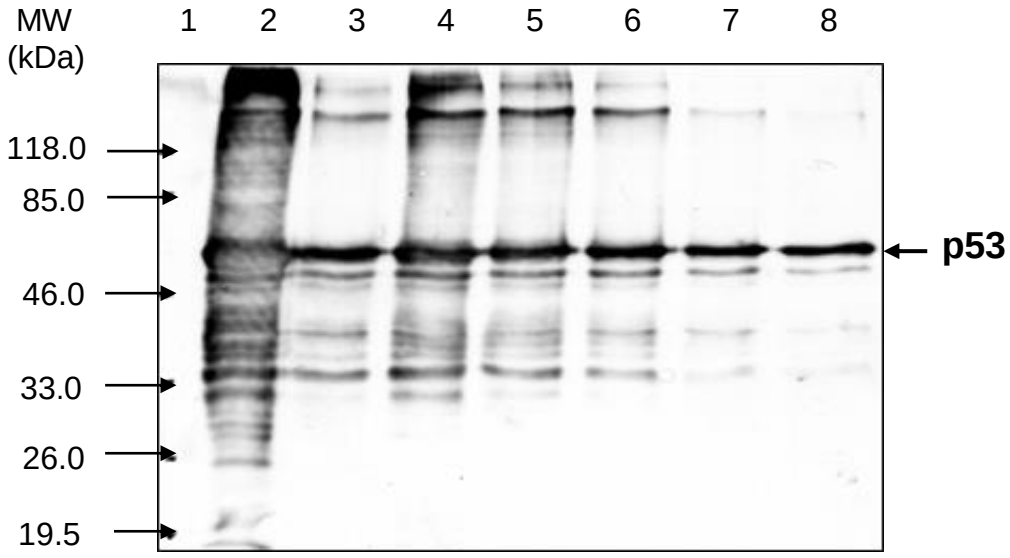

Figure 4.2(b). Western blot analysis showing purification profile of resolubilised p53 protein expressed in *E. coli* BL21(DE3) purified from a gradient elution (50 mM to 1 M NaCl in Buffer B) on a 5 ml Hi-Trap Heparin Sepharose column (1.65 cm X 2.5 cm) (Amersham Biosciences) using an FPLC system. 5 ml fractions were collected. The primary antibody used was mouse monoclonal anti-p53 (DO-1) and the secondary antibody was rabbit anti-mouse HRP conjugated polyclonal antibody (DAKO Cytomation).

Lane 1 – prestained protein molecular weight markers (Fermentas)

Lane 2 – resolubilised p53 extract

Lane 3 – fraction 9

Lane 4 - fraction 10

Lane 5 - fraction 11

Lane 6 - fraction 12

Lane 7 - fraction 13

Lane 8 - fraction 14

p53 protein on SDS-PAGE gels as it was likely due to the low levels of resolubilised p53 protein in the pooled fractions starting material (data not shown). As this problem persisted, it was decided not to proceed further purification with Phosphocellulose P-11 column but instead to purify and concentrate resolubilised p53 protein with a Centricon-30 with 30 kDa cut-off point in order to get purified resolubilised p53 protein.

4.1.2 Purification of soluble p53 protein

Since soluble p53 protein only constitutes ~ 2% of the total p53 protein expressed in *E. coli*, therefore it was quite a challenge to isolate it and subsequently purify it. This would require a substantial amount of soluble cell lysate, from at least several litres of IPTG-induced *E. coli* BL21(DE3) bacterial strain transformed with pT7.7Hup53 followed by purification. The preparation and purification of the soluble p53 protein was described in the Materials & Methods, Sections 2.10 & 2.15. The SDS-PAGE purification profile of soluble p53 protein is shown in Fig. 4.3. As can be seen in Fig. 4.3(a) and (b), Lane 2, there was a lot of soluble p53 protein in the initial lysate which was confirmed in Western blot analyses in Fig. 4.4(a) and (b), Lane 2. However, a lot of soluble p53 protein together with a lot of bacterial contaminating proteins passed through the column in flowthrough fraction 2 and wash fraction 3 (Lanes 4 and 5, respectively). This means that a big fraction of soluble p53 protein did not bind to the resin and therefore passed through the column. In the SDS-PAGE gel soluble p53 protein purification profiles, Figs. 4.3(a) and (b), we can only see that most purified soluble p53 proteins were eluted at fractions 9 and 10. This might be due to the soluble p53 was not in the correct conformation to bind to the resin and/or the charges on the soluble p53 protein was not balanced or not in the correct

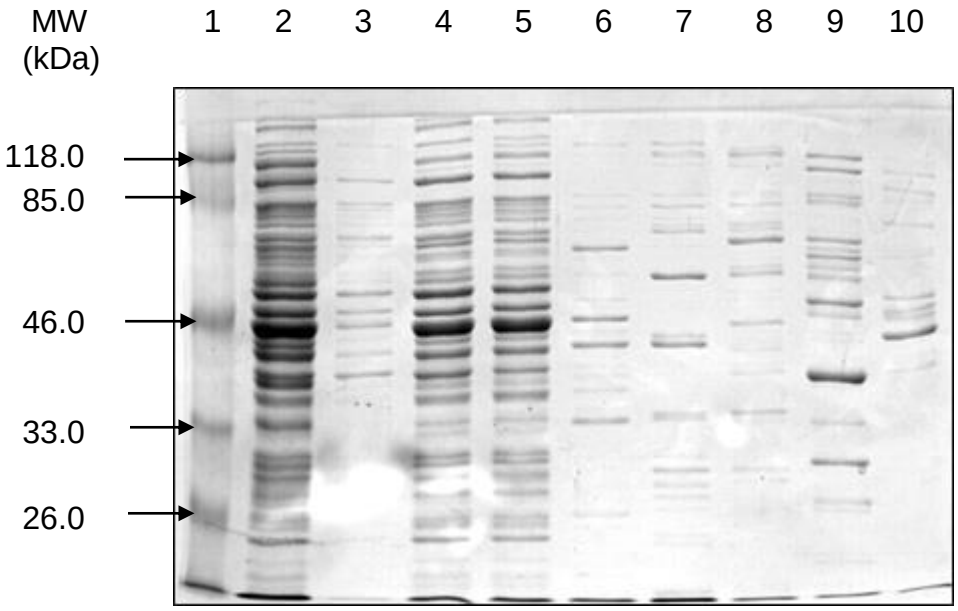

Figure 4.3(a). A 10% SDS PAGE gel showing purification profile of soluble p53 protein expressed in *E. coli* BL21(DE3) purified from a gradient elution (50 mM to 1 M KCl in Buffer C) on a 5 ml Hi-Trap Heparin Sepharose column (1.65 cm X 2.5 cm) (Amersham Biosciences) using an FPLC system. 5 ml fractions were collected. The gel was stained with Coomassie Blue staining.

Lane 1 - prestained protein molecular weight markers (Fermentas)

Lane 2 - non-purified soluble p53

Lane 3 - Fraction 1
Lane 4 - Fraction 2
} Flowthrough

Lane 5 - Fraction 3
Lane 6 - Fraction 4
} Washes with 50 mM KCl in Buffer C

Lane 7 - Fraction 5

Lane 8 - Fraction 6

Lane 9 - Fraction 7

Lane 10 - Fraction 8

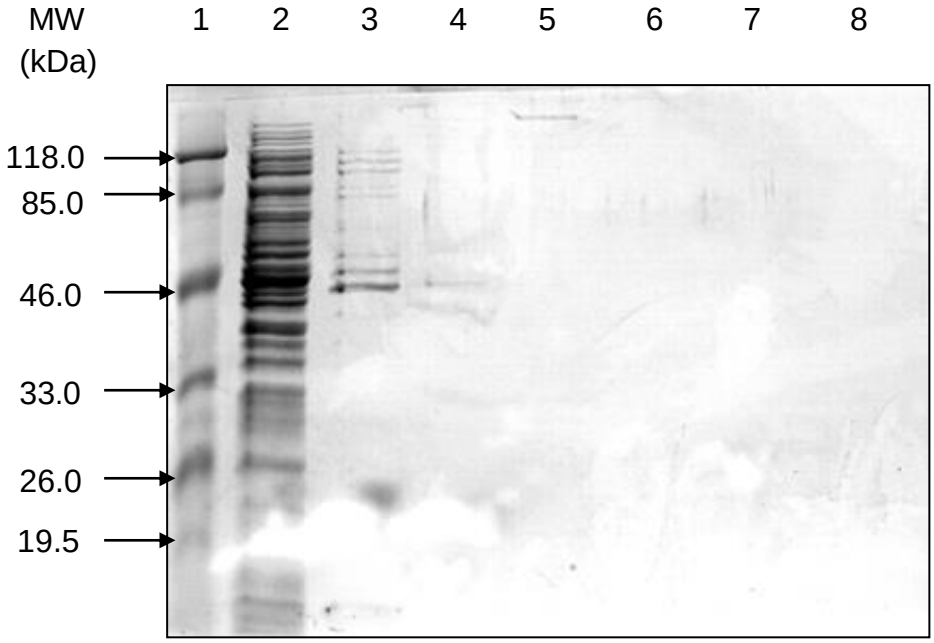

Figure 4.3(b). A 10% SDS PAGE gel showing purification profile of soluble p53 protein expressed in *E. coli* BL21(DE3) purified from a gradient elution (50 mM to 1 M KCl in Buffer C) on a 5 ml Hi-Trap Heparin Sepharose column (1.65 cm X 2.5 cm) (Amersham Biosciences) using an FPLC system. 5 ml fractions were collected. The gel was stained with Coomassie Blue staining.

Lane 1 - prestained protein molecular weight markers (Fermentas)

Lane 2 - non-purified soluble p53

Lane 3 - Fraction 9

Lane 4 - Fraction 10

Lane 5 - Fraction 11

Lane 6 - Fraction 12

Lane 7 - Fraction 13

Lane 8 - Fraction 14

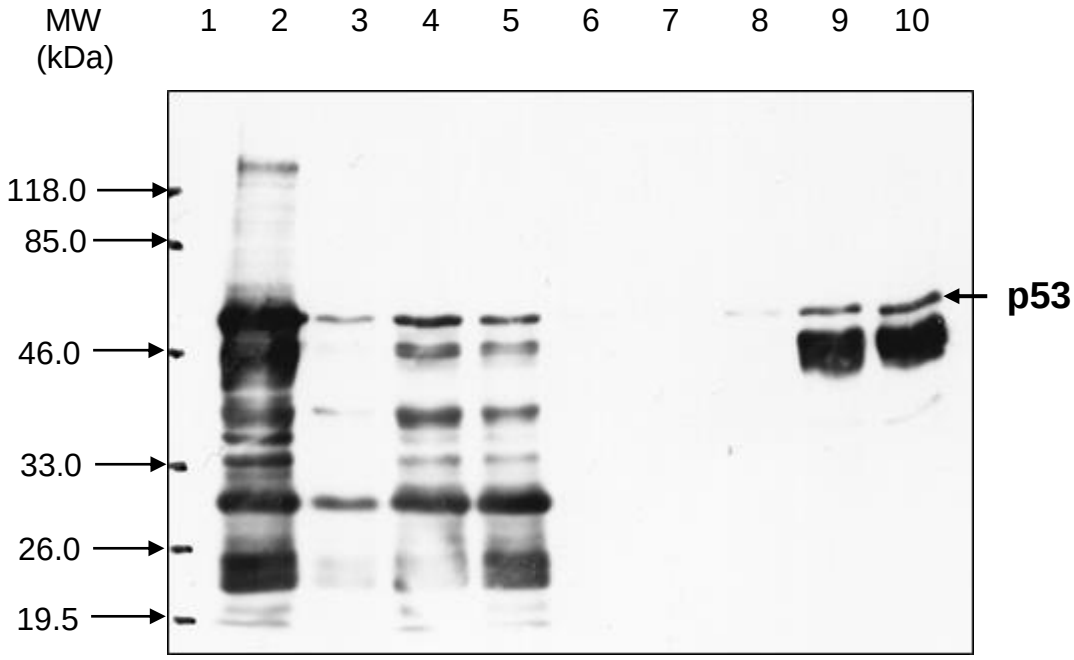

Figure 4.4(a). Western blot analysis showing purification profile of soluble p53 protein expressed in *E. coli* BL21(DE3) purified from a linear gradient elution (50 mM to 1 M KCl in Buffer C) on a 5 ml Hi-Trap Heparin Sepharose column (1.65 cm X 2.5 cm) (Amersham Biosciences) using an FPLC system. The primary antibody used was mouse monoclonal anti-p53 (DO-1) and the secondary antibody was rabbit anti-mouse HRP conjugated polyclonal antibody.

Lane 1 - prestained protein molecular weight markers (Fermentas)

Lane 2 - non-purified soluble p53

Lane 3 - Fraction 1
Lane 4 - Fraction 2
} Flowthrough

Lane 5 - Fraction 3
Lane 6 - Fraction 4
} Washes with 50 mM KCl in Buffer C

Lane 7 - Fraction 5

Lane 8 - Fraction 6

Lane 9 - Fraction 7

Lane 10 - Fraction 8

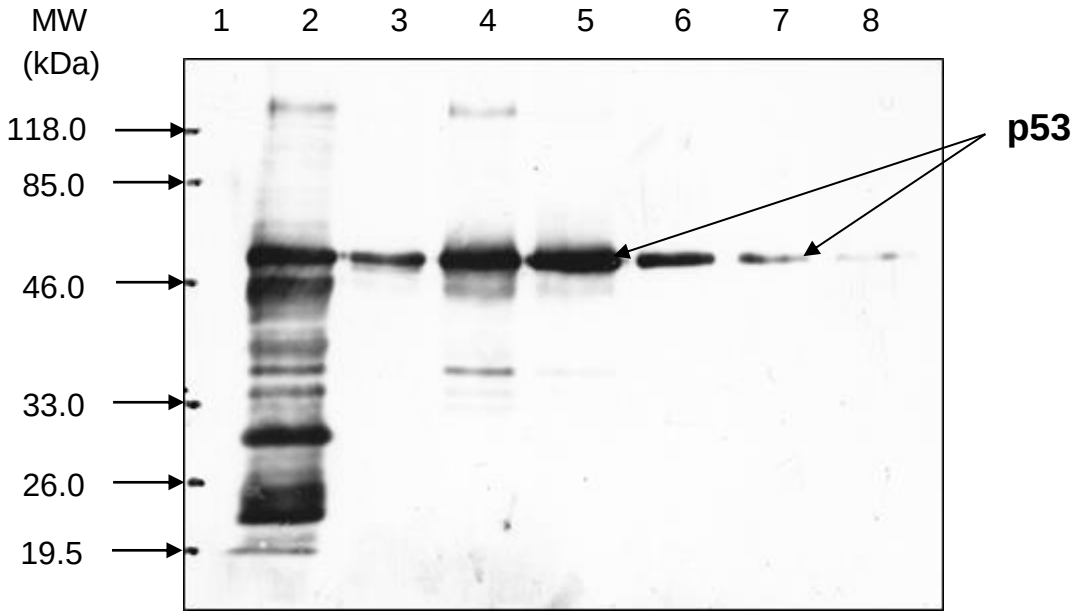

Figure 4.4(b). Western blot analysis showing purification profile of soluble p53 protein expressed in *E. coli* BL21(DE3) purified from a linear gradient elution (50 mM to 1 M KCl in Buffer C) on a 5 ml Hi-Trap Heparin Sepharose column (1.65 cm X 2.5 cm) (Amersham Biosciences) using an FPLC system**.** The primary antibody used was mouse monoclonal anti-p53 (DO-1) and the secondary antibody was rabbit anti-mouse HRP conjugated polyclonal antibody (DAKO Cytomation).

Lane 1 - prestained protein molecular weight markers (Fermentas)

Lane 2 - non-purified soluble p53

Lane 3 - Fraction 9

Lane 4 - Fraction 10

Lane 5 - Fraction 11

Lane 6 - Fraction 12

Lane 7 - Fraction 13

Lane 8 - Fraction 14

ratio with the charges on the resin thus their binding was weak resulting in a large fraction of soluble p53 protein passed through the column. However, Western blot analyses (Figs. 4.4(a) and (b)) show that purified full length soluble p53 proteins were mostly obtained in eluted fractions 9-13 (Figs. 4.4(b), Lanes 3-7). Eluted fractions 7 and 8 were predominantly p53 degradation products. Therefore we selected and pooled together eluted fractions 9-13 for further purification on a Superose 12 gel filtration column.

Before proceeding with gel filtration purification on a Superose 12 gel filtration column (10 mm X 310 mm) (Amersham Biosciences), the column had to be calibrated with gel filtration molecular weight markers (following protocol from Sigma gel filtration molecular weight markers) on a 30 ml gel filtration column using an FPLC system at a flowrate of 0.2 ml/min. Blue Dextran (2000 kDa) was used to determine the void volume (V_o). The other protein markers were eluted from the column according to their molecular weights, the heavier the earlier. Fig. 4.5 shows the elution profile of gel filtration molecular weight markers as they passed through the gel filtration column. The elution volume (V_e) of each protein marker was determined from the distance of their peaks to the starting point. The V_e / V_o ratio for each protein marker was then determined and the gel filtration markers standard curve was generated by plotting log molecular weights versus the V_e / V_o ratio (Fig. 4.6).

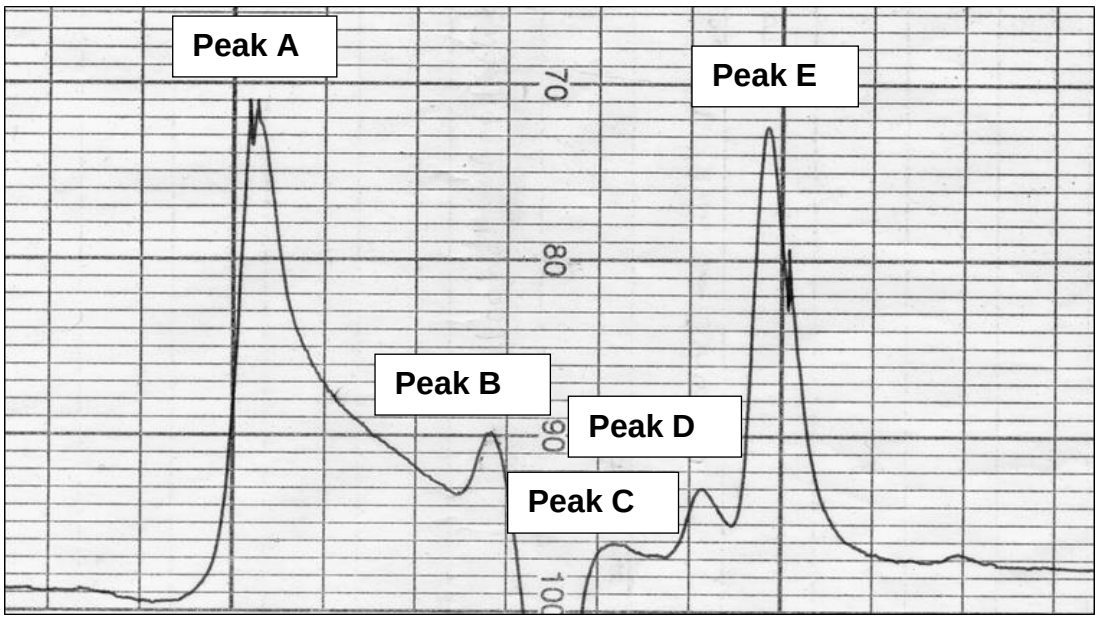

Figure 4.5. A chart showing distinct peaks produced when gel filtration molecular weight markers (Sigma) were passed through a 30 ml gel filtration column Superose 12 (10 mm X 310 mm) (Amersham Biosciences) at a flowrate of 0.2 ml/min using an FPLC system. These proteins eluted from the column according to their molecular weights, the heavier the earlier.

Peak A - Blue Dextran, 2000 kDa (V_o = 11.1)

Peak B - Alcohol Dehydrogenase, 150 kDa (V_e = 15.3)

Peak C - Bovine Serum Albumin, 66 kDa (Ve =16.9)

Peak D - Carbonic Anhydrase, 29 kDa (Ve = 18.2)

Peak E - Cytochrome c, 12.4 kDa (Ve =19.3)

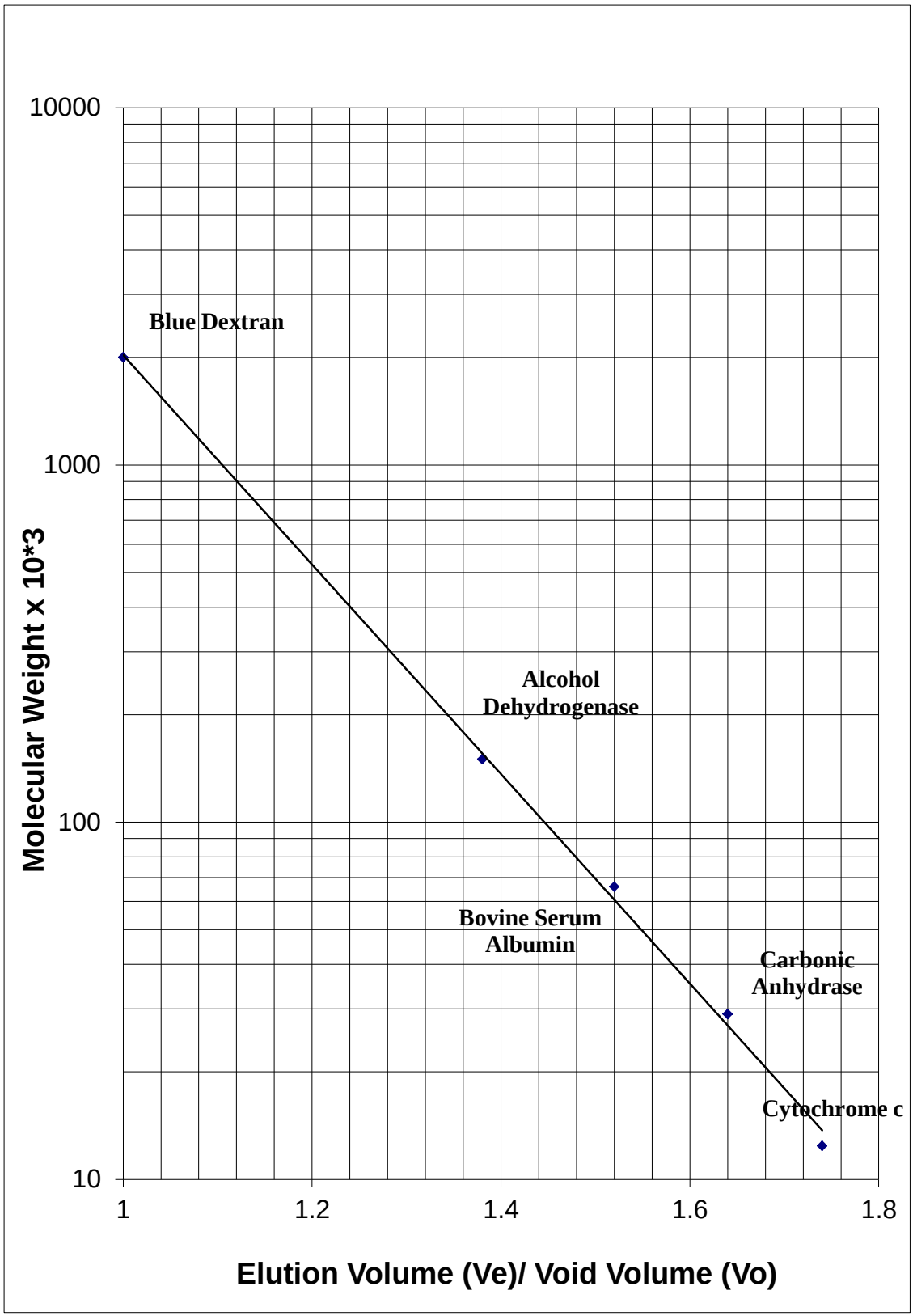

Figure 4.6. Standard curve for gel filtration markers

Table 4.1 below shows the values for V_e and V_e / V_o ratio of gel filtration molecular weight markers (from Sigma).

Table 4.1: Showing V_e and V_e / V_o ratio of gel filtration molecular weight markers with their molecular weights indicated

Components	MW (kDa)	V_e	V_e / V_o
Blue Dextran	2000	11.1	1.00
Alcohol Dehydrogenase	150	15.3	1.38
Bovine Serum Albumin (BSA)	66	16.9	1.52
Carbonic Anhydrase	29	18.2	1.64
Cytochrome c	12.4	19.3	1.74

* Void volume (V_o) for Blue Dextran was 11.1

The next step was to further purify p53 protein isolated from the Hi-Trap Heparin sepharose purification procedure. Fractions 9-13 which were enriched in p53 protein were pooled together and further purified and concentrated by ultrafiltration using a Centricon-30 with 30 kDa cut-off point before being loaded onto Superose 12 gel filtration column for further purification. Several batches of p53 gel filtration purifications of soluble p53 protein on Superose 12 column were carried out at a flowrate of 0.2 ml/min where 1 ml fractions were collected in a total of 30 fractions. All the 30 fractions from the first purification batch were then run on SDS-PAGE gels and then subjected to Western blot analysis in order to screen for which fractions contained the purified soluble p53 proteins. From Western blots of the 30 fractions from the first batch purification we found that most of purified soluble p53 protein was in eluted fractions 9 to 16. Therefore, in subsequent gel filtration purifications of soluble p53 proteins only eluted fractions 9 to 16 were run on an SDS-PAGE gel and then electroblotted for Western blot analysis. However, there were variations in the degree of p53 protein being eluted in these fractions between batch to batch but a representative blot Fig. 4.7 shows high amounts of soluble p53 proteins were detected in eluted fractions 10 to 12 (Lanes 4-6). Weak p53 signals in fractions 9, 13 and 14 (Lanes 3, 7 and 8, respectively) (refer Table 4.2 for the calculated masses of

these fractions). No signals were detected in eluted fractions 15 and 16 (Lanes 9 and 10, respectively). From the calculation of p53 elution volume in corresponse to its molecular weight, it is expected that p53 protein as a tetramer is eluted between fractions 14 and 15 when taking into account the masses of p53 monomer, 43-53 kDa obtained (43 kDa is obtained by multiplying 393 a.a. of p53 protein sequence with the average amino acid mass of 110 Da and 53 kDa is observed as an apparent mass of p53 protein migrating in denaturing SDS-polyacrylamide gel) multiplied by 4, so the masses of p53 tetramers will be between 172-212 kDa which contradict with our findings shown by western blot analysis Fig. 4.7 as described above where most p53 protein was eluted from fractions as early as fraction 9 throughout fraction 14 and none p53 protein was eluted in fractions 15 and beyond. As mass/molecular weight is indirectly proportional to elution volume (see gel filtration standard curve Fig. 4.6), thus bigger mass has low elution volume so elutes earlier than smaller mass with high elution volume. The bigger p53 protein masses obtained in this experiment (especially fractions earlier than fraction 14) show that p53 protein masses eluted were between 350-1700 kDa which were 2-10 fold higher than the masses of the expected p53 protein tetramers (Table 4.2). This might be due to the p53 protein tetramers clumped to each other to form multiple of tetramers/oligomers under the buffer condition parameters used (pH, ionic strength and temperature). This is not surprising as p53 forms tetramers in solution, which is the form p53 protein predominantly assembled both *in vitro* and *in vivo* (Friedman *et al*., 1993; Wang *et al*., 1994; review in Okorokov and Orlova, 2009) but the evidence for multiples of tetramers i.e. 2-10x tetramers, is weak. However, we still pooled fractions 9-14 since western blot analysis showed the p53 protein was enriched in these fractions and thus could then be used for later nitration work.

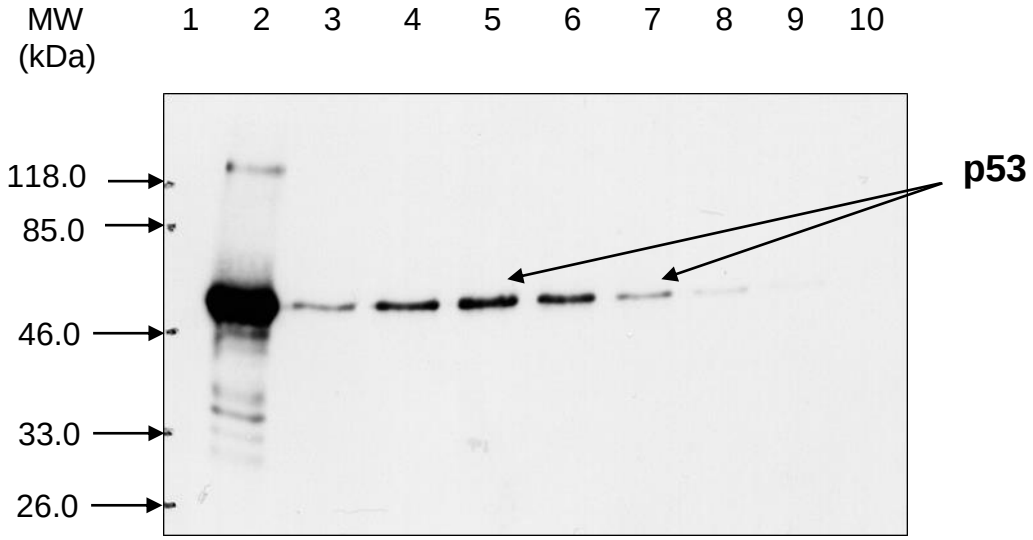

Figure 4.7. Western blot analysis showing purification of soluble p53 protein expressed in *E. coli* BL21(DE3) purified from Superose 12 gel filtration column (10 mm X 310 mm)(Amersham Biosciences) using an FPLC system. 26 fractions were collected altogether, 1 ml each. Eluted fractions 9-16, where expected soluble p53 protein were eluted, were selected and run onto an SDS-PAGE gel and then electroblotted. The volumes of the samples loaded were 20 µl. The primary antibody used was mouse monoclonal anti-p53 (DO-1) and the secondary antibody was rabbit anti-mouse HRP conjugated polyclonal antibody (DAKO Cytomation).

Lane 1 - prestained protein molecular weight markers (Fermentas)

Lane 2 - soluble p53 extract

Lane 3 - eluted fraction 9

Lane 4 - eluted fraction 10

Lane 5 - eluted fraction 11

Lane 6 - eluted fraction 12

Lane 7 - eluted fraction 13

Lane 8 - eluted fraction 14

Lane 9 - eluted fraction 15

Lane 10 - eluted fraction 16

Table 4.2: Showing the masses of p53 protein at fractions 9-14 determined from the gel filtration standard curve (Fig. 4.6) by the correlation of the V_e / V_o ratio of each fraction to their masses

Fractions	V_e	V_e / V_o	Masses (kDa)
9	9	0.81	1700
10	10	0.90	1290
11	11	0.99	1100
12	12	1.08	1030
13	13	1.17	650
14	14	1.26	350

* Void volume (V_o) for Blue Dextran was 11.1

4.2 Expression and purification of GST and GST-MDM2 proteins

MDM2 protein is known to be a negative regulator of p53 protein by inactivating p53 transcriptional activity by masking the N-terminal region [mapped at residues 18-23 (TFSDLW)] (Picksley *et al*., 1994; Bottger *et al*., 1996) of p53 protein from binding to its transcriptional machinery proteins and it also ubiquitinates p53 protein, shuttles p53 protein from the nucleus to the cytoplasm and finally targets p53 protein for 26S proteosomal degradation in the cytoplasm (Momand *et al*., 1992; Chen *et al*., 1993 & 1995; Oliner *et al.*, 1993; Kussie *et al*., 1996; Moll & Petrenko, 2003). This thus raises the question what will happen to the interactions between p53 and MDM2 proteins when p53 protein is nitrated especially at the N-terminal region where it binds MDM2 protein especially at Trp 23 to form nitro-tryptophan (however no nitro-tryptophan antibody available in the market yet) as Phe19, Trp23 and Leu26 are the most critical contact points (Chen *et al*., 1993; Picksley *et al*., 1994). Will it inhibit their interactions and thus will it lead to p53 protein stabilisation and activity? As MDM2 protein binds p53 protein also through its N-terminal region (residues 1-188 a.a), we also would like to look at the other angle by also attempting to nitrate MDM2 protein and hopefully to gain insights of the effects of nitrated MDM2 protein on its interaction with p53 protein. This is because 2 tyrosine residues, located at

amino acids 54 and 61 at the N-terminal region of MDM2 protein, are potential targets for nitration to form nitro-tyrosines.

In this work, we also heterologously overexpressed GST-MDM2 fusion protein from the expression construct of Bottger *et al*. (1996) by which a PCR product of human MDM2 cDNA (encompassing a.a. 1-188) was ligated into the pGEX-2T plasmid (Pharmacia). GST protein, as a control protein, was obtained form the expression plasmid pGEX-2T (Pharmacia). The plasmids were then introduced to *E. coli* BL21 strains (Bottger *et al*., 1996; Bottger *et al*., 1997) and the protein expression was induced by 1 mM IPTG for 4 hrs at 37°C before being harvested. This was then followed by a batch purification of the proteins using Glutathione Sepharose 4B (Amersham Biosciences). The purpose of this work was to prepare purified GST-MDM2 protein and its control protein GST, either being nitrated or not, for future experiments to see their effects on the interactions with both nitrated and non-nitrated p53 protein. But first we needed to do a small scale expression of GST and GST-MDM2 proteins in order to determine the optimal conditions for the expression of both proteins.

4.2.1 Small scale expression of GST and GST-MDM2 in *E. coli* BL21 strain

In order to determine the optimal expression conditions for GST and GST-MDM2 proteins**,** *E. coli* BL21 strains transformed either with pGEX-2T or pGEX-2T-MDM2 carrying the GST-MDM2 fusion protein were grown at a small scale until late log phase, the $OD_{600\ nm}$ of ~ 0.8 – 1.0 before they were induced by the addition of IPTG to 1 mM. Uninduced BL21 strain transformed with pGEX-2T-MDM2 and induced BL21 alone were also grown in parallel. Growth curves for the 4 cultures were plotted as shown in Fig. 4.8 (BL21 + IPTG and pGEX-2T + IPTG served as controls. The IPTG-induced BL21 cultures either untransformed or transformed with pGEX-2T-MDM2 or transformed with pGEX-2T vector showed similar growth curves where their $OD_{600\ nm}$ values increased gradually when compared to the uninduced pGEX-2T-MDM2 transformed BL21 with markedly increased in $OD_{600\ nm}$

values. This showed that IPTG induction retarded the growth of the BL21 strain. Another way to explain this observation is by a direct comparison of the BL21 cultures transformed with pGEX-2T-MDM2 either induced with IPTG or not indicated that the expression relied on a strong promoter that dominated cellular transcription making the GST-MDM2 protein in the IPTG-induced transformed BL21, consequently their own growth was halted. Thus, we can see that in the uninduced transformed BL21 the cells kept growing since they did not produce foreign proteins.

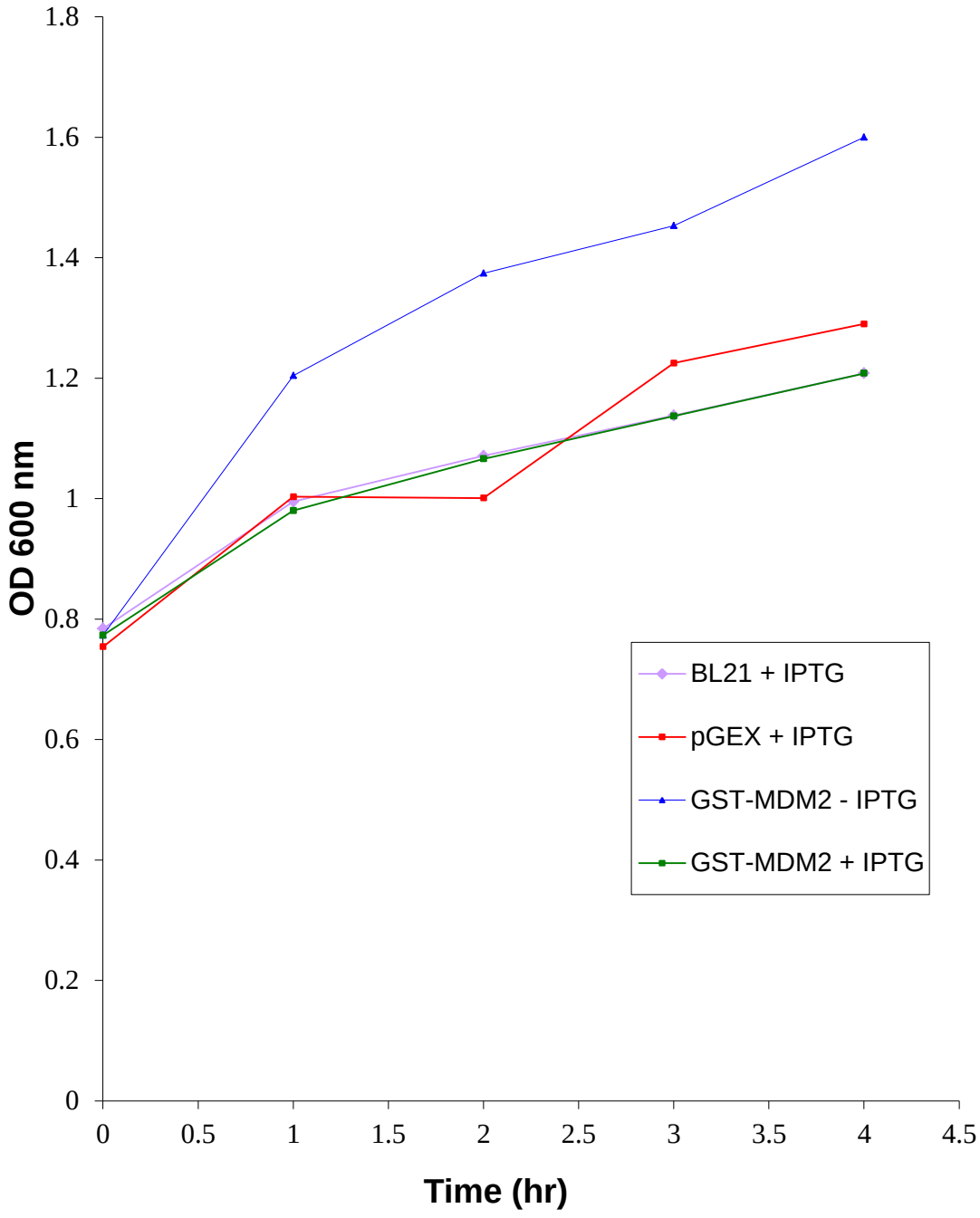

Figure 4.8. Growth curve of BL21 either untransformed or transformed with pGEX-2T or pGEX-2T-MDM2 and either non-induced or induced with 1 mM IPTG for a period of 4 hrs.

4.2.2 Uninduced and IPTG induction profiles of GST-MDM2 protein

1 ml of each culture was also removed and then pelleted at 13,000 rpm for 2 min and the pellets were resuspended in SDS loading dye with freshly added 1 mM reducing agent DTT. The cultures were removed at 0 time and every hour until 4 hrs period after IPTG addition. Fig. 4.9 shows the uninduced GST-MDM2 protein profile together with untransformed BL21 and BL21 transformed with pGEX-2T vector, both uninduced, as experimental controls (Lanes 2 and 3, respectively). A 4 hrs-IPTG-induced pGEX-2T-MDM2 transformed BL21 was used as a positive control for GST-MDM2 protein expression (Lane 9). In this profile, we can see that the levels of GST-MDM2 protein slightly increased from 1 to 4 hrs period even though they were not induced (Lanes 5-8). Hardly any GST-MDM2 protein was seen at 0 time (Lane 4). In order to explain this observation, it was likely due to a leaky promoter where the protein was induced to express even without the inducer IPTG. This explanation is further confirmed by the presence of high levels of GST protein in uninduced pGEX-2T transformed BL21 grown in parallel for 4 hrs (Lane 3). The leaky promoter, however, can be reduced by growing the bacterial BL21 strain in Minimal Media (M63, M9 etc.) which contain minimum nutrients typically glucose as a carbon source for bacterial growth (Studier *et al*., 1990). However, we did not do this because we were not going to do further work with the uninduced bacterial cells and only the IPTG-induced cells were to be lysed to purify the GST and GST-MDM2 proteins.

Fig. 4.10 shows an IPTG-induced GST-MDM2 protein profile together with untransformed BL21 and BL21 transformed with pGEX-2T vector, both induced for 4 hrs, as experimental controls (Lanes 2 and 3, respectively). A 4 hrs non-induced pGEX-2T-MDM2 transformed BL21 was used as a negative control eventhough there were some GST-MDM2 proteins present probably due to a leaky promoter as mentioned earlier (Lane 4). As can be seen in Fig. 4.10, there was an increased in the expression levels of GST-MDM2 proteins when induced with IPTG from 0 to 4 hrs. Hardly any GST-MDM2 protein was observed at 0 time induction and the highest levels of GST-MDM2 protein at 4 hrs after induction. This indicates that the optimal

conditions for the expression of GST-MDM2 protein is to IPTG induce the cells at 1 mM at late log phase (~ 0.8-1.0) and then harvesting at least 4 hrs after IPTG addition.

The above results were further verified by Western blot analysis using anti-GST mouse monoclonal antibody HRP-conjugated by selecting only a few samples. In Fig. 4.11, untransformed BL21 IPTG-induced at 0 min and after 4 hrs show no bands as expected as the bacteria did not have any GST or GST-MDM2 genes, and thus no expression of the proteins (Lanes 2 and 3, respectively). These two samples acted as negative controls for the experiment. It can be seen that GST protein was expressed even at 0 min after induction and the levels increased at 4 hrs after the IPTG-induction together with a few smaller sizes degradation products (Lanes 4 and 5). We can also see GST-MDM2 protein being expressed at 0 min after IPTG-induction (Lane 6). GST-MDM2 protein was also expressed in the pGEX-2T-MDM2 transformed BL21 uninduced for 4 hrs (Lane 7). This band confirms the SDS-PAGE result we have in Fig. 4.9, Lane 8. A high level of GST-MDM2 proteins with a lot of smaller sizes degradation products were observed in pGEX-2T-MDM2 transformed BL21 induced with IPTG for 4 hrs. This band confirms the previous SDS-PAGE gel (Fig. 4.10, Lane 9). These degradation products might be due to the proteolysis of the proteins by proteases other than *lon* and *omp*T proteases in BL21 and/or due to the handling of the proteins. Therefore, in order to minimise protein degradation, the protein preparation must be done very fast and the samples should be kept cold on ice all the time.

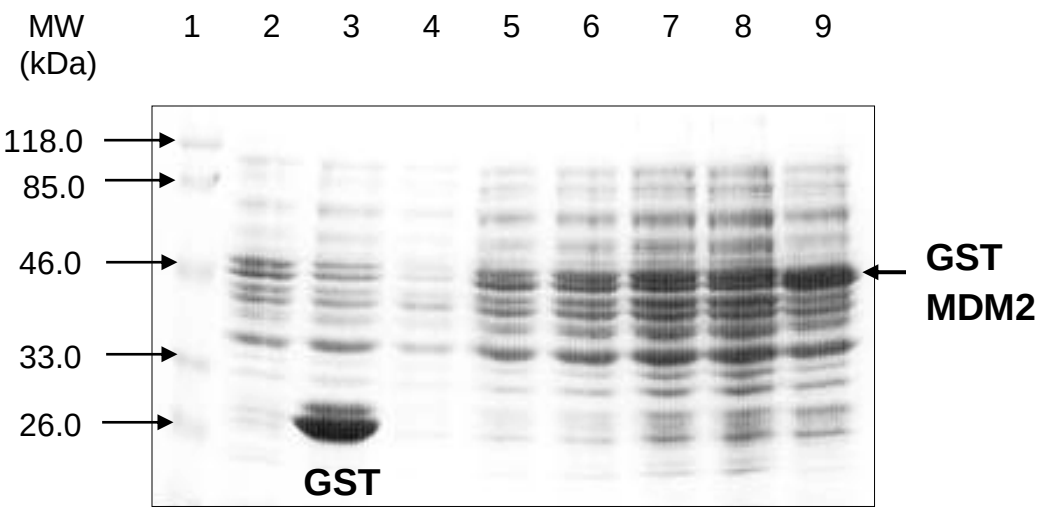

Figure 4.9. A 10% SDS-PAGE gel showing uninduced GST-MDM2 protein. 4 hr- IPTG-induced GST-MDM2 protein was loaded in parallel as a positive control.

Lane 1 - prestained protein molecular weight markers (Fermentas)

Lane 2 - BL21 (4 hr)

Lane 3 - pGEX-2T (4 hr)

Lane 4 - non-induced GST-MDM2 (0 hr)

Lane 5 - non-induced GST-MDM2 (1 hr)

Lane 6 - non-induced GST-MDM2 (2 hr)

Lane 7 - non-induced GST-MDM2 (3 hr)

Lane 8 - non-induced GST-MDM2 (4 hr)

Lane 9 - IPTG-induced GST-MDM2 (4 hr)

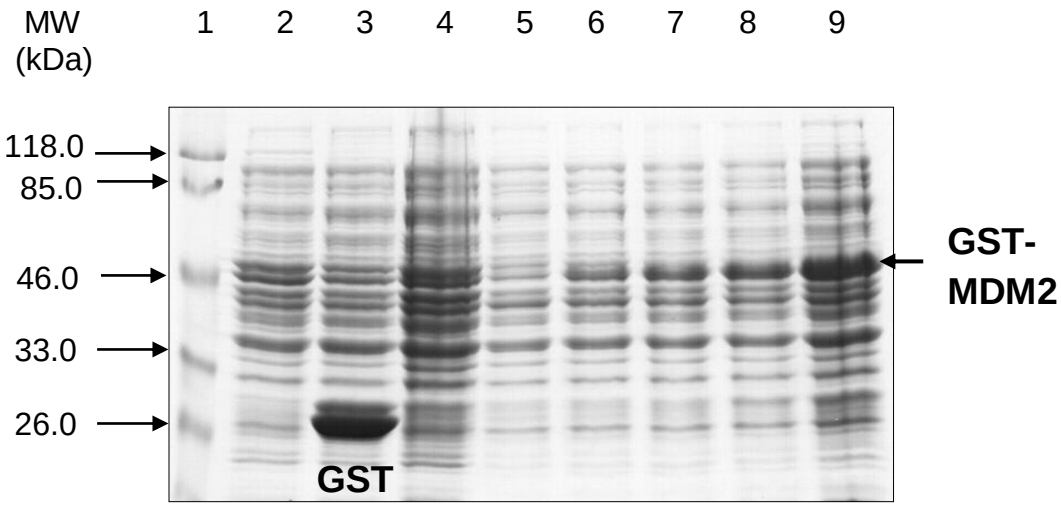

Figure 4.10. A 10% SDS-PAGE gel showing 1 mM IPTG-induced GST-MDM2 protein. 4 hr-uninduced GST-MDM2 was run in parallel as a negative control.

Lane 1 - prestained protein molecular weight markers (Fermentas)

Lane 2 - IPTG-induced BL21 (4 hr)

Lane 3 - IPTG-induced pGEX-2T (4 hr)

Lane 4 - non-induced GST-MDM2 (4 hr)

Lane 5 - IPTG-induced GST-MDM2 (0 hr)

Lane 6 - IPTG-induced GST-MDM2 (1 hr)

Lane 7 - IPTG-induced GST-MDM2 (2 hr)

Lane 8 - IPTG-induced GST-MDM2 (3 hr)

Lane 9 - IPTG-induced GST-MDM2 (4 hr)

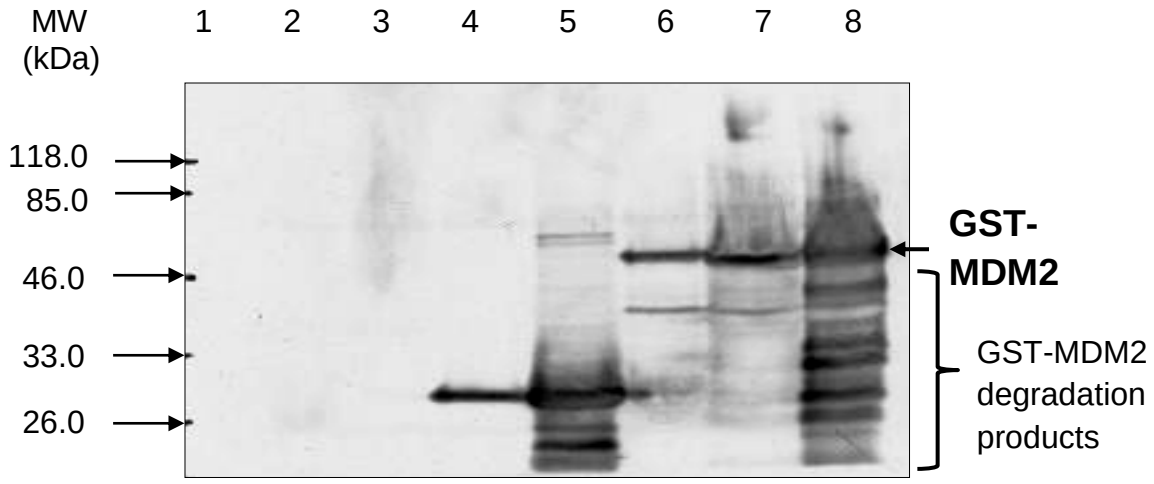

Figure 4.11. A Western blot analysis of pGEX-2T and GST-MDM2 non-induced or induced with 1 mM PTG. The blot was probed with anti-GST mouse monoclonal antibody conjugated with HRP (DAKO Cytomation).

Lane 1 - prestained protein molecular weight markers (Fermentas)

Lane 2 - BL21 (0 min)

Lane 3 - BL21 induced with IPTG (4 hr)

Lane 4 - pGEX-2T (0 min)

Lane 5 - pGEX-2T induced with IPTG (4 hr)

Lane 6 - GST-MDM2 (0 min)

Lane 7 - GST-MDM2 non-induced (4 hr)

Lane 8 - GST-MDM2 induced with IPTG (4 hr)

4.2.3 Large scale expression of GST and GST-MDM2 proteins and their purification using Glutathione Sepharose 4B.

After determining the optimal conditions for the expression of GST and GST-MDM2 proteins i.e. to IPTG induce the cells at 1 mM at late log phase (~ 0.8-1.0) and then harvesting at least 4 hrs after IPTG addition, we then proceeded with a large scale expression of both the proteins followed by a batch purification of the proteins using Glutathione Sepharose 4B (Amersham Biosciences) as described in the Materials and Methods, Section 2.19.2. This was in order to get a large amount of purified GST and GST-MDM2 proteins for nitration work.

4.2.3.1 GST protein gel purification profile

As can be seen in Fig. 4.12, a lot of GST protein among other contaminating host proteins in the sonicated GST lysate (Lane 2). However, hardly any GST protein can be seen in the initial GST lysate (Lane 9). Decreased amounts of GST protein when compared to its amount in the sonicated lysate (Lane 2) were observed in the supernatant after solubilisation and in the supernatant after beads binding (Lanes 3 and 4, respectively). Very pure GST proteins were found in all the three elutions 1, 2 and 3 (Lane 5, 6 and 7, respectively). A lot of GST proteins were found in the GST final beads (Lane 8) which might be due to inefficient or incomplete elution of the protein from the beads. The purified GST proteins in elutions 1, 2 and 3 was verified by western blot analysis using anti-GST mouse monoclonal antibody HRP-conjugated (Fig. 4.13). These results were quite satisfactory as we managed to obtain relatively pure GST proteins with only minor contaminations.

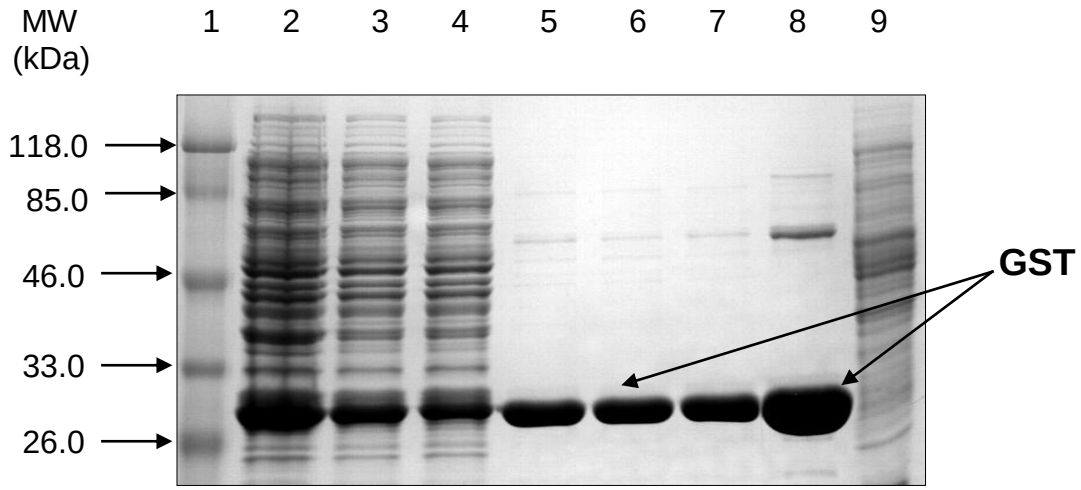

Figure 4.12. A 10% SDS PAGE gel showing a batch purification profile of GST protein using Glutathione Sepharose 4B (Amersham Biosciences). The gel was stained with Coomassie Blue stain for 15 min and then destained overnight.

Lane 1 - prestained protein molecular weight markers (Fermentas)

Lane 2 - sonicated GST lysate

Lane 3 - supernatant after solubilisation

Lane 4 - supernatant after beads binding

Lane 5 - elution 1

Lane 6 - elution 2

Lane 7 - elution 3

Lane 8 - GST final beads

Lane 9 - initial GST lysate

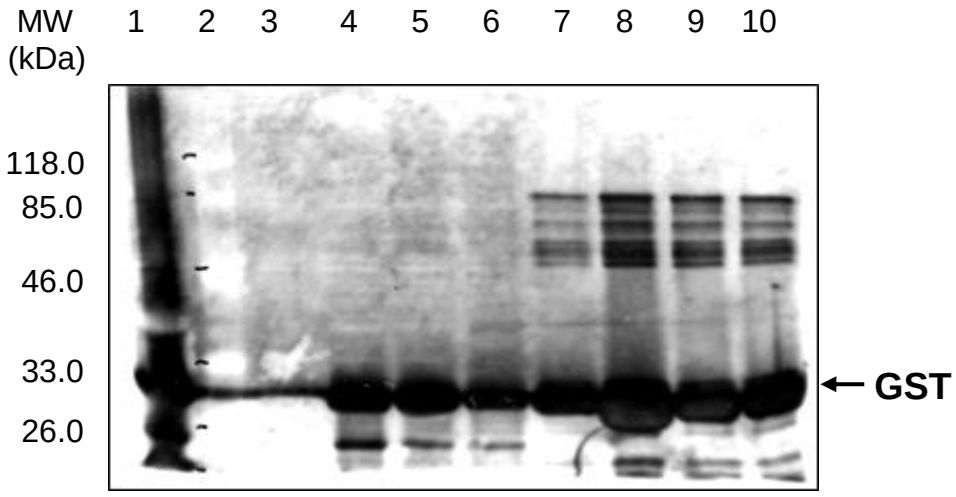

Figure 4.13. A Western blot analysis of a batch purification profile of GST protein by Glutathione Sepharose 4B (Amersham Biosciences). The blot was probed with anti-GST mouse monoclonal antibody conjugated with HRP (DAKO Cytomation).

Lane 1 - initial GST lysate

Lane 2 - prestained protein molecular weight markers (Fermentas)

Lane 3 - right after sonication

Lane 4 - supernatant after solubilisation

Lane 5 - pellet after solubilisation

Lane 6 - supernatant after beads binding

Lane 7 - elution 1

Lane 8 - elution 2

Lane 9 - elution 3

Lane 10 - beads after elution

4.2.3.2 GST-MDM2 protein gel purification profile

Upon induction of GST-MDM2 fusion protein expression with 1 mM IPTG for 4 hr, the BL21 cells were harvested and the pellet resuspended with ice-cold PBS was sonicated. Then the sonicated pellet was solubilized with Triton X-100 to 1% followed by centrifugation at 12,000 x g for 10 min at 4°C. The supernatant was transferred into a fresh container. The supernatant and the pellet after solubilisation were run in parallel as shown in Fig. 4.14, Lanes 4 and 5, respectively. In Fig. 4.14, we can see a lot of GST-MDM2 protein among other contaminating host proteins in the supernatant after solubilisation (Lane 4) of the GST-MDM2 fusion proteins (See Protocol 2.19.1) but hardly any GST-MDM2 protein was found in the sonicated GST-MDM2 lysate (Lane 3). A higher amount of GST-MDM2 in the supernatant after solubilisation when compared to it in the sonicated GST-MDM2 lysate might be due to solubilisation had enriched the GST-MDM2 protein levels. However, the levels of GST-MDM2 protein decreased in the pellet after solubilisation and in the supernatant after beads binding (Lanes 5 and 6) when compared to its levels in the supernatant after solubilisation (Lane 4). However, we are not interested in the pellet after solubilisation as we obtained higher levels of GST-MDM2 in the supernatant. This was just to show that fewer GST-MDM2 proteins remained in the pellet but most were in the supernatant (Lanes 4 and 5, respectively). Lower levels of GST-MDM2 proteins in the supernatant after beads binding (Lane 6) when compared to it in the supernatant after solubilisation (Lane 4) was as expected as most of GST-MDM2 proteins formed complexes with the beads and thus very little left in the supernatant.

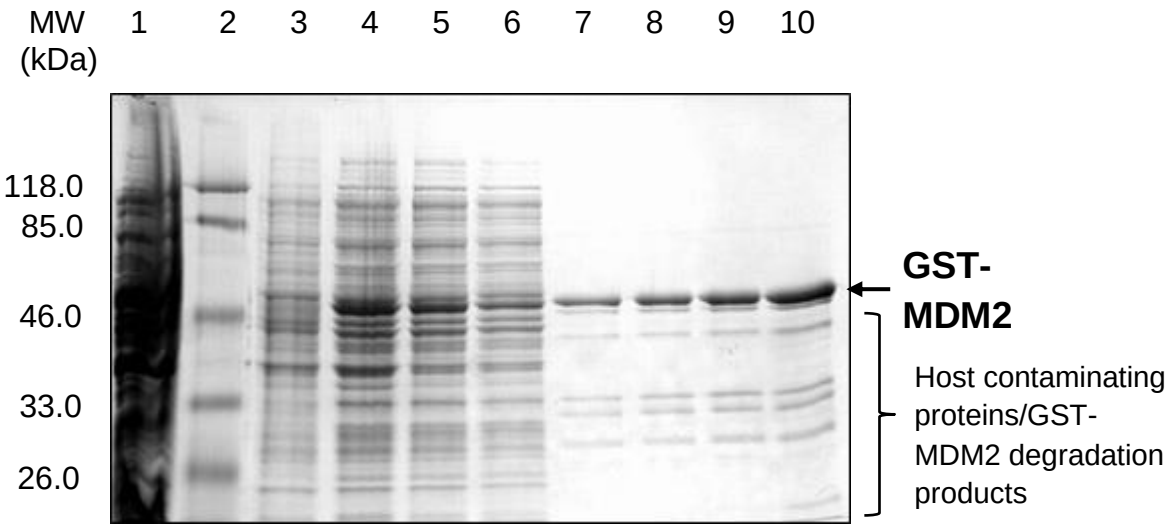

Figure 4.14. A 10% SDS PAGE gel showing a batch purification profile of GST-MDM2 protein using Glutathione Sepharose 4B (Amersham Biosciences). The gel was stained with Coomassie Blue stain for 15 min and then destained overnight.

Lane 1 - initial GST-MDM2 lysate

Lane 2 - prestained protein molecular weight markers (Fermentas)

Lane 3 - sonicated GST-MDM2 lysate

Lane 4 - supernatant after solubilisation

Lane 5 - pellet after solubilisation

Lane 6 - supernatant after beads binding

Lane 7 - elution 1

Lane 8 - elution 2

Lane 9 - elution 3

Lane 10 - GST-MDM2 final beads

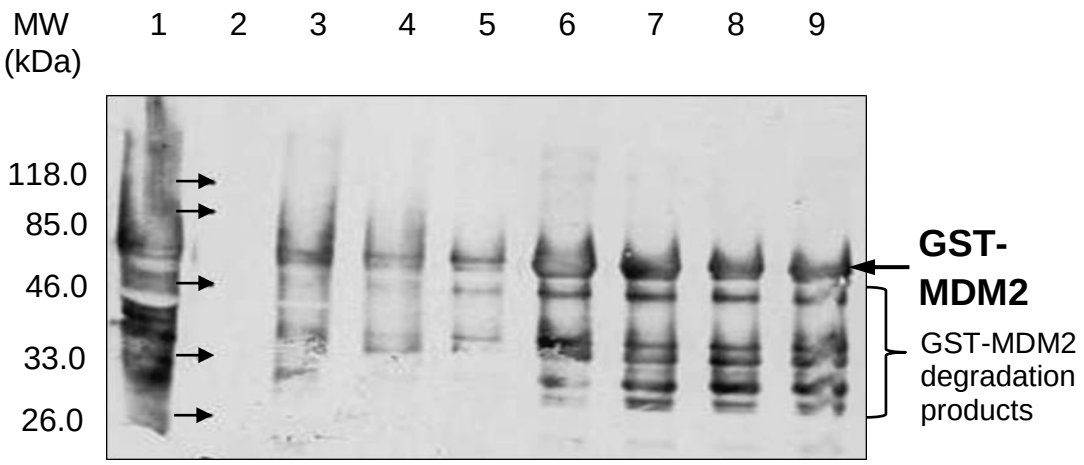

Figure 4.15. A Western blot analysis of a batch purification profile of GST-MDM2 protein by Glutathione Sepharose 4B (Amersham Biosciences). The blot was probed with anti-GST mouse monoclonal antibody conjugated with HRP (DAKO Cytomation).

Lane 1 - pellet

Lane 2 - prestained protein molecular weight markers (Fermentas)

Lane 3 - right after sonication

Lane 4 - supernatant after solubilisation

Lane 5 - supernatant after beads binding

Lane 6 - elution 1

Lane 7 - elution 2

Lane 8 - elution 3

Lane 9 - beads after elution

Quite a lot of highly enriched GST-MDM2 proteins were eluted in all the three beads elutions 1, 2 and 3 with a few smaller sizes host contaminating proteins and/or its degradation products (Lanes 7, 8 and 9). As can be seen in Lane 10, a lot of GST-MDM2 proteins were remained in GST-MDM2 final beads which might due to inefficient or incomplete elution of GST-MDM2 proteins. The GST-MDM2 protein gel purification profile finding was further verified by a Western blot analysis as shown in Fig. 4.15. As we are interested to see the elution part, a lot of GST-MDM2 proteins were found in all the three elutions 1, 2 and 3 with a few smaller sizes GST-MDM2 degradation products (Lanes 6, 7 and 8). We confirmed that the smaller sizes proteins lower than the GST-MDM2 protein were its degradation products since they were picked up by anti-GST mouse monoclonal antibody HRP-conjugated. The three elutions 1, 2 and 3 were then pooled together to be used for nitration work.

Now that we have obtained purified soluble native p53 protein, though at very low concentrations, and purified resolubilised p53 protein, supposedly at sufficient amounts, from a few litres of pT7.7Hup53 transformed *E.coli* bacterial culture and purified GST-MDM2 fusion proteins to be used for nitration work in order to see the effects of nitration on the stability and the levels of the proteins and on the interactions between the two proteins. In order to get substantial amounts of purified soluble native p53 protein, it is apparently clear to grow more pT7.7Hup53 transformed *E.coli* BL21(DE3) bacterial culture and then combine the purified batches and concentrate by ultracentrifugation by using centricon-30. Failing this, it is worth trying to transform pT7.7Hup53 construct into Lemo21(DE3) (New England Biolabs, 2013-2014 Catalog & Technical Reference), a derivative of BL21(DE23), which features tunable T7 expression for potential elimination of inclusion body formation so more soluble p53 protein will be obtained in supernatant of the cell lysates.

4.3 Discussion

The difficulties encountered when p53 protein was expressed in BL21(DE) in inclusion bodies include the incomplete resolubilisation resulting in reduced amount of soluble crude extracts. Also, several steps to follow from resolubilisation to dialysis and then through a series of purification steps resulted in the loss of p53 protein and ultimately a low yield of purified p53 protein. The purification of soluble p53 protein using gel filtration column on the FPLC system is easy and fast. The other advantage is only a small volume of starting crude extracts were applied to the column, thus eliminating the preparation of a large volume of samples. However, purification of soluble p53 protein is very challenging as the total yield was quite little.

The expression of MDM2 protein fused with GST using pGEX vector with in-built GST gene is very convenient, fast and only employed a single step purification on Glutathione Sepharose affinity chromatography. The GST-MDM2 protein expressed was soluble. Purification of the protein gave a high yield although low molecular weight contaminating proteins or degradation products were present. This can be improved by selecting the most efficient protease inhibitors at the correct concentrations. Thus, in the future should consider to fuse p53 gene with pGEX vector in order to get soluble p53 protein, thus eliminating the difficulty and lengthy processes of resolubilisation and refolding of inclusion bodies, which ultimately influence the biological activity of the protein (Young *et al*., 2012). The purification uses very mild elution conditions thus retaining the antigenicity and functional activity of the protein (GE Healthcare). Furthermore, the yield of pure protein is quite high.

RESULTS CHAPTER 5

In vitro generation of peroxynitrite and optimisation of nitration methods and conditions using BSA as a model protein for nitration

5.1 *In vitro* generation of peroxynitrite

In order to conduct *in vitro* nitration of proteins, we had to generate peroxynitrite, a potent nitrating agent used to nitrate protein, in the lab since due to its labile nature. Peroxynitrite was prepared by simultaneously flushing together 1.2 M $NaNO_2$ and 1 M HNO_3/H_2O_2 in plungers connected to a T-junction tube where the mixture was collected in a beaker containing 1.5 M NaOH. Excess H_2O_2 was then removed from the mixture by passing through manganese oxide (MnO_2) on a filter paper support (Naseem *et al*., 2004). The concentration of the resulting peroxynitrite could then be determined by spectroscopy. Scanning spectroscopy could also be used to determine the quality of the peroxynitrite produced.

5.2 Multiwavelength scanning of generated peroxynitrite

Individual components that made up peroxynitrite such as 1.5 M NaOH, 1 M HNO_3 alone, 1M HNO_3/H_2O_2 and 1.2 M $NaNO_2$ were scanned after calibrating the spectrophotometer with 1.5 M NaOH over a wavelength range 200-400 nm. As was expected no distinct UV absorbance spectrum for NaOH was observed as shown in Fig. 5.1(a) as it was blanked against itself. The UV absorbance spectra for HNO_3 alone and a combination of HNO_3/H_2O_2 showed no significant differences which were a single broad peak spanning from 200 nm to 350 nm as shown in Figs. 5.1(b) and 5.1(c), respectively. No distinct spectrum for $NaNO_2$ was seen as shown in Fig.5.1(d) where there was another single broad peak from 200 nm and to over 400 nm. Combination of all these components resulted in a peroxynitrite solution, the absorbance spectrum of which as shown in Fig. 5.2. The spectrum for the peroxynitrite solution gave two peaks, A and B, where peak B had a maximum absorbance approximately at 302 nm as expected

(approximately 70% peroxynitrite) (Robinson and Beckman, 2005). Peak A might be due to unreacted HNO_3 or a by-product of peroxynitrite formation (nitrate) or possibly due to other contaminants (remaining 30%) (Robinson and Beckman, 2005).

5.3 Determination of appropriate nitration method

Before nitration experiments could proceed, we needed to evaluate two nitration procedures. Because peroxynitrite is very labile, we needed to optimise the exposure of the target protein to peroxynitrite. The two methods recommended by Prof. Naseem (University of Bradford) were using an aggregometer set at 37°C at maximum speed and using vortex and a rocking water bath set at 37°C at vigorous speed. Free fatty acid bovine serum albumin (BSA) (Sigma) dissolved in 10 mM PBS was used as a model protein for preliminary nitration experiments since it is available commercially and 99.8% pure, and furthermore it is easily nitrated mainly because of its high content of tyrosine residues (19 tyrosine residues). BSA was subjected to nitrating agent peroxynitrite at various concentrations ranging from 10 µM to 500 µM using both mentioned nitration methods. Stronger signals of nitrated BSA were observed when it was nitrated using vortex and a rocking water bath set at 37°C (Fig. 5.3(b)) when compared to using an aggregometer (Fig. 5.3(a)). Thus, nitration with vortex and a rocking water bath was the preferred method for all the following nitration work.

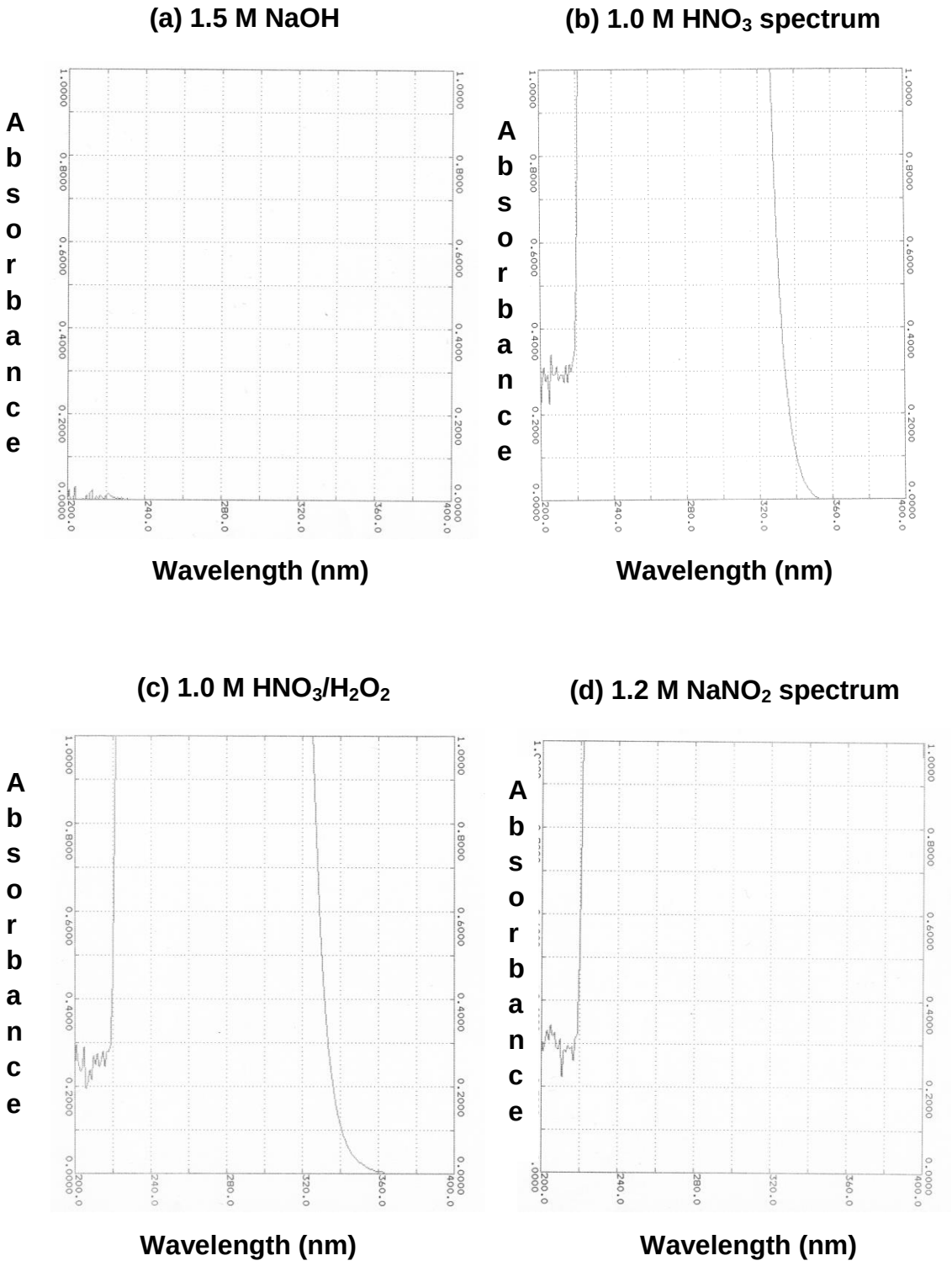

Figure 5.1. A multiwavelength scan of each component to prepare peroxynitrite solution indicated above which was first calibrated with NaOH using a Beckman DU-64 spectrophotometer at wavelengths ranging from 200 nm to 400 nm and absorbance limits from 0.0000 to 1.0000.

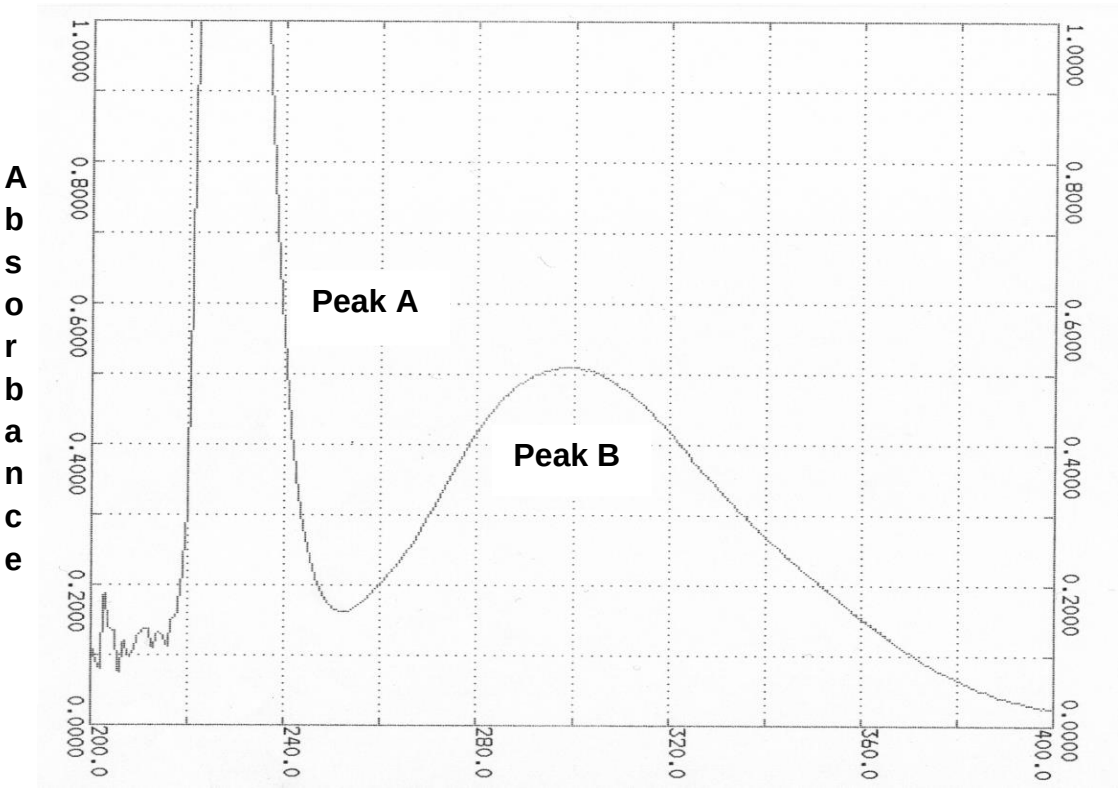

Figure 5.2. A multiwavelength scan of a peroxynitrite solution showing the quality of peroxynitrite formation using a Beckman DU-64 spectrophotometer at wavelengths ranging from 200 nm to 400 nm and absorbance limits from 0.0000 to 1.0000.

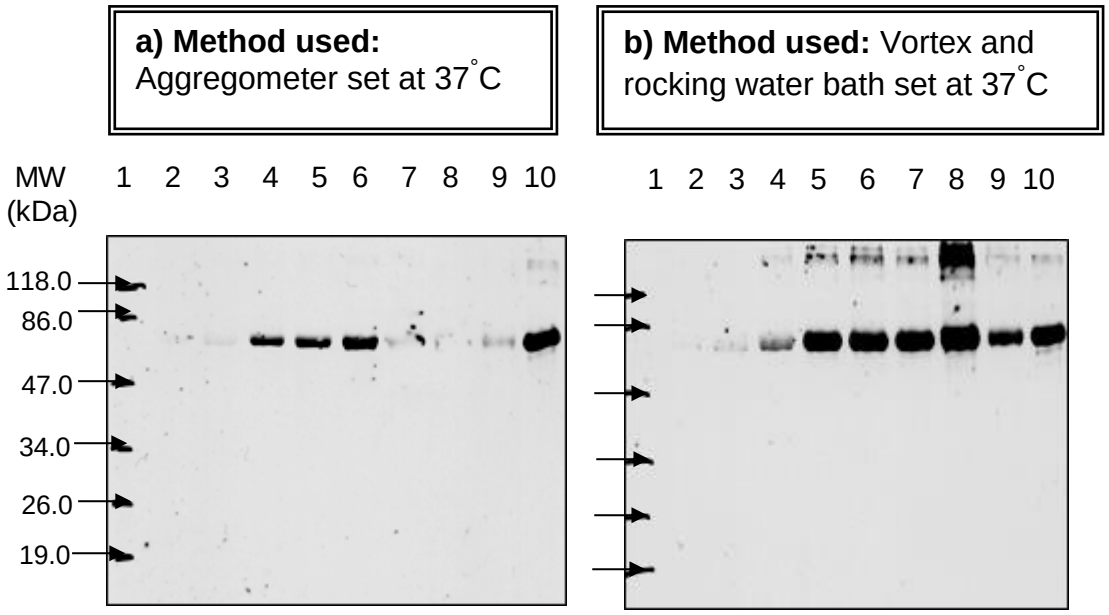

Figure 5.3. A comparison of two methods used to nitrate 2 mg/ml BSA dissolved in PBS : **a)** Method used was aggregometer set at 37°C and **b)** Method used was vortex and rocking water bath set at 37°C. The samples were incubated for 15 min with peroxynitrite. The same amounts of non-nitrated and nitrated BSA (2 µg) were loaded onto SDS-PAGE gels. The primary antibody used for both blots was anti-nitrotyrosine mouse monoclonal IgG, Clone 1A6 (Upstate Biotechnology) and the secondary antibody polyclonal rabbit anti-mouse IgG/HRP conjugated from DAKO Cytomation.

Lane 1 - prestained protein molecular weight markers (Fermentas)

Lane 2 - non-nitrated BSA as a negative control

Lane 3 - 10 µM peroxynitrite nitrated BSA

Lane 4 - 50 µM peroxynitrite nitrated BSA

Lane 5 - 100 µM peroxynitrite nitrated BSA

Lane 6 - 200 µM peroxynitrite nitrated BSA

Lane 7 - 300 µM peroxynitrite nitrated BSA

Lane 8 - 400 µM peroxynitrite nitrated BSA

Lane 9 - 500 µM peroxynitrite nitrated BSA

Lane 10 - 100 µM peroxynitrite previously nitrated BSA as a positive control

5.4 Optimisation of nitration conditions

In our preliminary nitration study, we nitrated a model protein BSA and dialysed p53 lysate with 3 mM peroxynitrite using the preferred method vortexing and a rocking water bath set at 37˚C as determined above in Section 5.3. The samples were then run on a 10% SDS-PAGE gel along with their non-nitrated counterparts (Fig. 5.4). As can be seen in Fig. 5.4, the levels of BSA protein and dialysed p53 protein nitrated with 3 mM were lower than their non-nitrated total proteins. This might be due to the degrading properties of peroxynitrite which resulted in the degradation of the proteins especially at its high concentration (3 mM) as shown by Ischiropoulos and Al-Mehdi on fatty acid-free BSA fragmentation when treated with peroxynitrite (Ischiropoulos and Al-Mehdi, 1995). To check for nitro-BSA and nitro-p53 protein, Western blot analyses were carried out on the same samples in Fig. 5.4. Two blots of the same samples were either probed with anti-nitrotyrosine mouse monoclonal IgG, Clone 1A6 (Upstate Biotechnology) and then with the secondary antibody sheep anti-mouse HRP conjugated (a kind gift of Dr Patel, University of Bradford) (Fig. 5.5(a)) or with the same secondary antibody alone (Fig. 5.5(b)). In Fig. 5.5(a), we can see that there was a weak nitrotyrosine signal in non-nitrated BSA and a relatively strong nitrotyrosine signal was detected in 3 mM peroxynitrite nitrated BSA (Fig.5.5(a), Lanes 2 and 3, respectively). The weak nitrotyrosine signal in non-nitrated BSA might be due to BSA was endogenously nitrated in cow as it is

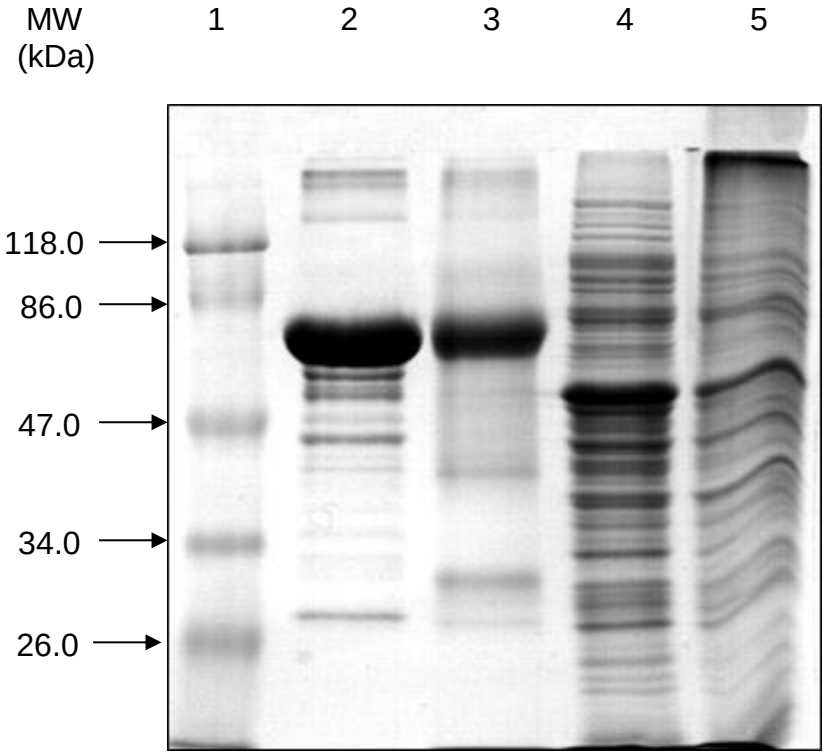

Figure 5.4. A 10% SDS-PAGE gel preliminary nitration of bovine serum albumin (BSA) and dialysed p53 lysate in PBS in comparison with Western blot analysis of the same samples as shown on Figure 5.5. The samples were subjected to 3 mM peroxynitrite and incubated for 15 min in a rocking water bath at 37°C.

Lane 1 – prestained protein molecular weight markers (Fermentas)

Lane 2 – non-nitrated BSA (15 µg)

Lane 3 – nitrated BSA (15 µg)

Lane 4 – non-nitrated dialysed p53 lysate (13.7 µg)

Lane 5 – nitrated dialysed p53 lysate (13.7 µg)

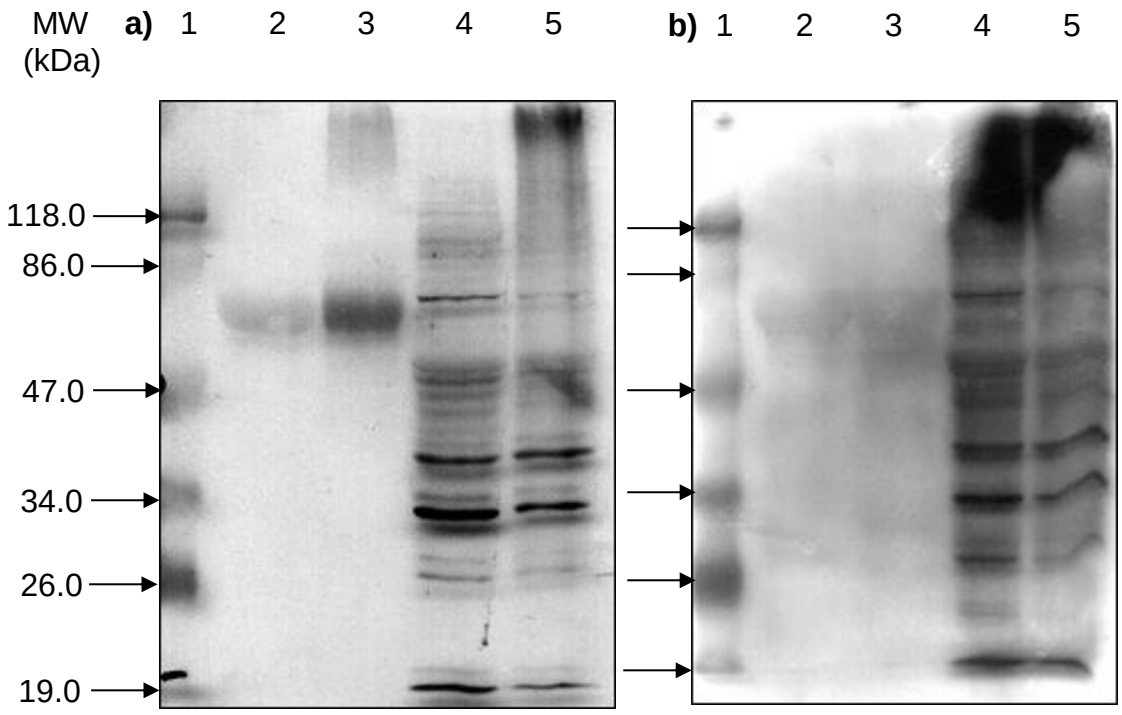

Figure 5.5. Western Blot analysis showing preliminary nitration of bovine serum albumin (BSA) and dialysed p53 lysate in PBS. Nitrated samples were subjected to 3 mM nitrating agent peroxynitrite and incubated for 15 min in a rocking water bath at 37°C: **a)** The primary antibody used was anti-nitrotyrosine mouse monoclonal IgG, Clone 1A6 (Upstate Biotechnology) and the secondary antibody sheep anti-mouse HRP conjugated (Amersham Biosciences, a kind gift of Mr Patel, University of Bradford. **b)** The secondary antibody sheep anti-mouse HRP conjugated alone (Amersham Biosciences) was used to probe the blot to act as a negative control.

Lane 1 – prestained protein molecular weight markers (Fermentas)

Lane 2 – non-nitrated BSA (15 µg)

Lane 3 – nitrated BSA (15 µg)

Lane 4 – non-nitrated dialysed p53 lysate (13.7 µg)

Lane 5 – nitrated dialysed p53 lysate (13.7 µg)

believed that tyrosine nitration is part of normal physiological processes in humans (Moncada *et al*., 1991; Beckman and Koppenol., 1996) and presumably also in other mammals and organisms. Dialysed p53 lysate gave about similar nitrotyrosine signals of the host contaminating proteins in both the non-nitrated and the nitrated (Fig. 5.5(a), Lanes 4 and 5, respectively), showing a very weak nitro-p53 protein signal in non-nitrated lysate but no additional one in response to nitration. A possible explanation to this phenomenon is that the bacterial proteins were endogenously nitrated. However, in Fig. 5.5(b), as the secondary antibody used picked up bacterial proteins in both non-nitrated and nitrated dialysed p53 lysate (Fig. 5.5(b), Lanes 4 and 5, respectively), it is clear that the non-specific binding of the secondary antibody resulted in false-positive nitrotyrosine signals for both the samples when probed with the primary antibody anti-nitrotyrosine mouse monoclonal IgG, Clone 1A6. Nevertheless, both non-nitrated and nitrated BSA were not obviously picked up by the secondary antibody alone as no signals were observed (Fig. 5.5(b), Lanes 2 and 3, respectively). This shows that the primary antibody anti-nitrotyrosine might work. The nitrotyrosine signals depicted in Fig 5.5(a) might be due to the overlapping actions between the primary antibody anti-nitrotyrosine and the secondary antibody sheep anti-mouse HRP conjugated or the secondary antibody used was not good enough, therefore, it is unlikely to comment on the primary antibody (Dr Picksley, personal communication).

Similar experiments were repeated but this time using a variety of samples such as bacterial lysate, BSA, bovine platelet, dialysed p53 lysate and purified resolubilised p53 protein. The samples except bacterial lysate were nitrated with 3 mM peroxynitrite and their non-nitrated counterparts were run in parallel. The primary antibody used was the same as before i.e. Clone 1A6 antibody with a change in secondary antibody rabbit anti-mouse IgG HRP conjugated polyclonal antibody (DAKO Cytomation). As can be seen in Fig. 5.6, the bacterial lysate, non-nitrated and nitrated BSA, non-nitrated and nitrated bovine platelet and non-nitrated dialysed p53 lysate but not nitrated dialysed p53 lysate gave nitrotyrosine signals (Fig. 5.6, Lanes 2-7). No nitrotyrosine signals were detected in nitrated dialysed p53 lysate and in both

non-nitrated and nitrated purified resolubilised p53 protein (Fig. 5.6, Lanes 8, 9 and 10, respectively). A possible explanation for no nitrotyrosine signal in nitrated dialysed p53 lysate is that high peroxynitrite concentration (3 mM) used to nitrate the proteins resulted in their degradation or loss. Since the starting amount of purified resolubilised p53 protein was quite low, thus, no detectable nitrotyrosine signal was observed in nitrated purified resolubilised p53 protein (Fig. 5.6, Lane 10). The nitrotysrosine signals observed in both the non-nitrated and the nitrated (Fig. 5.6, Lanes 2-7) are probably due to the presence of endogenous nitrated proteins or due to the secondary antibody problem where it non-specifically bound to the proteins in the samples.

In order to find out further the causes of this problem, nitration experiments were done using BSA nitrated at various concentrations of peroxynitrite ranging from 10 µM to 3 mM using this time around a different primary antibody rabbit anti-nitrotyrosine polyclonal antibody (from SIGMA) and therefore a different secondary antibody swine anti-rabbit polyclonal antibody (from DAKO Cytomation). Two negative control blots were used by preabsorbing the primary antibody with 10 mM 3-nitro-tyrosine right before its incubation to the blot and incubation of a blot with the secondary antibody alone Fig. 5.7(a) and (b), respectively). Both these blots gave false positive nitrotyrosine signals where blot in Fig 5.7(b) gave weaker nitrotyrosine signals when compared to blot in Fig. 5.7(a). Blot in Fig. 5.7(c) where the blot was incubated with the primary rabbit anti-nitrotyrosine polyclonal antibody and the secondary swine anti-rabbit polyclonal antibody showed about similar nitrotyrosine signals intensity as blot in Fig. 5.7(a). Secondary antibody was still a problem here where it non-specifically bound to BSA both non-nitrated and nitrated, indicating that it was not fit for the purpose.

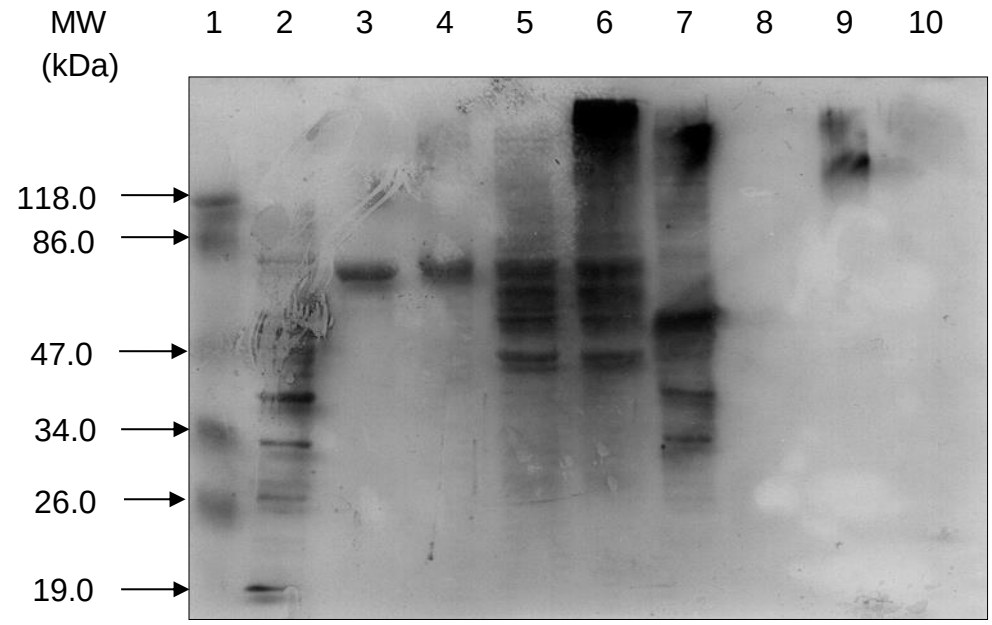

Figure 5.6. Western Blot analysis showing various samples nitrated with 3 mM peroxynitrite and incubated for 15 min in a rocking water bath at 37°C. The primary antibody used was anti-nitrotyrosine monoclonal antibody (Clone 1A6) (Upstate Biotechnology) and the secondary antibody was rabbit anti-mouse IgG HRP conjugated polyclonal antibody (Dako Cytomation).

Lane 1 - prestained protein molecular weight markers (Fermentas)

Lane 2 - BL21(DE3) bacterial lysate grown for 4 hours

Lane 3 - non-nitrated BSA (5 µg)

Lane 4 - nitrated BSA (5 µg)

Lane 5 - non-nitrated bovine platelet (20 µg)

Lane 6 - nitrated bovine platelet (20 µg)

Lane 7 - non- nitrated dialysed p53 lysate (20.6 µg)

Lane 8 - nitrated dialysed p53 lysate (20.6 µg)

Lane 9 - non-nitrated purified resolubilised p53 (2.6 µg)

Lane 10 - nitrated purified resolubilised p53 (2.6 µg)

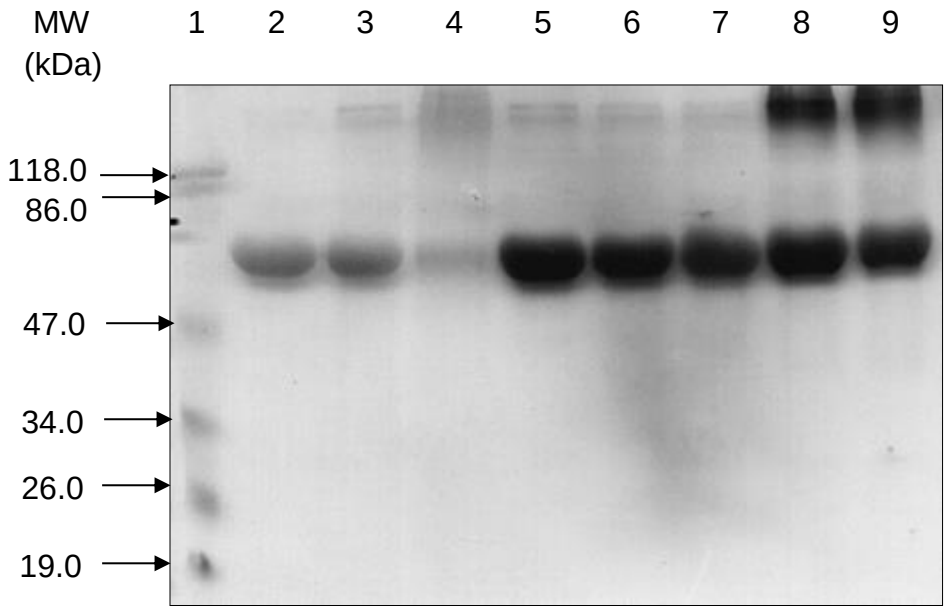

Figure 5.7(a). Western Blot showing non-nitrated and nitrated BSA at various peroxynitrite concentrations and incubated for 15 min in a rocking water bath at 37°C. Rabbit anti-nitrotyrosine polyclonal antibody (Sigma) was used as the primary antibody which was first preabsorbed with 10 mM 3-nitro-tyrosine (Sigma) and swine anti-rabbit polyclonal antibody (DAKO Cytomation) as the secondary antibody. The amount of all the samples loaded was 10 µg. This blot acts as a negative control blot.

Lane 1 – prestained protein molecular weight markers (Fermentas)

Lane 2 – non-nitrated BSA

Lane 3 – 10 µM peroxynitrite nitrated BSA

Lane 4 – 100 µM peroxynitrite nitrated BSA

Lane 5 – 250 µM peroxynitrite nitrated BSA

Lane 6 – 500 µM peroxynitrite nitrated BSA

Lane 7 – 1 mM peroxynitrite nitrated BSA

Lane 8 – 2 mM peroxynitrite nitrated BSA

Lane 9 – 3 mM peroxynitrite nitrated BSA

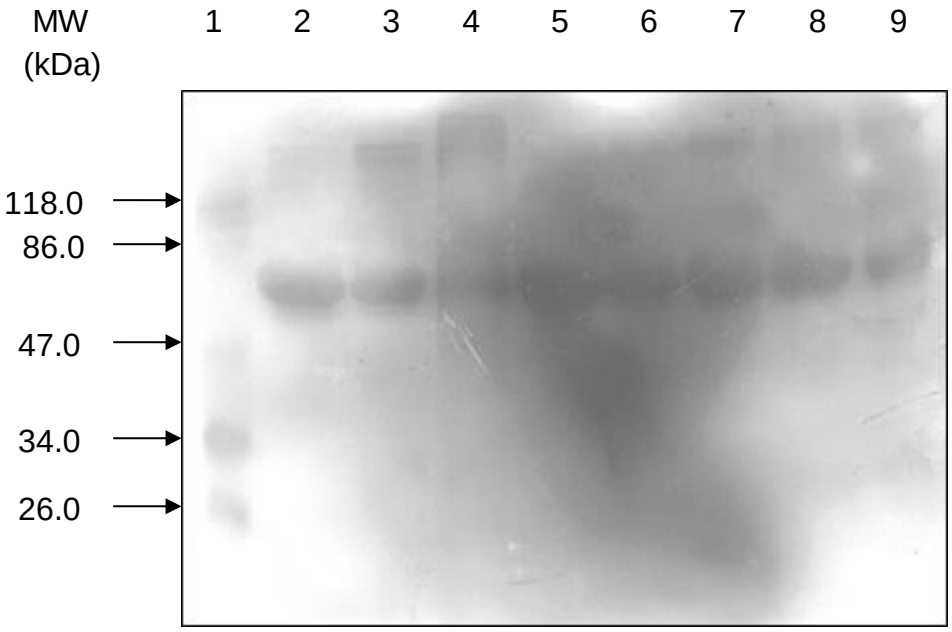

Figure 5.7(b). Western Blot showing non- nitrated and nitrated BSA at various peroxynitrite concentrations and incubated for 15 min in a rocking water bath at 37°C. The secondary antibody used was swine anti-rabbit polyclonal antibody (DAKO Cytomation) alone. The amount of all the samples loaded was 10 µg.

Lane 1 – prestained protein molecular weight markers (Fermentas)

Lane 2 – non-nitrated BSA

Lane 3 – 10 µM peroxynitrite nitrated BSA

Lane 4 – 100 µM peroxynitrite nitrated BSA

Lane 5 – 250 µM peroxynitrite nitrated BSA

Lane 6 – 500 µM peroxynitrite nitrated BSA

Lane 7 – 1 mM peroxynitrite nitrated BSA

Lane 8 – 2 mM peroxynitrite nitrated BSA

Lane 9 – 3 mM peroxynitrite nitrated BSA

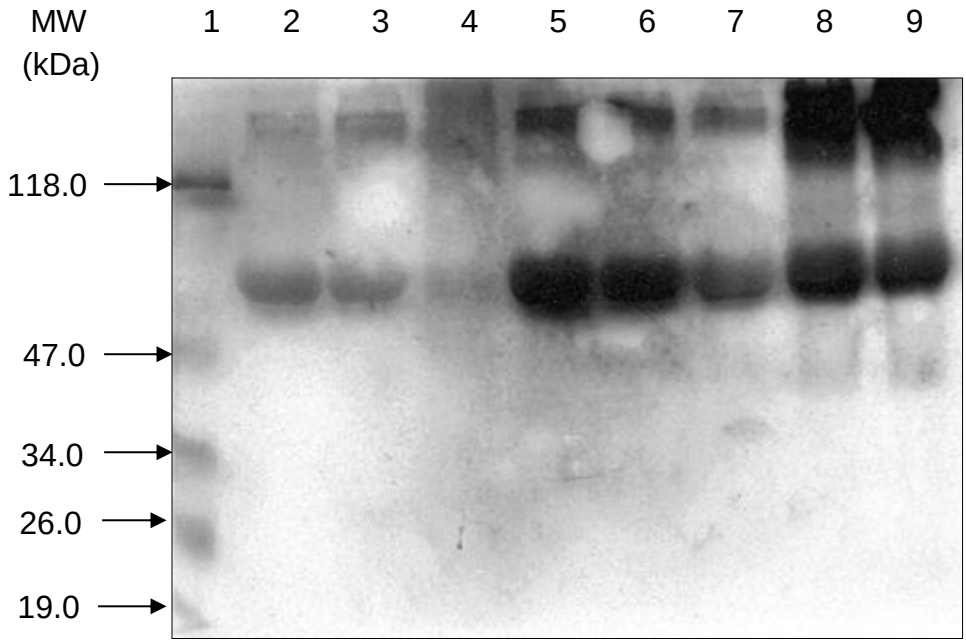

Figure 5.7(c). Western Blot showing non- nitrated and nitrated BSA at various concentrations of peroxynitrite and incubated for 15 min in a rocking water bath at 37°C. Rabbit anti-nitrotyrosine polyclonal antibody (Sigma) was used as the primary antibody and swine anti-rabbit polyclonal antibody (DAKO Cytomation) as the secondary antibody. The amount of all samples loaded was 10 µg.

Lane 1 – prestained protein molecular weight markers (Fermentas)

Lane 2 – non-nitrated BSA

Lane 3 – 10 µM peroxynitrite nitrated BSA

Lane 4 – 100 µM peroxynitrite nitrated BSA

Lane 5 – 250 µM peroxynitrite nitrated BSA

Lane 6 – 500 µM peroxynitrite nitrated BSA

Lane 7 – 1 mM peroxynitrite nitrated BSA

Lane 8 – 2 mM peroxynitrite nitrated BSA

Lane 9 – 3 mM peroxynitrite nitrated BSA

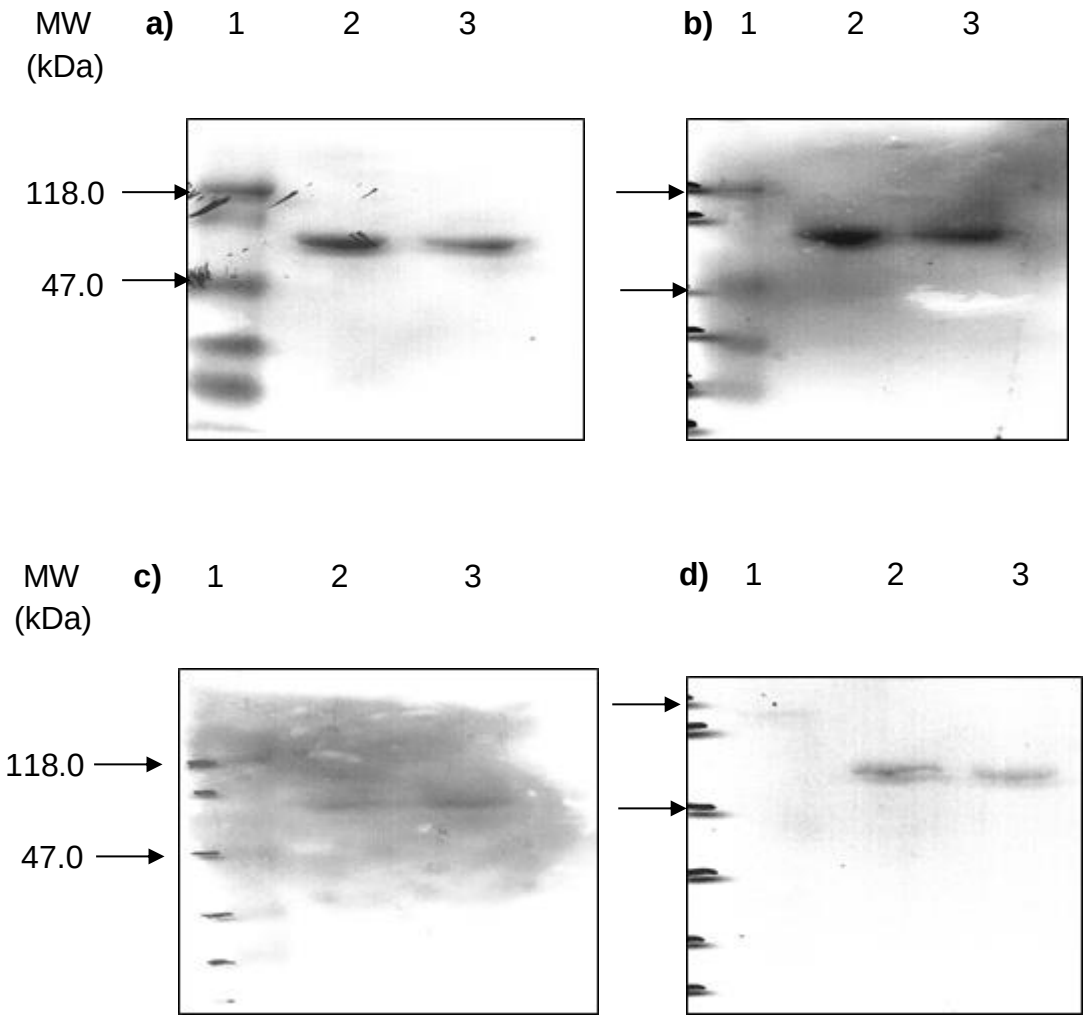

Figure 5.8. Western Blot analysis showing non-nitrated and nitrated BSA with 250 µM peroxynitrite and incubated for 15 min in a rocking water bath at 37°C. The samples were blotted with different anti-rabbit secondary antibody alone: **a)** swine anti-rabbit IgG/HRP conjugated (DAKO Cytomation), **b)** anti-rabbit HRP conjugated (Cell Signalling), **c)** goat anti-rabbit IgG/HRP conjugated (Amersham Biosciences), **d)** sheep anti-rabbit IgG/HRP conjugated. The amount of BSA loaded was 2 µg.

Lane 1 – prestained protein molecular weight markers (Fermentas)

Lane 2 - non-nitrated BSA

Lane 3 - 250 µM peroxynitrite nitrated BSA

This therefore led us to use a variety of secondary antibodies alone including the ones we used in the previous experiments namely swine anti-rabbit IgG HRP conjugated (DAKO Cytomation), anti-rabbit HRP conjugated (Cell Signalling), goat anti-rabbit IgG HRP conjugated (Amershan Biosciences) and sheep anti-rabbit IgG HRP conjugated (a kind gift of Dr Patel, University of Bradford) to incubate strips of small cut blots containing non-nitrated and 250 µM peroxynitrite nitrated BSA (Fig. 5.8(a), (b), (c) and (d), respectively). These data show that all the four secondary antibodies used gave signals indicating that these antibodies picked up both non-nitrated and nitrated BSA. From these data, we then came to identify that secondary antibodies were the cause of the problems for false positive signals.

In order to solve the secondary antibody problems, we then explored different blocking conditions with secondary antibody alone using non-nitrated BSA as a sample. Two representative secondary antibodies were used namely rabbit anti-mouse polyclonal antibody HRP conjugated and swine anti-rabbit polyclonal antibody HRP conjugated (both from DAKO Cytomation). Four blocking conditions were used as summarised in Materials & Methods, Section 2.14, Table 2.7. Briefly, the blocking conditions used were (i) 5% non-fat dry milk in PBS, (ii) 5% non-fat dry milk/0.2% Tween 20 in PBS, (iii) 0.2% Tween 20 in PBS, (iv) 3% BSA in PBS. As can be seen in Fig. 5.9, Very clear background was found in blocking conditions (i) and (ii) whereas non-specific binding of both secondary antibodies to non-nitrated BSA were found when using blocking conditions (iii) and (iv). From this experiment, we finally determined the best blocking conditions to be used namely either with 5% non-fat milk in PBS or with 5% non-fat dry milk/0.2% Tween 20 in PBS.

Having solved the problems, we now proceeded with nitration of purified resolubilised p53 protein with various concentrations of peroxynitrite ranging from 10 µM to 3 mM but this time we probed the membrane with the primary rabbit anti-nitrotyrosine polyclonal antibody (Sigma). A dirty background was observed when we incubated a blot containing nitrated purified resolubilised p53 samples with this primary antibody [Fig. 5.10(a)]. However, we could

only see a moderate nitrotyrosine signal in purified resolubilised p53 protein nitrated with 250 μM peroxynitrite (Fig. 5.10(a), Lane 5). In addition, the non-nitrated purified resolublised p53 protein as expected and the rest of the nitrated samples gave no nitrotyrosine signals. A negative control blot where the primary antibody rabbit polyclonal anti-nitrotyrosine was first preabsorbed with 10 mM 3-nitrotyrosine showed a clear background or reduced signal (Fig. 5.10(b)), consistent with the antigen binding sites were blocked as expected. In Fig. 5.10(c), a lot of p53 protein degradation products were observed in non-nitrated samples and nitrated samples with peroxynitrite from 10 μM to 1 mM (Fig. 5.10(c), Lanes 2-7). The levels of nitrated purified resolubilised p53 protein nitrated with 2 and 3 mM peroxynitrite seem to be reduced (Fig. 5.10(c), Lanes 8 and 9, respectively). The experiments had been repeated with 2 repeats (n=2).

As the primary rabbit anti-nitrotyrosine polyclonal antibody (Sigma) [see Fig. 5.10(a)] resulted in a dirty background, we then decided to switch back to use anti-nitrotyrosine mouse monoclonal IgG, Clone 1A6 (Upstate Biotechnology) for the following nitration work as so far it did not give a dirty background.

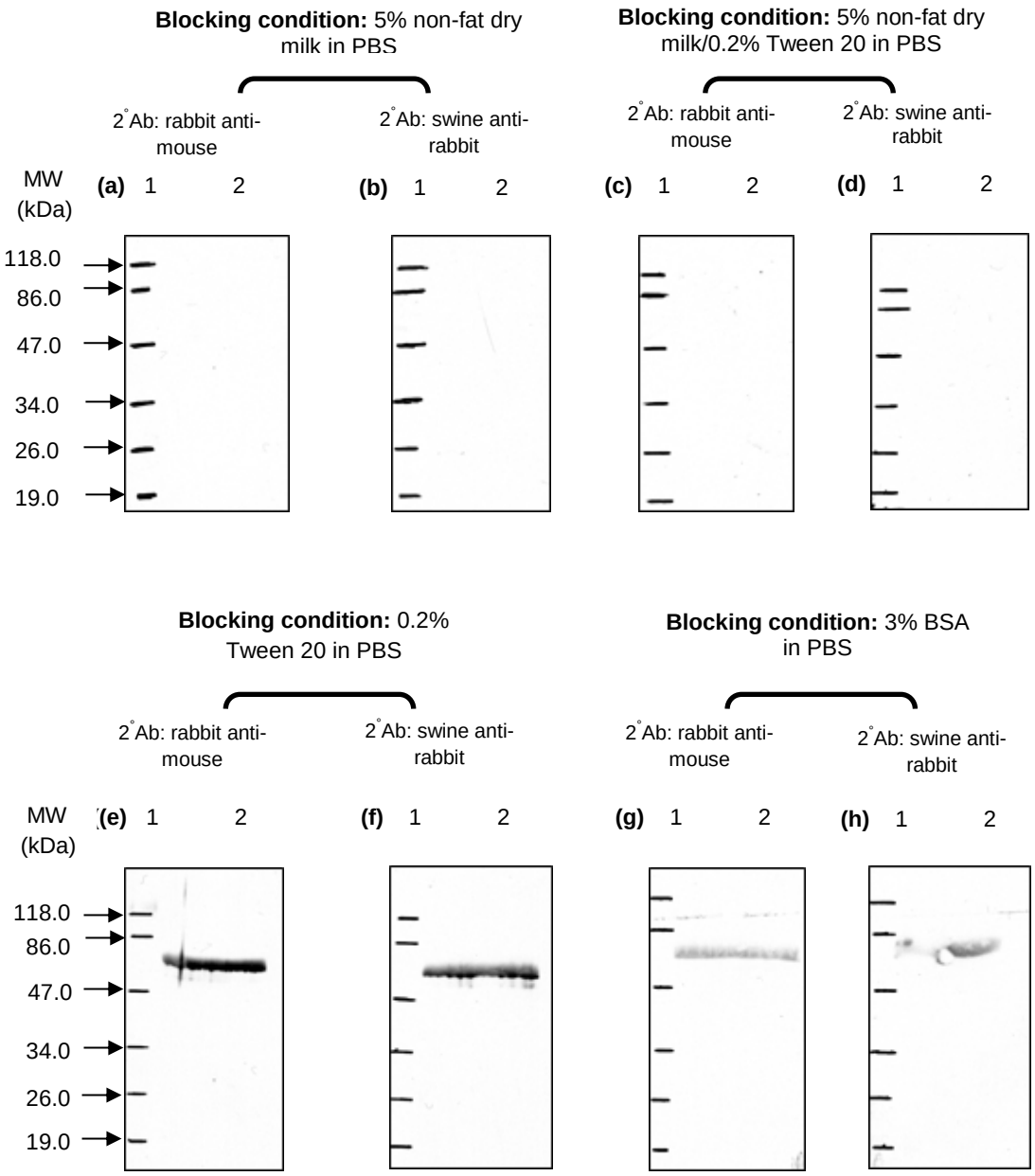

Figure 5.9. Western Blot analysis showing different blocking conditions used and all the blots were probed only with secondary antibody alone either with rabbit anti-mouse monoclonal antibody HRP conjugated or with swine anti-rabbit polyclonal antibody HRP conjugated, both of which from DAKO Cytomation. 9 out of 10 wells were combined together with a cellotape to form one big well. 100 µl of 1mg/ml BSA was loaded onto the well, thus making the amount of BSA in each small blot about 20 µg when one big blot was cut into 4 small strips. Since MW marker was not visible, therefore a Strategene marker was placed on top of cling film used to wrap the blots after poured with ECL and then exposed to X-ray film before being developed and fixed. However, the cut blots were first marked with a red pen on its upper part and with a black pen on its lower part in order to aid marking of the marker.

Lane 1 - prestained protein molecular weight markers (Fermentas)

Lane 2 - bovine serum albumin (BSA) (non-nitrated)

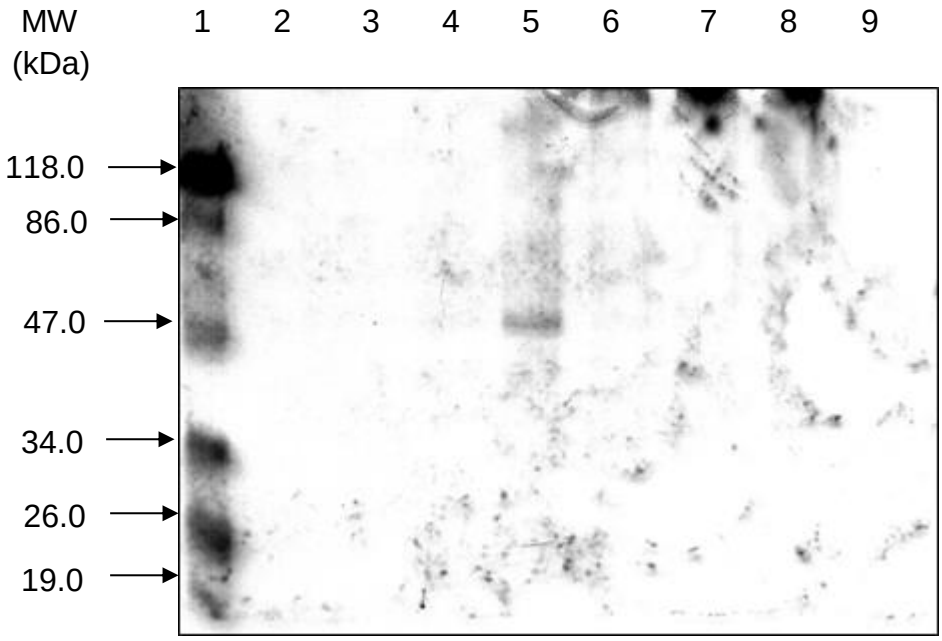

Figure 5.10(a). Western Blot analysis showing purified resolubilised p53 protein nitrated with various concentrations of peroxynitrite ranging from 10 µM to 3 mM and incubated for 15 min in a rocking water bath at 37°C. Non-nitrated purified resolubilised p53 protein was used as a negative control. The amount of all samples loaded was 2.04 µg. The primary antibody used was rabbit polyclonal anti-nitrotyrosine (Sigma) and the secondary antibody was swine anti-rabbit IgG/HRP conjugated (DAKO Cytomation) (n=2 repeats).

Lane 1 - prestained protein molecular weight markers (Fermentas)

Lane 2 - non-nitrated purified p53

Lane 3 - 10 µM peroxynitrite nitrated purified resolubilised p53

Lane 4 - 100 µM peroxynitrite nitrated purified resolubilised p53

Lane 5 - 250 µM peroxynitrite nitrated purified resolubilised p53

Lane 6 - 500 µM peroxynitrite nitrated purified resolubilised p53

Lane 7 - 1 mM peroxynitrite nitrated purified resolubilised p53

Lane 8 - 2 mM peroxynitrite nitrated purified resolubilised p53

Lane 9 - 3 mMperoxynitrite nitrated purified resolubilised p53

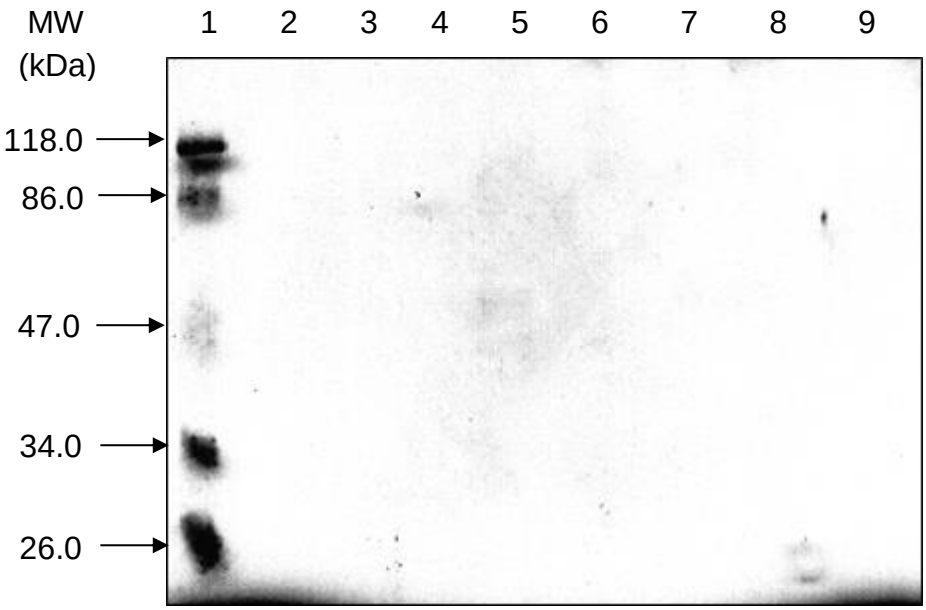

Figure 5.10(b). Western Blot analysis showing purified resolubilised p53 protein nitrated with various concentrations of peroxynitrite ranging from 10 µM to 3 mM and incubated for 15 min in a rocking water bath at 37°C. Non-nitrated purified p53 protein was used as a negative control. The amount of all samples loaded was 2.04 µg. The primary antibody used was rabbit polyclonal anti-nitrotyrosine (Sigma) which was first pre-absorbed with 10 mM 3-nitro-L-tyrosine (Sigma) and the secondary antibody was swine anti-rabbit IgG/HRP conjugated (DAKO Cytomation). This blot acted as a negative control blot.

Lane 1 - prestained protein molecular weight markers (Fermentas)

Lane 2 - non-nitrated purified p53

Lane 3 - 10 µM peroxynitrite nitrated purified resolubilised p53

Lane 4 - 100 µM peroxynitrite nitrated purified resolubilised p53

Lane 5 - 250 µM peroxynitrite nitrated purified resolubilised p53

Lane 6 - 500 µM peroxynitrite nitrated purified resolubilised p53

Lane 7 - 1 mM peroxynitrite nitrated purified resolubilised p53

Lane 8 - 2 mM peroxynitrite nitrated purified resolubilised p53

Lane 9 - 3 mM peroxynitrite nitrated purified resolubilised p53

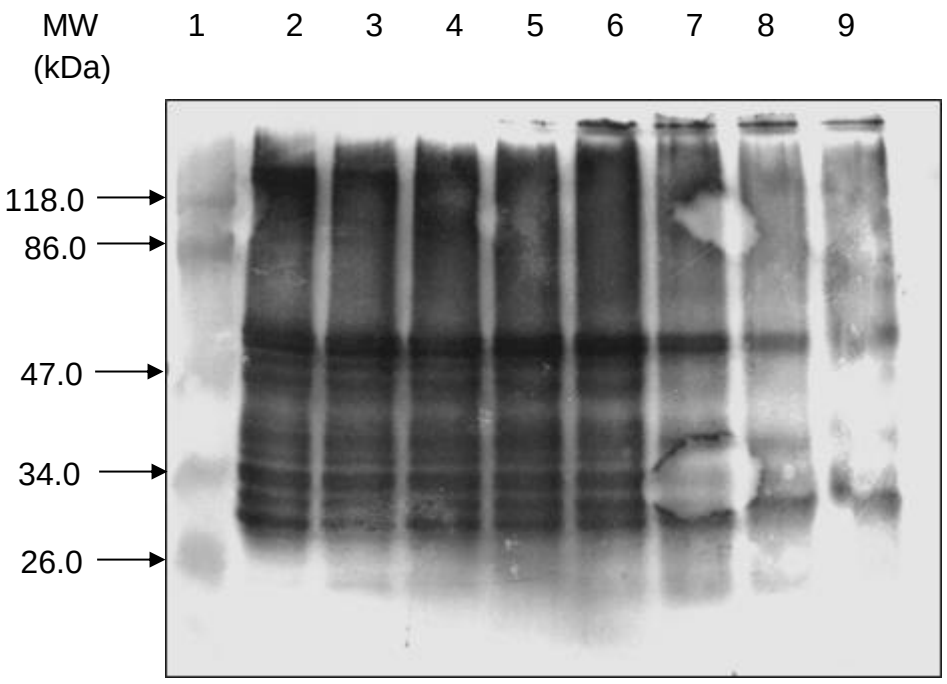

Figure 5.10(c). Western Blot analysis showing purified resolubilised p53 protein nitrated with various concentrations of peroxynitrite ranging from 10 µM to 3 mM and incubated for 15 min in a rocking water bath at 37°C. Non-nitrated purified p53 protein was used as a negative control. The amount of all samples loaded was 2.04 µg. The primary antibody used was anti-p53 monoclonal antibody (DO-1), a kind gift of Dr Borivoj Vojtesek from the Czech Republic and the secondary antibody was polyclonal rabbit anti-mouse IgG from DAKO Cytomation.

Lane 1 - prestained protein molecular weight markers (Fermentas)

Lane 2 - non-nitrated purified resolubilised p53

Lane 3 - 10 µM peroxynitrite nitrated purified resolubilised p53

Lane 4 - 100 µM peroxynitrite nitrated purified resolubilised p53

Lane 5 - 250 µM peroxynitrite nitrated purified resolubilised p53

Lane 6 - 500 µM peroxynitrite nitrated purified resolubilised p53

Lane 7 - 1 mM peroxynitrite nitrated purified resolubilised p53

Lane 8 - 2 mM peroxynitrite nitrated purified resolubilised p53

Lane 9 - 3 mMperoxynitrite nitrated purified resolubilised p53

We now proceeded with nitration of BSA but this time we narrowed down the concentrations of peroxynitrite used from 10 µM to 1 mM in order to see a dose response. In Fig. 5.11(a), increasing the concentrations of peroxynitrite increased the nitrotyrosine signals up to 200 µM peroxynitrite. However, the nitrotyrosine signals started to level off beyond 200 µM peroxynitrite namely at 300 µM, 400 µM, 500 µM and 1 mM. A blot with the same BSA samples as in a blot in Fig. 5.11(a) where the primary anti-nitrotyrosine Clone 1A6 was first preabsorbed with 10 mM 3-nitro-L-tyrosine before being incubated to the blot acted as a negative control blot (Fig. 5.11(b)). We expected to get no signals at all, however, there were nitrotyrosine signals and a weaker signal in BSA samples nitrated with 50 µM and 100 µM peroxynitrite, respectively (Fig. 5.11(b), Lanes 4 and 5, respectively). A possible reason for this is that BSA nitrated with 50 µM peroxynitrite had the strongest nitrotyrosine levels and then followed by BSA nitrated with 100 µM peroxynitrite where even after the primary antibody Clone 1A6 had been pre-absorbed with 10 mM 3-nitro-L-tyrosine, a little amount of unabsorbed antibody would still react with the abundant nitro-BSA protein. The fact is 100 µM peroxynitrite can be seen as a pathological relevant concentration of the nitrating agent *in vivo*.

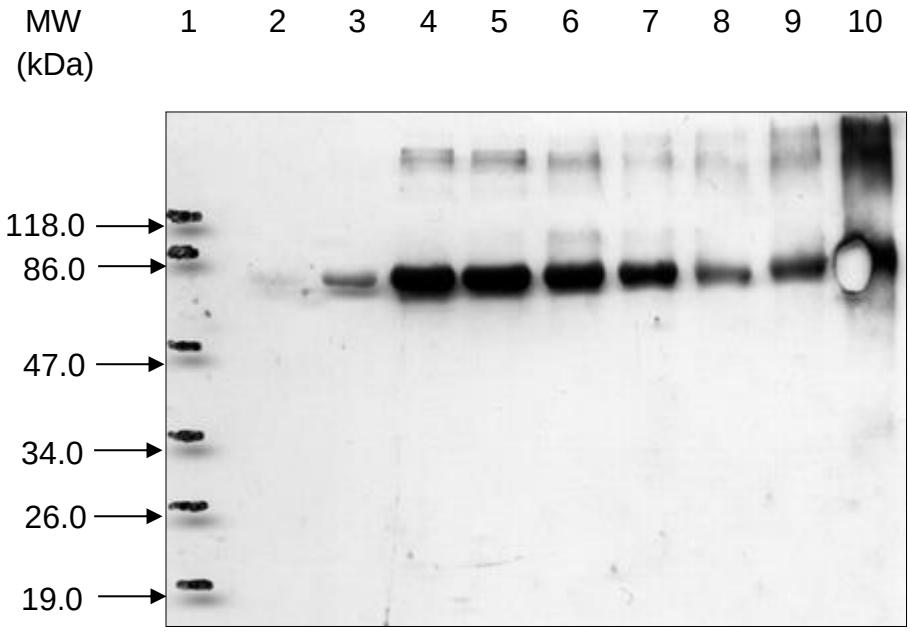

Figure 5.11(a). Western Blot analysis showing non-nitrated BSA and nitrated BSA with various concentrations of peroxynitrite and incubated for 15 min in a rocking water bath at 37°C. The primary antibody used was anti-nitrotyrosine mouse monoclonal IgG, Clone 1A6 (Upstate Biotechnology) and the secondary antibody was polyclonal rabbit anti-mouse IgG/HRP conjugated (Dako Cytomation). The amount of BSA loaded was 2 µg.

Lane 1 - prestained protein molecular weight markers (Fermentas)

Lane 2 - non-nitrated BSA

Lane 3 - 10 µM peroxynitrite nitrated BSA

Lane 4 - 50 µM peroxynitrite nitrated BSA

Lane 5 - 100 µM peroxynitrite nitrated BSA

Lane 6 - 200 µM peroxynitrite nitrated BSA

Lane 7 - 300 µM peroxynitrite nitrated BSA

Lane 8 - 400 µM peroxynitrite nitrated BSA

Lane 9 - 500 µM peroxynitrite nitrated BSA

Lane 10 - 1 mM peroxynitrite nitrated BSA

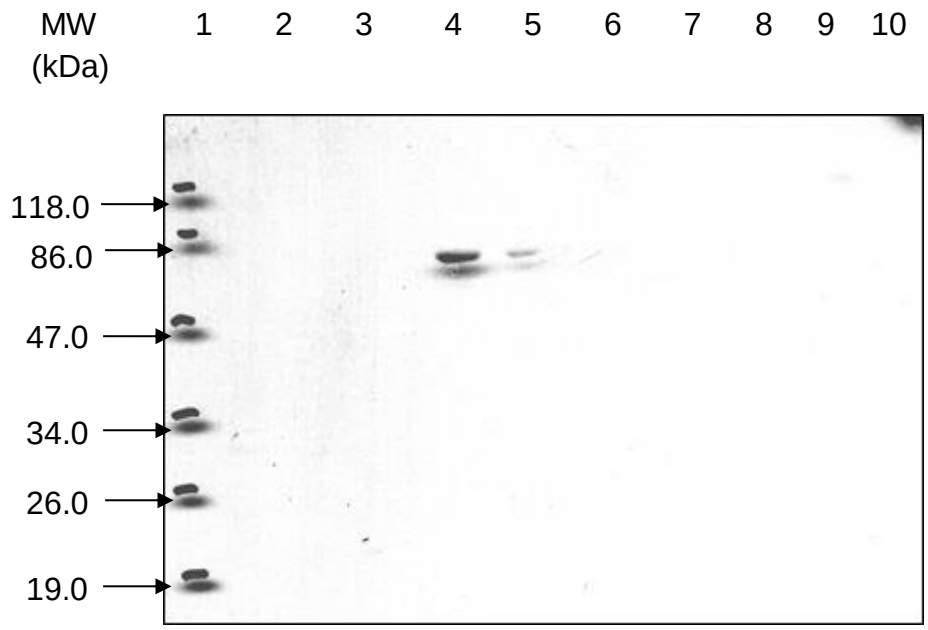

Figure 5.11(b). Western Blot analysis showing non-nitrated BSA and nitrated BSA with various concentrations of peroxynitrite and incubated for 15 min in a rocking water bath at 37°C. The primary antibody used was anti-nitrotyrosine mouse monoclonal IgG, Clone 1A6 (Upstate Biotechnology) which was first pre-absorbed with 10 mM 3-nitrotyrosine (Sigma) and the secondary antibody was polyclonal rabbit anti-mouse IgG/HRP conjugated (Dako Cytomation). The amount of BSA loaded was 2 µg. This blot acts as a negative control blot.

Lane 1 - prestained protein molecular weight markers (Fermentas)

Lane 2 - non-nitrated BSA

Lane 3 - 10 µM peroxynitrite nitrated BSA

Lane 4 - 50 µM peroxynitrite nitrated BSA

Lane 5 - 100 µM peroxynitrite nitrated BSA

Lane 6 - 200 µM peroxynitrite nitrated BSA

Lane 7 - 300 µM peroxynitrite nitrated BSA

Lane 8 - 400 µM peroxynitrite nitrated BSA

Lane 9 - 500 µM peroxynitrite nitrated BSA

Lane 10 - 1 mM peroxynitrite nitrated BSA

We then repeated the dose response of increasing concentrations of peroxynitrite on purified resolubilised p53 protein. The dose response effects of nitrated purified resolubilised p53 protein was a bit different from the dose response effects of nitrated BSA. In Fig. 5.12(a), we can see that the nitrotyrosine signals increased from 50 µM to 400 µM peroxynitrite (Fig. 5.12(a), Lanes 5 to 9). Weaker signals were observed in purified resolubilised p53 protein samples nitrated with 50 µM and 100 µM peroxynitrite (Fig. 5.12(a), Lanes 5 and 6, respectively). No nitrotyrosine signal was obtained in non-nitrated purified resolubilised p53 protein as expected where it acted as a negative control for nitration (Fig. 5.12(a), Lane 3). No signal was also found in 10 µM peroxynitrite nitrated purified resolubilised p53 protein samples (Fig. 5.12(a), Lane 4). We can see very strong nitro-p53 protein signals in purified resolubilised p53 protein samples nitrated with 200, 300 and 400 µM peroxynitrite with unreduced high molecular weight aggregates (Fig. 5.12(a), Lanes 7-9) which were also seen by Calmels *et al*. (1997) and Cobbs *et al*. (2001) in MCF7 and D54MG cells at 0.5-1 mM and 10-100 µM, peroxynitrite, respectively. This is believed to be due to the formation of carbonyl or dityrosine (i.e. tyrosine oxidation by peroxynitrite) or loss of zinc from p53 active site (Cobbs *et al*., 2001), which has been shown when p53 protein was treated with zinc chelators or with oxidizing agents (Hainut and Milner, 1993; Hainut *et al*., 1995). This modification on the p53 protein might affects p53 structure and functions. However, at 500 µM peroxynitrite, no nitro-p53 protein signal was observed at 53 kDa but we can see that there were still some unreduced high molecular weight aggregates present (Fig. 5.12(a), Lane 10). A possible explanation for the loss of nitrotyrosine signal at high concentration of peroxynitrite used (500 µM) is that due to the degrading properties of peroxynitrite on proteins as evident by a study by Ischiropoulos and Al-Mehdi which showed that fatty acid-free BSA was fragmented after exposure to peroxynitrite (Ischiropoulos and Al-Mehdi, 1995). 50 µM peroxynitrite nitrated BSA was run in parallel to act as a positive control for nitration (Fig. 5.12(a), Lane 2). A negative blot by pre-absorbing the primary antibody Clone 1A6 with 10 mM 3-nitro-L-tyrosine prior to incubating the blot was acceptable as no nitrotyrosine signals for all the samples on the blot except that we can see

a weak nitrotyrosine signal of 50 µM peroxynitrite nitrated BSA (Fig. 5.12(b)). The possible reason for this is that due to a high amount of nitrotyrosine shown in Fig. 5.12(a), thus the incomplete pre-absorbed anti-nitrotyrosine antibody could easily pick up the excess nitrated BSA. In Fig. 5.12(c), the blot with the same samples as the blots in Figs. 5.12(a) and (b), was probed with anti-p53 monoclonal antibody (DO-1) in order to check p53 protein levels after nitration with different concentrations of peroxynitrite and also to compare with non-nitrated purified resolubilised p53 protein sample. As can be seen in Fig. 5.12(c), a lot of p53 degradation products were observed from non-nitrated to 500 µM peroxynitrite nitrated purified resolubilised p53 protein samples. We cannot see an obvious increasing trend of p53 protein degradation products with increasing concentrations of peroxynitrite in this figure as reported by Cobbs and co-workers (2001 and 2003) where they found that tyrosine nitration of purified baculovirus-derived recombinant wt p53 protein and of p53 protein in D54MG cells system treated with 0-100 µM peroxynitrite caused increased p53 protein degradation. Non-reduced high molecular weight aggregates are also seen in samples in Lanes 3-9 (Fig. 5.12(c)) with higher intensities in samples 7-9.

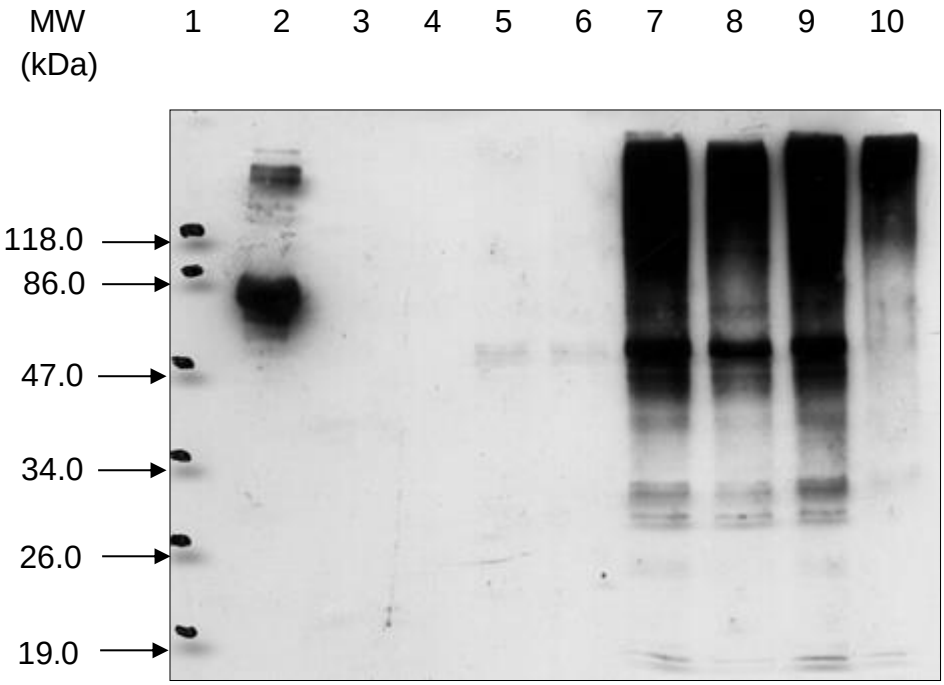

Figure 5.12(a). Western Blot analysis showing nitrated purified resolubilised p53 protein with various concentrations of peroxynitrite ranging from 10 μM to 500 μM and incubated for 15 min in a rocking water bath at 37°C. 50 μM peroxynitrite nitrated BSA was used as a positive control and non-nitrated purified resolubilised p53 protein as a negative control. The amount of nitrated BSA loaded was 2 μg and non-nitrated and nitrated purified resolubilised p53 protein was 2.04 μg. The primary antibody used was anti-nitrotyrosine mouse monoclonal IgG, Clone 1A6 (Upstate Biotechnology) and the secondary antibody was polyclonal rabbit anti-mouse IgG/HRP conjugated (Dako Cytomation).

Lane 1 - prestained protein molecular weight markers (Fermentas)

Lane 2 - 50 μM peroxynitrite nitrated BSA

Lane 3 - non-nitrated purified resolubilised p53

Lane 4 - 10 μM peroxynitrite nitrated purified resolubilised p53

Lane 5 - 50 μM peroxynitrite nitrated purified resolubilised p53

Lane 6 - 100 μM peroxynitrite nitrated purified resolubilised p53

Lane 7 - 200 μM peroxynitrite nitrated purified resolubilised p53

Lane 8 - 300 μM peroxynitrite nitrated purified resolubilised p53

Lane 9 - 400 μM peroxynitrite nitrated purified resolubilised p53

Lane 10 - 500 μM peroxynitrite nitrated purified resolubilised p53

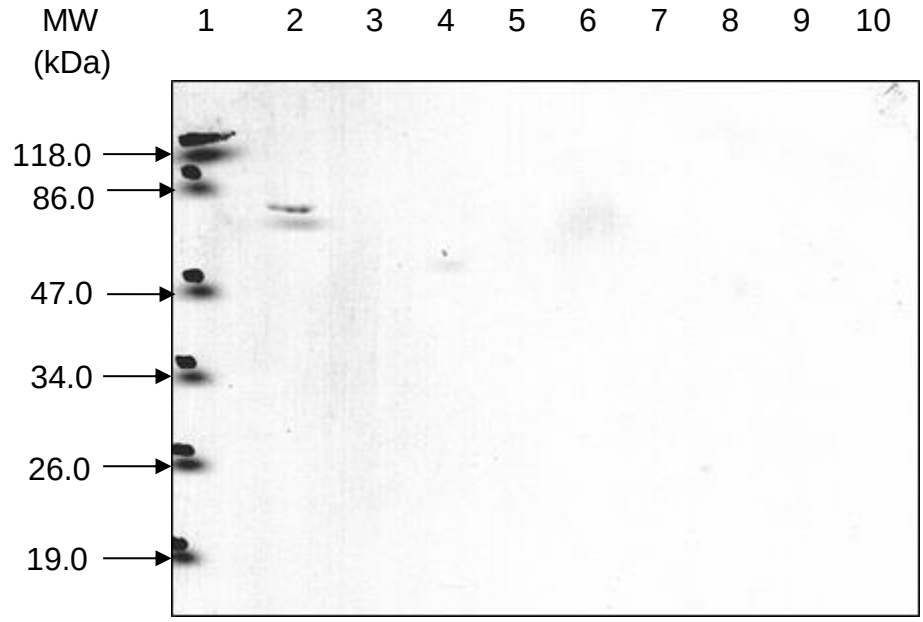

Figure 5.12(b). Western Blot analysis showing nitrated purified resolubilised p53 protein with various concentrations of peroxynitrite ranging from 10 μM to 500 μM and incubated for 15 min in a rocking water bath at 37°C. 50 μM peroxynitrite nitrated BSA was used as a positive control and non-nitrated purified p53 protein as a negative control. The amount of nitrated BSA loaded was 2 μg and non-nitrated and nitrated purified p53 protein was 2.04 μg. The primary antibody used was anti-nitrotyrosine mouse monoclonal IgG, Clone 1A6 (Upstate Biotechnology) which was first pre-absorbed with 3-nitro-L-tyrosine (Sigma) and the secondary antibody was polyclonal rabbit anti-mouse IgG/HRP conjugated (Dako Cytomation). This blot acts as a negative control blot.

Lane 1 - prestained protein molecular weight markers (Fermentas)

Lane 2 - 50 μM peroxynitrite nitrated BSA

Lane 3 - non-nitrated purified resolubilised p53

Lane 4 - 10 μM peroxynitrite nitrated purified resolubilised p53

Lane 5 - 50 μM peroxynitrite nitrated purified resolubilised p53

Lane 6 - 100 μM peroxynitrite nitrated purified resolubilised p53

Lane 7 - 200 μM peroxynitrite nitrated purified resolubilised p53

Lane 8 - 300 μM peroxynitrite nitrated purified resolubilised p53

Lane 9 - 400 μM peroxynitrite nitrated purified resolubilised p53

Lane 10 - 500 μM peroxynitrite nitrated purified resolubilised p53

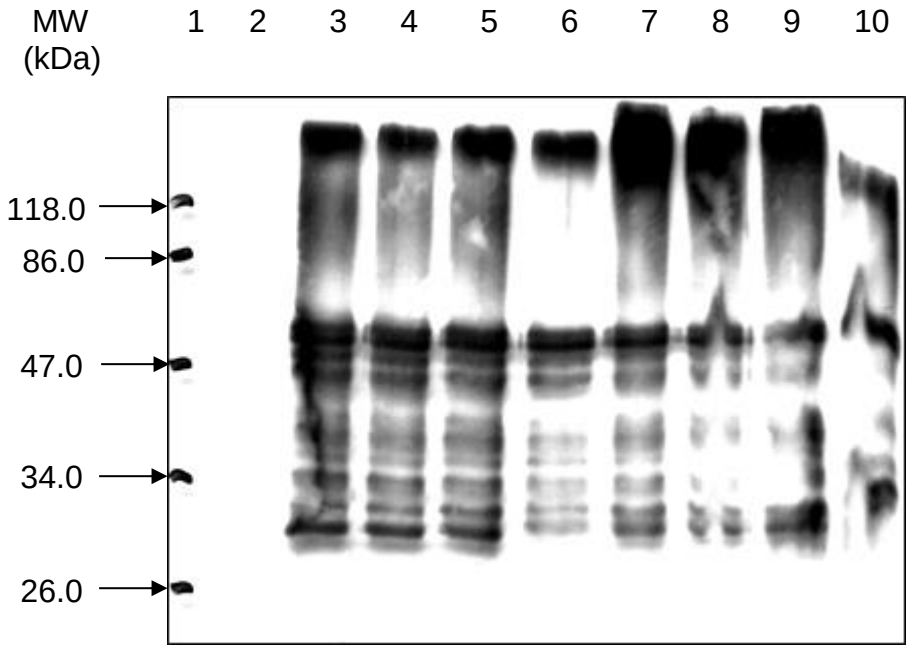

Figure 5.12(c). Western Blot analysis showing nitrated purified resolubilised p53 protein with various concentrations of peroxynitrite ranging from 10 μM to 500 μM and incubated for 15 min in a rocking water bath at 37°C. 50 μM peroxynitrite nitrated BSA was used as a positive control and non-nitrated purified resolubilised p53 protein as a negative control. The amount of nitrated BSA loaded was 2 μg and non-nitrated and nitrated purified resolubilised p53 protein was 2.04 μg. The primary antibody used was anti-p53 monoclonal antibody (DO-1), a kind gift of Dr Borivoj Vojtesek from the Czech Republic and the secondary antibody was rabbit polyclonal anti-mouse IgG HRP conjugated (DAKO Cytomation).

Lane 1 - prestained protein molecular weight markers (Fermentas)

Lane 2 - 50 μM peroxynitrite nitrated BSA

Lane 3 - non-nitrated purified resolubilised p53

Lane 4 - 10 μM peroxynitrite nitrated purified resolubilised p53

Lane 5 - 50 μM peroxynitrite nitrated purified resolubilised p53

Lane 6 - 100 μM peroxynitrite nitrated purified resolubilised p53

Lane 7 - 200 μM peroxynitrite nitrated purified resolubilised p53

Lane 8 - 300 μM peroxynitrite nitrated purified resolubilised p53

Lane 9 - 400 μM peroxynitrite nitrated purified resolubilised p53

Lane 10 - 500 μM peroxynitrite nitrated purified resolubilised p53

5.5 Nitration of a model protein BSA at different amounts

In order to get the most suitable conditions for nitration, as usual we used BSA as a model protein for nitration. BSA was nitrated at different amounts i.e. 100, 200, 300 and 500 µg with 100 µM peroxynitrite. From the results in Fig. 5.13, we found that there was no obvious different signals or nitrotyrosine levels in nitrated BSA in all the four amounts. But in a large scale nitration (20 mg), we can see that weak nitrotyrosine signals in 50 µM, 200 µM and 1 mM peroxynitrite when compared to 3 mM peroxynitrite which shows the strongest signal among the four concentrations of peroxynitrite used (Fig. 5.14) and interestingly the signal was about similar to signal in Lane 3 (500 µg BSA previously nitrated with 100 uM peroxynitrite) as also evident in Fig. 5.13, Lane 4, 100 µM peroxynitrite in 500 µg BSA. In non-nitrated BSA (Lane 2, Fig. 5.14) we can see a very weak signal of nitrotyrosine which was probably due to BSA being endogenously nitrated in cow as it is believed that nitration may occur as part of a normal physiological process with a potential role in signal transduction mechanisms, possibly by influencing tyrosine phosphorylation or dephosphorylation (Bruckdorfer, 2001).

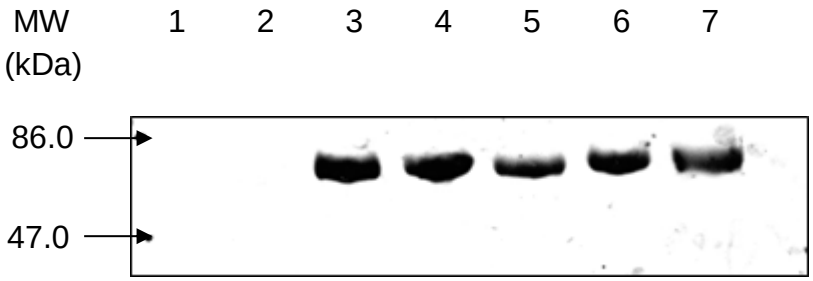

Figure 5.13. Western blot analysis showing 100 µM peroxynitrite nitration of BSA at different amounts in order to determine the effects of amounts on nitrotyrosine signals. The samples were incubated with peroxynitrite for 15 min in a rocking water bath at 37°C. The primary antibody used was anti-nitrotyrosine mouse monoclonal IgG, Clone 1A6 (Upstate Biotechnology) and the secondary antibody was rabbit anti-mouse IgG/HRP conjugated (DAKO Cytomation). The amount of BSA loaded was 2 µg.

Lane 1 - prestained protein molecular weight markers (Fermentas)

Lane 2 - non-nitrated BSA

Lane 3 - 100 µM peroxynitrite previously nitration of 500 µg BSA as a positive control

Lane 4 - 100 µM peroxynitrite nitration of 500 µg BSA

Lane 5 - 100 µM peroxynitrite nitration of 300 µg BSA

Lane 6 - 100 µM peroxynitrite nitration of 200 µg BSA

Lane 7 - 100 µM peroxynitrite nitration of 100 µg BSA

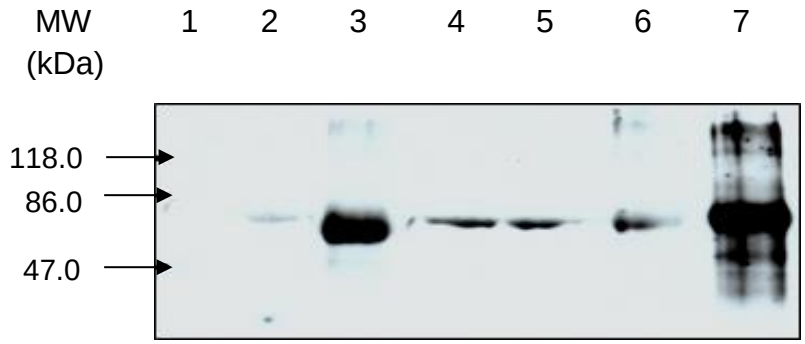

Figure 5.14. Western blot analysis showing a large scale nitration (20 mg) of BSA at various concentrations of peroxynitrite and incubated for 15 min in a rocking water bath at 37°C. 100 µM peroxynitrite previously nitration of 500 µg BSA was used as a positive control. The primary antibody used was anti-nitrotyrosine mouse monoclonal IgG, Clone 1A6 (Upstate Biotechnology and the secondary antibody was rabbit anti-mouse IgG/HRP conjugated (DAKO Cytomation). The amount of BSA loaded was 2 µg.

Lane 1 - prestained protein molecular weight markers (Fermentas)

Lane 2 - non-nitrated BSA

Lane 3 - 100 µM peroxynitrite previously nitration of 500 µg BSA

Lane 4 - 50 µM peroxynitrite nitration of 20 mg BSA

Lane 5 - 200 µM peroxynitrite nitration of 20 mg BSA

Lane 6 - 1 mM peroxynitrite nitration of 20 mg BSA

Lane 7 - 3 mM peroxynitrite nitration of 20 mg BSA

5.6 Increased in the amounts of nitrated BSA resulted in increased in nitrotyrosine signals

We also attempted to determine whether nitrotyrosine signals increased with increasing amount of nitrated BSA loaded (from 0.5 to 6.0 µg) onto an SDS polyacrylamide gel. BSA was nitrated with 3 mM peroxynitrite, loaded onto a SDS polyacryamide gel and then immunoblotted onto a nitrocellulose membrane and was subsequently detected with anti-nitrotyrosine monoclonal antibody (Upstate Biotechnology). From Fig. 5.15, we can see that the nitrotyrosine signals increased from 0.5 to 3.0 µg nitrated BSA loaded (Lanes 4-8) and then the signals seemed to plateau from 3.0 to 6.0 µg nitrated BSA loaded (Lanes 8-15).

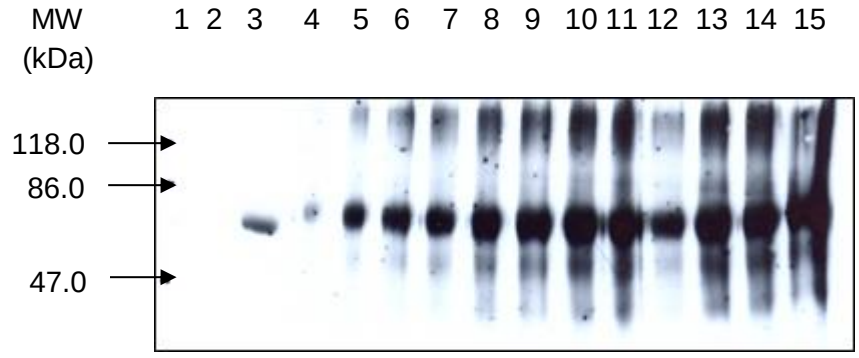

Figure 5.15. Western blot analysis showing 3 mM peroxynitrite nitrated BSA was incubated for 15 min in a rocking water bath at 37°C. The samples were loaded on an SDS-PAGE gel with increasing in amount from 0.5 µg to 6.0 µg to detect whether an increase in nitrotyrosine signal with increasing amounts of nitrated BSA. The primary antibody used was anti-nitrotyrosine mouse monoclonal IgG, Clone 1A6 (Upstate Biotechnology) and the secondary antibody was rabbit anti-mouse IgG/HRP conjugated (DAKO Cytomation).

Lane 1 - prestained protein molecular weight markers (Fermentas)

Lane 2 - non-nitrated BSA (2 µg)

Lane 3 -100 µM peroxynitrite previously nitrated BSA (2 µg)

Lane 4 - 3 mM peroxynitrite nitrated BSA (0.5 µg)

Lane 5 - 3 mM peroxynitrite nitrated BSA (1.0 µg)

Lane 6 - 3 mM peroxynitrite nitrated BSA (1.5 µg)

Lane 7 - 3 mM peroxynitrite nitrated BSA (2.0 µg)

Lane 8 - 3 mM peroxynitrite nitrated BSA (2.5 µg)

Lane 9 - 3 mM peroxynitrite nitrated BSA (3.0 µg)

Lane 10 - 3 mM peroxynitrite nitrated BSA (3.5 µg)

Lane 11 - 3 mM peroxynitrite nitrated BSA (4.0 µg)

Lane 12 - 3 mM peroxynitrite nitrated BSA (4.5 µg)

Lane 13 - 3 mM peroxynitrite nitrated BSA (5.0 µg)

Lane 14 - 3 mM peroxynitrite nitrated BSA (5.5 µg)

Lane 15 - 3 mM peroxynitrite nitrated BSA (6.0 µg)

5.7 Use of platelets in the pilot nitration study

Peroxynitrite affects platelet functions in a concentration-dependent manner. At higher concentrations (> 150 µM), peroxynitrite acts as a platelet agonist by stimulating platelet aggregation (Moro *et al*., 1994). However, at lower concentrations (3-10 µM) , peroxynitrite acts as a platelet inhibitor with an $I.C._{50}$ of 3 µM, but less effective than NO (Moro *et al*., 1994; Naseem, 1995). It has been shown that the addition of peroxynitrite leads to the nitration of specific platelet proteins and the regulation of platelet functions (Mandoro *et al*., 1997). Among the most prominently nitrated proteins had molecular weights of 187, 164, 113, 89, and 61 kDa. Platelet proteins nitrated to a lesser extent were of molecular weights of 208, 182, 122, 91, 70, and 50 kDa (Mondoro *et al*., 1997). Therefore, in order to reproduce this finding using our nitration system, we then tried to nitrate bovine platelets as recommended by Prof. Naseem (Biomedical Sciences Department). The platelets were either lysed or left intact (kindly prepared by Dr Andrew Milward, Biomedical Sciences Department) and then were nitrated with peroxynitrite concentrations ranging from 5 to 100 µM and BSA was nitrated in parallel with 100 µM peroxynitrite to act as a positive control for nitration. As can be seen on an SDS polyacrylamide gel stained with Commassie blue in Fig. 5.16(a), the platelet proteins profiles for both unlysed and lysed platelets were very similar either they were nitrated or not. The platelet proteins were hardly nitrated as evident in Fig. 5.16(b) where very weak signals of nitrotyrosine detected in both nitrated unlysed and lysed platelets with the exception that at 50 µM and 100 µM peroxynitrite-treated unlysed bovine platelets where quite strong signals were detected when compared to the rest. Interestingly, the size of the nitrated platelet protein is about the same size as the nitrated BSA (66 kDa). This might be residual BSA remained in the unlysed washed platelet as BSA is very readily nitrated due to its high content of tyrosine residues and these results show a clear evident for the readily nitrated BSA at 50 µM and 100 µM peroxynitrite.

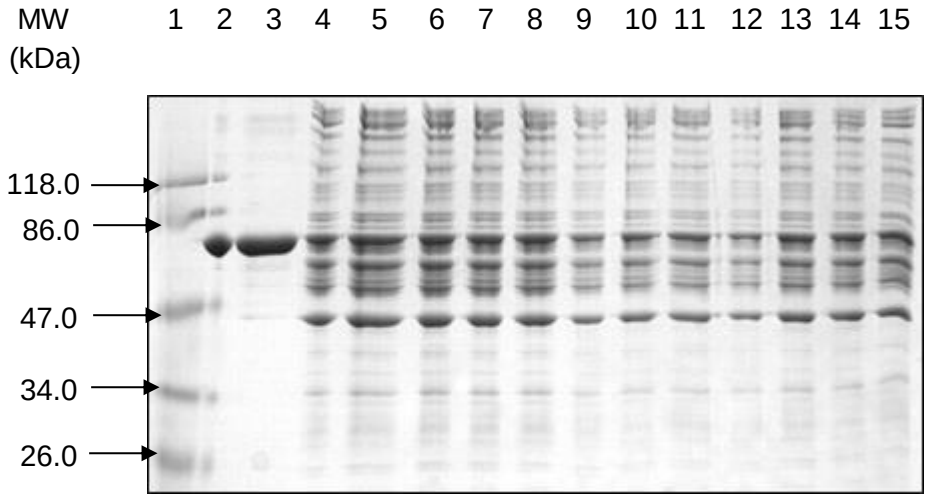

Figure 5.16(a). A 10% SDS-PAGE gel showing nitration of unlysed and lysed bovine platelets with peroxynitrite concentrations ranging from 5 to 100 µM and incubated for 15 min in a rocking water bath at 37°C. BSA was nitrated at the same time with 100 µM peroxynitrite to act as a positive control for nitration. The amount of BSA loaded was 2 µg. The gel was stained with Coomassie Blue for 15 minutes and then destained overnight.

Lane 1 - prestained protein molecular weight markers (Fermentas)

Lane 2 - non-nitrated BSA dissolved in PBS

Lane 3 - 100 µM peroxynitrite nitrated BSA dissolved in PBS

Lane 4 - non-nitrated unlysed bovine platelets

Lane 5 - 5 µM peroxynitrite nitrated unlysed bovine platelets

Lane 6 - 10 µM peroxynitrite nitrated unlysed bovine platelets

Lane 7 - 25 µM peroxynitrite nitrated unlysed bovine platelets

Lane 8 - 50 µM peroxynitrite nitrated unlysed bovine platelets

Lane 9 - 100 µM peroxynitrite nitrated unlysed bovine platelets

Lane 10 - non-nitrated lysed bovine platelets

Lane 11 - 5 µM peroxynitrite nitrated lysed bovine platelets

Lane 12 - 10 µM peroxynitrite nitrated lysed bovine platelets

Lane 13 - 25 µM peroxynitrite nitrated lysed bovine platelets

Lane 14 - 50 µM peroxynitrite nitrated lysed bovine platelets

Lane 15 - 100 µM peroxynitrite nitrated lysed bovine platelets

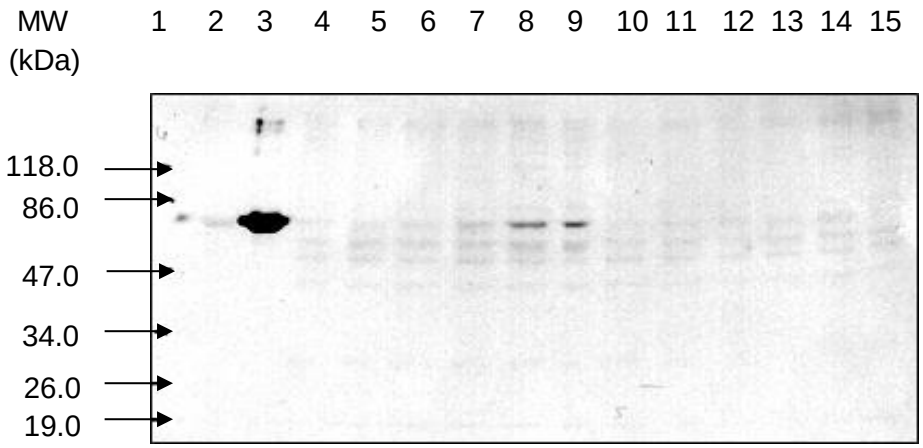

Figure 5.16(b). A western blot analysis showing nitration of unlysed and lysed bovine platelets with peroxynitrite concentrations ranging from 5 to 100 µM and incubated for 15 min in a rocking water bath at 37°C. BSA was nitrated at the same time with 100 µM peroxynitrite to act as a positive control for nitration. The primary antibody used was mouse monoclonal anti-nitrotyrosine (Upstate Biotechnology) and the secondary antibody was rabbit anti-mouse HRP conjugated polyclonal antibody (DAKO Cytomation). The amount of BSA loaded was 2 µg.

Lane 1 - prestained protein molecular weight markers (Fermentas)

Lane 2 - non-nitrated BSA dissolved in PBS

Lane 3 - 100 µM peroxynitrite nitrated BSA dissolved in PBS

Lane 4 - non-nitrated unlysed bovine platelets

Lane 5 - 5 µM peroxynitrite nitrated unlysed bovine platelets

Lane 6 - 10 µM peroxynitrite nitrated unlysed bovine platelets

Lane 7 - 25 µM peroxynitrite nitrated unlysed bovine platelets

Lane 8 - 50 µM peroxynitrite nitrated unlysed bovine platelets

Lane 9 - 100 µM peroxynitrite nitrated unlysed bovine platelets

Lane 10 - non-nitrated lysed bovine platelets

Lane 11 - 5 µM peroxynitrite nitrated lysed bovine platelets

Lane 12 - 10 µM peroxynitrite nitrated lysed bovine platelets

Lane 13 - 25 µM peroxynitrite nitrated lysed bovine platelets

Lane 14 - 50 µM peroxynitrite nitrated lysed bovine platelets

Lane 15 - 100 µM peroxynitrite nitrated lysed bovine platelets

5.8 pH measurements of peroxynitrite, NaOH, Potassium Phosphate Buffer (KPi), PBS and distilled water and $OD_{302\ nm}$ of diluted peroxynitrite

The objective of this work was to determine whether the differences in the pH values of diluents used to dilute peroxynitrite (PN) would affect its stability and its effectiveness as a nitrating agent. First, we measured the pH of each solution employed and then the pH of peroxynitrite diluted in each diluent and their corresponding optical densities (ODs) at 302 nm were read using a spectrophotometer. The pH of stock of freshly prepared peroxynitrite, 1.5 M NaOH, 50 mM KPi, PBS and distilled water (both sterile and non-sterile) were measured by using pH indicator sticks. We found that the pH of peroxynitrite (30 mM) was around 13.0. 1.5 M NaOH was the most alkaline with a pH of 14.0. KPi with a pH of 8.0 was more alkaline than PBS (pH 7.5). These results are summarised in Table 5.1 below.

Table 5.1: pH checking of 30 mM stock peroxynitrite (PN), 1.5 M NaOH, 50 mM Potassium Phosphate Buffer (KPi), PBS and distilled water (both sterile and non-sterile) using pH indicator sticks.

Reagents	pH
Peroxynitrite (30 mM)	13.0
1.5 M NaOH	14.0
50 mM KPi	8.0
PBS	7.5
Sterile distilled water	5.0
Non-sterile distilled water	4.7

Stock peroxynitrite was diluted 1:2, 1:10 and 1:20 in 1.5 M NaOH, 50 mM KPi, PBS or sterile distilled water to see the effects of these solutions on the pH of peroxynitrite. As shown in Table 5.2 below, the pH of stock peroxynitrite diluted in 1.5 M NaOH increased to 14.0 in all the 3 dilutions. The pH of stock peroxynitrite remained at 13.0 when diluted 1:2 in 50 mM KPi, PBS or sterile distilled water. The pH dropped to 12.0 and then further

dropped to 11.0 when diluted 1:10 and 1:20, respectively in 50 mM KPi, PBS or sterile distilled water.

Table 5.2: pH checking of peroxynitrite (PN) after 1:2, 1:10 and 1:20 dilution either in 1.5 M NaOH, 50 mM KPi, PBS or sterile distilled water using pH indicator sticks

Diluent / Dilution	**pH**		
	1:2	**1:10**	**1:20**
1.5 M NaOH	14.0	14.0	14.0
50 mM KPi	13.0	12.0	11.0
PBS	13.0	12.0	11.0
Sterile distilled water	13.0	12.0	11.0

The stock peroxynitrite diluted 1:2, 1:10 or 1:20 in 1.5 M NaOH, 50 mM KPi, PBS or sterile distilled water was measured at $OD_{302\ nm}$. $OD_{302\ nm}$ of peroxynitrite diluted in 1.5 M NaOH at all the 3 dilutions were slightly higher than that of in 50 mM KPi, PBS or distilled water, however, were still lower than the expected $OD_{302\ nm}$. As we increased dilution from 1:2 to 1:10 to 1:20, by right the ODs would decrease 2 fold to 5 fold to 10 fold as calculated in the expected $OD_{302\ nm}$. The decrease in ODs corresponds to the decrease in the peroxynitrite concentration. As what can be seen in Table 5.3 below, peroxynitrite was quite stable in 1.5 M NaOH when compared to in 50 mM KPi, PBS or sterile distilled water. The data are also presented graphically in Fig. 5.17. The half-life of peroxynitrite in solution at physiological pH 7.4 is approximately 1 s (Koppenol et al., 1992). Once prepared, peroxynitrite needs to be stored in 1.5 M NaOH to increase its stability.

Table 5.3: Summary of OD 302 nm of peroxynitrite (PN) diluted either in 1.5 M NaOH, 50 mM KPi, PBS or sterile distilled water. Expected ODs were also included

	OD 302 nm				
PN dilution	**Expected $OD_{302\ nm}$**	**1.5 M NaOH**	**50 mM KPi**	**PBS**	**Sterile distilled water**
1:2	0.349	0.313	0.283	0.252	0.271
1:10	0.070	0.024	0.012	0.016	0.024
1:20	0.035	0.011	-0.008	0.003	0.004

Peroxynitrite solution diluted 1:2, 1:10 and 1:30 either in distilled water, PBS or 1.5 M NaOH were scanned with a multiwavelength spectrophotometer (Beckman DU-64) (Fig. 5.18). The absorbance peak at 302 nm of peroxynitrite diluted 1:2 in distilled water was slightly lower than that of diluted in PBS and 1.5 M NaOH (Fig. 5.18(a)). In 1:10 dilution, we expected to get a 5-fold lower of OD 302 nm where this can only be seen in 1.5 M NaOH diluent but the other two diluent gave much lower ODs. Reduction in OD 302 nm of peroxynitrite diluted 1:30 in 1.5 M NaOH was as expected (15-fold reduction) however in 1:30 dilution in PBS, no peak at OD 302 nm was detected and a very low peak in distilled water when compared to in 1.5 M NaOH. We can conclude here that peroxynitrite diluted in 1.5 M NaOH was more stable since NaOH is very alkaline (pH 14.0) and is therefore more efficient in nitrating proteins.

Figure 5.17. A comparison of OD 302 nm of dilution of stock peroxynitrite (PN) either in NaOH, KPi, PBS or distilled water (dH_2O).

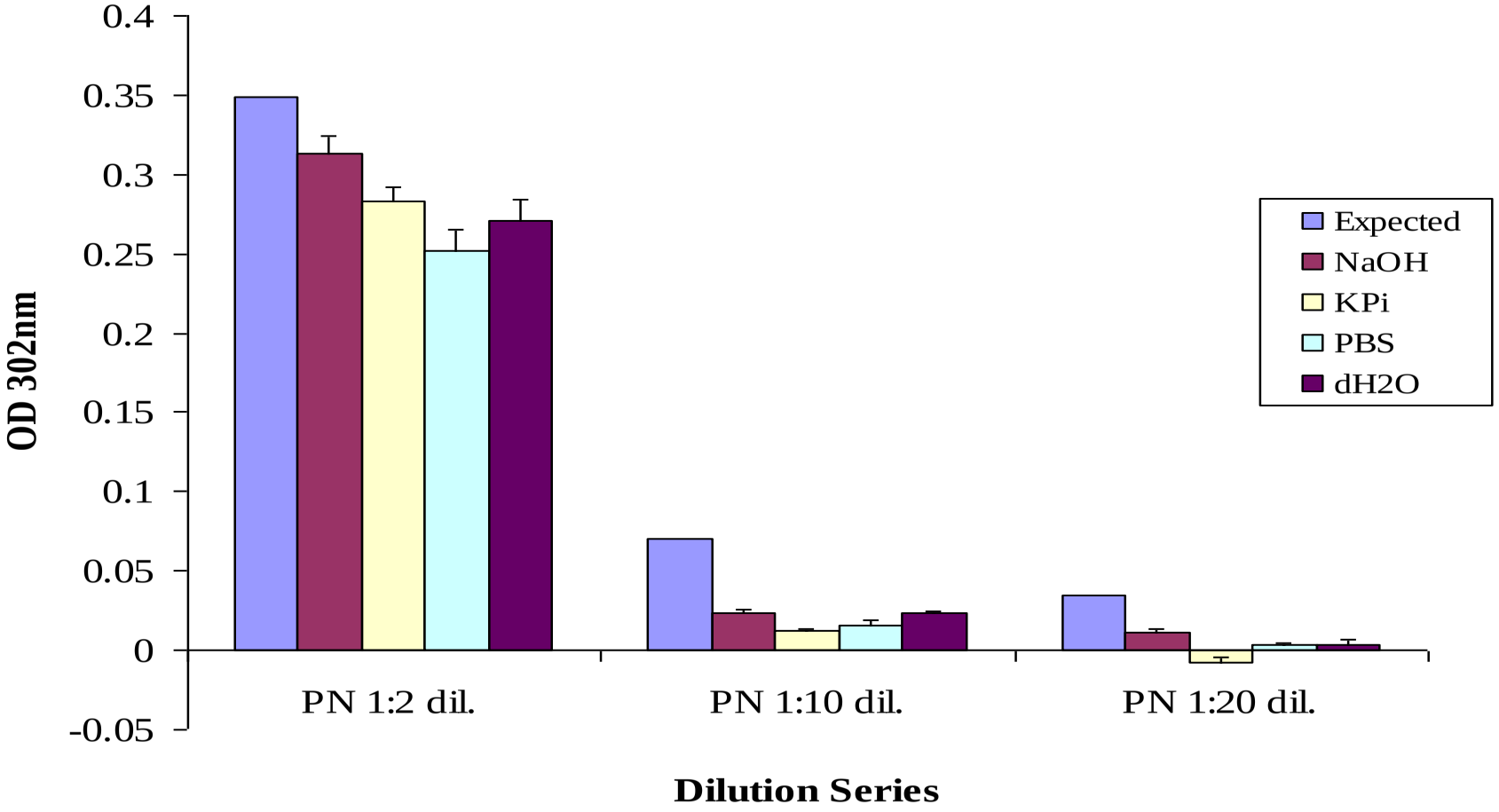

Figure 5.18(a). A multiwavelength scan of a peroxynitrite solution diluted 1:2 in distilled water (dH_2O), PBS or 1.5 M NaOH using a Beckman DU-64 spectrophotometer at wavelengths ranging from 200 nm to 400 nm and absorbance limits from 0.0000 to 1.0000.

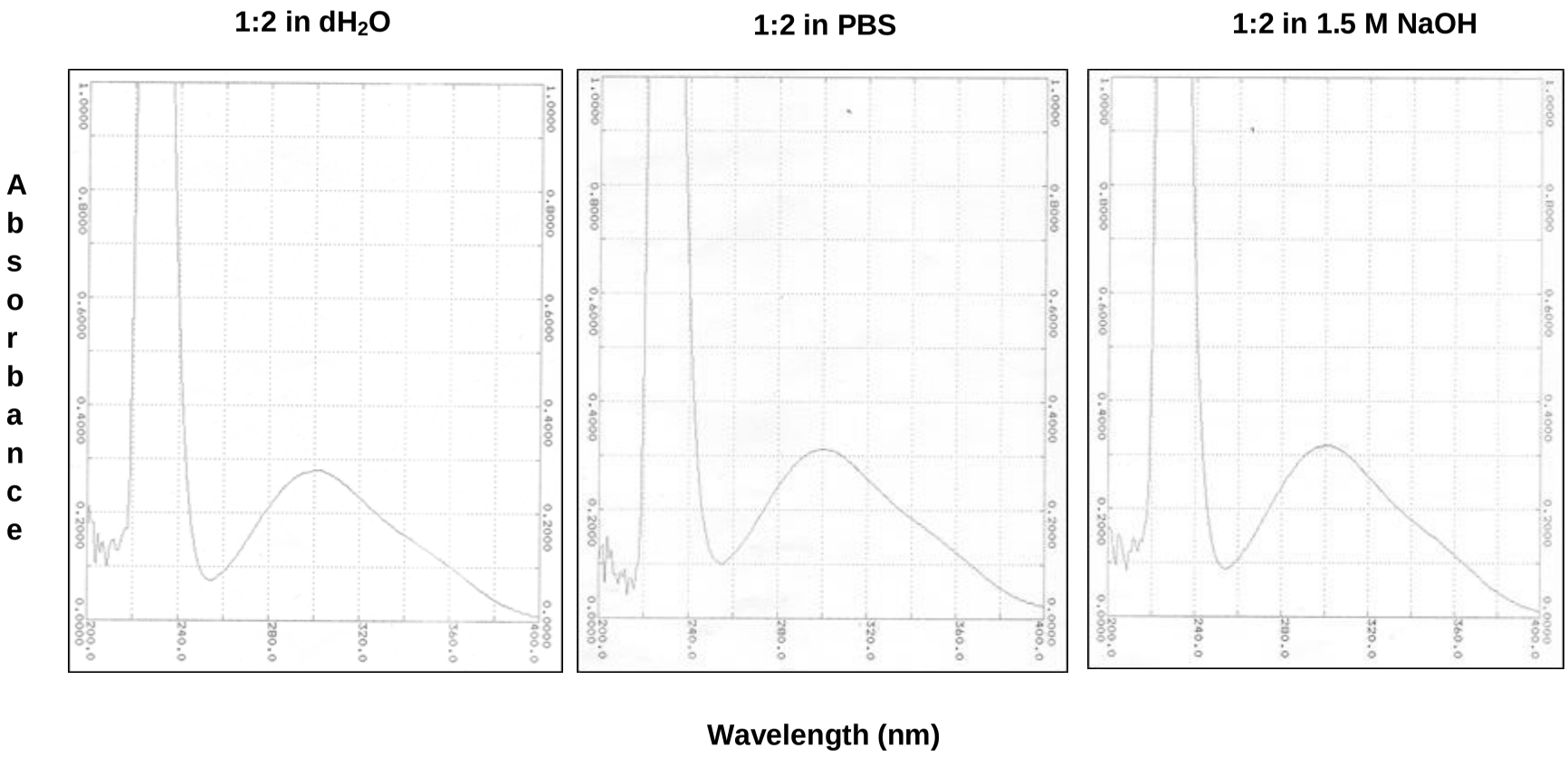

Figure 5.18(b). A multiwavelength scan of a peroxynitrite solution diluted 1:10 in distilled water (dH_2O), PBS or 1.5 M NaOH using a Beckman DU-64 spectrophotometer at wavelengths ranging from 200 nm to 400 nm and absorbance limits from 0.0000 to 1.0000.

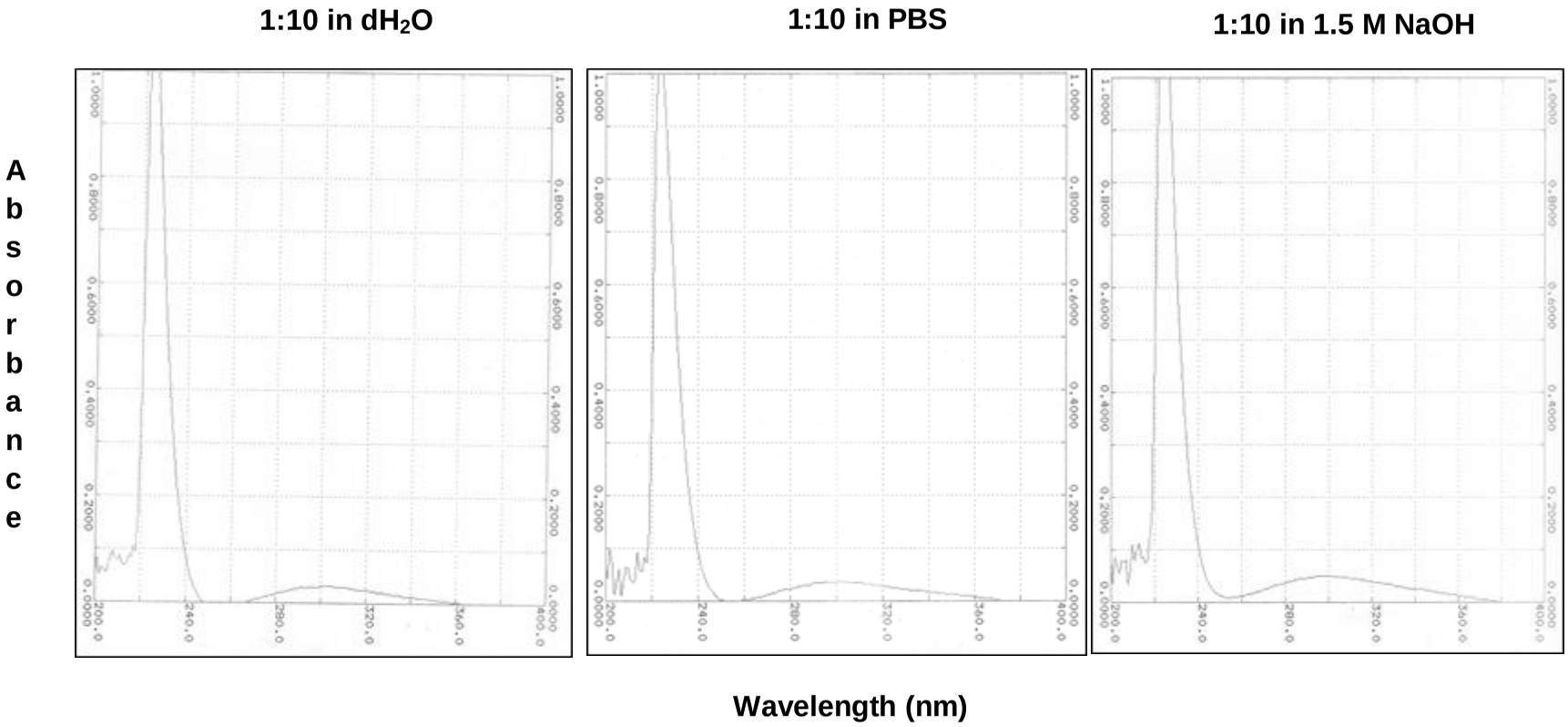

Figure 5.18(c). A multiwavelength scan of a peroxynitrite solution diluted 1:30 in distilled water (dH_2O), PBS or 1.5 M NaOH using a Beckman DU-64 spectrophotometer at wavelengths ranging from 200 nm to 400 nm and absorbance limits from 0.0000 to 1.0000.

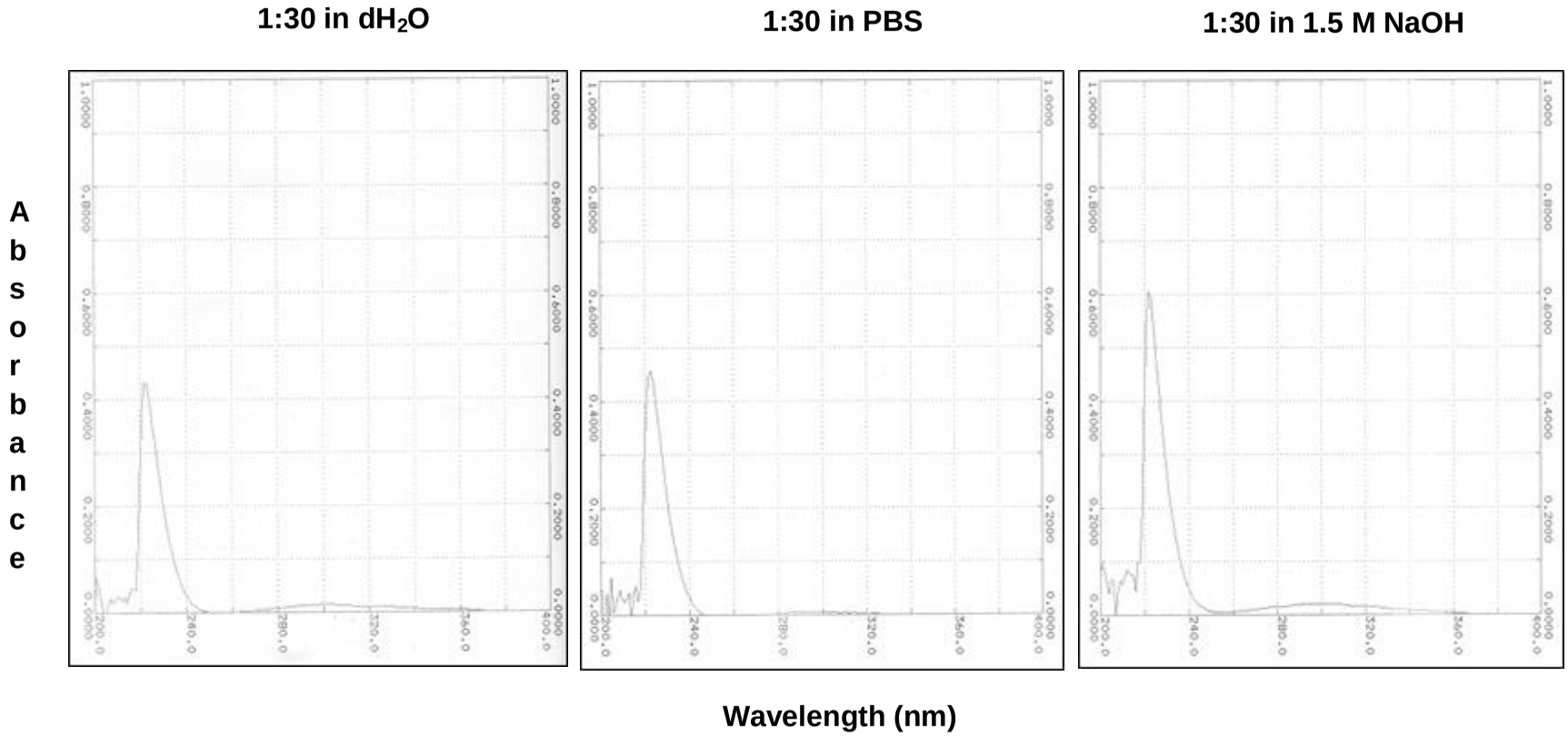

5.9 Effects of buffers used in dissolving BSA on nitration

We then carried out experiments to determine whether buffer used to dissolve BSA would affect its nitration. Two different buffers were used namely PBS (pH 7.4) or 50 mM Potassium Phosphate Buffer (KPi, pH 8.2, as used in the literature). As can be seen in Fig. 5.19(a), the levels of nitrated BSA were lower when it was dissolved in PBS (Lanes 4-8) when compared to nitrated BSA dissolved in KPi (Lanes 9-14). This is supported by a western blot analysis (Fig. 5.19(b)) where nitrotyrosine levels of BSA dissolved in KPi shows a dose response increase from 5 µM to 100 µM peroxynitrite. BSA dissolved in PBS shows the strongest signal at 100 µM peroxynitrite while the rest gave weak nitrotyrosine signals. This means that peroxynitrite concentration at 100 µM used to nitrate BSA gave an optimal nitration. We then proceeded to the nitration of different amounts (20.3, 40.6 and 60.9 µg) of purified resolubilised p53 protein after being dialysed in PBS with 100 µM Peroxynitrite in order to determine the effects of amounts on the nitrotyrosine signals (see Fig. 5.20). However, the experiment was unsuccessful as we could not get any nitrotyrosine signals for all the amounts. This shows that p53 protein is not easily nitrated. We then attempted to nitrate both purified resolubilised and purified soluble p53 protein with 100 µM and 1.5 mM peroxynitrite from 30 mM stock (Fig.5.21(a)) but no nitroytrosine signals were detected for both forms of p53 protein. BSA which was nitrated at the same time showed strong nitrotyrosine signals. Again non-nitrated BSA showed a very weak signal of nitrotyrosine indicating that BSA was endogenously nitrated in cow. Both non-nitrated purified resolubilised p53 and purified soluble p53 protein showed high levels of p53 protein as seen in Fig. 5.21(b) Lane 6 and Lane 9, respectively, however the p53 protein levels dramatically reduced in nitrated purified soluble p53 protein (Fig. 5.21(b), Lanes 10-11) and almost altogether disappeared in nitrated purified reolubilised p53 protein (Fig. 5.21(b), Lanes 7-8).

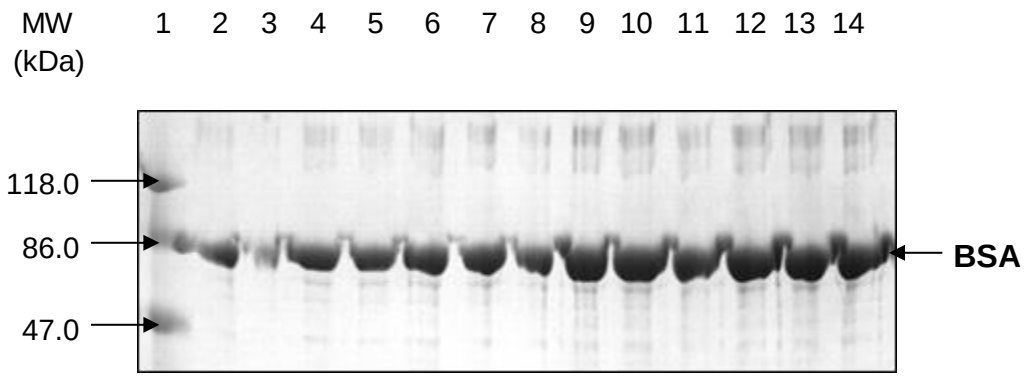

Figure 5.19(a). A 10% SDS-PAGE gel showing a comparison of nitration of BSA which was incubated with peroxynitrite for 15 min in a rocking water bath at 37°C. The samples were either dissolved in PBS (pH 7.4) or 50 mM Potassium Phosphate Buffer (KPi, pH 8.2). The amount of BSA loaded was 2 µg. The gel was stained with Coomassie Blue for 15 mins and then destained overnight.

Lane 1 - prestained protein molecular weight markers (Fermentas)

Lane 2 - non-nitrated BSA dissolved in PBS

Lane 3 - 100 µM peroxynitrite previously nitrated BSA dissolved in PBS

Lane 4 - 5 µM peroxynitrite nitrated BSA dissolved in PBS

Lane 5 - 10 µM peroxynitrite nitrated BSA dissolved in PBS

Lane 6 - 25 µM peroxynitrite nitrated BSA dissolved in PBS

Lane 7 - 50 µM peroxynitrite nitrated BSA dissolved in PBS

Lane 8 - 100 µM peroxynitrite nitrated BSA dissolved in PBS

Lane 9 - non-nitrated BSA dissolved in KPi

Lane 10 - 5 µM peroxynitrite nitrated BSA dissolved in KPi

Lane 11 - 10 µM peroxynitrite nitrated BSA dissolved in KPi

Lane 12 - 25 µM peroxynitrite nitrated BSA dissolved in KPi

Lane 13 - 50 µM peroxynitrite nitrated BSA dissolved in KPi

Lane 14 - 100 µM peroxynitrite nitrated BSA dissolved in KPi

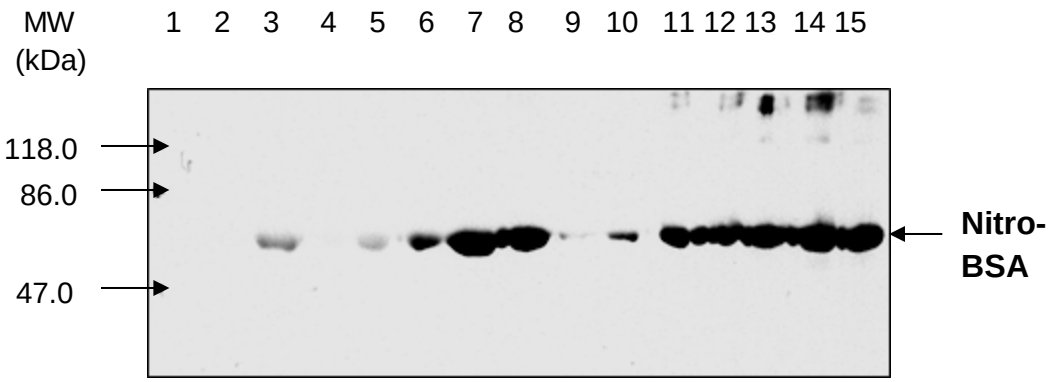

Figure 5.19(b). A western blot analysis showing a comparison of nitration of BSA which was incubated with peroxynitrite for 15 min in a rocking water bath at 37°C. The samples were either dissolved in PBS (pH 7.4) or 50 mM Potassium Phosphate Buffer (KPi, pH 8.2). The amount of BSA loaded was 2 µg. The primary antibody used was mouse anti-nitrotyrosine monoclonal antibody (Upstate Biotechnology) and the secondary antibody was rabbit anti-mouse HRP conjugated polyclonal antibody (DAKO Cytomation).

Lane 1 - prestained protein molecular weight markers (Fermentas)

Lane 2 - non-nitrated BSA dissolved in PBS

Lane 3 - 5 µM peroxynitrite nitrated BSA dissolved in PBS

Lane 4 - 10 µM peroxynitrite nitrated BSA dissolved in PBS

Lane 5 - 25 µM peroxynitrite nitrated BSA dissolved in PBS

Lane 6 - 50 µM peroxynitrite nitrated BSA dissolved in PBS

Lane 7 - 100 µM peroxynitrite nitrated BSA dissolved in PBS

Lane 8 - 100 µM peroxynitrite previously nitrated BSA dissolved in PBS

Lane 9 - non-nitrated BSA dissolved in KPi

Lane 10 - 5 µM peroxynitrite nitrated BSA dissolved in KPi

Lane 11 - 10 µM peroxynitrite nitrated BSA dissolved in KPi

Lane 12 - 25 µM peroxynitrite nitrated BSA dissolved in KPi

Lane 13 - 50 µM peroxynitrite nitrated BSA dissolved in KPi

Lane 14 - 100 µM peroxynitrite nitrated BSA dissolved in KPi

Lane 15 - 100 µM peroxynitrite previously nitrated BSA dissolved in PBS

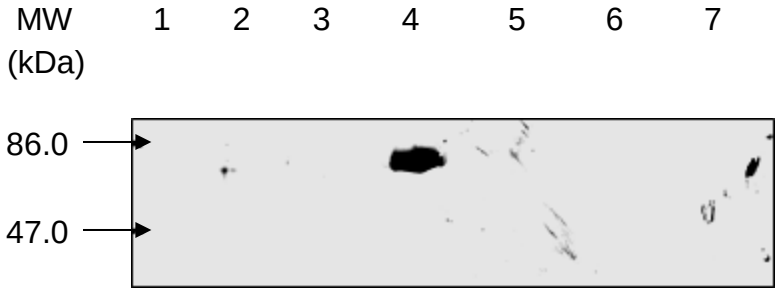

Figure 5.20. A Western blot analysis showing 100 µM peroxynitritre nitration of purified resolubilised p53 protein after being dialysed in PBS at different amounts which was incubated with peroxynitrite for 15 min in a rocking water bath at 37°C. This was in order to determine the effects of volumes/amounts on nitrotyrosine signals. The primary antibody used was anti-nitrotyrosine mouse monoclonal IgG, Clone 1A6 (Upstate Biotechnology) and the secondary antibody was rabbit anti-mouse IgG/HRP conjugated (DAKO Cytomation). Non-nitrated purified resolubilised p53 protein was used as a negative control. Non-nitrated and 100 µM peroxynitrite nitrated BSA were also used as controls. The amount of BSA loaded was 2 µg.

Lane 1 - prestained protein molecular weight markers (Fermentas)

Lane 2 - non-nitrated purified resolubilised p53 protein

Lane 3 - non-nitrated BSA

Lane 4 - 100 µM peroxynitrite previously nitration of 500 µg BSA as a positive control

Lane 5 - 100 µM peroxynitrite nitration of 60.9 µg purified resolubilised p53 protein

Lane 6 - 100 µM peroxynitrite nitration of 40.6 µg purified resolubilised p53 protein

Lane 7 - 100 µM peroxynitrite nitration of 20.3 µg purified resolubilised p53 protein

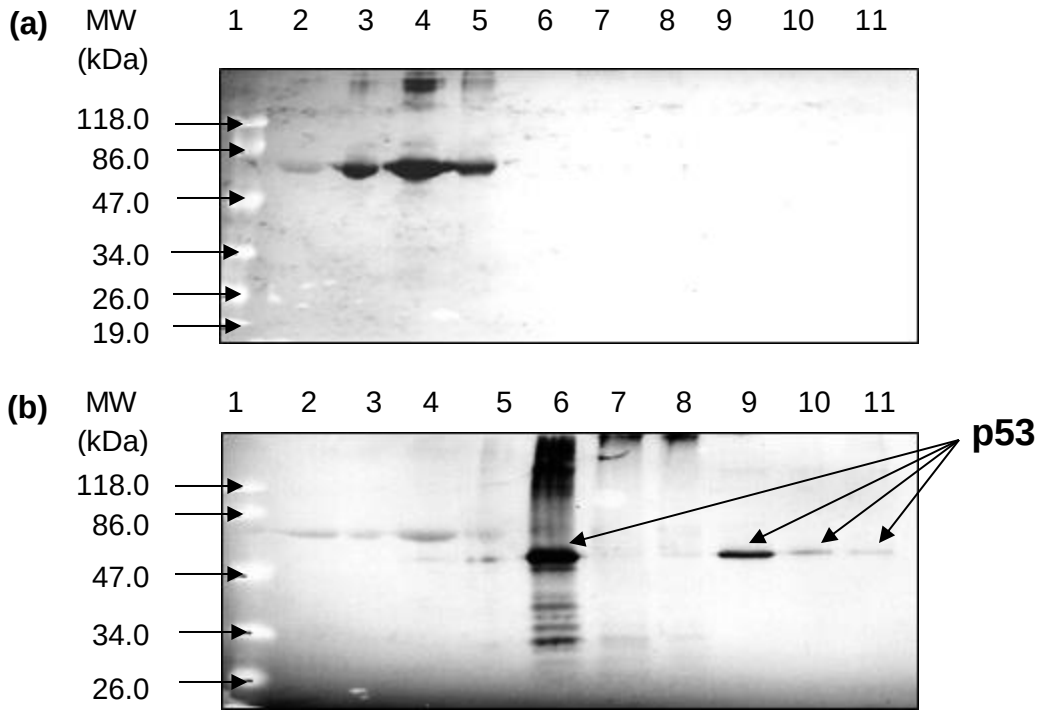

Figure 5.21. Nitration of purified resolubilised and soluble p53 protein with 100 µM peroxynitrite directly from 30 mM stock and also 2.5 µl from the stock where the final concentration was 1.5 mM which were incubated with peroxynitrite for 15 min in a rocking water bath at 37°C. The samples BSA was also nitrated alongside to act as a positive control for nitration. The primary antibody used for blot **(a)** was mouse monoclonal anti-nitrotyrosine (Upstate Biotechnology) and DO-1 for blot **(b)**. The secondary antibody used for both blots were rabbit anti-mouse polyclonal antibody (DAKO Cytomation).

Lane 1 - prestained protein molecular weight markers (Fermentas)

Lane 2 - non-nitrated BSA (2 µg)

Lane 3 - 100 µM peroxynitrite previously nitrated BSA (2 µg)

Lane 4 - 100 µM peroxynitrite nitrated BSA (2 µg)

Lane 5 - 2.5 µl peroxynitrite nitrated BSA (2 µg)

Lane 6 - non-nitrated purified resolubilised p53 protein (2.04 µg)

Lane 7 - 100 µM peroxynitrite nitrated purified resolubilised p53 protein (2.04 µg)

Lane 8 - 2.5 µl peroxynitrite nitrated purified resolubilised p53 protein (2.04 µg)

Lane 9 - non-nitrated purified soluble p53 protein (1.14 µg)

Lane 10 -100 µM peroxynitrite nitrated purified soluble p53 protein (1.14 µg)

Lane 11 - 2.5 µl peroxynitrite nitrated purified soluble p53 protein (1.14 µg)

5.10 Attempted nitration of purified resolubilised p53 protein

This was the first ever work to nitrate purified recombinant wt p53 protein expressed in *E. coli*. Other works done earlier include nitration of purified baculovirus-derived p53 protein (Cobbs *et al*., 2001), nitration of recombinant mwt p53 expressed in cell-free rabbit-reticulocyte lysates (Calmels et *al*., 1997), nitration of cell lysates of cancer cell lines with peroxynitrite (0-100 µM), and an endogenous or GSNO-induced (1 mM) NO-production in RAW 264.7. In some work, cancer cell lines such as MCF7 human breast cancer cells, HepG2 human hepatoma cells, D54MG cancer cells, and HCT 116 colon carcinoma cells (with wt p53, null-p53 and null-p21 genes) were treated with NO donors such as GSNO, SNAP, SIN-1, NONOate etc. (Calmels et *al*., 1997; Chazotte-Aubert *et al*., 2000; Cobbs *et al*., 2001; Hofseth *et al*., 2003).

We then attempted to nitrate purified resolubilised p53 protein with increasing concentrations of peroxynitrite to determine the dose-response effects of peroxynitrite on the nitrotyrosine levels of nitrated p53 protein. The basal nitrotyrosine signal observed in non-nitrated purified resolubilised p53 protein might be due to the p53 protein was endogenously nitrated *E. coli* BL21 strain where it was being expressed (Fig. 5.22(a), Lane 4). This suggests that the recombinant p53 protein was exposed to a nitrating species present *in vivo* in *E. coli* BL21. Similar basal nitrotyrosine signals were also observed in all nitrated purified resolubilised p53 protein samples (Fig. 5.22 (a), Lanes 5-13) when compared to a basal nitro-p53 signal in non-nitrated purified resolubilised p53 protein control (Fig. 5.22(a), Lane 4) except sample in Lane 14 (Fig. 5.22 (a)) (nitrated with 3 mM peroxynitrite) where no nitrotyrosine signal was detected. From these observations it is clear that there was no dose-response effects of peroxynitrite on the nitrotyrosine signals in nitrated purified resolubilised p53 protein. Fig. 5.22(b) shows that increasing doses of peroxynitrite from 10 µM to 2 mM (Lanes 5-13) seemed not to reduce the levels of the nitrated purified resolubilised p53 protein where their levels were almost similar compared to the p53 protein level in non-nitrated purified resolubilised p53 protein (Lane 4).

There was a slight reduction in the p53 protein level in purified resolubilised p53 protein nitrated with 3 mM peroxynitrite (Fig. 5.22(b), Lane 14) when compared to the non-nitrated (Lane 4) and the other nitrated counterparts (nitrated with 10 µM to 2 mM peroxynitrite) (Lane 5-13). This shows that peroxynitrite at 3 mM concentration is quite degrading and did not give any nitrotyrosine signal in nitrated purified resolubilised p53 protein.

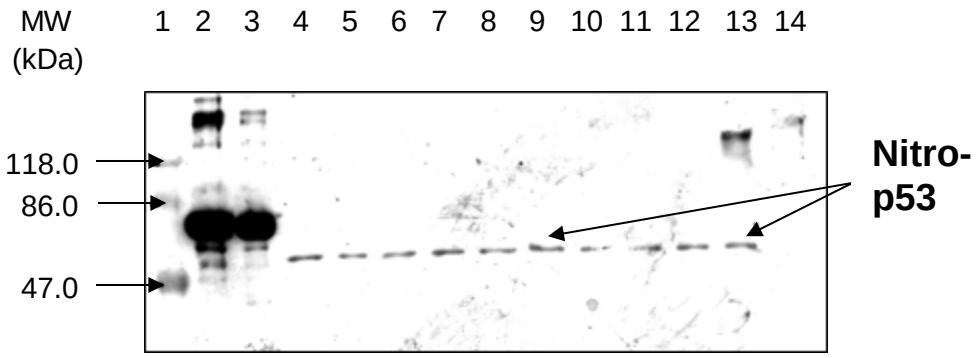

Figure 5.22(a). Western blot analysis showing nitration of 40.6 µg purified resolubilised p53 protein with increasing concentrations of peroxynitrite ranging from 10 µM to 3 mM which were incubated with peroxynitrite for 15 min in a rocking water bath at 37°C. The samples The same amounts of non-nitrated and nitrated purified resolubilised p53 protein were loaded onto SDS-PAGE gelS (2.04 µg). The primary antibody used was anti-nitrotyrosine monoclonal mouse monoclonal IgG, Clone 1A6 (Upstated Biotechnology) and the secondary antibody was rabbit polyclonal anti-mouse IgG/HRP conjugated (DAKO Cytomation).

Lane 1 - prestained protein molecular weight markers (Fermentas)

Lane 2 - 100 µM peroxynitrite previously nitrated BSA

Lane 3 - 100 µM peroxynitrite freshly nitrated BSA

Lane 4 - non-nitrated purified resolubilised p53 protein

Lane 5 - 10 µM peroxynitrite nitrated purified resolubilised p53 protein

Lane 6 - 50 µM peroxynitrite nitrated purified resolubilised p53 protein

Lane 7 - 100 µM peroxynitrite nitrated purified resolubilised p53 protein

Lane 8 - 200 µM peroxynitrite nitrated purified resolubilised p53 protein

Lane 9 - 300 µM peroxynitrite nitrated purified resolubilised p53 protein

Lane 10 - 400 µM peroxynitrite nitrated purified resolubilised p53 protein

Lane 11 - 500 µM peroxynitrite nitrated purified resolubilised p53 protein

Lane 12 - 1 mM peroxynitrite nitrated purified resolubilised p53 protein

Lane 13 - 2 mM peroxynitrite nitrated purified resolubilised p53 protein

Lane 14 - 3 mM peroxynitrite nitrated purified resolubilised p53 protein

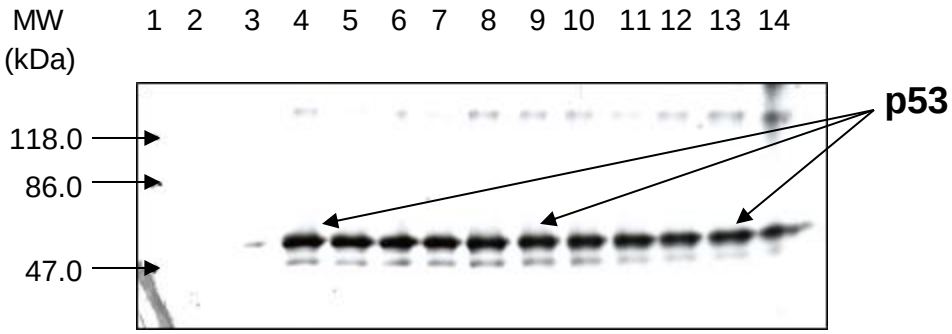

Figure 5.22(b). Western blot analysis showing nitration of 40.6 µg purified resolubilised p53 protein with increasing concentrations of peroxynitrite ranging from 10 µM to 3 mM which were incubated with peroxynitrite for 15 min in a rocking water bath at 37°C. The samples The same amounts of non-nitrated and nitrated purified resolubilised p53 protein were loaded onto SDS-PAGE gels (2.04 µg). The primary antibody used was anti-p53 mouse monoclonal antibody, DO-1. The secondary antibody used was rabbit polyclonal anti-mouse IgG/HRP conjugated (DAKO Cytomation).

Lane 1 - prestained protein molecular weight markers (Fermentas)

Lane 2 - 100 µM peroxynitrite previously nitrated BSA

Lane 3 - 100 µM peroxynitrite freshly nitrated BSA

Lane 4 - non-nitrated purified resolubilised p53 protein

Lane 5 - 10 µM peroxynitrite nitrated purified resolubilised p53 protein

Lane 6 - 50 µM peroxynitrite nitrated purified resolubilised p53 protein

Lane 7 - 100 µM peroxynitrite nitrated purified resolubilised p53 protein

Lane 8 - 200 µM peroxynitrite nitrated purified resolubilised p53 protein

Lane 9 - 300 µM peroxynitrite nitrated purified resolubilised p53 protein

Lane 10 - 400 µM peroxynitrite nitrated purified resolubilised p53 protein

Lane 11 - 500 µM peroxynitrite nitrated purified resolubilised p53 protein

Lane 12 - 1 mM peroxynitrite nitrated purified resolubilised p53 protein

Lane 13 - 2 mM peroxynitrite nitrated purified resolubilised p53 protein

Lane 14 - 3 mM peroxynitrite nitrated purified resolubilised p53 protein

5.11 Attempted nitration of GST and GST-MDM2 protein

This was the first ever work to nitrate purified GST and purified GST-MDM2 proteins expressed in *E. coli*. Our attempts for the nitration of purified GST and purified GST-MDM2 proteins were unsuccessful where there were no nitrotyrosine signals detected (data not shown). However, Fig. 5.23 shows an SDS-polyacrylamide gel stained with Commassie brilliant blue of nitrated and non-nitrated purified GST and purified GST-MDM2 proteins. Both GST and GST-MDM2 proteins disappeared when nitrated with 500 µM peroxynitrite (Lane 3 and Lane 4, respectively) when compared to non-nitrated proteins loaded at the same amounts (Lane 2 and Lane 5, respectively). We can assume that peroxynitrite treatment might cause degradation or loss of the proteins. In Fig. 5.23, it can be noticed that increasing in the amounts of purified GST-MDM2 protein loaded resulted in the increase in the levels of the proteins together with its contaminating proteins and/or its degradation products.

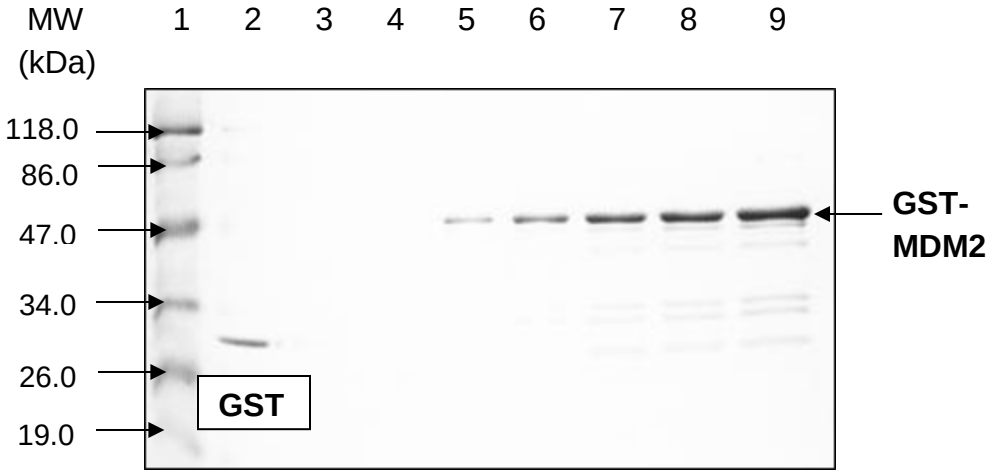

Figure 5.23. A 10% SDS-PAGE gel of purified GST, 500 µM peroxynitrite nitrated purified GST, purified MDM2 and 500 µM peroxynitrite nitrated purified MDM2 which were incubated with peroxynitrite for 15 min in a rocking water bath at 37°C. The samples loaded at different volumes. The gel was stained with Coomassie Blue for 15 minutes and then destained overnight.

Lane 1 - prestained protein molecular weight markers (Fermentas)

Lane 2 - purified GST (5 µl)

Lane 3 - 500 µM peroxynitrite nitrated purified GST (5 µl)

Lane 4 - 500 µM peroxynitrite nitrated purified GST-MDM2 (5 µl)

Lane 5 - purified GST-MDM2 (5 µl)

Lane 6 - purified GST-MDM2 (10 µl)

Lane 7 - purified GST-MDM2 (15 µl)

Lane 8 - purified GST-MDM2 (20 µl)

Lane 9 - purified GST-MDM2 (30 µl)

5.12 Discussion

The weak nitrotyrosine signal in non-nitrated BSA might be due to BSA was endogenously nitrated in cow as it is believed that tyrosine nitration is part of normal physiological processes in humans (Moncada *et al*., 1991; Beckman and Koppenol, 1996) and presumably also in other mammals and organisms, with a potential role in signal transduction mechanisms, possibly by influencing tyrosine phosphorylation or dephosphorylation (Bruckdorfer, 2001). A possible explanation for the loss of nitrotyrosine signal at high concentration of peroxynitrite used (500 µM) is that due to the degrading properties of peroxynitrite on proteins as evident by a study by Ischiropoulos and Al-Mehdi which showed that fatty acid-free BSA was fragmented after exposure to peroxynitrite (Ischiropoulos and Al-Mehdi, 1995). The incomplete pre-absorbed anti-nitrotyrosine antibody could easily pick up the excess nitrated BSA resulting in a high level of nitrotyrosine. We cannot see an obvious increasing trend of p53 protein degradation products with increasing concentrations of peroxynitrite as reported by Cobbs and co-workers (2001 and 2003) where they found that tyrosine nitration of purified baculovirus-derived recombinant wt p53 protein and of p53 protein in D54MG cells system treated with 0-100 µM peroxynitrite caused increased p53 protein degradation.

In summary, there raises a need to improve the yield of the in vitro generation of peroxynitrite by either modifying certain steps or by comparing several laboratory methods present at the moment which will give sufficient yield of peroxynitrite. The most appropriate nitrating method was determined i.e vortexing and rocking water bath set 37°C with vigorous speed. Optimisation of western blot steps for nitration such as optimal blocking solution used was obtained. BSA was readily nitrated especially when dissolved in KPi buffer (pH 8.2) where nitro-tyrosine was detected at low concentration of peroxynitrite (10 uM) in comparison to when it was dissolved in PBS (pH 7.4). Attempts to nitrate purified resolubilised p53 protein and purified GST-MDM2 protein were unsuccessful, indicating these proteins are not readily nitrated which might be

due to cryptic location of tyrosine residues in the proteins which made them not accessible to nitration. Another factor to take into consideration is that nitration is a very selective process where not every tyrosine is nitrated, only certain one is susceptible to nitration, possibly those next to glutamate residue as observed in neurofilaments, among others (Crow *et al*., 1997). Peroxynitrite shows degrading properties where both nitrated purified resolubilised and soluble p53 protein and also nitrated purified GST and GST-MDM2 proteins reduced in levels or totally loss when compared to their non-nitrated counterparts.

RESULTS CHAPTER 6

In this chapter the aim was to isolate and characterise nitrated p53 protein from selected cancer cell lines with different p53 status either wild type, mutant or null-p53 proteins. These cell lines, either intact or lysed, were untreated or treated with peroxynitrite in order to determine whether these p53 proteins and their nitro-p53 forms could be successfully immunoprecipitated with anti-p53 antibodies. In another experiment, a cell line with wt-p53 was incubated with NO donor S-Nitrosoglutathione (GSNO) to see its effect on nitro-p53 signal and on p53 protein levels.

6.1 Immunoprecipitation studies of p53 and nitro-p53 proteins from selected cancer cell lines

A panel of human cancer cell lines with different p53 status were chosen for nitration study using nitrating agent peroxynitrite in the test tubes or incubating the cultured cells with nitric oxide donor GSNO at certain concentrations. The cells were either lysed or still intact before being nitrated, while the intact cells were either first washed with PBS or not before being nitrated. The cell lysates were directly nitrated with peroxynitrite before being immunoprecipitated for p53 protein or nitro-p53 protein and then were subjected to Western blotting by probing with the anti-nitrotyrosine and anti-p53 antibodies, respectively. The cell lysates were also indirectly nitrated by first immunoprecipitating with the anti-p53 polyclonal antisera (CM-1) where CM-1 antisera formed complexes with p53 protein and protein G beads and then were subjected to Western blotting by probing with the anti-nitrotyrosine antibody or vice versa. Table 6.1 shows the selected human cancer cell lines used in this study.

Table 6.1: Human cancer cell lines used in this study

Cell lines	Description and Characteristics	Source
MCF7	Breast cancer cell line with wild type *p53* gene.	ICT, University of Bradford
PANC-1	Pancreatic cancer cell line with mutant *p53* gene.	ICT, University of Bradford
SW620	Colorectal cancer cell line with mutant *p53* gene.	ICT, University of Bradford
HCT116 p53+/+	Colorectal cancer cell line with wild type *p53* gene.	ICT, University of Bradford
HCT116 p53-/-	Colorectal cancer cell line with deleted *p53* gene.	ICT, University of Bradford

*ICT: The Institute of Cancer Therapeutics

6.2 Pilot nitration study of human cancer cell lines

SW620 cells were used for our pilot nitration study as the cells have accumulated amount of mutant p53 protein. The cells were grown to ~80% confluent before being harvested by trypsin and then resuspended in PBS. The intact cells were then nitrated with increasing concentrations of peroxynitrite ranging from 10 µM to 3 mM. MCF7 cells harbouring wt-p53, which were priorly incubated with 500 ng/ml Actinomycin D, an anti-cancer drug commonly used to inhibit transcription, for 24 hrs to induce the expression of wt p53 protein (as used by Cobbs *et al*., 2001), were also treated in parallel with 100 µM peroxynitrite. Non-nitrated BSA, MCF7 and SW620 were used as negative controls for nitration. BSA was also nitrated at the same time with the cells to act as a positive control for nitration and also to determine whether the nitration process was successful. No nitrotyrosine signal was detected in non-nitrated BSA as expected (Fig. 6.1, Lane 2) and very strong signals of nitro-BSA were detected in BSA either freshly or previously nitrated with 100 µM (Fig. 6.1, Lanes 3 and 4, respectively).

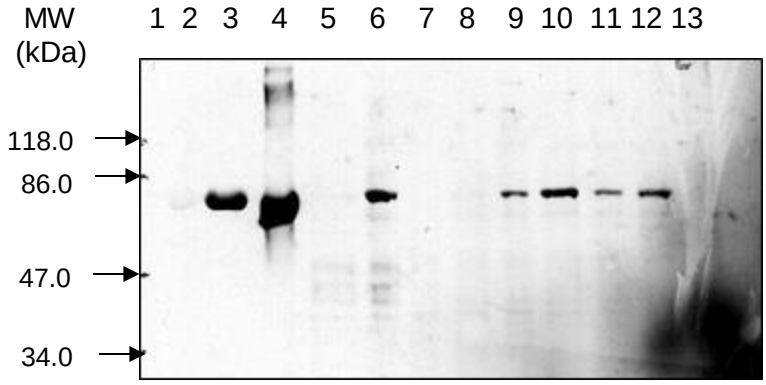

Figure 6.1. A Western blot analysis showing nitration of SW620 cells with various concentrations of peroxynitrite ranging from 10 µM to 3 mM. The cells were grown to ~80% confluent in T75 culture flask before being trypsinised and resuspended in PBS and then treated with peroxynitrite and incubated for 15 min in a rocking water bath at 37°C. 2 mg/ml BSA was nitrated at the same time to act as a positive control for nitration. The primary antibody used was anti-nitrotyrosine mouse monoclonal IgG, Clone 1A6 (Upstate Biotechnology) and the secondary antibody was rabbit polyclonal anti-mouse IgG/HRP conjugated (DAKO Cytomation).

Lane 1 - prestained protein molecular weight markers (Fermentas)

Lane 2 - non-nitrated BSA

Lane 3 - 100 µM peroxynitrite freshly nitrated BSA

Lane 4 - 100 µM peroxynitrite previously nitrated BSA

Lane 5 - non-nitrated MCF7 cells

Lane 6 - 100 µM peroxynitrite nitrated MCF7 cells

Lane 7 - non-nitrated SW620 cells

Lane 8 - 10 µM peroxynitrite nitrated SW620 cells

Lane 9 - 50 µM peroxynitrite nitrated SW620 cells

Lane 10 - 100 µM peroxynitrite nitrated SW620 cells

Lane 11 - 300 µM peroxynitrite nitrated SW620 cells

Lane 12 - 500 µM peroxynitrite nitrated SW620 cells

Lane 13 - 3 mM peroxynitrite nitrated SW620 cells

No nitrotyrosine signal was observed in non-nitrated MCF7 cells as expected (Fig. 6.1, Lane 5). A moderate signal of nitrotyrosine of proteins in MCF7 cells was detected when the cells were treated with 100 µM peroxynitrite (Fig. 6.1, Lane 6). This signal was probably nitrated BSA of ~66.4 kDa. No nitrotyrosine signals were detected in non-nitrated SW620 cells and also in SW620 cells treated with 10 µM peroxynitrite (Fig. 6.1, Lanes 7 and 8). Relatively weak nitrotyrosine signals were obtained in SW620 nitrated with 50, 300 and 500 µM peroxynitrite (Fig. 6.1, Lanes 9, 11 and 12 respectively) when compared to SW620 cells treated with 100 µM peroxynitrite which gave the strongest signal among all the concentrations of peroxynitrite used (Fig. 6.1, Lane 10). However, no nitrotyrosine signal was detected when SW620 cells were treated with 3 mM peroxynitrite (Fig. 6.1, Lane 13). This might suggest that a strong concentration of peroxynitrite resulted in the degradation or reduction in the levels of the protein. We suspected the nitrated proteins in both PBS resuspended MCF7 and SW620 cells were residual serum proteins from complete culture media used to culture the cells.

As determined above and by Cobbs *et al* (2001 & 2003), 100 µM peroxynitrite used to nitrate cancer cells gave the optimal and strong nitro-tyrosine signals, mimicking the concentration in inflamed tissues, we therefore further explored the nitration of MCF7 and SW620 cells in various experimental conditions. Non-nitrated and 100 µM peroxynitrite-nitrated BSA were used as a negative and a positive control, respectively. Non-nitrated BSA gave no nitrotyrosine signal as expected and 100 µM peroxynitrite-nitrated BSA gave a very strong nitro-tyrosine signal (Fig. 6.2(a), Lanes 2 and 3, respectively). Whole cells without lysing in sample buffer were used in these experiments to see whether peroxynitrite could diffuse into whole cells and nitrate p53 protein in comparison to direct protein nitration in cell lysates. Also, this is in order to see whether it was possible to detect nitrated protein when whole cells which were lysed upon boiling in SDS loading buffer were loaded into gels for Western blotting. Both non-nitrated unwashed and washed intact MCF7 cells gave negative results

where no nitrotyrosine signals were detected as expected (Fig. 6.2(a), Lanes 4and 6, respectively). 100 µM peroxynitrite-nitrated unwashed intact MCF7 cells gave a very weak nitrotyrosine signal whereas no signal observed in 100 µM peroxynitrite-nitrated washed intact MCF7 cells (Fig. 6.2(a), Lanes 5 and 7, respectively). We suspected the nitrated protein in the unwashed intact MCF7 cells was a serum protein used in the cell culture media. No nitrotyrosine signals were observed in the non-nitrated washed MCF cell lysates as expected (Fig. 6.2(a), Lane 8). No nitrotyrosine signal was detected in 100 µM peroxynitrite-nitrated washed MCF7 cell lysates as the serum was washed away when preparing the cell lysates (Fig. 6.2(a), Lane 9). Similar results to the MCF7 cells were observed in SW620 cells for all the conditions used where no nitrotyrosine signals were detected in all the samples except that a very strong nitrotyrosine signal was detected in 100 µM peroxynitrite-nitrated unwashed intact SW620 cells (Fig. 6.2(a), Lane 11) when compared to a weak nitrotyrosine signal in 100 µM peroxynitrite-nitrated unwashed intact MCF7 cells (Fig. 6.2(a), Lane 5), which indicates a higher serum protein level present in unwashed intact SW620 cells prepared in comparison to a lower level of serum protein in the prepared unwashed intact MCF7 cells. In another blot (Fig. 6.2(b)) with the same samples loaded as in Fig. 6.2(a) but was probed with mouse monoclonal anti-p53 antibody (DO-1), wt p53 protein in MCF7 cells was barely detected (Fig. 6.2(b), Lanes 4-9) whereas strong signals of mutant p53 protein were detectable in SW620 cells when probed with DO-1 (Fig. 6.2(b), Lanes 10-15).

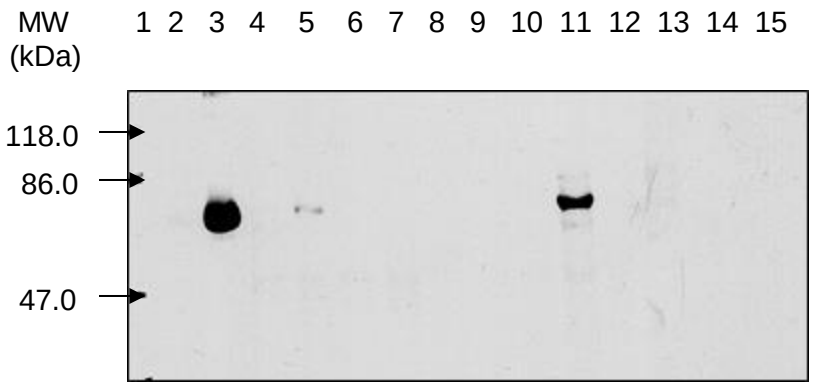

Figure 6.2(a). Western blot analysis showing a pilot nitration study of MCF7 and SW620 cells nitrated with 100 µM peroxynitrite and incubated for 15 min in a rocking water bath at 37°C. 2 mg/ml BSA was nitrated at the same time to act as a positive control for nitration. Non-nitrated BSA, MCF7 cells and SW620 cells were served as negative controls for nitration. The primary antibody used was mouse monoclonal anti-nitrotyrosine (Upstate Biotechnology) and the secondary antibody was rabbit polyclonal anti-mouse HRP conjugated (DAKO Cytomation).

Lane 1 - prestained protein molecular weight markers (Fermentas)

Lane 2 - non-nitrated BSA

Lane 3 - 100 µM peroxynitrite nitrated BSA

Lane 4 - non-nitrated unwashed intact MCF7 cells

Lane 5 - 100 µM peroxynitrite nitrated unwashed intact MCF7 cells

Lane 6 - non-nitrated washed intact MCF7 cells

Lane 7 - 100 µM peroxynitrite nitrated washed intact MCF7 cells

Lane 8 - non-nitrated washed MCF7 cell lysates

Lane 9 - 100 µM peroxynitrite nitrated washed MCF7 cell lysates

Lane 10 - non-nitrated unwashed intact SW620 cells

Lane 11 - 100 µM peroxynitrite nitrated unwashed intact SW620 cells

Lane 12 - non-nitrated washed intact SW620 cells

Lane 13 - 100 µM peroxynitrite nitrated washed intact SW620 cells

Lane 14 - non-nitrated washed SW620 cell lysates

Lane 15 - 100 µM peroxynitrite nitrated washed SW620 cell lysates

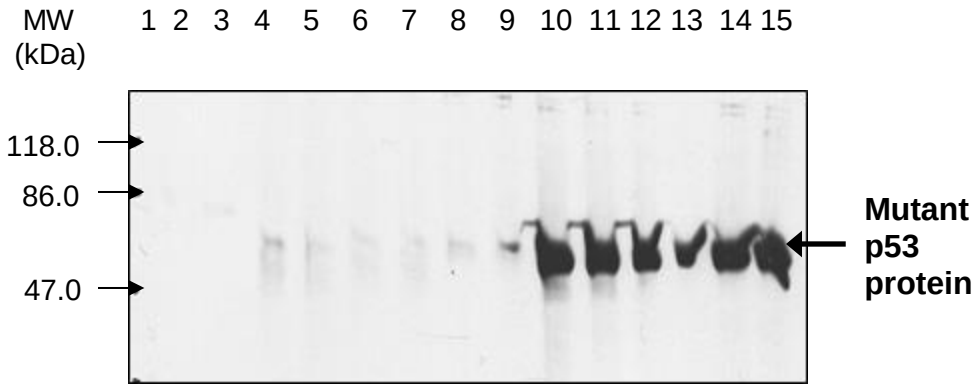

Figure 6.2(b). Western blot analysis showing a pilot nitration study of MCF7 and SW620 cells nitrated with 100 µM peroxynitrite and incubated for 15 min in a rocking water bath at 37°C. 2 mg/ml BSA was nitrated at the same time to act as a positive control for nitration. Non-nitrated BSA, MCF7 cells and SW620 cells were served as negative controls for nitration. The primary antibody used was mouse monoclonal anti- p53 (DO-1) and the secondary antibody was rabbit polyclonal anti-mouse HRP conjugated (DAKO Cytomation).

Lane 1 - prestained protein molecular weight markers (Fermentas)

Lane 2 - non-nitrated BSA

Lane 3 - 100 µM peroxynitrite nitrated BSA

Lane 4 - non-nitrated unwashed intact MCF7 cells

Lane 5 - 100 µM peroxynitrite nitrated unwashed intact MCF7 cells

Lane 6 - non-nitrated washed intact MCF7 cells

Lane 7 - 100 µM peroxynitrite nitrated washed intact MCF7 cells

Lane 8 - non-nitrated washed MCF7 cell lysates

Lane 9 - 100 µM peroxynitrite nitrated washed MCF7 cell lysates

Lane 10 - non-nitrated unwashed intact SW620 cells

Lane 11 - 100 µM peroxynitrite nitrated unwashed intact SW620 cells

Lane 12 - non-nitrated washed intact SW620 cells

Lane 13 - 100 µM peroxynitrite nitrated washed intact SW620 cells

Lane 14 - non-nitrated washed SW620 cell lysates

Lane 15 - 100 µM peroxynitrite nitrated washed SW620 cell lysates

6.3 Nitration of cell lysates of selected cancer cell lines followed by immunoprecipitation of p53 protein

This section is to describe the attempted nitration of MCF7, PANC-1 and SW260 cell lysates with different p53 status (wild-type *p53* gene for MCF7 cells and mutant *p53* gene for both PANC-1 and SW260 cells) in order to determine whether the p53 protein both wild-type and mutant forms were successfully nitrated and to determine the nitration effects on p53 protein levels.

6.3.1 Attempted nitration of MCF7, PANC-1 and SW260 cell lysates (1)

Nitration experiments were then conducted in three cancer cell lines namely MCF7, PANC-1 and SW620. The cells were grown until ~80% confluency before being harvested by trypsin and then lysed with NET buffer [150 mM NaCl, 5 mM EDTA pH 8.0, 50 mM Tris-HCl pH 8.0, 1% (v/v) Igepal s protease inhibitors cocktail]. However, MCF7 cells were first incubated with 500 ng/ml Actinomycin-D for 24 hr, the purpose of which was to induce wt p53 protein expression before being harvested since wt p53 protein is barely detectable in MCF7 cells, - see Material & Methods, Section 2.18 for further details of the method used. The cell lysates for each cell line were then either directly nitrated with 100 µM peroxynitrite or were first immunoprecipitated for p53 protein by CM-1 antibody before being nitrated with 100 µM peroxynitrite. In the Western blot analyses as shown in Figs. 6.3(a) and (b), just protein G beads bound to the three antibodies namely CM-1, DO-1 or the mouse monoclonal anti-nitrotyrosine antibody, Clone Clone 16A (Upstate Biotechnology) were loaded onto SDS-PAGE gels (Lanes 4, 5 and 6) and also the three non-nitrated cell lysates (Lanes 7, 8 and 9) to act as negative controls for the experiment. The non-nitrated and nitrated BSA were run in parallel to act as a negative and a positive control for nitration, respectively (Fig. 6.3(a) & (b), Lanes 2 and 3, respectively). As can be seen in Fig. 6.3(a) and (b), the rabbit anti-mouse polyclonal secondary antibody very weakly recognised the heavy and light chains of the rabbit polyclonal CM-1 sera as p53 could be easily be confused with the heavy chain of the CM-1 serum (Lane 4). As both DO-1 and the mouse monoclonal

anti-tyrosine antibody were both mouse monoclonal antibodies, these antibodies were greatly picked up by the secondary anti-mouse antibody and that is why the heavy and light chains signals for both the antibodies were very strong (Lanes 5 and 6, respectively). No nitro-tyrosine signals were detected in all the three cell lysates indicating that p53 protein was not endogenously nitrated in these cell lines (Fig. 6.3(a), Lanes 7-9). As PANC-1 and SW620 cells contain mutant p53 protein which is stable and at a high level, there were strong signals of mutant p53 protein in these two cells (Fig. 6.3(b), Lanes 8 and 9, respectively). As wt p53 protein accumulated in MCF7 cells induced with Actinomycin-D, we can see quite a strong signal of p53 protein in this cell (Fig. 6.3(b), Lane 7), nevertheless it was lower than that of mutant p53 proteins in both PANC-1 and SW620 (Fig. 6.3(b) Lanes 8 and 9, respectively), which could be due to protein load and wavy gel effect (Dr Steven Picksley, personal communication). No nitrotyrosine signal of p53 protein was detected in Actinomycin-induced MCF7 cell lysates nitrated with 100 µM peroxynitrite which was then immunoprecipitated with CM-1 (Fig. 6.3(a), Lane 10). However, very weak nitro-tyrosine signals of mutant p53 proteins were detected in PANC-1 and SW620 cell lysates nitrated with 100 µM peroxynitrite which were then immunoprecipitated with CM-1 (Fig. 6.3(a), Lanes 11 and 12). After immunoprecipitation with CM-1, 100 µM peroxynitrite-nitrated MCF7 lysates, which were priorly induced with 500 ng/ml Actinomycin D for 24 hr, showed no signal of p53 protein (Fig. 6.3(b), Lane 10). This might be due to quite a lower level of the starting wt p53 protein induced in MCF7 cells by Actinomycin D or because it did not work. We can also use this evidence of the lower level of starting wt p53 protein to reason why there was no nitro-tyrosine signal of this sample (Fig. 6.3(a), Lane 10). The levels of mutant p53 protein in PANC-1 and SW620 cell lysates nitrated with 100 µM peroxynitrite which were then immunoprecipitated with CM-1 were still high (Fig. 6.3(b), Lanes 11 and 12) even though their levels were a bit lower than just the lysates (not immunoprecipitated) (Fig. 6.3(b), Lanes 8 and 9, respectively). As can be seen in Fig. 6.3(a), CM-1- immunoprecipitated p53 protein in MCF7, PANC-1 and

SW620 cell lysates nitrated with 100 μM peroxynitrite show strong signals of nitrotyrosine (Lanes 13-14) in comparison to their negative control sample (just beads bound to CM-1) in Lane 4 in the same Fig. 6.3(a). Stronger signals of mutant p53 protein were found in CM1-immunoprecipitated p53 protein in PANC-1 and SW620 cell lysates nitrated with 100 μM peroxynitrite (Fig. 6.3(b), Lanes 14 and 15, respectively) when compared to their counterpart MCF7 cells containing wt p53 protein and a negative control sample (just beads bound to CM-1) (Fig. 6.3(b), Lanes 13 and 4, respectively).

Figure 6.3(a). Attempted nitration of CM-1 immunoprecipitated p53 proteins from Actinomycin D-treated MCF7, PANC-1 or SW620 cell lysates with 100 µM peroxynitrite and incubated for 15 min in a rocking water bath at 37°C. The primary antibody used was mouse monoclonal anti-nitrotyrosine (Upstate Biotechnology) and the secondary antibody was rabbit anti-mouse HRP conjugated polyclonal antibody (DAKO Cytomation).

Lane 1 - prestained protein molecular weight markers (Fermentas)

Lane 2 - non-nitrated BSA (2 µg)

Lane 3 - 100 µM peroxynitrite nitrated BSA (2 µg)

Lane 4 - just beads bound to CM-1

Lane 5 - just beads bound to DO-1

Lane 6 - just beads bound to mouse monoclonal anti-nitrotyrosine

Lane 7 - MCF7 cell lysates (10 µg)

Lane 8 - PANC-1 cell lysates (10 µg)

Lane 9 - SW620 cell lysates (10 µg)

Lane 10 - 100 µM peroxynitrite nitrated Actinomycin D-treated MCF7 cell lysates immunoprecipitated with CM-1

Lane 11 - 100 µM peroxynitrite nitrated PANC-1 immunoprecipitated with CM-1

Lane 12 - 100 µM peroxynitrite nitrated SW620 immunoprecipitated with CM-1

Lane 13 - CM-1 immunoprecipitated Actinomycin D-treated MCF7 cell lysates nitrated with 100 µM peroxynitrite

Lane 14 - CM-1 immunoprecipitated PANC-1 cell lysates nitrated with 100 µM peroxynitrite

Lane 15 - CM-1 immunoprecipitated SW620 cell lysates nitrated with 100 µM peroxynitrite

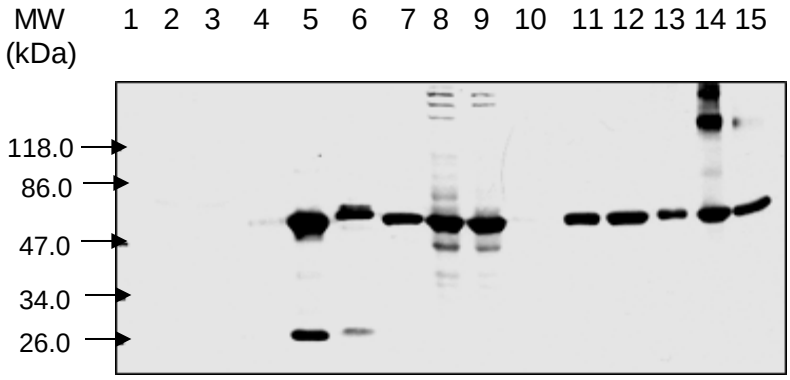

Figure 6.3(b). Attempted nitration of CM-1 immunoprecipitated p53 proteins from Actinomycin D-treated MCF7, PANC-1 or SW620 cell lysates with 100 µM peroxynitrite and incubated for 15 min in a rocking water bath at 37°. The primary antibody used was mouse monoclonal anti-p53 (DO-1) and the secondary antibody was rabbit anti-mouse HRP conjugated polyclonal antibody (DAKO Cytomation).

Lane 1 - prestained protein molecular weight markers (Fermentas)

Lane 2 - non-nitrated BSA (2 µg)

Lane 3 - 100 µM peroxynitrite nitrated BSA (2 µg)

Lane 4 - just beads bound to CM-1

Lane 5 - just beads bound to DO-1

Lane 6 - just beads bound to mouse monoclonal anti-nitrotyrosine

Lane 7 - MCF7 cell lysates (10 µg)

Lane 8 - PANC-1 cell lysates (10 µg)

Lane 9 - SW620 cell lysates (10 µg)

Lane 10 - 100 µM peroxynitrite nitrated Actinomycin D-treated MCF7 cell lysates immunoprecipitated with CM-1

Lane 11 - 100 µM peroxynitrite nitrated PANC-1 immunoprecipitated with CM-1

Lane 12 - 100 µM peroxynitrite nitrated SW620 immunoprecipitated with CM-1

Lane 13 - CM-1 immunoprecipitated Actinomycin D-treated MCF7 cell lysates nitrated with 100 µM peroxynitrite

Lane 14 - CM-1 immunoprecipitated PANC-1 cell lysates nitrated with 100 µM peroxynitrite

Lane 15 - CM-1 immunoprecipitated SW620 cell lysates nitrated with 100 µM peroxynitrite

6.3.2 Attempted nitration of MCF7, PANC-1 and SW620 cell lysates (2)

In order to confirm and support the experimental results on section 6.3.1, the experiments were repeated but with some modifications such that some of the samples were not only immunoprecipitated with CM-1 but were also reverse-order immunoprecipitated i.e. with the mouse monoclonal anti-nitrotyrosine antibody. Non-nitrated BSA and 100 μM peroxynitrite-nitrated BSA were served as a negative and a positive control for nitration, respectively. No nitrotyrosine signal was observed in non-nitrated BSA as expected (Fig. 6.4(a), Lane 2), whereas a strong nitrotyrosine signal was detected in BSA nitrated with 100 μM peroxynitrite (Fig. 6.4(a), Lane 3). A weak band for the heavy and light chains of the rabbit polyclonal CM-1 sera as the anti-mouse secondary antibody weakly recognised the two chains (Fig. 6.4(a), Lane 4). Very strong signals for the heavy and light chains of DO-1 (the anti-p53 mouse monoclonal antibody) and the anti-nitrotyrosine mouse monoclonal antibody as they were greatly picked up by the polyclonal anti-mouse secondary antibody (Fig. 6.4(a), lanes 5 and 6, respectively). MCF7 cell lysates nitrated with 100 μM peroxynitrite showed a few bands corresponding to moderate nitrotyrosine signals (Fig. 6.4(a), Lane 7) whereas very weak bands corresponding to very weak nitrotyrosine signals observed in both PANC-1 and SW620 cell lysates nitrated with 100 μM peroxynitrite (Fig. 6.4(a), Lanes 8 and 9, respectively). The wt p53 protein levels were higher in MCF-7 cells incubated 24 hrs with 500 ng/ml Actinomycin D (Fig. 6.4(b), Lane 7). As expected, very high mutant p53 protein levels were observed in PANC-1 and SW620 cell lysates as the mutant p53 proteins are stable and at high levels (Fig. 6.4(b), Lanes 8 and 9, respectively). In addition, there were also smaller p53 degradation products noticed, which might be due to proteolysis or handling of the samples. Samples in Lanes 10 to 12 acted as controls for samples in Lanes 13 to 14 in Fig. 6.4. In Fig. 6.4(a) (Lanes 10-12), non-nitrated MCF7, PANC-1 and SW620 cell lysates were immunoprecipitated with CM-1 while the cell lysates were immunoprecipitated with the mouse monoclonal anti-tyrosine antibody in Fig. 6.4(b) (Lanes 10 to 12) to detect p53 nitrotyrosine and

p53 protein, respectively. The blot in Fig. 6.4(a) was probed with the anti-nitrotyrosine mouse monoclonal antibody while the blot in Fig. 6.4(b) was probed with CM-1. Samples in Lanes 13 to 15 were 100 μM peroxynitrite-nitrated MCF7, PANC-1 and SW620 cell lysates immunoprecipitated with either CM-1 (Fig. 6.4(a)) or immunoprecipitated with the mouse monoclonal anti-tyrosine antibody (Fig. 6.4(b)) to detect p53 nitrotyrosine or p53 protein, respectively. As can be seen in Fig. 6.4(a), very weak signals of p53 nitrotyrosine were detected in both non-nitrated and nitrated MCF7, PANC-1 and SW620 cell lysates immunoprecipitated with CM-1 (Lanes 10 to 15) with sample in Lane 13 showed almost no signal at all. No p53 protein was observed in a sample in Lane 10, Fig. 6.4(b) i.e. non-nitrated MCF7 lysates immunoprecipitated with the mouse monoclonal anti-nitrotyrosine antibody and also a sample in Lane 13, the same figure i.e. 100 μM peroxynitrite-nitrated MCF7 lysates immunoprecipitated with the mouse monoclonal anti-nitrotyrosine. Non-nitrated PANC-1 and SW620 cell lysates immunoprecipitated with the mouse monoclonal anti-tyrosine antibody showed moderate levels of mutant p53 protein (Fig. 6.4(b), Lanes 11 and 12, respectively). However, the mutant p53 protein levels in these samples were far lower than their counterparts non-nitrated lysates (not immunoprecipitated) (Fig. 6.4(b), Lanes 8 and 9, respectively). The mutant p53 proteins in 100 μM peroxynitrite-nitrated PANC-1 and SW620 cell lysates immunoprecipitated with the mouse monoclonal anti-tyrosine were almost undetected (Fig. 6.4(b), Lanes 14 and 15, respectively). This might due to inefficient nitration of p53 protein in these cell lysates as seen in Fig. 6.4 (a) where hardly no nitro-p53 signals in samples in Lanes 13-15 or could be due to proteolysis of the protein.

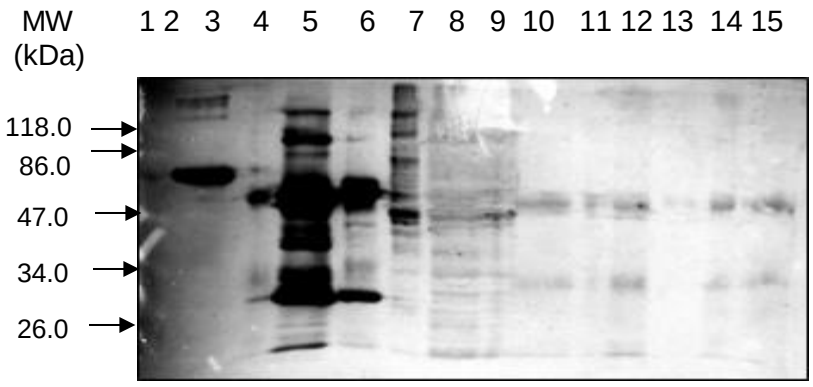

Figure 6.4(a). Attempted immuniprecipitation study of non-nitrated and nitrated MCF7, PANC-1 and SW620 cell lysates. The samples were nitrated with 100 µM peroxynitrite and incubated for 15 min in a rocking water bath at 37°C. The nitrated and non-nitrated SW620 cell lysates were either immuniprecipitated with CM-1 or mouse monoclonal anti-nitrotyrosine (Upstate Biotechnology). Beads just bound to either CM-1, DO-1 or mouse monoclonal anti-nitrotyrosine (Upstate Biotechnology) were used as controls. The samples were then subjected to western blot study. The primary antibody used was mouse monoclonal anti-nitrotyrosine (Upstate Biotechnology) and the secondary antibody was rabbit polyclonal anti-mouse HRP conjugated (DAKO Cytomation).

Lane 1 - prestained protein molecular weight markers (Fermentas)

Lane 2 - non-nitrated BSA (2 µg)

Lane 3 - 100 µM peroxynitrite nitrated BSA (2 µg)

Lane 4 - just beads bound to CM-1

Lane 5 - just beads bound to DO-1

Lane 6 - just beads bound to mouse monoclonal anti-nitrotyrosine

Lane 7 - 100 µM peroxynitrite nitrated MCF7 lysates

Lane 8 - 100 µM peroxynitrite nitrated PANC-1 lysates

Lane 9 - 100µM peroxynitrite nitrated SW620 lysates

Lane 10 – non-nitrated MCF7 lysates immunoprecipitated with CM-1

Lane 11 – non-nitrated PANC-1 lysates immunoprecipitated with CM-1

Lane 12 - non-nitrated SW620 lysates immunoprecipitated with CM-1

Lane 13 - 100 µM peroxynitrite nitrated MCF7 lysates immunoprecipitated with CM-1

Lane 14 - 100 µM peroxynitrite nitrated PANC-1 lysates immunoprecipitated with CM-1

Lane 15 - 100 µM peroxynitrite nitrated SW620 lysates immunoprecipitated with CM-1

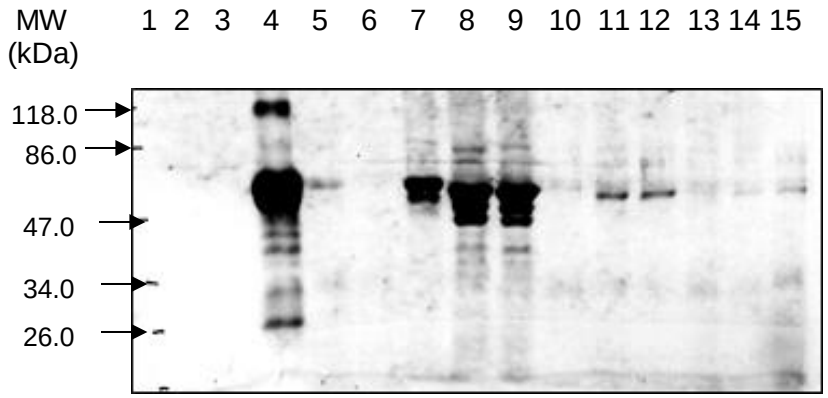

Figure 6.4(b). Attempted immuniprecipitation study of non-nitrated and nitrated MCF7, PANC-1 and SW620 cell lysates. The samples were nitrated with 100 µM peroxynitrite and incubated for 15 min in a rocking water bath at 37°C. The nitrated and non-nitrated cell lysates were immuniprecipitated mouse monoclonal anti-nitrotyrosine (Upstate Biotechnology). Beads just bound to either CM-1, DO-1 or mouse monoclonal anti-nitrotyrosine (Upstate Biotechnology) were used as controls. The samples were then subjected to western blot study. The primary antibody used was anti-p53 polyclonal antibody (CM-1) and the secondary antibody was swine polyclonal anti-rabbit HRP conjugated.

Lane 1 - prestained protein molecular weight markers (Fermentas)

Lane 2 - non-nitrated BSA (2 µg)

Lane 3 - 100 µM peroxynitrite nitrated BSA (2 µg)

Lane 4 - just beads bound to CM-1

Lane 5 - just beads bound to DO-1

Lane 6 - just beads bound to mouse monoclonal anti-nitrotyrosine

Lane 7 - just MCF7 lysates

Lane 8 - just PANC-l lysates (b)

Lane 9 - just SW620 lysates (b)

Lane 10 – non-nitrated MCF7 lysates immunoprecipitated with mouse monoclonal anti-nitrotyrosine

Lane 11 – non-nitrated PANC-1 lysates immunoprecipitated with mouse monoclonal anti-nitrotyrosine

Lane 12 - non-nitrated SW620 lysates immunoprecipitated with mouse monoclonal anti-nitrotyrosine

Lane 13 - 100 µM peroxynitrite nitrated MCF7 lysates immunoprecipitated with mouse monoclonal anti-nitrotyrosine

Lane 14 - 100 µM peroxynitrite nitrated PANC-1 lysates immunoprecipitated with mouse monoclonal anti-nitrotyrosine

Lane 15 - 100 µM peroxynitrite nitrated SW620 lysates immunoprecipitated with mouse monoclonal anti-nitrotyrosine

6.3.3 Nitration of HCT116 null-p53 and HCT116 wt-p53 cell lines

HCT116 null-p53 and HCT116 wt-p53 cell lines were used in this next study of nitration since null p53 served as a good control for p53 protein as the HCT116 null- p53 cells do not contain any p53 gene and thus no p53 protein is being expressed. In this study, non-nitrated BSA was used as a negative control for nitration where a very weak endogenous nitrotyrosine signal was observed (Fig. 6.5(a), Lane 2). A possible explanation for this observation is that BSA might be endogenously nitrated in cow as considerable evidence showed that tyrosine nitration is part of both physiological and pathological processes in the human body (Moncada *et al*., 1991; Beckman and Koppenol., 1996) and presumably also in other organisms. A very strong nitrotyrosine signal was detected in 100 µM peroxynitrite-previously nitrated BSA as compared to BSA freshly nitrated with 100 µM peroxynitrite where a very weak nitrotyrosine signal was observed (Fig. 6.5(a), Lanes 3 and 4, respectively). The anti-mouse secondary antibody very weakly recognised the heavy and light chains of the rabbit polyclonal CM-1 sera (Fig. 6.5(a), Lane 5). Very strong signals for the heavy and light chains of DO-1 (the anti-p53 mouse monoclonal antibody) and the anti-nitrotyrosine mouse monoclonal antibody as they were greatly picked up by the anti-mouse secondary antibody (Fig. 6.5(a), lanes 6 and 7, respectively). A few very weak signals of nitrotyrosine were detected throughout the samples in Lanes 8 to 13 (Fig. 6.5(a)), where non-nitrated HCT116 null-p53 cell lysates and non-nitrated Actinomycin D-induced HCT116 wt-p53 cell lysates showed very weak nitrotyrosine signals indicating that some of the proteins in both the cell lysates were endogenously nitrated (Fig. 6.5(a), Lanes 8 and 9, respectively). There was no obvious difference in the nitrotyrosine signals in 100 µM peroxynitrite-nitrated HCT116 null-p53 cell lysates and 100 µM peroxynitrite-nitrated Actinomycin D-induced HCT116 wt-p53 cell lysates (Fig. 6.5(a), Lanes 10 and 11, respectively) when compared to their non-nitrated counterparts (Fig. 6.5(a), Lanes 8 and 9, respectively). No nitrotyrosine signal was detected in 100 µM peroxynitrite-nitrated HCT116 null-p53 cell lysates immunoprecipitated with CM-1 as was expected as no p53 protein present (Fig. 6.5(a), Lane 12). Hardly any

nitrotyrosine signal was detected in 100 µM peroxynitrite-nitrated Actinomycin D-treated HCT116 wt-p53 cell lysates immunoprecipitated with CM-1 (Fig. 6.5(a), Lane 13). CM-1 immunoprecipitated HCT116 null-p53 cell lysates nitrated with 100 µM peroxynitrite shows very weak nitrotyrosine signals whereas very strong nitrotyrosine signals were observed in CM-1 immunoprecipitated Actinomycin D-treated HCT116 wt-p53 cell lysates nitrated with 100 µM peroxynitrite (Fig. 6.5(a), Lanes 14 and 15, respectively). This, therefore, needs to be further studied in other cancer cell lines with different p53 status (null, wild type or mutant) in order to get full significant insights of the experimental findings.

Fig. 6.5(b) was a Western blot analysis of similar samples to Fig. 6.5(a) but was probed with DO-1 (the anti-p53 mouse monoclonal antibody) to detect p53 protein. As can be seen in Lane 5, a very weak signal of the heavy chain of CM-1 was picked up the anti-mouse secondary antibody. However, very strong signals of the heavy and light chains of both DO-1 and the anti-tyrosine mouse monoclonal antibody were greatly picked up by the anti-mouse secondary antibody (Fig. 6.5(b), Lanes 6 and 7, respectively). As expected, no p53 proteins were found in non-nitrated HCT116 null-p53 cell lysates, in 100 µM peroxynitrite-nitrated HCT116 null-p53 cell lysates and also in CM-1 immunoprecipitated HCT116 null-p53 lysates nitrated with 100 µM peroxynitrite (Fig. 6.5(b), Lanes 8, 10 and 14, respectively). However, a weak signal of p53 was observed in 100 µM peroxynitrite-nitrated HCT116 null-p53 cell lysates immunoprecipitated with CM-1 (Fig. 6.5(b), Lane 12) which should not be the case as the cells did not contain the p53 gene. A reason for this might be due to overflow of samples at either side of the well, problems with the secondary antibody and/or cross reaction with CM-1 (Dr Steven Picksley, personal communication). Strong signals for p53 were observed in non-nitrated Actinomycin D-treated HCT116 wt-p53 cell lysates and in 100 µM peroxynitrite-nitrated Actinomycin D-treated HCT116 wt-p53 cell lysates (Fig. 6.5(b), Lanes 9 and 11, respectively) which indicates that Actinomycin D had successfully

induced the expression of wt p53 proteins. A p53 signal was observed in 100 µM peroxynitrite-nitrated Actinomycin D-treated HCT116 wt-p53 cell lysates immunoprecipitated with CM-1 (Fig. 6.5(b), Lane 13). A possible explanation for this observation is that not all the total p53 proteins bound to CM-1 (the anti-p53 polyclonal antibody), maybe some percentages of the p53 proteins were unbound to CM-1. No signal for p53 protein was observed in CM-1 immunoprecipitated HCT116 null-p53 cell lysates nitrated with 100 µM peroxynitrite (Fig. 6.5(b), Lane 14) whereas a very weak signal for p53 protein was found in CM-1 immunoprecipitated Actinomycin D-treated HCT116 wt-p53 cell lysates nitrated with 100 µM peroxynitrite (Fig. 6.5(b), Lane 15).

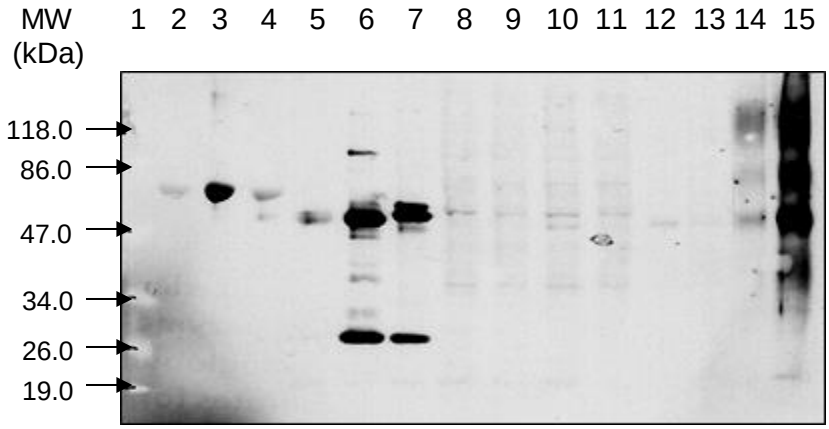

Figure 6.5(a). Nitration of CM-1 immunoprecipitated p53 proteins from HCT116 null-p53 and HCT116 wt-p53 cell lysates with 100 µM peroxynitrite and incubated for 15 min in a rocking water bath at 37°C. The primary antibody used was mouse monoclonal anti-nitrotyrosine (Upstate Biotechnology). The secondary antibody used was rabbit anti-mouse HRP conjugated polyclonal antibody (DAKO Cytomation).

Lane 1 - prestained protein molecular weight markers (Fermentas)

Lane 2 - non-nitrated BSA (2 µg)

Lane 3 - previously 100 µM peroxynitrite nitrated BSA (2 µg)

Lane 4 - 100 µM peroxynitrite nitrated BSA (2 µg)

Lane 5 - just beads bound to CM-1

Lane 6 - just beads bound to DO-1

Lane 7 - just beads bound to mouse monoclonal anti-nitrotyrosine

Lane 8 - non-nitrated HCT116 null-p53 cell lysates (10 µg)

Lane 9 - non-nitrated Actinomycin D-treated HCT116 wt-p53 cell lysates (10 µg)

Lane 10 - 100 µM peroxynitrite nitrated HCT116 null-p53 cell lysates

Lane 11 - 100 µM peroxynitrite nitrated Actinomycin D-treated HCT116 wt-p53 cell lysates

Lane 12 - 100 µM peroxynitrite nitrated HCT116 null-p53 cell lysate immunoprecipitated with CM-1

Lane 13 - 100 µM peroxynitrite nitrated Actinomycin D-treated HCT116 wt-p53 cell lysates immunoprecipitated with CM-1

Lane 14 - CM-1 immunoprecipitated HCT116 null-p53 cell lysates nitrated with 100 µM peroxynitrite

Lane 15 - CM-1 immunoprecipitated Actinomycin D-treated HCT116 wt-p53 cell lysates nitrated with 100 µM peroxynitrite

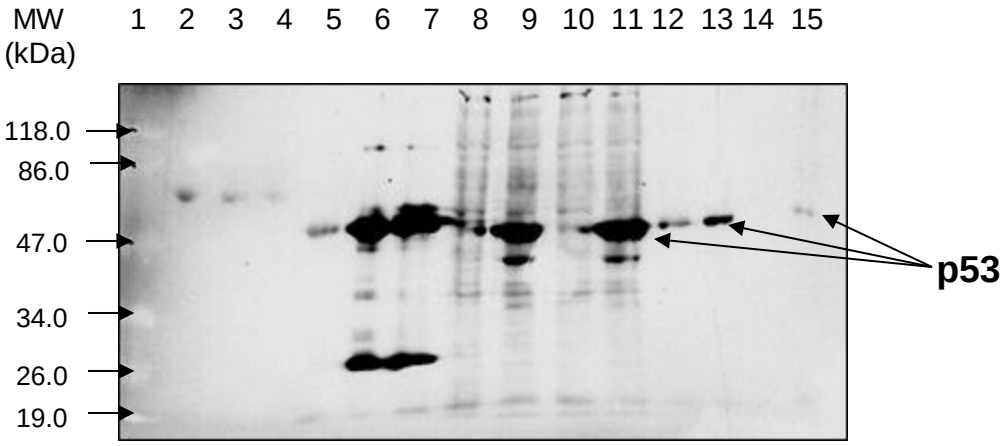

Figure 6.5(b). Nitration of CM-1 immunoprecipitated p53 proteins from HCT116 null-p53 and HCT116 wt-p53 cell lysates with 100 µM peroxynitrite and incubated for 15 min in a rocking water bath at 37°C. The primary antibody used was mouse monoclonal anti-p53 (DO-1) and the secondary antibody was rabbit anti-mouse HRP conjugated polyclonal antibody (DAKO Cytomation).

Lane 1 - prestained protein molecular weight markers (Fermentas)

Lane 2 - non-nitrated BSA (2 µg)

Lane 3 - previously 100 µM peroxynitrite nitrated BSA (2 µg)

Lane 4 - 100 µM peroxynitrite nitrated BSA (2 µg)

Lane 5 - just beads bound to CM-1

Lane 6 - just beads bound to DO-1

Lane 7 - just beads bound to mouse monoclonal anti-nitrotyrosine

Lane 8 - non-nitrated HCT116 null-p53 cell lysates (10 µg)

Lane 9 - non-nitrated Actinomycin D-treated HCT116 wt-p53 cell lysates (10 µg)

Lane 10 - 100 µM peroxynitrite nitrated HCT116 null-p53 cell lysates

Lane 11 - 100 µM peroxynitrite nitrated Actinomycin D-treated HCT116 wt-p53 cell lysates

Lane 12 - 100 µM peroxynitrite nitrated HCT116 null-p53 cell lysate immunoprecipitated with CM-1

Lane 13 - 100 µM peroxynitrite nitrated Actinomycin D-treated HCT116 wt-p53 cell lysates immunoprecipitated with CM-1

Lane 14 - CM-1 immunoprecipitated HCT116 null-p53 cell lysates nitrated with 100 µM peroxynitrite

Lane 15 - CM-1 immunoprecipitated Actinomycin D-treated HCT116 wt-p53 cell lysates nitrated with 100 µM peroxynitrite

6.4 Nitration study using NO donor, GSNO, using a model cell line MCF7

In order to look indirectly the effects of nitration on p53-nitro signals and p53 protein levels, we employed NO donor GSNO (S-Nitrosoglutathione) where in the cell NO will be released from GSNO and will react with superoxide to form peroxynitrite (Gunther et al., 1997; Goodwin et al., 1998). We attempted a pilot nitration study of wt-p53 expressing MCF7 cells incubated with NO donor, GSNO, at two selected concentrations namely 0.5 mM and 1.0 mM, optimal concentrations for p53 induction (Calmels et al., 1997; Chazotte-Aubert et al., 2000 & 2001), in culture flasks. Just protein G Sepharose beads bound to antibodies namely CM-1, DO-1 and the anti-nitrotyrosine mouse monoclonal antibodies were used as experimental controls. The protein G beads were added to the antibody and mixed by rotation for 15 minutes before the antibody and the beads complex were collected by centrifugation, added SDS loading dye and boiled before they were loaded onto SDS-polyacrylamide gel electrophoresis followed by Western blotting analyses. Very strong the light and heavy chains of DO-1 and the anti-nitrotyrosine mouse monoclonal antibodies were observed where they were greatly picked up by the anti-mouse secondary antibody (Fig. 6.6(a), Lanes 3 and 4, respectively).

There were strong signals in a sample in Lane 5, Fig. 6.6 (a) where the signals seem to be the heavy and light chains of antibody. This must be due to an overflow of a sample in Lane 4, in the same figure, i.e. just beads bound to the mouse monoclonal anti-nitrotyrosine antibody. Weaker nitrotyrosine signals were observed in 0.5 and 1.0 mM GSNO-treated MCF7 cell lysates (Fig. 6.6 (a), Lanes 6 and 7). Moderate nitrotyrosine signals were detected in 0.5 mM and 1.0 mM GSNO-treated MCF7 cell lysates immunoprecipitated with CM-1 (Fig. 6.6(a), Lanes 8 and 9, respectively). The levels of p53 protein in the untreated, 0.5 mM and 1.0 mM GSNO-treated MCF7 cell lysates were about similar (Fig. 6.6(b), Lanes 5-7) indicating that GSNO did not degrade the p53 protein at these 2 concentrations. The 0.5 mM and 1.0 mM GSNO-treated MCF7 cell lysates were also reverse-order immunoprecipitated with the mouse monoclonal

anti-nitrotyrosine antibody (Fig. 6.6(b), Lanes 8 and 9, respectively) and then probed with CM-1 in order to detect p53 protein. However, no p53 protein signals were detected in both the samples. A possible reason for this might be due to only a small percentage of the nitro-p53 protein had been immunoprecipitated as the nitro-p53 protein levels in both 0.5 mM and 1.0 mM GSNO-treated MCF7 cell lysates were initially quite low (Fig. 6.6(a), Lanes 6 and 7, respectively). For this reason, we could not reproduce the results by Chazotte-Aubert et al. (2000) which showed moderate signals of nitro-p53 in MCF7 cells treated with 1 mM and 2 mM GSNO. There are many possible reasons for the discrepancy in the results such as the culture conditions, the amounts of protein loaded onto SDS-PAGE gels, the primary and secondary antibodies used for immunoprecipitation and Western blotting and also the exposure time.

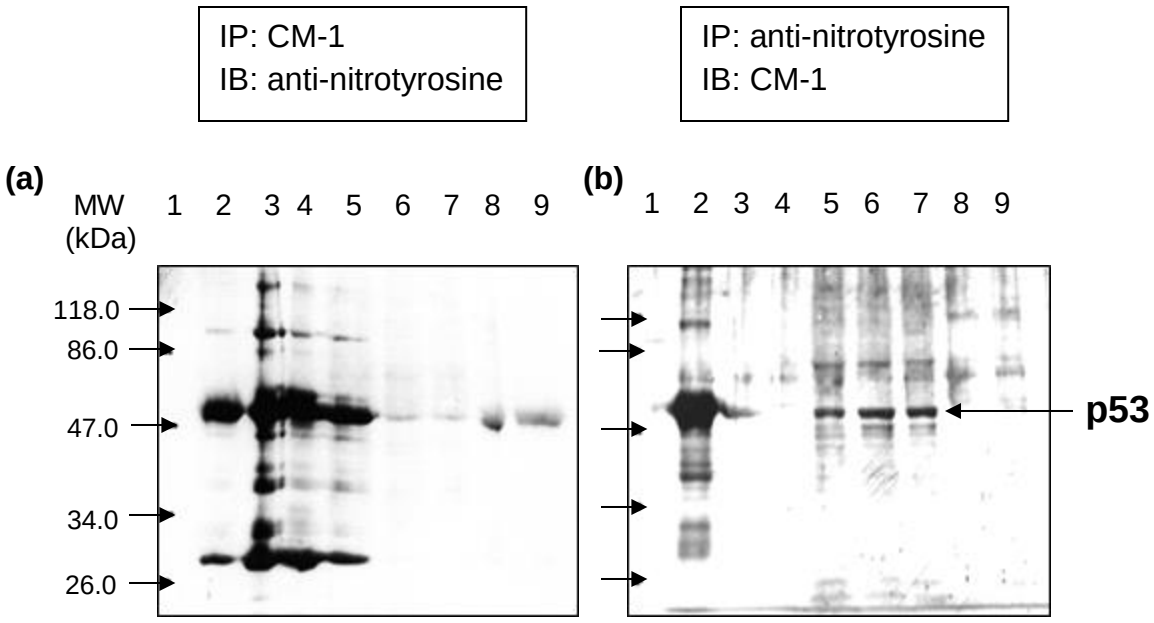

Figure 6.6. Western blot analysis of a pilot nitration study of MCF7 cancer cells incubated with the NO donor GSNO for 4 hrs. Nitrated cell lysates were immunoprecipitated with either rabbit polyclonal anti-p53 (CM-1) for **(a)** or mouse monoclonal anti-nitrotyrosine (Upstate Biotechnology) for **(b)** and then for Western blot analysis were probed with mouse monoclonal anti-nitrotyrosine or CM-1, respectively. The secondary antibody used for blot **(a)** was rabbit anti-mouse HRP conjugated polyclonal antibody (DAKO Cytomation) and swine anti-rabbit HRP conjugated polyclonal antibody for blot **(b).**

Lane 1 - prestained protein molecular weight markers (Fermentas)

Lane 2 - just beads bound to CM-1

Lane 3 - just beads bound to DO-1

Lane 4 - just beads bound to mouse monoclonal anti-nitrotyrosine

Lane 5 - untreated MCF7 cell lyates

Lane 6 - 0.5 mM GSNO treated MCF7 cell lysates (20 µg)

Lane 7 - 1.0 mM GSNO treated MCF7 cell lysates (20 µg)

Lane 8 - 0.5 mM GSNO treated MCF7 cell lysates immunoprecipitated with CM-1 (a) or immunoprecipitated with mouse monoclonal anti-nitrotyrosine (b)

Lane 9 - 1.0 mM GSNO treated MCF7 cell lysates immunoprecipitated with CM-1 (a) or immunoprecipitated with mouse monoclonal anti-nitrotyrosine (b)

6.5 Discussion

We suspected the nitrated proteins in both PBS resuspended MCF7 and SW620 cells were residual serum proteins from complete culture media used to culture the cells. A possible explanation for this observation is that BSA might be endogenously nitrated in cow as considerable evidence showed that tyrosine nitration is part of both physiological and pathological processes in the human body (Moncada *et al*., 1991; Beckman and Koppenol., 1996) and presumably also in other organisms. There are many possible reasons for the discrepancies in the results such as the culture conditions, the amounts of protein loaded onto SDS-PAGE gels, the primary and secondary antibodies used for immunoprecipitation and Western blotting and also the exposure time.

What can be summarised from the findings in this Chapter is that p53 protein, regardless of either wild type which was induced by Actinomycin-D (in MCF7 and HCT116 wt-p53 cells) or mutant (in PANC-1 and SW620 cells), was weakly and not efficiently nitrated either treating the cell lysates with peroxynitrite or incubating the cells with NO donor GSNO giving a very weak signal of nitro-p53 when compared to a readily nitrated BSA and also protein serum from residual culture media in unwashed intact cells. This therefore poses a question as to whether presumably low levels or undetectable nitro-p53 protein in the human system does significantly affect the p53-regulated pathways especially involving its established functions in cell cycle regulation and cell growth as it is famously known as a guardian of the genome, a cellular caretaker, a cellular gatekeeper etc. Therefore further insights of p53 nitration from cancer patient samples (clinical samples) such as blood, body fluids and tissues and also from a large number of various cancer cell lines and animal models of cancers need to be established before conclusive data on this unestablished type of post-translational modification of p53 protein and its effects thereof can be obtained.

CHAPTER 7

DISCUSSION

The main aim of this work was to characterise the effects of nitration on the levels and functions of p53 tumour suppressor protein. Initially, it was important to obtain a large amount of unmodified p53 protein to work with. Therefore, we used an *E. coli* expression system to express human p53 protein. Heterologous protein expression in the Gram-negative bacterium *E. coli* is the simplest and most inexpensive means to produce large amount of the desired product (Makrides, 1996; Hannig and Makrides, 1998). Additionally, *E. coli* has well-characterized genetics and there is an increasingly large number of cloning vectors and mutant host strains (reviewed by Baneyx, 1999). However, the main problem caused by *E. coli* expression of heterologous proteins is incorrect folding which results in the formation of insoluble aggregates known as inclusion bodies (Georgiou and Valax, 1996). However, the partially active protein can be obtained by *in vitro* solubilisation and followed by refolding by dialysis. Unmodified p53 produced in *E. coli* provides an excellent source for nitration study.

Expression levels of p53 protein were examined in two *E. coli* host strains namely BL21(DE3) and BL21(DE3)Star transformed with the pT7.7 vector carrying a full length human p53 gene under similar conditions as described by Midgley and coworkers (1992). It has been reported that the presence of mutation of the gene encoding RNAse E (*rne*131) in BL21(DE3)Star increases the expression of heterologous protein due to greater stabilization of mRNA with concomitant increase in protein translation (Invitrogen). Since no major differences in the expression levels of p53 protein between the two transformed strains were observed, thus, mRNA stability is not an issue here instead it is most probably due to different codon usage in *E. coli* and man. The choice of codon in both prokaryotes and eukaryotes is not random (Yokota *et al*, 1980). A

final year project student, Suzanne Camus (unpublished report, 2002), has investigated the expression levels of p53 protein in the Rosetta-gami (DE3), which supplies tRNAs for the codons AUA, AGG, AGA, CUA, CCC, GGA on a compatible chloramphenicol-resistant plasmid (Novagen), relative to the two *E. coli* strains, namely the BL21(DE3) strain and the BL21(DE3) Star strain, used in this study. The results showed there was not manifestly any difference in the expression levels of p53 in all the three strains. Thus, improved rare codon usage in the Rosetta strain does not significantly increase the yield of heterologous protein.

In this study, we found that the non-induced BL21(DE3) and BL21(DE3)Star transformed with the pT7.7Hup53 construct showed constitutive expression of p53 protein. This observation was confirmed by fresh transformation of the two strains with the pT7.7Hup53 construct and left uninduced. This is probably due to a leaky P_{tac} promoter where even without IPTG the promoter was initiated to transcribe the T7 RNA polymerase gene and subsequently resulted in p53 protein production. The leaky production of T7 RNA polymerase can be controlled by co-transforming *E. coli* cells with additional plasmids namely pLysE and pLysS both of which will constitutively produce T7 lysozyme, a natural inhibitor of T7 RNA polymerase (Dubendoff and Studier, 1991) but this would not change the overall yield of p53 protein produced (Midgley *et al*., 1992). T7 lysozyme will inactivate the basal level of T7 RNA polymerase activity which will promote some transcription of heterologous gene in the uninduced cells, but will be swamped, and thereby rendered ineffective, by the larger amount of T7 RNA polymerase produced during induction. T7 lysozyme acts by cutting a specific bond in the peptidoglycan layer of the *E. coli* cell wall and by binding to T7 RNA polymerase and hence inhibiting transcription (Studier *et al*, 1990). Cells carrying pLysE accumulate substantial levels of T7 lysozyme than cells carrying pLysS. pLysS has little effect on growth rate but pLysE significantly lowers the growth rate of the cells carrying it (Studier *et al*, 1990).

The presence of bands corresponding to p53 protein in non-induced BL21(DE3) pT7.7Hup53 and BL21(DE3)Star pT7.7Hup53 was confirmed by Western blotting using anti-p53 mouse monoclonal antibody DO-1 which is specific for amino acids close to conserved box 1 in the N terminus of human p53 protein (Vojtesek *et al*., 1992) as a primary antibody for immunodetection of p53 protein. Also evident was the absence of bands corresponding to p53 protein in the two induced strains transformed with the vector pT7.7 alone. The two induced strains transformed with the pT7.7Hup53 construct where IPTG was added at OD_{600nm} of 0.8-1.0 (late log phase) showed very strong signals corresponding to p53 protein. Verification that p53 protein was produced in the two induced strains transformed with the pT7.7Hup53 construct therefore led us to proceed to a large scale expression of p53 protein and subsequently to purify p53 protein through a series of column chromatography purification systems. Some p53 protein were not bound to the column and therefore found in the flowthroughs (Fig. 3.10(a)) which was most probably due to the fact the protein was not completely refolded during dialysis (Dr Picksley, personal communication). Overall, the purified p53 protein yield was modest but was good enough to do initial work. Therefore, a small scale optimisation of p53 protein expression in the two *E. coli* host strains above carrying the pT7.7Hup53 construct was carried out to get significant amount of p53 protein. The optimum conditions for the expression of p53 protein were finally determined as described in details in the Results Section 3.5. Therefore, a large scale production of p53 protein was carried out using BL21(DE3) pT7.7Hup53 and 12 litres of cultures of induced BL21(DE3) pT7.7Hup53 were grown using the optimum p53 expression conditions obtained earlier. Having established the optimisation conditions for p53 expression, a sufficient amount of purified resolubilised p53 protein was obtained and therefore sufficient to be used for the nitration study. However, in order to get more and improved soluble p53 protein, it is worth trying to express human p53 protein in Lemo21(DE3) (New England Biolabs, 2013-2014 Catalog & Technical Reference), derivative of BL21(DE23), which features tunable T7 expression for potential elimination of inclusion body

formation of which ~98% of p53 protein in inclusion bodies when expressed in conventional BL21(DE3) system. The p53 protein expression levels can be controlled by varying the level of T7 lysozyme (lysY), the natural inhibitor of T7 RNA polymerase.

Both resolubilised and soluble p53 protein were separately purified by following the methods by Hupp *et al*. (1992) and Midgley *et al*. (1992) with slight modifications. It was very challenging to purify soluble p53 protein as the protein is only present 2% of the total p53 protein, thus a large volume of several batches of BL21(DE3) *E. coli* bacterial culture transformed with pT7.7Hup53 were needed to be cultivated. After gel purification with Superose 12 column, most soluble p53 protein was eluted at fractions 9-14 with calculated masses from 340-1100 kDa which were 2-10 fold higher and not in agreement with the mass of p53 protein tetramers (172-212 kDa), however two independent studies by Hupp *et al*. and Friedman *et al*. showed the active p53 fractions were eluted at approximately 440 kDa (a multimer larger than a tetramer) (Hupp *et al*., 1992; Friedman *et al*., 1993), with < 20% of the total protein in the void volume of the column (which is around fraction 11 of our results), indicating the presence of larger forms of p53 protein (Friedman *et al*., 1993). The reason for this might be due to soluble p53 tetramers formed clumped in the buffer conditions used including factors such as pH, ionic strength and temperature but this is not of surprise as p53 forms tetramers in solution, both *in vitro* and *in vivo* (Friedman *et al*., 1993; Wang *et al*., 1994; review in Okorokov and Orlova, 2009), but the evidence for multi-tetramers is weak as these independent groups did not indicate the 2-10 fold increase of p53 tetramers (multiples of tetramers) in their studies. Separately, a reasonable amount of purified resolubilised p53 protein was obtained for subsequent nitration work. Since preliminary and optimisation of nitration had to be done repeatedly, we had to generate a lot of purified p53 protein both soluble and insoluble by cultivating 12 litres of BL21(DE3) *E. coli* bacterial culture transformed with pT7.7Hup53. The Glutathione S-transferase (GST) gene fusion system is a very powerful system to express, purify and

detect fusion proteins produced in *E. coli*. GST is of a molecular weight of 26 kDa. In fusion proteins, GST moiety is at the amino terminus and the protein of interest at the carboxyl terminus. The protein accumulates within the cell's cytoplasm. In this work, our GST-fusion protein of interest was GST-MDM2 protein from the expression construct of Bottger *et al*. (1996) by which a PCR product of human MDM2 cDNA (encompassing a.a. 1-188) was ligated into the pGEX-2T plasmid (Pharmacia). GST control protein was also expressed in BL21 *E. coli* and purified along with GST-MDM2 protein with reference to the work by Bottger *et al*. (1996) and Bottger *et al*. (1997). Both GST and GST-MDM2 proteins were purified from bacterial lysates by affinity chromatography using immobilised Glutathione Sepharose 4B (Amersham Biosciences), which is designed for the rapid, single-step purification of GST fusion proteins produced using the pGEX series of expression vectors. GST fusion proteins then bound to the affinity medium, and impurities or unbound contaminating bacterial proteins were removed by washing. The fusion proteins were then eluted under mild, non-denaturing conditions using reduced glutathione which preserve protein antigenicity and functionality. A lot of relatively pure GST and GST-MDM2 proteins were obtained in this single-step purification process (Figs. 4.12, 4.13, 4.14 & 4.15).

We used a simple, most convenient and possibly the cleanest way to synthesise peroxynitrite by simultaneously flushing together acidified hydrogen peroxide (H_2O_2) and sodium nitrite ($NaNO_2$) using a Y tubing. The two solutions were mixed evenly and rapidly in the Y-connector where the resulting yellow solution was immediately passed into alkaline solution 1.5 M NaOH to quench peroxynitrous acid ONOOH as peroxynitrite is stable in alkaline solutions. Thus, it is noteworthy that optimal conditions to yield higher concentrations of peroxynitrite with minimum concentrations of contaminants such as H_2O_2 and nitrite remaining in the resultant peroxynitrite solution, needs further exploration such as modifications of certain steps/conditions by varying initial concentrations of the reactants, different temperatures (such as at 0°, 20°C and

25°C which affects the rate of formation and decay of ONOOH), the flow rate where the reactants are efficiently mixed and the reaction is complete i.e. the time of quenching, or by comparing several available laboratory methods that give higher yield of peroxynitrite such as among others, those using a quenched-flow setup with a computerised syringe pump, though it is quite costly As a rule of thumb, peroxynitrite free from nitrite can be obtained by using slightly higher H_2O_2 than nitrite and vice versa (Saha *et al*., 1998).

In this work, fatty acid-free bovine serum albumin (BSA) (Sigma) was used as a model nitration substrate since it is easily nitrated and furthermore it is 99.8% pure and is available commercially. This is because BSA has 19 tyrosine residues which are targets for protein nitration. We used BSA for determining optimal nitration conditions. First, we had to determine the best nitration method by nitrating BSA at various concentrations of peroxynitrite (10 µM to 500 µM) by using either aggregometer set at 37ºC or vortexing and rocking water bath set at 37ºC (Fig. 5.3) (following Professor Khalid Naseem's suggestion). We found that vortexing and rocking water bath set at 37ºC gave strong nitrotyrosine signals at peroxynitrite concentrations at 100-400 µM when compared to using aggregometer set at 37ºC at the same concentrations of peroxynitrite. This is mainly because peroxynitrite reacted very fast and instantaneously with proteins and vortexing the mixture of peroxynitrite and BSA helped to speed up their reaction and also made the peroxynitrite worked effectively to nitrate the tyrosine residues of BSA. A rocking water bath set at 37ºC supposedly prolonged the reaction between peroxynitrite and BSA. Since there was still a lack of expertise for nitration of p53 protein (mostly confined to big chemistry groups in the USA), thus we had to start from scratch by first optimising nitration conditions by using BSA as a model protein, which had taken a lot of time. However, we finally found optimal conditions for Western blotting such as optimal conditions for blocking membranes and the best anti-nitrotyrosine antibody to be used i.e. mouse monoclonal anti-nitrotyrosine IgG Clone1A6 (Upstate Biotechnology) for our nitration work. We also used Western

blotting steps such as diluent used to dilute primary and secondary antibodies and washing steps involved by adapting a method in Dr Picksley's laboratory (see Table 2.8).

Small amounts of BSA used in nitration work did not seem to give different nitrotyrosine signals. As BSA was nitrated with 100 µM peroxynitrite at different amounts (100, 200, 300 and 500 µg) we could not see any different in the levels of nitrotyrosine signals in all the 4 amounts (Fig. 5.13). The possible reason to this might be due to almost complete nitration of BSA protein with 100 µM peroxynitrite when present in small amounts, so the nitrotyrosine signals among the different small amounts of BSA were almost similar. However, at larger amounts (20 mg), weak nitrotyrosine signals were observed in BSA nitrated with 50 µM, 200 µM and 1 mM peroxynitrite whereas a very strong signal was detected in BSA nitrated with 3 mM peroxynitrite which was about similar to 100 µM peroxynitrite previously nitrated 500 µg BSA (Fig. 5.14). A possible explanation to this phenomenon is that when at small amounts, peroxynitrite can completely react with all the amounts of BSA, therefore there is no difference in nitrotyrosine signals in all the 4 amounts of BSA used. At larger amount, only a very high concentration of peroxynitrite reaches and completely reacts with all the BSA amounts whereas, lower concentrations of peroxynitrite are far too low to completely react with the high amount of BSA. However, it is totally different in the case of nitration of purified resolubilised p53 protein at small amounts (20.3, 40.6 and 60.9 µg) with 100 µM. No nitrotyrosine signals were obtained in all the 3 amounts. One reason for this is that the starting p53 protein material was too low and another reason is that p53 protein is not readily nitrated when compared to BSA (19 tyrosine residues) as it only contains 9 tyrosine residues (8 in the DNA binding domain and 1 in the tetramerisation domain). The other reason is the tyrosine residues in the p53 protein prepared might perhaps be hidden away/cryptic in or not on the surface of the p53 protein structure like the Pab240 epitope (where Pab240 reacts with cryptic

epitope in wt p53 and exposed in many p53 mutants) (Stephen and Lane, 1992; Calmels *et al*., 1997).

We compared the effects of dissolving BSA in two different buffer systems (PBS, pH 7.4 and KPi, pH 8.2) on nitration. While nitrotyrosine signals were detected as low as 10 µM up to 100 µM peroxynitrite in BSA dissolved in KPi (pH 8.2), detection of nitrotyrosine signals were observed only at 50 µM and strongest at 100 µM peroxynitrite when PBS (pH 7.4) was used to dissolve peroxynitrite. Changes in the pH of buffers used to dissolve BSA from physiological (PBS, pH 7.4) to alkaline values (KPi, pH 8.2) can increase the half-life of peroxynitrite, therefore prolonging peroxynitrite activities towards BSA (Cantoni, 2002) and also buffer composition can substantially affect the reactivity of peroxynitrite (Beckman *et al*., 1994). Peroxynitrite is extremely short-lived and labile at physiological pH values (pH 7.4) with halflife of ~1 s due to its rapid decomposition (Koppenol *et al*., 1992; Mondoro *et al*., 1997). Thus, we can conclude that peroxynitrite would react more effectively in alkaline conditions with slow decomposition rate. Peroxynitrite has a degrading property as evident in experiment in Fig. 5.21(b), where both nitrated purified resolubilised and nitrated purified soluble p53 protein dramatically reduced in levels after they were nitrated with 100 µM and 1.5 mM peroxynitrite (Fig. 5.21(b), Lanes 7 & 8 and 10 & 11, respectively) when compared to their non-nitrated counterparts (Fig. 5.21(b), Lanes 6 and 9, respectively).

Very strong nitro-p53 protein signals in purified resolubilised p53 protein samples nitrated with 200, 300 and 400 µM peroxynitrite with unreduced high molecular weight aggregates (Fig. 5.12(a), Lanes 7-9) which were also seen by Calmels *et al*. (1997) and Cobbs *et al*. (2001) in MCF7 and D54MG cells at 0.5-1 mM and 10-100 µM, peroxynitrite, respectively. This is believed to be due to the formation of carbonyl or dityrosine (i.e. tyrosine oxidation by peroxynitrite) or loss of zinc from p53 active site (Cobbs *et al*., 2001), which has been shown when p53 protein was treated with zinc chelators or with oxidizing agents

(Hainut and Milner, 1993; Hainut *et al*., 1995). This modification on the p53 protein might affects p53 structure and functions. Our attempt to nitrate purified resolubilised p53 protein resulted in basal levels of nitrotyrosine signals for all the samples (10 µM to 2 mM) in correspond to non-nitrated purified resolubilised p53 protein (Fig. 5.22(a)). At nitration with 3 mM concentration of peroxynitrite, the nitro-p53 protein was undetected (Fig. 5.22(a), Lane 14) when compared to the rest of the samples (Lanes 4-13). This might be due to the degrading properties of peroxynitrite especially occurs at higher concentration. However, in this work, our attempts to nitrate GST and GST-MDM2 proteins were unsuccessful where the nitrotyrosine signals could not be detected in both GST and GST-MDM2 proteins nitrated with increasing concentrations of peroxynitrite (data not shown). The number of tyrosine residues in MDM2 protein alone is 9 and GST protein is 4, thus the total number of tyrosines in the GST-MDM2 fusion protein is 13. However, this did not help in the nitration which might be due to the cryptic locations of the tyrosines in the protein which resulted in the tyrosine residues not easily accessible to the nitration process. To further confirm the degrading properties of peroxynitrite, an SDS-PAGE analysis of 500 µM peroxynitrite nitrated purified GST and GST-MDM2 protein showed no bands corresponding to the proteins (Fig. 5.23, Lanes 3 and 4, respectively) when compared to their non-nitrated counterparts (Fig. 5.23, Lanes 2 and 5, respectively). This is supported by a study by Ischiropoulos and Al-Mehdi which showed that fatty acid-free BSA treated with peroxynitrite resulted in protein fragmentation with protein fragments with molecular weight lower than 66 kDa (Ischiropoulos and Al-Mehdi, 1995) although no evidence reported in p53 protein thus far. However, in the culture system it is due to ubiquitin-dependent proteolysis by proteasome although evidence for the underlying mechanisms are still lacking (Calmels *et al*., 1997; Cobbs *et al*., 2003).

A panel of human cancer cell lines with different p53 status were selected for nitration study. When the cells reached about ~80% confluent, they were harvested and either lysed in cold RIPA lysis buffer or remained intact. The

intact cells were either washed with PBS or left unwashed. As determined earlier, the concentration of peroxynitrite at 100 µM gave the strongest nitrotyrosine signal and also 0-100 µM peroxynitrite are equivalent to its concentrations *in vivo* during oxidative stress and inflammatory conditions (Cobbs *et al*., 2001), therefore we used this concentration, mimicking the concentration at oxidative stress and inflammation, in our nitration study on the chosen cell lysates and intact cells. We found that BSA in serum in unwashed intact cells were readily nitrated. This further confirms that BSA is a readily nitrated protein and therefore is very suitable to use as a model protein for preliminary nitration work. In all nitration studies on the cell lysates and immunprecipitation work we found that at 100 µM peroxynitrite hardly any nitrotyrosine signals or just basal signals were obtained. Thus, optimisation for nitration conditions for the cell lysates such as using different lysis buffers to lyse cells need to be further explored.

We then explored the effects of nitration on p53 protein levels using NO donor GSNO in MCF7 cancer cell line. The concentrations of NO that were released by GSNO are similar to those formed under intense inflammatory conditions (Chazotte-Aubert *et al*., 2000). GSNO (1 mM) has been shown to generate NO at the rate of 1 to 4 µmol/litre/min in culture medium with 10% foetal bovine serum (Wink *et al*., 1996). GSNO is not a strong nitrating agent itself *in vitro*, however, within the cell NO released from GSNO reacts with superoxide anion to form peroxynitrite, a strong oxidant and nitrating agent (Chazotte-Aubert *et al*., 2000). We found very weak nitrotyrosine signals in 0.5 mM and 1.0 mM GSNO treated MCF7 cell lysates while moderate nitrotyrosine signals in 0.5 mM and 1.0 mM GSNO treated MCF7 cell lysates immunoprecipitated with CM-1. This indicates that p53 protein in MCF7 cells were nitrated at tyrosine residues following GSNO treatment. The levels of p53 protein in 0.5 mM and 1.0 mM GSNO treated MCF7 cell lysates were almost similar to that of untreated MCF7 lysates. However, the p53 proteins were completely abolished in 0.5 mM and 1.0 mM GSNO treated MCF7 cell lysates

immunoprecipitated with mouse monoclonal anti-nitrotyrosine antibody. There are two possible reasons for this i) because the starting materials of p53 protein immunoprecipitated by CM-1 was low and/or ii) the degrading effect of GSNO resulted in the loss of p53 protein. Further studies need to be carried out to see the effects of other NO donors on p53 nitration and therefore its protein levels and also on p53 functions and activities such as on DNA binding activity of p53 on its specific consensus sequence using electrophoretic mobility shift assay (EMSA), on the expression of p53-target genes such as those involved in cell cycle arrest (eg*. p21, GADD4*), apoptosis (eg. *Bax, PUMA, NOXA*), DNA repair, differentiation and senescence by employing reverse-transcription PCR (RT-PCR) (expression at RNA levels), western blotting (expression at protein levels), or by luciferase reporter assay (co-transfection of a p53 construct with a plasmid containing a p53-response element fused with a luciferase gene), the effects on apoptosis and cell cycle regulation, protein-protein interactions with cellular proteins such as MDM2 and viral proteins by immunoprecipitation studies and ELISA.

Protein tyrosine nitration has been shown to occur under physiological conditions by the detection of 3-nitrotyrosine by analytical and immunological techniques (reviewed by Greenacre and Ischiropoulos, 2001). Nitration of tyrosine residues is a useful marker of the contribution of nitric oxide in oxidative damage (reviewed by Alvarez and Radi, 2003). Nitration may interfere with signaling cascades, since nitrated tyrosine residues cannot be phosphorylated (Gow *et al*., 1996; Kong *et al*., 1996). Protein tyrosine nitration is a selective process, which depends on the structure of the protein, the abundance of the protein and the number of tyrosine residues (Souza *et al*., 1999). In neurofilaments, tyrosine residues next to glutamate in amino acid sequence could be easily nitrated (Crow *et al*., 1997). In human p53 protein three tyrosines namely Y 205, Y 220 and Y 327 match these characteristics (Chazotte-Aubert *et al*., 2000). These tyrosine-glutamate sequences are located in the central DNA binding domain as well as in the tetramerisation domain of

p53 protein. Which tyrosine residues are nitrated in p53 protein and whether tyrosine nitration results in the activation or loss of p53 functions and activities need further elucidation. p53 tyrosine modification is dependent on the cell types, the redox state of the cells, the cell microenvironment which is variable and complex, the p53 mutational status, the p53 protein levels and localisation, the steady-state concentration and localisation of NO and its derivatives.

On the present Pubmed search under the keywords “p53 nitration”, the results showed only 25 publications so far, though some are not directly related to our study, versus other modifications such as “p53 phosphorylation” (6180 papers), “p53 acetylation” (1095 papers), “p53 ubiquitination” (1104 papers), “p53 sumoylation” (156 papers), “p53 neddylation” (28 papers), and also “p53 methylation” (1913 papers) and none papers directly showed “MDM2 nitration”. It would seem that nitration work generally has become limited to big chemistry groups in the USA etc. (Dr Steven Picksley, personal communication). There are two contradictory findings about p53 protein modification by NO and its derivatives. Only a handful papers have shown that wt p53 protein was inactivated as a transcription factor through being made defective in its DNA binding activity as determined by gel shift assays and thereby resulted in dysregulation of its downstream pathways (Cobbs *et al*., 2001 & 2003). 8 of 9 tyrosine residues of p53 protein are located in the central core DNA-binding domain where covalent modifications of these residues by NO possibly causes mutant p53 conformation or directly interferes with DNA binding residues. This was evident at high concentrations of NO where it inhibited p53 functions by altering its conformation and consequently impaired its DNA binding activity *in vitro*, in turn its function as a transcription factor (Ho *et al*., 1996; Calmels *et al*., 1997; Chazotte-Aubert *et al*., 2000). A study by Salem *et al*. in the Department of Biomedical Sciences, University of Bradford, showed that peroxynitrite, a potent oxidising and nitrating derivative of NO, abrogated p53 binding to DNA but this effect was counteracted by exposure to hydrogen peroxide (H_2O_2). They confirmed this result by computer simulation which shows that in the native

structure of p53 protein there are 7 interacting residues of p53 that bind to DNA (Lys120, Ser241, Arg248, Arg271, Ala276, Cys277 and Arg289), however Arg248 and Cys277 are lost upon exposure to peroxynitrite, presumably due to the conversion of 8 tyrosine residues in the DNA binding domain of p53 to 3-nitrotyrosine (Tyr103, Tyr107, Tyr126, Tyr163, Tyr205, Tyr220, Tyr234 and Tyr236) which causes severe conformational changes in the p53 protein structure and thus abrogates its DNA binding capacity. However, after H_2O_2-mediated oxidation, a marked increase in DNA binding based on the increase of the number of amino acids interacting from 7 to 15 (Salem *et al*., 2009). On the contrary, most papers show that NO treatment of a variety of cells led to p53 tyrosine nitration and enhanced its DNA binding activity, indicating that NO activates wt p53, however, the underlying mechanisms are still not known. It was reported that low concentrations of NO and its derivatives activate p53 protein as a transcription factor due to the induction of DNA damage by NO (Forrester *et al*., 1996; Ho *et al*., 1996). Upon treatment of various cells with NO, either produced endogenously via induction of iNOS or exogenously supplied through NO donors, p53 became phosphorylated at serine 15 and accumulated in the nucleus due to attenuated nuclear export by NO resulting in the stabilisation and activation of p53 protein which as a result affects cell cycle progression and/or apoptosis (Schneiderhan *et al*., 2003). Yakovlev *et al*. have shown that p53 nitrated at tyrosine 327, which is located in the tetramerisation domain, promoted p53 oligomerisation, nuclear accumulation and transcriptional activity without p53 Ser15 phosphorylation at low NO concentrations (Yakovlev *et al*., 2010). NO has been shown in several different cell types to downregulate MDM2 protein levels resulting in the accumulation of p53 protein due to reduced p53 ubiquitination but extended NO exposure increased MDM2 protein levels due to p53-dependent induction of MDM2 gene (Wang *et al*., 2002). Activated p53 protein by NO in several cell types led to the induction of p53 target genes p21 and MDM2, both at mRNA and protein levels (Wang *et al*., 2002). NO has been shown to have both pro- and anti-neoplastic effects (Hussain *et al*., 2003 & 2004). Peroxynitrite has been shown to induce apoptosis in HL-60 leukaemia

cells through the activation of multiple caspases mainly caspases 2, 3, 6 and 7. NO-induced apoptosis was the result of DNA damage and subsequent upregulation of p53 protein expression prior to apoptosis (MeBmer *et al*., 1994). NO induced p53 protein upregulation and apoptosis in a dose- and time-dependent manners in several different cell types (MeBmer *et al*., 1994; Lee *et al*., 2006; Natal *et al*., 2008) and NO-treated cells resulted in a decrease in anti-apoptotic Bcl-2 protein levels and an increase in pro-apoptotic Bax protein levels and also an increase in caspase-3 and -9 activities, both playing a major role in apoptosis (Natal *et al*., 2008). The specificity of the NO action was confirmed in that NOS inhibitors such as NMMA stopped inducible NO production as well as p53 protein expression and apoptosis (MeBmer *et al*., 1994). There is a close relationship, i.e. an autoregulatory feedback loop, between p53 and NO whereby upon treatment of cells with NO donors, p53 protein became accumulated in the nucleus (Messmer *et al*., 1994; Forrester *et al*., 1996; Messmer & Brune, 1996; Calmels *et al*., 1997; Chazotte-Aubert *et al*., 2000) and this was then followed by transrepression of transcription of iNOS mRNA expression (Forrester *et al*. 1996; Ambs *et al*., 1997; Chazotte-Aubert *et al*.; 2000). This is one of the mechanisms whereby p53 safeguards the cells from the potential of NO-induced DNA damage other than its well established roles in cell cycle arrest and/or apoptosis. In summary, NO inhibits cell proliferation (by p53-mediated growth arrest) or induces apoptosis, however, negative and positive modulators of apoptosis strongly determine the susceptibility of cells to the toxic insult of NO and its derivatives (MeBmer *et al*., 1994). NO effects depend on many factors such as the microenvironment that is variable, complex and unpredictable so no firm predictions on how NO will modify a particular protein in the cell system (reviewed in Leon *et al*., 2008).

FUTURE STUDIES

Provided that nitration of p53 protein is successful, the following studies should be further considered:

i) To map p53 nitration sites by trypsin digestion, 2-D PAGE gels and Western blotting with an anti-nitrotyrosine antibody. This is to determine which tyrosine residues are nitrated and at which position. To assist mapping, a deletion series of the p53 protein will be generated. Separately, whether the amino acid analyser can be used to detect nitrated amino acids and whether this could be used to extend the range of amino acids beyond nitrotyrosine i.e. can we detect nitrophenylalanine and nitrotryptophan. Another indirect method of possible detecting nitrated residues is to ask whether nitration of p53 protein blocks the binding sites of a range of p53 antibodies. Having detected and confirmed nitrated residues on p53 protein, we will mutate these sites by site-directed mutagenesis and to see whether residues on p53 protein affect its latent binding with DNA, and other transcription machinery.

ii) Also to determine whether nitrated p53 protein affects its interaction with cellular proteins such as MDM2, viral proteins such as Adenovirus E1B and with its transcription machinery proteins by employing immunoprecipitation assay followed by Western blotting or by sandwich ELISA. MDM2 and AdE1B proteins will be produced as GST fusion proteins expressed in *E. coli*. Nitrated p53 protein and cell extracts containing either MDM2 protein or AdE1B protein is mixed. A monoclonal antibody DO-1 raised against human p53 protein is then added. If MDM2 protein or AdE1B binds to nitrated p53 protein, they will form an immune complex with the monoclonal antibody DO-1 and therefore will be pulled down by protein G Sepharose beads upon centrifugation. SDS-PAGE and Western blotting will then be carried out. The MDM2-GST or AdE1B-GST fusion proteins binding to nitrated p53 protein can also be determined by mixing the proteins together with Glutathione Sepharose which then pull down the

complex upon centrifugation. This is then followed by SDS-PAGE and Western blotting. This can also be done by using Biacore assay (real time, label-free detection characterisation and analysis of biomolecular interactions) or failing that simply by employing sandwich ELISA.

iii) To check the effects of p53 nitration on its major roles in cell cycle regulation and apoptosis by employing flowcytometry and morphological detection of apoptotic cells by TUNEL assay, then verified by DNA fragmentation assay, and to a lesser extent on its role in DNA repair, differentiation and senescence. Apart from these analyses, regulation of genes responsible for these activities such as *p21, GADD4* (cell cycle checkpoints), *BAX, PUMA, NOXA* (pro-apoptotic genes), *Bcl-2, Bcl-xl*, *survivin* (anti-apoptotic) and other p53-regulated genes can be determined by RT-PCR (mRNA transcript levels) or Western blotting (protein levels). Novel genes downregulated or upregulated by p53 protein nitration can be determined by employing microarray analysis. Expression or repression of highly significant regulated genes having distinct roles will then be verified by Real-Time PCR (qPCR). This is also to delineate established as well as novel signalling pathways involved in p53 nitration. Apoptosis can also be determined by the outer mitochondrial membrane permeability (OMMP) leading to mitochondrial dysfunction and collapse resulting in the release of cytochrome c from the mitochondria and subsequently the activation of common effector caspases such as caspase-3 and caspase-7, determined by using caspase 3/7 assay. The cleavage and activated caspases 3 and 7 can also be detected by Western blotting. In addition, luciferase reporter assay can also be used to confirm transcriptional induction of genes transcribed by nitrated p53 protein compared to its native p53 protein counterpart.

iv) Proteomic studies can also be used to detect novel proteins being expressed which are associated with p53 protein nitration. Cell lysates from untreated control and nitrated samples will be used in order to compare total

protein expression profiling between the samples by employing two-dimensional gel electrophoresis (2-DE) by first subjecting the cleaned cell lysates to immobilised pH gradient (IPG) strips for isoelectric focusing (IEF) where the proteins are separated by their isoelectric points (pI) (1^{st} dimension separation) and then followed by standard SDS polyacrylamide gel electrophoresis by which the proteins are separated according to their molecular weights (2^{nd} dimension separation). These combined separations will give individual protein spots, also known as 2D map. The gels are stained with fluorescent dyes, Commassie Brilliant Blue staining or silver staining (the most sensitive staining) and differential in protein expressions and intensities between the gels are identified and the selected protein spots are excised and in-gel trypsin digested into smaller peptides before being subjected to mass spectrometry for peptide mapping or peptide mass fingerprinting by which the peptide sequence can be analysed using the protein databases such as ExPASY to identify and characterise the protein spots. This advanced proteomics technology thus can be used to identify protein biomarkers in nitrated samples compared to untreated control samples. In translational research, these novel protein biomarkers can be used in the clinical settings as early diagnosis and/or treatment response monitoring in human diseases particularly in specific types of cancers and inflammatory conditions. In addition, uniquely expressed proteins could be potentially useful targeted candidates for anti-cancer drug developments. If the main interest is just to look at specific tyrosine residues in p53 protein that are nitrated, after 2D electrophoresis, the gel is electroblotted and then probed with anti-p53 antibody. The different spots of p53 proteins can be processed by mass spectrometry to determine the specific amino acids that are modified, in this case nitrated. The Institute of Cancer Therapeutics (ICT), University of Bradford, has the facilities for the proteomics work.

v) To determine the localisation of nitro-p53 protein compared to non-nitrated native p53 protein and p53-regulated proteins in the nucleus or

cytoplasm by employing immunofluorescence and then confirmed by cell fractionation assay followed by Western blotting. The effects of nitration on p53 protein stability in cultured cells can be followed temporally by adding protein synthesis inhibitor cycloheximide after treatment of cells with NO donors or peroxynitrite at certain concentrations or time points.

vi) To check whether NO or its derivatives alone have effects on the cells viability by employing MTS assay, which is an improved version of MTT assay. Also to check whether NO or its derivatives can sensitise cancer cells to existing chemotherapeutic drugs or radiation.

vii) Since we have the baculovirus p53 construct, it is worth to look at human p53 protein expressed in baculovirus for nitration study. Insect cells possess similar posttranslational modifications to mammalian cells permitting proper folding, disulphide bond formation, glycosylation, acylation and phosphorylation. p53 protein produced in this system is expected to be soluble, correctly folded and biologically active and relatively easy to purify.

From all the above suggested further studies, it is worth noting and bearing in mind that, overall, the effects of p53 protein nitration depend on the cell types, p53 status, p53 protein levels, types of NO donors, doses of and time of exposure to NO and its derivatives.

REFERENCES

Abarzua, P., LoSardo, J.E., Gubler, M.L., and Neri, A. (1995). Microinjection of monoclonal antibody PAb421 into human SW480 colorectal carcinoma cells restores the transcription activation function to mutant p53. Cancer Res 55, 3490-3494.

Abarzua, P., LoSardo, J.E., Gubler, M.L., Spathis, R., Lu, Y.A., Felix, A., and Neri, A. (1996). Restoration of the transcription activation function to mutant P53 in human cancer cells. Oncogene 13, 2477-2482.

Abida, W.M., Nikolaev, A., Zhao, W., Zhang, W., and Gu, W. (2007). FBXO11 promotes the Neddylation of p53 and inhibits its transcriptional activity. The Journal of biological chemistry 282, 1797-1804.

Adorno, M., Cordenonsi, M., Montagner, M., Dupont, S., Wong, C., Hann, B., Solari, A., Bobisse, S., Rondina, M.B., Guzzardo, V., et al. (2009). A Mutant-p53/Smad complex opposes p63 to empower TGFbeta-induced metastasis. Cell 137, 87-98.

Ahn, B., Han, B.S., Kim, D.J., and Ohshima, H. (1999). Immunohistochemical localization of inducible nitric oxide synthase and 3-nitrotyrosine in rat liver tumors induced by N-nitrosodiethylamine. Carcinogenesis 20, 1337-1344.

Alarcon-Vargas, D., and Ronai, Z. (2002). p53-Mdm2--the affair that never ends. Carcinogenesis 23, 541-547.

Alberts B, J.A., Lewis J, et al. (2002). Intracellular Control of Cell-Cycle Events. Molecular Biology of the Cell 4th edition.

Alvarez, B., and Radi, R. (2003). Peroxynitrite reactivity with amino acids and proteins. Amino Acids 25, 295-311.

Ambs, S., Hussain, S.P., and Harris, C.C. (1997). Interactive effects of nitric oxide and the p53 tumor suppressor gene in carcinogenesis and tumor progression. FASEB J 11, 443-448.

Anderson, M.E., Woelker, B., Reed, M., Wang, P., and Tegtmeyer, P. (1997). Reciprocal interference between the sequence-specific core and nonspecific C-terminal DNA binding domains of p53: implications for regulation. Mol Cell Biol 17, 6255-6264.

Appelbaum, E.R., and Shatzman, A.R. (1999). Prokaryotic in vivo expression systems. In Protein expression: a practical approach, S.J. Higgins, and B.D. Hames, eds. (Oxford, Oxford University Press), pp. 169-200.

Appella, C.W.A.a.E. (2010). Signaling to the p53 Tumor Suppressor through Pathways Activated by Genotoxic and Non-Genotoxic Stresses. In Handbook of Cell Signaling, pp. 2185-2204.

Appella, E., and Anderson, C.W. (2000). Signaling to p53: breaking the posttranslational modification code. Pathol Biol (Paris) 48, 227-245.

Appella, E., and Anderson, C.W. (2001). Post-translational modifications and activation of p53 by genotoxic stresses. Eur J Biochem 268, 2764-2772.

Argentini, M., Barboule, N., and Wasylyk, B. (2001). The contribution of the acidic domain of MDM2 to p53 and MDM2 stability. Oncogene 20, 1267-1275.

Arrowsmith, C.H., and Morin, P. (1996). New insights into p53 function from structural studies. Oncogene 12, 1379-1385.

Ashcroft, M., Kubbutat, M.H., and Vousden, K.H. (1999). Regulation of p53 function and stability by phosphorylation. Mol Cell Biol 19, 1751-1758.

Bai, L., and Zhu, W.G.(2006). p53: structure, function and therapeutic applications. Journal of Cancer Molecules 2, 141-153.

Baneyx, F. (1999). Recombinant protein expression in Escherichia coli. Curr Opin Biotechnol 10, 411-421.

Baptiste, N., Friedlander, P., Chen, X., and Prives, C. (2002). The proline-rich domain of p53 is required for cooperation with anti-neoplastic agents to promote apoptosis of tumor cells. Oncogene 21, 9–21.

Bar, J.K., Slomska, I., Rabczynki, J., Noga, L., and Grybos, M. (2009). Expression of p53 protein phosphorylated at serine 20 and serine 392 in malignant and benign ovarian neoplasms: correlation with clinicopathological parameters of tumors. International journal of gynecological cancer : official journal of the International Gynecological Cancer Society 19, 1322-1328.

Barak, Y., and Oren, M. (1992). Enhanced binding of a 95 kDa protein to p53 in cells undergoing p53-mediated growth arrest. The EMBO journal 11, 2115-2121.

Barbieri, C.E., Tang, L.J., Brown, K.A., and Pietenpol, J.A. (2006). Loss of p63 leads to increased cell migration and up-regulation of genes involved in invasion and metastasis. Cancer Res 66, 7589-7597.

Bates, S., and Vousden, K.H. (1996). p53 in signaling checkpoint arrest or apoptosis. Curr Opin Genet Dev 6, 12-18.

Battinelli, E., and Loscalzo, J. (2000). Nitric oxide induces apoptosis in megakaryocytic cell lines. Blood 95, 3451-3459.

Bech-Otschir, D., Kraft, R., Huang, X., Henklein, P., Kapelari, B., Pollmann, C., and Dubiel, W. (2001). COP9 signalosome-specific phosphorylation targets p53 to degradation by the ubiquitin system. The EMBO journal 20, 1630-1639.

Beckman, J.S. (1996). Oxidative damage and tyrosine nitration from peroxynitrite. Chemical research in toxicology 9, 836-844.

Beckman, J.S., Beckman, T.W., Chen, J., Marshall, P.A., and Freeman, B.A. (1990). Apparent hydroxyl radical production by peroxynitrite: implications for endothelial injury from nitric oxide and superoxide. Proc Natl Acad Sci U S A 87, 1620-1624.

Beckman, J.S., Chen, J., Ischiropoulos, H., and Crow, J.P. (1994). Oxidative chemistry of peroxynitrite. Methods in enzymology 233, 229-240.

Beckman JS, K.W. (1996). Nitric oxide, superoxide, and peroxynitrite: the good, the bad, and ugly. Am J Physiol 271, C1424-1437.

Bennett, M., Macdonald, K., Chan, S.W., Luzio, J.P., Simari, R., and Weissberg, P. (1998). Cell surface trafficking of Fas: a rapid mechanism of p53-mediated apoptosis. Science 282, 290-293.

Bensaad, K., Tsuruta, A., Selak, M.A., Vidal, M.N., Nakano, K., Bartrons, R., Gottlieb, E., and Vousden, K.H. (2006). TIGAR, a p53-inducible regulator of glycolysis and apoptosis. Cell 126, 107-120.

Bensaad, K., and Vousden, K.H. (2007). p53: new roles in metabolism. Trends Cell Biol 17, 286-291.

Bieging, K.T., and Attardi, L.D. (2012). Deconstructing p53 transcriptional networks in tumor suppression. Trends Cell Biol 22, 97-106.

Birnboim, H.C., and Doly, J. (1979). A rapid alkaline extraction procedure for screening recombinant plasmid DNA. Nucleic Acids Res 7, 1513-1523.

Bischof O, S.K., Martin N, Werner A, Sustmann C, Grosschedl R, Dejean A. (2006). The E3 SUMO ligase PIASy is a regulator of cellular senescence and apoptosis. Mol Cell 22, 783-794.

Bode, A.M., and Dong, Z. (2004). Post-translational modification of p53 in tumorigenesis. Nat Rev Cancer 4, 793-805.

Bossi, G., Lapi, E., Strano, S., Rinaldo, C., Blandino, G., and Sacchi, A. (2006). Mutant p53 gain of function: reduction of tumor malignancy of human cancer cell lines through abrogation of mutant p53 expression. Oncogene 25, 304-309.

Bossi, G., Marampon, F., Maor-Aloni, R., Zani, B., Rotter, V., Oren, M., Strano, S., Blandino, G., and Sacchi, A. (2008). Conditional RNA interference in vivo to study mutant p53 oncogenic gain of function on tumor malignancy. Cell Cycle 7, 1870-1879.

Bottger, A., Bottger, V., Sparks, A., Liu, W.L., Howard, S.F., and Lane, D.P. (1997). Design of a synthetic Mdm2-binding mini protein that activates the p53 response in vivo. Current biology : CB 7, 860-869.

Bottger, V., Bottger, A., Garcia-Echeverria, C., Ramos, Y.F., van der Eb, A.J., Jochemsen, A.G., and Lane, D.P. (1999). Comparative study of the p53-mdm2 and p53-MDMX interfaces. Oncogene 18, 189-199.

Bottger, V., Bottger, A., Howard, S.F., Picksley, S.M., Chene, P., Garcia-Echeverria, C., Hochkeppel, H.K., and Lane, D.P. (1996). Identification of novel mdm2 binding peptides by phage display. Oncogene 13, 2141-2147.

Bourdon, J.C. (2007). p53 and its isoforms in cancer. British journal of cancer 97, 277-282.

Bourdon, J.C. (2007). p53 Family isoforms. Current pharmaceutical biotechnology 8, 332-336.

Bourdon, J.C., Fernandes, K., Murray-Zmijewski, F., Liu, G., Diot, A., Xirodimas, D.P., Saville, M.K., and Lane, D.P. (2005). p53 isoforms can regulate p53 transcriptional activity. Genes & development 19, 2122-2137.

Brady, C.A., and Attardi, L.D. (2010). p53 at a glance. J Cell Sci 123, 2527-2532.

Brady, C.A., Jiang, D., Mello, S.S., Johnson, T.M., Jarvis, L.A., Kozak, M.M., Kenzelmann Broz, D., Basak, S., Park, E.J., McLaughlin, M.E., et al. (2011). Distinct p53 transcriptional programs dictate acute DNA-damage responses and tumor suppression. Cell 145, 571-583.

Bredt, D.S., and Snyder, S.H. (1994). Nitric oxide: a physiologic messenger molecule. Annu Rev Biochem 63, 175-195.

Brockhaus, F., and Brune, B. (1999). Overexpression of CuZn superoxide dismutase protects RAW 264.7 macrophages against nitric oxide cytotoxicity. The Biochemical journal 338 (Pt 2), 295-303.

Brooks, C.L., and Gu, W. (2003). Ubiquitination, phosphorylation and acetylation: the molecular basis for p53 regulation. Curr Opin Cell Biol 15, 164-171.

Brooks, C.L., and Gu, W. (2010). New insights into p53 activation. Cell Res 20, 614-621.

Brooks, C.L., Li, M., Hu, M., Shi, Y., and Gu, W. (2007). The p53--Mdm2--HAUSP complex is involved in p53 stabilization by HAUSP. Oncogene 26, 7262-7266.

Brosh, R., and Rotter, V. (2009). When mutants gain new powers: news from the mutant p53 field. Nat Rev Cancer 2009 Oct;9(10):701-13.

Brown, C.J., Lain, S., Verma, C.S., Fersht, A.R., and Lane, D.P. (2009). Awakening guardian angels: drugging the p53 pathway. Nature reviews Cancer 9, 862-873.

Bruckdorfer, K.R. (2001). The nitration of proteins in platelets. Comptes rendus de l'Academie des sciences Serie III, Sciences de la vie 324, 611-615.

Brugarolas, J., Chandrasekaran, C., Gordon, J.I., Beach, D., Jacks, T., and Hannon, G.J. (1995). Radiation-induced cell cycle arrest compromised by p21 deficiency. Nature 377, 552-557.

Bruins, W., Bruning, O., Jonker, M.J., Zwart, E., van der Hoeven, T.V., Pennings, J.L., Rauwerda, H., de Vries, A., and Breit, T.M. (2008). The absence of Ser389 phosphorylation in p53 affects the basal gene expression level of many p53-dependent genes and alters the biphasic response to UV exposure in mouse embryonic fibroblasts. Molecular and cellular biology 28, 1974-1987.

Bruins, W., Jonker, M.J., Bruning, O., Pennings, J.L., Schaap, M.M., Hoogervorst, E.M., van Steeg, H., Breit, T.M., and de Vries, A. (2007). Delayed expression of apoptotic and cell-cycle control genes in carcinogen-exposed bladders of mice lacking p53.S389 phosphorylation. Carcinogenesis 28, 1814-1823.

Brune, B. (2003). Nitric oxide: NO apoptosis or turning it ON? Cell death and differentiation 10, 864-869.

Budanov, A.V., Sablina, A.A., Feinstein, E., Koonin, E.V., and Chumakov, P.M. (2004). Regeneration of peroxiredoxins by p53-regulated sestrins, homologs of bacterial AhpD. Science 304, 596-600.

Bulavin, D.V., Saito, S., Hollander, M.C., Sakaguchi, K., Anderson, C.W., Appella, E., and Fornace, A.J., Jr. (1999). Phosphorylation of human p53 by p38 kinase coordinates N-terminal phosphorylation and apoptosis in response to UV radiation. The EMBO journal 18, 6845-6854.

Burney, S., Niles, J.C., Dedon, P.C., and Tannenbaum, S.R. (1999). DNA damage in deoxynucleosides and oligonucleotides treated with peroxynitrite. Chemical research in toxicology 12, 513-520.

Buschmann, T., Fuchs, S.Y., Lee, C.G., Pan, Z.Q., and Ronai, Z. (2000). SUMO-1 modification of Mdm2 prevents its self-ubiquitination and increases Mdm2 ability to ubiquitinate p53. Cell 101, 753-762.

Buschmann, T., Lerner, D., Lee, C.G., and Ronai, Z. (2001). The Mdm-2 amino terminus is required for Mdm2 binding and SUMO-1 conjugation by the E2 SUMO-1 conjugating enzyme Ubc9. The Journal of biological chemistry 276, 40389-40395.

Buschmann, T., Potapova, O., Bar-Shira, A., Ivanov, V.N., Fuchs, S.Y., Henderson, S., Fried, V.A., Minamoto, T., Alarcon-Vargas, D., Pincus, M.R., et

al. (2001). Jun NH2-terminal kinase phosphorylation of p53 on Thr-81 is important for p53 stabilization and transcriptional activities in response to stress. Mol Cell Biol 21, 2743-2754.

Caelles, C., Helmberg, A., and Karin, M. (1994). p53-dependent apoptosis in the absence of transcriptional activation of p53-target genes. Nature 370, 220-223.

Cahilly-Snyder, L., Yang-Feng, T., Francke, U., and George, D.L. (1987). Molecular analysis and chromosomal mapping of amplified genes isolated from a transformed mouse 3T3 cell line. Somat Cell Mol Genet 13, 235-244.

Cairns, R.A., Harris, I.S., and Mak, T.W. (2011). Regulation of cancer cell metabolism. Nat Rev Cancer 11, 85-95.

Calmels, S., Hainaut, P., and Ohshima, H. (1997). Nitric oxide induces conformational and functional modifications of wild-type p53 tumor suppressor protein. Cancer Res 57, 3365-3369.

Campisi, J. (2005). Senescent cells, tumor suppression, and organismal aging: good citizens, bad neighbors. Cell 120, 513-522.

Candau, R., Scolnick, D.M., Darpino, P., Ying, C.Y., Halazonetis, T.D., and Berger, S.L. (1997). Two tandem and independent sub-activation domains in the amino terminus of p53 require the adaptor complex for activity. Oncogene 1997 Aug 14;15(7):807-16.

Canman, C.E., Lim, D.S., Cimprich, K.A., Taya, Y., Tamai, K., Sakaguchi, K., Appella, E., Kastan, M.B., and Siliciano, J.D. (1998). Activation of the ATM kinase by ionizing radiation and phosphorylation of p53. Science 281, 1677-1679.

Cantoni, O., Palomba, L., Guidarelli, A., Tommasini, I., Cerioni, L., and Sestili, P. (2002). Cell signaling and cytotoxicity by peroxynitrite. Environmental health perspectives 110 Suppl 5, 823-825.

Casciano I, M.K., Boni L, Pagnan G, Banelli B, Allemanni G, Ponzoni M, Tonini GP, Romani M. (2002). Expression of DeltaNp73 is a molecular marker for adverse outcome in neuroblastoma patients. Cell Death Differ 9, 246-251.

Chao, C., Wu, Z., Mazur, S.J., Borges, H., Rossi, M., Lin, T., Wang, J.Y., Anderson, C.W., Appella, E., and Xu, Y. (2006). Acetylation of mouse p53 at lysine 317 negatively regulates p53 apoptotic activities after DNA damage. Molecular and cellular biology 26, 6859-6869.

Chazotte-Aubert, L., Hainaut, P., and Ohshima, H. (2000). Nitric oxide nitrates tyrosine residues of tumor-suppressor p53 protein in MCF-7 cells. Biochem Biophys Res Commun 267, 609-613.

Chazotte-Aubert, L., Pluquet, O., Hainaut, P., and Ohshima, H. (2001). Nitric oxide prevents gamma-radiation-induced cell cycle arrest by impairing p53

function in MCF-7 cells. Biochemical and biophysical research communications 281, 766-771.

Chehab, N.H., Malikzay, A., Appel, M., and Halazonetis, T.D. (2000). Chk2/hCds1 functions as a DNA damage checkpoint in G(1) by stabilizing p53. Genes & development 14, 278-288.

Chen, J., Lin, J., and Levine, A.J. (1995). Regulation of transcription functions of the p53 tumor suppressor by the mdm-2 oncogene. Molecular medicine 1, 142-152.

Chen, J., Marechal, V., and Levine, A.J. (1993). Mapping of the p53 and mdm-2 interaction domains. Molecular and cellular biology 13, 4107-4114.

Chen, L., and Chen, J. (2003). MDM2-ARF complex regulates p53 sumoylation. Oncogene 22, 5348-5357.

Chen, P.L., Chen, Y.M., Bookstein, R., and Lee, W.H. (1990). Genetic mechanisms of tumor suppression by the human p53 gene. Science 250, 1576-1580.

Chen, X., Ko, L.J., Jayaraman, L., and Prives, C. (1996). p53 levels, functional domains, and DNA damage determine the extent of the apoptotic response of tumor cells. Genes & development 10, 2438-2451.

Chipuk, J.E., Kuwana, T., Bouchier-Hayes, L., Droin, N.M., Newmeyer, D.D., Schuler, M., and Green, D.R. (2004). Direct activation of Bax by p53 mediates mitochondrial membrane permeabilization and apoptosis. Science 303, 1010-1014.

Cho, Y., Gorina, S., Jeffrey, P.D., and Pavletich, N.P. (1994). Crystal structure of a p53 tumor suppressor-DNA complex: understanding tumorigenic mutations. Science 265, 346-355.

Choudhari, S.K., Chaudhary, M., Bagde, S., Gadbail, A.R., and Joshi, V. (2013). Nitric oxide and cancer: a review. World journal of surgical oncology 11, 118.

Chuikov, S., Kurash, J.K., Wilson, J.R., Xiao, B., Justin, N., Ivanov, G.S., McKinney, K., Tempst, P., Prives, C., Gamblin, S.J., et al. (2004). Regulation of p53 activity through lysine methylation. Nature 432, 353-360.

Clarke, A.R., Purdie, C.A., Harrison, D.J., Morris, R.G., Bird, C.C., Hooper, M.L., and Wyllie, A.H. (1993). Thymocyte apoptosis induced by p53-dependent and independent pathways. Nature 362, 849-852.

Clore, G.M., Omichinski, J.G., Sakaguchi, K., Zambrano, N., Sakamoto, H., Appella, E., and Gronenborn, A.M. (1994). High-resolution structure of the oligomerization domain of p53 by multidimensional NMR. Science 265, 386-391.

Cobbs, C.S., Samanta, M., Harkins, L.E., Gillespie, G.Y., Merrick, B.A., and MacMillan-Crow, L.A. (2001). Evidence for peroxynitrite-mediated modifications to p53 in human gliomas: possible functional consequences. Arch Biochem Biophys 394, 167-172.

Cobbs, C.S., Whisenhunt, T.R., Wesemann, D.R., Harkins, L.E., Van Meir, E.G., and Samanta, M. (2003). Inactivation of wild-type p53 protein function by reactive oxygen and nitrogen species in malignant glioma cells. Cancer research 63, 8670-8673.

Cordon-Cardo, C., Latres, E., Drobnjak, M., Oliva, M.R., Pollack, D., Woodruff, J.M., Marechal, V., Chen, J., Brennan, M.F., and Levine, A.J. (1994). Molecular abnormalities of mdm2 and p53 genes in adult soft tissue sarcomas. Cancer Res 54, 794-799.

Courtois, S., Caron de Fromentel, C., and Hainaut, P. (2004). p53 protein variants: structural and functional similarities with p63 and p73 isoforms. Oncogene 23, 631-638.

Craig, A., Scott, M., Burch, L., Smith, G., Ball, K., and Hupp, T. (2003). Allosteric effects mediate CHK2 phosphorylation of the p53 transactivation domain. EMBO reports 4, 787-792.

Craig, A.L., Burch, L., Vojtesek, B., Mikutowska, J., Thompson, A., and Hupp, T.R. (1999). Novel phosphorylation sites of human tumour suppressor protein p53 at Ser20 and Thr18 that disrupt the binding of mdm2 (mouse double minute 2) protein are modified in human cancers. The Biochemical journal 342 (Pt 1), 133-141.

Crighton, D., Wilkinson, S., O'Prey, J., Syed, N., Smith, P., Harrison, P.R., Gasco, M., Garrone, O., Crook, T., and Ryan, K.M. (2006). DRAM, a p53-induced modulator of autophagy, is critical for apoptosis. Cell 126, 121-134.

Crow, J.P., Ye, Y.Z., Strong, M., Kirk, M., Barnes, S., and Beckman, J.S. (1997). Superoxide dismutase catalyzes nitration of tyrosines by peroxynitrite in the rod and head domains of neurofilament-L. J Neurochem 69, 1945-1953.

Dai, C., and Gu, W. (2010). p53 post-translational modification: deregulated in tumorigenesis. Trends in molecular medicine 16, 528-536.

Dang, C.V. (2010). Glutaminolysis: supplying carbon or nitrogen or both for cancer cells? Cell Cycle 9, 3884-3886.

Dang, C.V., and Lee, W.M. (1989). Nuclear and nucleolar targeting sequences of c-erb-A, c-myb, N-myc, p53, HSP70, and HIV tat proteins. J Biol Chem 264, 18019-18023.

Dash, P.R., Cartwright, J.E., Baker, P.N., Johnstone, A.P., and Whitley, G.S. (2003). Nitric oxide protects human extravillous trophoblast cells from apoptosis

by a cyclic GMP-dependent mechanism and independently of caspase 3 nitrosylation. Experimental cell research 287, 314-324.

de Oca Luna, R.M., Tabor, A.D., Eberspaecher, H., Hulboy, D.L., Worth, L.L., Colman, M.S., Finlay, C.A., and Lozano, G. (1996). The organization and expression of the mdm2 gene. Genomics 33, 352-357.

Delphin, C., Huang, K.P., Scotto, C., Chapel, A., Vincon, M., Chambaz, E., Garin, J., and Baudier, J. (1997). The in vitro phosphorylation of p53 by calcium-dependent protein kinase C--characterization of a protein-kinase-C-binding site on p53. European journal of biochemistry / FEBS 245, 684-692.

Deng, C., Zhang, P., Harper, J.W., Elledge, S.J., and Leder, P. (1995). Mice lacking p21CIP1/WAF1 undergo normal development, but are defective in G1 checkpoint control. Cell 82, 675-684.

Derksen, P.W., Liu, X., Saridin, F., van der Gulden, H., Zevenhoven, J., Evers, B., van Beijnum, J.R., Griffioen, A.W., Vink, J., Krimpenfort, P., et al. (2006). Somatic inactivation of E-cadherin and p53 in mice leads to metastatic lobular mammary carcinoma through induction of anoikis resistance and angiogenesis. Cancer Cell 10, 437-449.

Deyoung MP, E.L. (2007). p63 and p73 in human cancer: defining the network. Oncogene 2007 26, 5169-5183.

Di Agostino, S., Cortese, G., Monti, O., Dell'Orso, S., Sacchi, A., Eisenstein, M., Citro, G., Strano, S., and Blandino, G. (2008). The disruption of the protein complex mutantp53/p73 increases selectively the response of tumor cells to anticancer drugs. Cell Cycle 7, 3440-3447.

Dias, C.S., Liu, Y., Yau, A., Westrick, L., and Evans, S.C. (2006). Regulation of hdm2 by stress-induced hdm2alt1 in tumor and nontumorigenic cell lines correlating with p53 stability. Cancer research 66, 9467-9473.

Ding, Q., Zhang, Z., Liu, J.J., Jiang, N., Zhang, J., Ross, T.M., Chu, X.J., Bartkovitz, D., Podlaski, F., Janson, C., et al. (2013). Discovery of RG7388, a potent and selective p53-MDM2 inhibitor in clinical development. J Med Chem 56, 5979-5983.

Donehower, L.A., Harvey, M., Slagle, B.L., McArthur, M.J., Montgomery, C.A., Jr., Butel, J.S., and Bradley, A. (1992). Mice deficient for p53 are developmentally normal but susceptible to spontaneous tumours. Nature 356, 215-221.

Donehower, L.A., Harvey, M., Vogel, H., McArthur, M.J., Montgomery, C.A., Jr., Park, S.H., Thompson, T., Ford, R.J., and Bradley, A. (1995). Effects of genetic background on tumorigenesis in p53-deficient mice. Molecular carcinogenesis 14, 16-22.

Dong, P., Karaayvaz, M., Jia, N., Kaneuchi, M., Hamada, J., Watari, H., Sudo, S., Ju, J., and Sakuragi, N. (2013). Mutant p53 gain-of-function induces epithelial-mesenchymal transition through modulation of the miR-130b-ZEB1 axis. Oncogene 2013 Jul 4;32(27):3286-95.

Dong, P., Xu, Z., Jia, N., Li, D., and Feng, Y. (2009). Elevated expression of p53 gain-of-function mutation R175H in endometrial cancer cells can increase the invasive phenotypes by activation of the EGFR/PI3K/AKT pathway. Mol Cancer 8, 1476-4598.

D'Orazi, G., Cecchinelli, B., Bruno, T., Manni, I., Higashimoto, Y., Saito, S., Gostissa, M., Coen, S., Marchetti, A., Del Sal, G., et al. (2002). Homeodomain-interacting protein kinase-2 phosphorylates p53 at Ser 46 and mediates apoptosis. Nat Cell Biol 4, 11-19.

Dornan, D., Shimizu, H., Perkins, N.D., and Hupp, T.R. (2003). DNA-dependent acetylation of p53 by the transcription coactivator p300. The Journal of biological chemistry 278, 13431-13441.

Dubendorff, J.W., and Studier, F.W. (1991). Controlling basal expression in an inducible T7 expression system by blocking the target T7 promoter with lac repressor. J Mol Biol 219, 45-59.

Dumaz, N., and Meek, D.W. (1999). Serine15 phosphorylation stimulates p53 transactivation but does not directly influence interaction with HDM2. The EMBO journal 18, 7002-7010.

Dumont, P., Leu, J.I., Della Pietra, A.C., 3rd, George, D.L., and Murphy, M. (2003). The codon 72 polymorphic variants of p53 have markedly different apoptotic potential. Nature genetics 33, 357-365.

Dutta, A., Ruppert, J.M., Aster, J.C., and Winchester, E. (1993). Inhibition of DNA replication factor RPA by p53. Nature 365, 79-82.

Eizirik, D.L., Delaney, C.A., Green, M.H., Cunningham, J.M., Thorpe, J.R., Pipeleers, D.G., Hellerstrom, C., and Green, I.C. (1996). Nitric oxide donors decrease the function and survival of human pancreatic islets. Molecular and cellular endocrinology 118, 71-83.

el-Deiry, W.S., Kern, S.E., Pietenpol, J.A., Kinzler, K.W., and Vogelstein, B. (1992). Definition of a consensus binding site for p53. Nat Genet 1, 45-49.

el-Deiry, W.S., Tokino, T., Velculescu, V.E., Levy, D.B., Parsons, R., Trent, J.M., Lin, D., Mercer, W.E., Kinzler, K.W., and Vogelstein, B. (1993). WAF1, a potential mediator of p53 tumor suppression. Cell 75, 817-825.

Elenbaas, B., Dobbelstein, M., Roth, J., Shenk, T., and Levine, A.J. (1996). The MDM2 oncoprotein binds specifically to RNA through its RING finger domain. Mol Med 2, 439-451.

Eliyahu, D., Michalovitz, D., Eliyahu, S., Pinhasi-Kimhi, O., and Oren, M. (1989). Wild-type p53 can inhibit oncogene-mediated focus formation. Proc Natl Acad Sci U S A 86, 8763-8767.

Eliyahu, D., Raz, A., Gruss, P., Givol, D., and Oren, M. (1984). Participation of p53 cellular tumour antigen in transformation of normal embryonic cells. Nature 312, 646-649.

el-Remessy AB, B.M., Platt DH, Fulton D, Caldwell RB. (2005). Oxidative stress inactivates VEGF survival signaling in retinal endothelial cells via PI 3-kinase tyrosine nitration. J Cell Sci 118, 243-252.

Fabbro, M., and Henderson, B.R. (2003). Regulation of tumor suppressors by nuclear-cytoplasmic shuttling. Experimental Cell Research 282, 59–69.

Fang, S., Jensen, J.P., Ludwig, R.L., Vousden, K.H., and Weissman, A.M. (2000). Mdm2 is a RING finger-dependent ubiquitin protein ligase for itself and p53. J Biol Chem 275, 8945-8951.

Fang, X., Feng, Y., Wang, J., and Dai, J. (2010). Perfluorononanoic acid-induced apoptosis in rat spleen involves oxidative stress and the activation of caspase-independent death pathway. Toxicology 267, 54-59.

Feng, Z., Zhang, H., Levine, A.J., and Jin, S. (2005). The coordinate regulation of the p53 and mTOR pathways in cells. Proceedings of the National Academy of Sciences of the United States of America 102, 8204-8209.

Finch, R.A., Donoviel, D.B., Potter, D., Shi, M., Fan, A., Freed, D.D., Wang, C.Y., Zambrowicz, B.P., Ramirez-Solis, R., Sands, A.T., et al. (2002). mdmx is a negative regulator of p53 activity in vivo. Cancer research 62, 3221-3225.

Finlan, L., and Hupp, T.R. (2004). The N-terminal interferon-binding domain (IBiD) homology domain of p300 binds to peptides with homology to the p53 transactivation domain. The Journal of biological chemistry 279, 49395-49405.

Flores, E.R., Sengupta, S., Miller, J.B., Newman, J.J., Bronson, R., Crowley, D., Yang, A., McKeon, F., and Jacks, T. (2005). Tumor predisposition in mice mutant for p63 and p73: evidence for broader tumor suppressor functions for the p53 family. Cancer cell 7, 363-373.

Flores, E.R., Tsai, K.Y., Crowley, D., Sengupta, S., Yang, A., McKeon, F., and Jacks, T. (2002). p63 and p73 are required for p53-dependent apoptosis in response to DNA damage. Nature 416, 560-564.

Fogal, V., Gostissa, M., Sandy, P., Zacchi, P., Sternsdorf, T., Jensen, K., Pandolfi, P.P., Will, H., Schneider, C., and Del Sal, G. (2000). Regulation of p53 activity in nuclear bodies by a specific PML isoform. Embo J 19, 6185-6195.

Forrester, K., Ambs, S., Lupold, S.E., Kapust, R.B., Spillare, E.A., Weinberg, W.C., Felley-Bosco, E., Wang, X.W., Geller, D.A., Tzeng, E., et al. (1996). Nitric oxide-induced p53 accumulation and regulation of inducible nitric oxide synthase expression by wild-type p53. Proc Natl Acad Sci U S A 93, 2442-2447.

Freedman, D.A., and Levine, A.J. (1998). Nuclear export is required for degradation of endogenous p53 by MDM2 and human papillomavirus E6. Mol Cell Biol 18, 7288-7293.

Friedlander, P., Haupt, Y., Prives, C., and Oren, M. (1996). A mutant p53 that discriminates between p53-responsive genes cannot induce apoptosis. Mol Cell Biol 16, 4961-4971.

Friedman, P.N., Chen, X., Bargonetti, J., and Prives, C. (1993). The p53 protein is an unusually shaped tetramer that binds directly to DNA. Proceedings of the National Academy of Sciences of the United States of America 90, 3319-3323.

Fu, L., Minden, M.D., and Benchimol, S. (1996). Translational regulation of human p53 gene expression. Embo J 15, 4392-4401.

Fu, T., Min, H., Xu, Y., Chen, J., and Li, G.(2012). Molecular dynamic simulation insights into the normal state and restoration of p53 function. Int. J. Mol. Sci. 13, 9709-9740.

Fuchs, S.Y., Adler, V., Buschmann, T., Wu, X., and Ronai, Z. (1998). Mdm2 association with p53 targets its ubiquitination. Oncogene 17, 2543-2547.

Gaiddon, C., Lokshin, M., Ahn, J., Zhang, T., and Prives, C. (2001). A subset of tumor-derived mutant forms of p53 down-regulate p63 and p73 through a direct interaction with the p53 core domain. Mol Cell Biol 21, 1874-1887.

Galleno, M., and Sick, A.J. (1999). Baculovirus expression vector system. In Gene expression systems, J.M. Fernandez, and J.P. Hoeffler, eds. (California, Academic Press), pp. 331-363.

Gannon, H.S., Woda, B.A., and Jones, S.N. (2012). ATM phosphorylation of Mdm2 Ser394 regulates the amplitude and duration of the DNA damage response in mice. Cancer Cell 21, 668-679.

Garcia, P.B., and Attardi, L.D. (2014). Illuminating p53 function in cancer with genetically engineered mouse models. Semin Cell Dev Biol 27, 74-85.

Gatti, A., Li, H.H., Traugh, J.A., and Liu, X. (2000). Phosphorylation of human p53 on Thr-55. Biochemistry 39, 9837-9842.

Georgiou, G., and Valax, P. (1996). Expression of correctly folded proteins in Escherichia coli. Curr Opin Biotechnol 7, 190-197.

Ghosh, A., Stewart, D., and Matlashewski, G. (2004). Regulation of human p53 activity and cell localization by alternative splicing. Molecular and cellular biology 24, 7987-7997.

Giaccia, A.J., and Kastan, M.B. (1998). The complexity of p53 modulation: emerging patterns from divergent signals. Genes Dev 12, 2973-2983.

Giono, L.E., and Manfredi, J.J. (2006). The p53 tumor suppressor participates in multiple cell cycle checkpoints. J Cell Physiol 209, 13-20.

Goh, A.M., Coffill, C.R., and Lane, D.P. (2011). The role of mutant p53 in human cancer. J Pathol 223, 116-126.

Goldberg, Z., Vogt Sionov, R., Berger, M., Zwang, Y., Perets, R., Van Etten, R.A., Oren, M., Taya, Y., and Haupt, Y. (2002). Tyrosine phosphorylation of Mdm2 by c-Abl: implications for p53 regulation. The EMBO journal 21, 3715-3727.

Good, P.F., Werner, P., Hsu, A., Olanow, C.W., and Perl, D.P. (1996). Evidence of neuronal oxidative damage in Alzheimer's disease. Am J Pathol 149, 21-28.

Goodman, J.E., Hofseth, L.J., Hussain, S.P., and Harris, C.C. (2004). Nitric oxide and p53 in cancer-prone chronic inflammation and oxyradical overload disease. Environ Mol Mutagen 44, 3-9.

Goodwin, D.C., Gunther, M.R., Hsi, L.C., Crews, B.C., Eling, T.E., Mason, R.P., and Marnett, L.J. (1998). Nitric oxide trapping of tyrosyl radicals generated during prostaglandin endoperoxide synthase turnover. Detection of the radical derivative of tyrosine 385. The Journal of biological chemistry 273, 8903-8909.

Gostissa, M., Hengstermann, A., Fogal, V., Sandy, P., Schwarz, S.E., Scheffner, M., and Del Sal, G. (1999). Activation of p53 by conjugation to the ubiquitin-like protein SUMO-1. Embo J 18, 6462-6471.

Gottlieb, T.M., Leal, J.F., Seger, R., Taya, Y., and Oren, M. (2002). Cross-talk between Akt, p53 and Mdm2: possible implications for the regulation of apoptosis. Oncogene 21, 1299-1303.

Goudelock DM, J.K., Pereira E, Russell B, Sanchez Y (2003). Regulatory interactions between the checkpoint kinase Chk1 and the proteins of the DNA-dependent protein kinase complex. J Biol Chem 278, 29940-29947.

Gow, A., Duran, D., Thom, S.R., and Ischiropoulos, H. (1996). Carbon dioxide enhancement of peroxynitrite-mediated protein tyrosine nitration. Arch Biochem Biophys 333, 42-48.

Gow, A.J., Duran, D., Malcolm, S., and Ischiropoulos, H. (1996). Effects of peroxynitrite-induced protein modifications on tyrosine phosphorylation and degradation. FEBS Lett 385, 63-66.

Green, D. R. (2006). At the gates of death. Cancer Cell 9, 328–330.

Green, D.R., and Kroemer, G. (2009). Cytoplasmic functions of the tumour suppressor p53. Nature 458, 1127-1130.

Greenarce SA, I.H. (2001). Tyrosine nitration: localisation, quantification, consequences for protein function and signal transduction. Free Radic Res 34, 541-581.

Greenblatt, M.S., Bennett, W.P., Hollstein, M., and Harris, C.C. (1994). Mutations in the p53 tumor suppressor gene: clues to cancer etiology and molecular pathogenesis. Cancer Res 54, 4855-4878.

Grossman, S.R., Deato, M.E., Brignone, C., Chan, H.M., Kung, A.L., Tagami, H., Nakatani, Y., and Livingston, D.M. (2003). Polyubiquitination of p53 by a ubiquitin ligase activity of p300. Science 300, 342-344.

Grossman, S.R., Perez, M., Kung, A.L., Joseph, M., Mansur, C., Xiao, Z.X., Kumar, S., Howley, P.M., and Livingston, D.M. (1998). p300/MDM2 complexes participate in MDM2-mediated p53 degradation. Molecular cell 2, 405-415.

Gu, J., Kawai, H., Nie, L., Kitao, H., Wiederschain, D., Jochemsen, A.G., Parant, J., Lozano, G., and Yuan, Z.M. (2002). Mutual dependence of MDM2 and MDMX in their functional inactivation of p53. J Biol Chem 277, 19251-19254.

Gu, W., and Roeder, R.G. (1997). Activation of p53 sequence-specific DNA binding by acetylation of the p53 C-terminal domain. Cell 90, 595-606.

Gu, X., P.J. Coates, L. Boldrup, and K. Nylander (2008). p63 contributes to cell invasion and migration in squamous cell carcinoma of the head and neck. Cancer Letter 263, 26-34.

Gunther, M.R., Hsi, L.C., Curtis, J.F., Gierse, J.K., Marnett, L.J., Eling, T.E., and Mason, R.P. (1997). Nitric oxide trapping of the tyrosyl radical of prostaglandin H synthase-2 leads to tyrosine iminoxyl radical and nitrotyrosine formation. The Journal of biological chemistry 272, 17086-17090.

Guo, A., Salomoni, P., Luo, J., Shih, A., Zhong, S., Gu, W., and Pandolfi, P.P. (2000). The function of PML in p53-dependent apoptosis. Nat Cell Biol 2, 730-736.

Hainaut P, M.J. (1993). A structural role for metal ions in the "wild-type" conformation of the tumor suppressor protein p53. Cancer research 53, 1739-1742.

Hainaut P, R.N., Davies M, Milner J. (1995). Modulation by copper of p53 conformation and sequence-specific DNA binding: role for Cu(II)/Cu(I) redox mechanism. Oncogene 2007 10, 27-32.

Hall, S.R., Campbell, L.E., and Meek, D.W. (1996). Phosphorylation of p53 at the casein kinase II site selectively regulates p53-dependent transcriptional repression but not transactivation. Nucleic Acids Res 24, 1119-1126.

Han, L., Zhang, A., Zhou, X., Xu, P., Wang, G.X., Pu, P.Y., and Kang, C.S. (2010). Downregulation of Dicer enhances tumor cell proliferation and invasion. Int J Oncol 37, 299-305.

Hanahan, D. (1983). Studies on transformation of Escherichia coli with plasmids. J Mol Biol 166, 557-580.

Hanahan, D., and Weinberg, R.A. (2011). Hallmarks of cancer: the next generation. Cell 144, 646–674.

Hannig, G., and Makrides, S.C. (1998). Strategies for optimizing heterologous protein expression in Escherichia coli. Trends Biotechnol 16, 54-60.

Harlow ED, L.D. (1988). Antibodies: A Laboratory Manual.

Harris, S.L., and Levine, A.J. (2005). The p53 pathway: positive and negative feedback loops. Oncogene 24, 2899-2908.

Haupt, Y., Maya, R., Kazaz, A., and Oren, M. (1997). Mdm2 promotes the rapid degradation of p53. Nature 387, 296-299.

Haupt, Y., Rowan, S., Shaulian, E., Vousden, K.H., and Oren, M. (1995). Induction of apoptosis in HeLa cells by trans-activation-deficient p53. Genes Dev 9, 2170-2183.

Hay, T.J., and Meek, D.W. (2000). Multiple sites of in vivo phosphorylation in the MDM2 oncoprotein cluster within two important functional domains. FEBS Lett 478, 183-186.

He, Z., Brinton, B.T., Greenblatt, J., Hassell, J.A., and Ingles, C.J. (1993). The transactivator proteins VP16 and GAL4 bind replication factor A. Cell 73, 1223-1232.

Hellberg CB, B.S., Lapetina EG (1998). Phosphatidylinositol 3-kinase is a target for protein tyrosine nitration. Biochemical and biophysical research communications 252, 313-317.

Helton, E.S., and Chen, X. (2007). p53 modulation of the DNA damage response. Journal of cellular biochemistry 100, 883-896.

Henry, Y., Lepoivre, M., Drapier, J.C., Ducrocq, C., Boucher, J.L., and Guissani, A. (1993). EPR characterization of molecular targets for NO in mammalian cells and organelles. FASEB J 7, 1124-1134.

Hermeking, H., Lengauer, C., Polyak, K., He, T.C., Zhang, L., Thiagalingam, S., Kinzler, K.W., and Vogelstein, B. (1997). 14-3-3 sigma is a p53-regulated inhibitor of G2/M progression. Mol Cell 1, 3-11.

Herrmann, C.P., Kraiss, S., and Montenarh, M. (1991). Association of casein kinase II with immunopurified p53. Oncogene 6, 877-884.

Higashimoto, Y., Saito, S., Tong, X.H., Hong, A., Sakaguchi, K., Appella, E., and Anderson, C.W. (2000). Human p53 is phosphorylated on serines 6 and 9 in response to DNA damage-inducing agents. The Journal of biological chemistry 275, 23199-23203.

Hirao, A., Kong, Y.Y., Matsuoka, S., Wakeham, A., Ruland, J., Yoshida, H., Liu, D., Elledge, S.J., and Mak, T.W. (2000). DNA damage-induced activation of p53 by the checkpoint kinase Chk2. Science 287, 1824-1827.

Hjerrild M, M.D., Dumaz N, Hay T, Issinger OG, Meek D (2001). Phosphorylation of murine double minute clone 2 (MDM2) protein at serine-267 by protein kinase CK2 in vitro and in cultured cells. Biochem J 355, 347-356.

Ho, Y.S., Wang, Y.J., and Lin, J.K. (1996). Induction of p53 and p21/WAF1/CIP1 expression by nitric oxide and their association with apoptosis in human cancer cells. Molecular carcinogenesis 16, 20-31.

Hoffman, W.H., Biade, S., Zilfou, J.T., Chen, J., and Murphy, M. (2002). Transcriptional repression of the anti-apoptotic survivin gene by wild type p53. The Journal of biological chemistry 277, 3247-3257.

Hofseth, L.J., Saito, S., Hussain, S.P., Espey, M.G., Miranda, K.M., Araki, Y., Jhappan, C., Higashimoto, Y., He, P., Linke, S.P., et al. (2003). Nitric oxide-induced cellular stress and p53 activation in chronic inflammation. Proc Natl Acad Sci U S A 100, 143-148.

Hollstein, M., Sidransky, D., Vogelstein, B., and Harris, C.C. (1991). p53 mutations in human cancers. Science 253, 49-53.

Honda, R., Tanaka, H., and Yasuda, H. (1997). Oncoprotein MDM2 is a ubiquitin ligase E3 for tumor suppressor p53. FEBS Lett 420, 25-27.

Honda, R., and Yasuda, H. (1999). Association of p19(ARF) with Mdm2 inhibits ubiquitin ligase activity of Mdm2 for tumor suppressor p53. Embo J 18, 22-27.

Hu, M.C., Qiu, W.R., and Wang, Y.P. (1997). JNK1, JNK2 and JNK3 are p53 N-terminal serine 34 kinases. Oncogene 15, 2277-2287.

Hu, W., Feng, Z., and Levine, A.J. (2012). The regulation of multiple p53 stress responses is mediated through MDM2. Genes & Cancer 3, 199–208.

Hu, W., Zhang, C., Wu, R., Sun, Y., Levine, A., and Feng, Z. (2010). Glutaminase 2, a novel p53 target gene regulating energy metabolism and antioxidant function. Proc Natl Acad Sci U S A 107, 7455-7460.

Huang, J., Dorsey, J., Chuikov, S., Perez-Burgos, L., Zhang, X., Jenuwein, T., Reinberg, D., and Berger, S.L. (2010). G9a and Glp methylate lysine 373 in the tumor suppressor p53. The Journal of biological chemistry 285, 9636-9641.

Huang, J., Perez-Burgos, L., Placek, B.J., Sengupta, R., Richter, M., Dorsey, J.A., Kubicek, S., Opravil, S., Jenuwein, T., and Berger, S.L. (2006). Repression of p53 activity by Smyd2-mediated methylation. Nature 444, 629-632.

Huang, J., Sengupta, R., Espejo, A.B., Lee, M.G., Dorsey, J.A., Richter, M., Opravil, S., Shiekhattar, R., Bedford, M.T., Jenuwein, T., et al. (2007). p53 is regulated by the lysine demethylase LSD1. Nature 449, 105-108.

Huhmer, A.F., Nishida, C.R., Ortiz de Montellano, P.R., and Schoneich, C. (1997). Inactivation of the inducible nitric oxide synthase by peroxynitrite. Chemical research in toxicology 10, 618-626.

Hupp, T.R., and Lane, D.P. (1994). Allosteric activation of latent p53 tetramers. Curr Biol 1994 Oct 1;4(10):865-75.

Hupp, T.R., and Lane, D.P. (1995). Two distinct signaling pathways activate the latent DNA binding function of p53 in a casein kinase II-independent manner. J Biol Chem 270, 18165-18174.

Hupp, T.R., Meek, D.W., Midgley, C.A., and Lane, D.P. (1992). Regulation of the specific DNA binding function of p53. Cell 71, 875-886.

Hupp, T.R., Meek, D.W., Midgley, C.A., and Lane, D.P. (1993). Activation of the cryptic DNA binding function of mutant forms of p53. Nucleic Acids Res 21, 3167-3174.

Hupp, T.R., Sparks, A., and Lane, D.P. (1995). Small peptides activate the latent sequence-specific DNA binding function of p53. Cell 83, 237-245.

Hussain, S.P., Hofseth, L.J., and Harris, C.C. (2003). Radical causes of cancer. Nat Rev Cancer 3, 276-285.

Hussain, S.P., Trivers, G.E., Hofseth, L.J., He, P., Shaikh, I., Mechanic, L.E., Doja, S., Jiang, W., Subleski, J., Shorts, L., et al. (2004). Nitric oxide, a mediator of inflammation, suppresses tumorigenesis. Cancer Res 64, 6849-6853.

Ide, T., Brown-Endres, L., Chu, K., Ongusaha, P.P., Ohtsuka, T., El-Deiry, W.S., Aaronson, S.A., and Lee, S.W. (2009). GAMT, a p53-inducible modulator of apoptosis, is critical for the adaptive response to nutrient stress. Molecular cell 36, 379-392.

Ignarro, L.J., Buga, G.M., Wood, K.S., Byrns, R.E., and Chaudhuri, G. (1987). Endothelium-derived relaxing factor produced and released from artery and vein is nitric oxide. Proceedings of the National Academy of Sciences of the United States of America 84, 9265-9269.

Ignarro, L.J., Byrns, R.E., Buga, G.M., and Wood, K.S. (1987). Endothelium-derived relaxing factor from pulmonary artery and vein possesses pharmacologic and chemical properties identical to those of nitric oxide radical. Circulation research 61, 866-879.

Ikemura, T. (1981). Correlation between the abundance of Escherichia coli transfer RNAs and the occurrence of the respective codons in its protein genes: a proposal for a synonymous codon choice that is optimal for the E. coli translational system. J Mol Biol 151, 389-409.

Ischiropoulos, H. (1998). Biological tyrosine nitration: a pathophysiological function of nitric oxide and reactive oxygen species. Arch Biochem Biophys 356, 1-11.

Ischiropoulos, H., and al-Mehdi, A.B. (1995). Peroxynitrite-mediated oxidative protein modifications. FEBS letters 364, 279-282.

Ischiropoulos, H., Zhu, L., Chen, J., Tsai, M., Martin, J.C., Smith, C.D., and Beckman, J.S. (1992). Peroxynitrite-mediated tyrosine nitration catalyzed by superoxide dismutase. Arch Biochem Biophys 298, 431-437.

Ish-Horowicz, D., and Burke, J.F. (1981). Rapid and efficient cosmid cloning. Nucleic Acids Res 9, 2989-2998.

Ito, A., Kawaguchi, Y., Lai, C.H., Kovacs, J.J., Higashimoto, Y., Appella, E., and Yao, T.P. (2002). MDM2-HDAC1-mediated deacetylation of p53 is required for its degradation. The EMBO journal 21, 6236-6245.

Ito, A., Lai, C.H., Zhao, X., Saito, S., Hamilton, M.H., Appella, E., and Yao, T.P. (2001). p300/CBP-mediated p53 acetylation is commonly induced by p53-activating agents and inhibited by MDM2. Embo J 20, 1331-1340.

Ivanov, G.S., Ivanova, T., Kurash, J., Ivanov, A., Chuikov, S., Gizatullin, F., Herrera-Medina, E.M., Rauscher, F., 3rd, Reinberg, D., and Barlev, N.A. (2007). Methylation-acetylation interplay activates p53 in response to DNA damage. Molecular and cellular biology 27, 6756-6769.

Jackson, J.G., and Lozano, G. (2013). The mutant p53 mouse as a pre-clinical model. Oncogene 32, 4325-4330.

Jackson, M.W., and Berberich, S.J. (2000). MdmX protects p53 from Mdm2-mediated degradation. Molecular and cellular biology 20, 1001-1007.

Jansson, M., Durant, S.T., Cho, E.C., Sheahan, S., Edelmann, M., Kessler, B., and La Thangue, N.B. (2008). Arginine methylation regulates the p53 response. Nature cell biology 10, 1431-1439.

Jayaraman, J., and Prives, C. (1995). Activation of p53 sequence-specific DNA binding by short single strands of DNA requires the p53 C-terminus. Cell 81, 1021-1029.

Jayaraman, L., and Prives, C. (1999). Covalent and noncovalent modifiers of the p53 protein. Cellular and molecular life sciences : CMLS 55, 76-87.

Jeffers, J.R., Parganas, E., Lee, Y., Yang, C., Wang, J., Brennan, J., MacLean, K.H., Han, J., Chittenden, T., Ihle, J.N., et al. (2003). Puma is an essential mediator of p53-dependent and -independent apoptotic pathways. Cancer cell 4, 321-328.

Jeffrey, P.D., Gorina, S., and Pavletich, N.P. (1995). Crystal structure of the tetramerization domain of the p53 tumor suppressor at 1.7 angstroms. Science 267, 1498-1502.

Jenkins, J.R., Rudge, K., and Currie, G.A. (1984). Cellular immortalization by a cDNA clone encoding the transformation- associated phosphoprotein p53. Nature 312, 651-654.

Jensen, M.D. (2003). Fate of fatty acids at rest and during exercise: regulatory mechanisms. Acta Physiol Scand 178, 385-390.

Jiang, D., Brady, C.A., Johnson, T.M., Lee, E.Y., Park, E.J., Scott, M.P., and Attardi, L.D. (2011). Full p53 transcriptional activation potential is dispensable for tumor suppression in diverse lineages. Proc Natl Acad Sci U S A 108, 17123-17128.

Johnson, T.M., and Attardi, L.D. (2006). Dissecting p53 tumor suppressor function in vivo through the analysis of genetically modified mice. Cell death and differentiation 13, 902-908.

Johnson, T.M., Hammond, E.M., Giaccia, A., and Attardi, L.D. (2005). The p53QS transactivation-deficient mutant shows stress-specific apoptotic activity and induces embryonic lethality. Nature genetics 37, 145-152.

Jones, L.H. (2012). Chemistry and biology of biomolecule nitration. Chem Biol 19, 1086-1092.

Jones, R.G., Plas, D.R., Kubek, S., Buzzai, M., Mu, J., Xu, Y., Birnbaum, M.J., and Thompson, C.B. (2005). AMP-activated protein kinase induces a p53-dependent metabolic checkpoint. Molecular cell 18, 283-293.

Jones, S.N., Roe, A.E., Donehower, L.A., and Bradley, A. (1995). Rescue of embryonic lethality in Mdm2-deficient mice by absence of p53. Nature 378, 206-208.

Jost, C.A., Marin, M.C., and Kaelin, W.G., Jr. (1997). p73 is a simian [correction of human] p53-related protein that can induce apoptosis. Nature 389, 191-194.

JS., A. (2006). The role of the mitochondrial permeability transition in cell death. Mitochondrion 6, 225-234.

K, M. (2000). Tumor suppressor genes. Current Opinion in Genetics & Development 10, 81-93.

Kaghad, M., Bonnet, H., Yang, A., Creancier, L., Biscan, J.C., Valent, A., Minty, A., Chalon, P., Lelias, J.M., Dumont, X., et al. (1997). Monoallelically expressed gene related to p53 at 1p36, a region frequently deleted in neuroblastoma and other human cancers. Cell 90, 809-819.

Kane, J.F. (1995). Effects of rare codon clusters on high-level expression of heterologous proteins in Escherichia coli. Curr Opin Biotechnol 6, 494-500.

Kastan, M.B., Onyekwere, O., Sidransky, D., Vogelstein, B., and Craig, R.W. (1991). Participation of p53 protein in the cellular response to DNA damage. Cancer Res 51, 6304-6311.

Kastan, M.B., Zhan, Q., el-Deiry, W.S., Carrier, F., Jacks, T., Walsh, W.V., Plunkett, B.S., Vogelstein, B., and Fornace, A.J., Jr. (1992). A mammalian cell cycle checkpoint pathway utilizing p53 and GADD45 is defective in ataxia-telangiectasia. Cell 71, 587-597.

Kaur, H., and Halliwell, B. (1994). Evidence for nitric oxide-mediated oxidative damage in chronic inflammation. Nitrotyrosine in serum and synovial fluid from rheumatoid patients. FEBS Lett 350, 9-12.

Kawai H, L.-P.V., Kim MM, Wiederschain D, Yuan ZM (2007). RING domain-mediated interaction is a requirement for MDM2's E3 ligase activity. Cancer research 67, 6026-6030.

Kawauchi, K., Araki, K., Tobiume, K., and Tanaka, N. (2008). Activated p53 induces NF-kappaB DNA binding but suppresses its transcriptional activation. Biochem Biophys Res Commun 2008 Jul 18;372(1):137-41.

Kawauchi, K., Araki, K., Tobiume, K., and Tanaka, N. (2008). p53 regulates glucose metabolism through an IKK-NF-kappaB pathway and inhibits cell transformation. Nat Cell Biol 10, 611-618.

Keller, D.M., Zeng, X., Wang, Y., Zhang, Q.H., Kapoor, M., Shu, H., Goodman, R., Lozano, G., Zhao, Y., and Lu, H. (2001). A DNA damage-induced p53 serine 392 kinase complex contains CK2, hSpt16, and SSRP1. Molecular cell 7, 283-292.

Kessis, T.D., Slebos, R.J., Nelson, W.G., Kastan, M.B., Plunkett, B.S., Han, S.M., Lorincz, A.T., Hedrick, L., and Cho, K.R. (1993). Human papillomavirus 16

E6 expression disrupts the p53-mediated cellular response to DNA damage. Proc Natl Acad Sci U S A 90, 3988-3992.

Keyes WM, W.Y., Vogel H, Guo X, Lowe SW, Mills AA. (2005). p63 deficiency activates a program of cellular senescence and leads to accelerated aging. Genes Dev 19, 1986-1999.

Khandrika, L., Kumar, B., Koul, S., Maroni, P., and Koul, H.K. (2009). Oxidative stress in prostate cancer. Cancer letters 282, 125-136.

Khanna, K.K., Keating, K.E., Kozlov, S., Scott, S., Gatei, M., Hobson, K., Taya, Y., Gabrielli, B., Chan, D., Lees-Miller, S.P., et al. (1998). ATM associates with and phosphorylates p53: mapping the region of interaction. Nature genetics 20, 398-400.

Khoo, K.H., Verma, C.S., and Lane, D.P. (2014). Drugging the p53 pathway: understanding the route to clinical efficacy. Nat Rev Drug Discov 13, 217-236.

Khoury, M.P., and Bourdon, J.C. (2010). The isoforms of the p53 protein. Cold Spring Harbor perspectives in biology 2.

Khoury, K., Popowicz, G.M., Holak, T.A., and Dömling, A. (2011). The p53 MDM2/MDMX axis – A chemotype perspective. Medchemcomm 2, 246–260.

Kim, E., and Deppert, W. (2006). The versatile interactions of p53 with DNA: when flexibility serves specificity. Cell Death Differ 13, 885–9.

Knights, C.D., Catania, J., Di Giovanni, S., Muratoglu, S., Perez, R., Swartzbeck, A., Quong, A.A., Zhang, X., Beerman, T., Pestell, R.G., et al. (2006). Distinct p53 acetylation cassettes differentially influence gene-expression patterns and cell fate. The Journal of cell biology 173, 533-544.

Knippschild, U., Milne, D.M., Campbell, L.E., DeMaggio, A.J., Christenson, E., Hoekstra, M.F., and Meek, D.W. (1997). p53 is phosphorylated in vitro and in vivo by the delta and epsilon isoforms of casein kinase 1 and enhances the level of casein kinase 1 delta in response to topoisomerase-directed drugs. Oncogene 15, 1727-1736.

Ko, L.J., and Prives, C. (1996). p53: puzzle and paradigm. Genes Dev 10, 1054-1072.

Ko, L.J., Shieh, S.Y., Chen, X., Jayaraman, L., Tamai, K., Taya, Y., Prives, C., and Pan, Z.Q. (1997). p53 is phosphorylated by CDK7-cyclin H in a p36MAT1-dependent manner. Mol Cell Biol 17, 7220-7229.

Kobet, E., Zeng, X., Zhu, Y., Keller, D., and Lu, H. (2000). MDM2 inhibits p300-mediated p53 acetylation and activation by forming a ternary complex with the two proteins. Proc Natl Acad Sci U S A 97, 12547-12552.

Kong, S.K., Yim, M.B., Stadtman, E.R., and Chock, P.B. (1996). Peroxynitrite disables the tyrosine phosphorylation regulatory mechanism: Lymphocyte-specific tyrosine kinase fails to phosphorylate nitrated cdc2(6-20)NH2 peptide. Proc Natl Acad Sci U S A 93, 3377-3382.

Koppenol, W.H., Moreno, J.J., Pryor, W.A., Ischiropoulos, H., and Beckman, J.S. (1992). Peroxynitrite, a cloaked oxidant formed by nitric oxide and superoxide. Chemical research in toxicology 5, 834-842.

Korde Choudhari, S., Sridharan, G., Gadbail, A., and Poornima, V. (2012). Nitric oxide and oral cancer: a review. Oral oncology 48, 475-483.

Kracikova, M., Akiri, G., George, A., Sachidanandam, R., and Aaronson, S.A. (2013). A threshold mechanism mediates p53 cell fate decision between growth arrest and apoptosis. Cell Death Differ 20, 576-588.

Kraiss, S., Quaiser, A., Oren, M., and Montenarh, M. (1988). Oligomerization of oncoprotein p53. J Virol 62, 4737-4744.

Kroemer, G., Marino, G., and Levine, B. (2010). Autophagy and the integrated stress response. Mol Cell 2010 Oct 22;40(2):280-93.

Kruse, J.P., and Gu, W. (2008). SnapShot: p53 posttranslational modifications. Cell 133, 930-930 e931.

Kruse, J.P., and Gu, W. (2009). Modes of p53 regulation. Cell 137, 609-622.

Kubbutat, M.H., Jones, S.N., and Vousden, K.H. (1997). Regulation of p53 stability by Mdm2. Nature 387, 299-303.

Kubbutat, M.H., Ludwig, R.L., Levine, A.J., and Vousden, K.H. (1999). Analysis of the degradation function of Mdm2. Cell Growth Differ 10, 87-92.

Kubbutat, M.H., and Vousden, K.H. (1998). Keeping an old friend under control: regulation of p53 stability. Mol Med Today 4, 250-256.

Kubbutat MH, L.R., Ashcroft M, Vousden KH (1998). Regulation of Mdm2-directed degradation by the C terminus of p53. Mol Cell Biol 18, 5690-5698.

Kuerbitz, S.J., Plunkett, B.S., Walsh, W.V., and Kastan, M.B. (1992). Wild-type p53 is a cell cycle checkpoint determinant following irradiation. Proc Natl Acad Sci U S A 89, 7491-7495.

Kuilman, T., Michaloglou, C., Mooi, W.J., and Peeper, D.S. (2010). The essence of senescence. Genes & development 24, 2463-2479.

Kumar, M.S., Pester, R.E., Chen, C.Y., Lane, K., Chin, C., Lu, J., Kirsch, D.G., Golub, T.R., and Jacks, T. (2009). Dicer1 functions as a haploinsufficient tumor suppressor. Genes Dev 23, 2700-2704.

Kumari, S.R., Mendoza-Alvarez, H., and Alvarez-Gonzalez, R. (1998). Functional interactions of p53 with poly(ADP-ribose) polymerase (PARP) during apoptosis following DNA damage: covalent poly(ADP-ribosyl)ation of p53 by exogenous PARP and noncovalent binding of p53 to the M(r) 85,000 proteolytic fragment. Cancer Res 58, 5075-5078.

Kurash, J.K., Lei, H., Shen, Q., Marston, W.L., Granda, B.W., Fan, H., Wall, D., Li, E., and Gaudet, F. (2008). Methylation of p53 by Set7/9 mediates p53 acetylation and activity in vivo. Molecular cell 29, 392-400.

Kussie, P.H., Gorina, S., Marechal, V., Elenbaas, B., Moreau, J., Levine, A.J., and Pavletich, N.P. (1996). Structure of the MDM2 oncoprotein bound to the p53 tumor suppressor transactivation domain. Science 274, 948-953.

Lambert, P.F., Kashanchi, F., Radonovich, M.F., Shiekhattar, R., and Brady, J.N. (1998). Phosphorylation of p53 serine 15 increases interaction with CBP. The Journal of biological chemistry 273, 33048-33053.

Lancaster, J.R., Jr. (1994). Simulation of the diffusion and reaction of endogenously produced nitric oxide. Proc Natl Acad Sci U S A 91, 8137-8141.

Lane, D.P. (1992). Cancer. p53, guardian of the genome. Nature 358, 15-16.

Lane, D.P., and Crawford, L.V. (1979). T antigen is bound to a host protein in SV40-transformed cells. Nature 278, 261-263.

Lane, K.H.V.a.D.P. (2007). p53 in health and disease. Nature Molecular Cell Biology 8, 275-283.

Lang, G.A., Iwakuma, T., Suh, Y.A., Liu, G., Rao, V.A., Parant, J.M., Valentin-Vega, Y.A., Terzian, T., Caldwell, L.C., Strong, L.C., et al. (2004). Gain of function of a p53 hot spot mutation in a mouse model of Li-Fraumeni syndrome. Cell 119, 861-872.

Lechner, M., Lirk, P., and Rieder, J. (2005). Inducible nitric oxide synthase (iNOS) in tumor biology: the two sides of the same coin. Seminars in cancer biology 15, 277-289.

Lee, H.O., Lee, J.H., Choi, E., Seol, J.Y., Yun, Y., and Lee, H. (2006). A dominant negative form of p63 inhibits apoptosis in a p53-independent manner. Biochem Biophys Res Commun 2006 May 26;344(1):166-72 Epub 2006 Apr 17.

Lee, J.T., and Gu, W. (2010). The multiple levels of regulation by p53 ubiquitination. Cell Death Differ 17, 86-92.

Lee, S.J., Kim, D.C., Choi, B.H., Ha, H., and Kim, K.T. (2006). Regulation of p53 by activated protein kinase C-delta during nitric oxide-induced dopaminergic cell death. The Journal of biological chemistry 281, 2215-2224.

Lees-Miller, S.P., Chen, Y.R., and Anderson, C.W. (1990). Human cells contain a DNA-activated protein kinase that phosphorylates simian virus 40 T antigen, mouse p53, and the human Ku autoantigen. Mol Cell Biol 10, 6472-6481.

Lees-Miller, S.P., Sakaguchi, K., Ullrich, S.J., Appella, E., and Anderson, C.W. (1992). Human DNA-activated protein kinase phosphorylates serines 15 and 37 in the amino-terminal transactivation domain of human p53. Mol Cell Biol 12, 5041-5049.

Leng, R.P., Lin, Y., Ma, W., Wu, H., Lemmers, B., Chung, S., Parant, J.M., Lozano, G., Hakem, R., and Benchimol, S. (2003). Pirh2, a p53-induced ubiquitin-protein ligase, promotes p53 degradation. Cell 112, 779-791.

Lenos, K., and Jochemsen, A.G. (2011). Functions of MDMX in the modulation of the p53-response. Journal of biomedicine & biotechnology 2011, 876173.

Leon, L., Jeannin, J.F., and Bettaieb, A. (2008). Post-translational modifications induced by nitric oxide (NO): implication in cancer cells apoptosis. Nitric Oxide 19, 77-83.

Leroy, B., Fournier, J.L., Ishioka, C., Monti, P., Inga, A., Fronza, G., and Soussi, T. (2013). The TP53 website: an integrative resource centre for the TP53 mutation database and TP53 mutant analysis. Nucleic Acids Res 41, 17.

Leu, J.I., Dumont, P., Hafey, M., Murphy, M.E., and George, D.L. (2004). Mitochondrial p53 activates Bak and causes disruption of a Bak-Mcl1 complex. Nature cell biology 6, 443-450.

Levine, A.J. (1997). p53, the cellular gatekeeper for growth and division. Cell 88, 323-331.

Levine, A.J., and Oren, M. (2009). The first 30 years of p53: growing ever more complex. Nat Rev Cancer 9, 749-758.

Li, H.H., Li, A.G., Sheppard, H.M., and Liu, X. (2004). Phosphorylation on Thr-55 by TAF1 mediates degradation of p53: a role for TAF1 in cell G1 progression. Molecular cell 13, 867-878.

Li, J., Billiar, T.R., Talanian, R.V., and Kim, Y.M. (1997). Nitric oxide reversibly inhibits seven members of the caspase family via S-nitrosylation. Biochem Biophys Res Commun 240, 419-424.

Li, L.M., Kilbourn, R.G., Adams, J., and Fidler, I.J. (1991). Role of nitric oxide in lysis of tumor cells by cytokine-activated endothelial cells. Cancer research 51, 2531-2535.

Li, M., Brooks, C.L., Kon, N., and Gu, W. (2004). A dynamic role of HAUSP in the p53-Mdm2 pathway. Molecular cell 13, 879-886.

Li, M., Brooks, C.L., Wu-Baer, F., Chen, D., Baer, R., and Gu, W. (2003). Mono- versus polyubiquitination: differential control of p53 fate by Mdm2. Science 302, 1972-1975.

Li, R., and Botchan, M.R. (1993). The acidic transcriptional activation domains of VP16 and p53 bind the cellular replication protein A and stimulate in vitro BPV-1 DNA replication. Cell 73, 1207-1221.

Li, R., Waga, S., Hannon, G.J., Beach, D., and Stillman, B. (1994). Differential effects by the p21 CDK inhibitor on PCNA-dependent DNA replication and repair. Nature 371, 534-537.

Li, Y.C., and Wahl, G.M. (2012). What a difference a phosphate makes: life or death decided by a single amino acid in MDM2. Cancer Cell 21, 595-596.

Liang, Y., Liu, J., and Feng, Z. (2013). The regulation of cellular metabolism by tumor suppressor p53. Cell Biosci 3, 2045-3701.

Liaudet L, V.G., Pacher P. (2009). Role of peroxynitrite in the redox regulation of cell signal transduction pathways. Front Biosci (Landmark Ed) 14, 4809-14.

Lin, J., Chen, J., Elenbaas, B., and Levine, A.J. (1994). Several hydrophobic amino acids in the p53 amino-terminal domain are required for transcriptional activation, binding to mdm-2 and the adenovirus 5 E1B 55-kD protein. Genes Dev 8, 1235-1246.

Ling Bai, W.-G.Z. (2006). p53: Structure, Function and Therapeutic Applications. J Cancer Mol, 141-153.

Linzer, D.I., and Levine, A.J. (1979). Characterization of a 54kDa cellular SV40 tumor antigen present in SV40-transformed cells and uninfected embryonal carcinoma cells. Cell 17, 43-52.

Liu, B., and Shuai, K. (2008). Regulation of the sumoylation system in gene expression. Current opinion in cell biology 20, 288-293.

Liu, D.P., Song, H., and Xu, Y. (2010). A common gain of function of p53 cancer mutants in inducing genetic instability. Oncogene 29, 949-956.

Liu, G., and Xirodimas, D.P. (2010). NUB1 promotes cytoplasmic localization of p53 through cooperation of the NEDD8 and ubiquitin pathways. Oncogene 29, 2252-2261.

Liu G, N.S., Xiao H, Chen X. (2004). DeltaNp73beta is active in transactivation and growth suppression. Mol Cell Biol 24, 487-501.

Liu, L., Scolnick, D.M., Trievel, R.C., Zhang, H.B., Marmorstein, R., Halazonetis, T.D., and Berger, S.L. (1999). p53 sites acetylated in vitro by PCAF and p300 are acetylated in vivo in response to DNA damage. Mol Cell Biol 19, 1202-1209.

Liu, X., Yue, P., Khuri, F.R., and Sun, S.Y. (2004). p53 upregulates death receptor
4 expression through an intronic p53 binding site. Cancer Res 64, 5078-5083.

Liu, Y., and Kulesz-Martin, M. (2001). p53 protein at the hub of cellular DNA damage response pathways through sequence-specific and non-sequence-specific DNA binding. Carcinogenesis 22, 851-860.

Liu, Y., Lagowski, J.P., Vanderbeek, G.E., and Kulesz-Martin, M.F. (2004). Facilitated search for specific genomic targets by p53 C-terminal basic DNA binding domain. Cancer Biol Ther 2004 Nov;3(11):1102-8 Epub 2004 Nov 24.

Lohrum, M.A., Ashcroft, M., Kubbutat, M.H., and Vousden, K.H. (2000). Contribution of two independent MDM2-binding domains in p14(ARF) to p53 stabilization. Curr Biol 10, 539-542.

Lowe, S.W., Jacks, T., Housman, D.E., and Ruley, H.E. (1994). Abrogation of oncogene-associated apoptosis allows transformation of p53-deficient cells. Proc Natl Acad Sci U S A 91, 2026-2030.

Lowe, S.W., Schmitt, E.M., Smith, S.W., Osborne, B.A., and Jacks, T. (1993). p53 is required for radiation-induced apoptosis in mouse thymocytes. Nature 362, 847-849.

Lozano, G. (2007). The oncogenic roles of p53 mutants in mouse models. Curr Opin Genet Dev 2007 Feb;17(1):66-70 Epub 2007 Jan 8.

Lozano, G., and Zambetti, G.P. (2005). What have animal models taught us about the p53 pathway? J Pathol 205, 206-220.

Lu, H., and Levine, A.J. (1995). Human TAFII31 protein is a transcriptional coactivator of the p53 protein. Proc Natl Acad Sci U S A 92, 5154-5158.

Lu, J., Getz, G., Miska, E.A., Alvarez-Saavedra, E., Lamb, J., Peck, D., Sweet-Cordero, A., Ebert, B.L., Mak, R.H., Ferrando, A.A., et al. (2005). MicroRNA expression profiles classify human cancers. Nature 435, 834-838.

Lu, X., and Lane, D.P. (1993). Differential induction of transcriptionally active p53 following UV or ionizing radiation: defects in chromosome instability syndromes? Cell 75, 765-778.

Lu, X., Nguyen, T.A., Zhang, X., and Donehower, L.A. (2008). The Wip1 phosphatase and Mdm2: cracking the "Wip" on p53 stability. Cell Cycle 7, 164-168.

Ludwig, R.L., Bates, S., and Vousden, K.H. (1996). Differential activation of target cellular promoters by p53 mutants with impaired apoptotic function. Mol Cell Biol 16, 4952-4960.

Luo, J., Su, F., Chen, D., Shiloh, A., and Gu, W. (2000). Deacetylation of p53 modulates its effect on cell growth and apoptosis. Nature 408, 377-381.

Ma, X.L., Gao, F., Lopez, B.L., Christopher, T.A., and Vinten-Johansen, J. (2000). Peroxynitrite, a two-edged sword in post-ischemic myocardial injury-dichotomy of action in crystalloid- versus blood-perfused hearts. J Pharmacol Exp Ther 292, 912-920.

Machado-Silva A, P.S., Bourdon JC (2010). p53 family members in cancer diagnosis and treatment. Semin Cancer Biol 20, 57-62.

Macleod, K. (2000). Tumor suppressor genes. Curr Opin Genet Dev 10(1): 81-93.

MacMillan-Crow, L.A., and Thompson, J.A. (1999). Tyrosine modifications and inactivation of active site manganese superoxide dismutase mutant (Y34F) by peroxynitrite. Archives of biochemistry and biophysics 366, 82-88.

Maddocks, O.D., and Vousden, K.H. (2011). Metabolic regulation by p53. J Mol Med 89, 237-245.

Makrides, S.C. (1996). Strategies for achieving high-level expression of genes in Escherichia coli. Microbiol Rev 60, 512-538.

Malkin, D., Li, F.P., Strong, L.C., Fraumeni, J.F., Jr., Nelson, C.E., Kim, D.H., Kassel, J., Gryka, M.A., Bischoff, F.Z., Tainsky, M.A., et al. (1990). Germ line p53 mutations in a familial syndrome of breast cancer, sarcomas, and other neoplasms. Science 250, 1233-1238.

Mallozzi, C., Di Stasi, A.M., and Minetti, M. (1997). Peroxynitrite modulates tyrosine-dependent signal transduction pathway of human erythrocyte band 3. Faseb J 11, 1281-1290.

Maltzman, W., and Czyzyk, L. (1984). UV irradiation stimulates levels of p53 cellular tumor antigen in nontransformed mouse cells. Mol Cell Biol 4, 1689-1694.

Marechal, V., Elenbaas, B., Piette, J., Nicolas, J.C., and Levine, A.J. (1994). The ribosomal L5 protein is associated with mdm-2 and mdm-2-p53 complexes. Mol Cell Biol 14, 7414-7420.

Marin MC, K.W.J. (2000). p63 and p73: old members of a new family. Biochim Biophys Acta 1470, 93-100.

Marine JC, D.M., Jochemsen AG (2007). MDMX: from bench to bedside. J Cell Sci 120, 371-8.

Marston, N.J., Jenkins, J.R., and Vousden, K.H. (1995). Oligomerisation of full length p53 contributes to the interaction with mdm2 but not HPV E6. Oncogene 10, 1709-1715.

Martindale, J.L., and Holbrook, N.J. (2002). Cellular response to oxidative stress: signaling for suicide and survival. Journal of cellular physiology 192, 1-15.

Mateu, M.G., and Fersht, A.R. (1998). Nine hydrophobic side chains are key determinants of the thermodynamic stability and oligomerization status of tumour suppressor p53 tetramerization domain. Embo J 17, 2748-2758.

Matoba, S., Kang, J.G., Patino, W.D., Wragg, A., Boehm, M., Gavrilova, O., Hurley, P.J., Bunz, F., and Hwang, P.M. (2006). p53 regulates mitochondrial respiration. Science 312, 1650-1653.

Matsuda, K., Yoshida, K., Taya, Y., Nakamura, K., Nakamura, Y. and Arakawa, H. (2002). p53AIP1 regulates the mitochondrial apoptotic pathway. Cancer Research 62, 2883–2889.

Matsumoto, M., Furihata, M., Kurabayashi, A., and Ohtsuki, Y. (2004). Phosphorylation state of tumor-suppressor gene p53 product overexpressed in skin tumors. Oncology reports 12, 1039-1043.

Matsumoto, M., Furihata, M., Kurabayashi, A., Sasaguri, S., Araki, K., Hayashi, H., and Ohtsuki, Y. (2004). Prognostic significance of serine 392 phosphorylation in overexpressed p53 protein in human esophageal squamous cell carcinoma. Oncology 67, 143-150.

Matsumoto, M., Furihata, M., and Ohtsuki, Y. (2006). Posttranslational phosphorylation of mutant p53 protein in tumor development. Medical molecular morphology 39, 79-87.

Maya, R., Balass, M., Kim, S.T., Shkedy, D., Leal, J.F., Shifman, O., Moas, M., Buschmann, T., Ronai, Z., Shiloh, Y., et al. (2001). ATM-dependent phosphorylation of Mdm2 on serine 395: role in p53 activation by DNA damage. Genes Dev 15, 1067-1077.

Mayer, B., and Hemmens, B. (1997). Biosynthesis and action of nitric oxide in mammalian cells. Trends Biochem Sci 22, 477-481.

Mayo, L.D., Dixon, J.E., Durden, D.L., Tonks, N.K., and Donner, D.B. (2002). PTEN protects p53 from Mdm2 and sensitizes cancer cells to chemotherapy. J Biol Chem 277, 5484-5489.

Mayo, L.D., and Donner, D.B. (2001). A phosphatidylinositol 3-kinase/Akt pathway promotes translocation of Mdm2 from the cytoplasm to the nucleus. Proc Natl Acad Sci U S A 98, 11598-11603.

Mayo, L.D., Turchi, J.J., and Berberich, S.J. (1997). Mdm-2 phosphorylation by DNA-dependent protein kinase prevents interaction with p53. Cancer Res 57, 5013-5016.

McCoy, M., Stavridi, E.S., Waterman, J.L., Wieczorek, A.M., Opella, S.J., and Halazonetis, T.D. (1997). Hydrophobic side-chain size is a determinant of the three-dimensional structure of the p53 oligomerization domain. Embo J 16, 6230-6236.

McKinney, K., Mattia, M., Gottifredi, V., and Prives, C. (2004). p53 linear diffusion along DNA requires its C terminus. Mol Cell 2004 Nov 5;16(3):413-24.

Mebmer U.K., A.M., Nicotera P, Brune B (1994). p53 expression in nitric oxide-induced apoptosis. FEBS letters 355, 23-26.

Mebmer U.K., R.J.C., Brune B (1996). Bcl-2 protects macrophages from nitric oxide-induced apoptosis. The Journal of biological chemistry 271, 20192-20197.

Meek, D.W. (2004). The p53 response to DNA damage. DNA repair 3, 1049-1056.

Meek, D.W. (2009). Tumour suppression by p53: a role for the DNA damage response? Nature reviews Cancer 9, 714-723.

Meek, D.W., and Anderson, C.W. (2009). Posttranslational modification of p53: cooperative integrators of function. Cold Spring Harbor perspectives in biology 1, a000950.

Meek DW, H.T. (2010). The regulation of MDM2 by multisite phosphorylation--opportunities for molecular-based intervention to target tumours? Seminars in cancer biology 20, 19-28.

Meek DW, K.U. (2003). Posttranslational modification of MDM2. Mol Cancer Res 1, 1017-1026.

Melino G, L.X., Gasco M, Crook T, Knight RA (2003). Functional regulation of p73 and p63: development and cancer. Trends Biochem Sci 28, 663-670.

Menendez, D., Inga, A., and Resnick, M.A. (2009). The expanding universe of p53 targets. Nat Rev Cancer 9, 724-37.

Merritt, A.J., Potten, C.S., Kemp, C.J., Hickman, J.A., Balmain, A., Lane, D.P., and Hall, P.A. (1994). The role of p53 in spontaneous and radiation-induced apoptosis in the gastrointestinal tract of normal and p53-deficient mice. Cancer Res 54, 614-617.

Meselson, M., and Yuan, R. (1968). DNA restriction enzyme from E. coli. Nature 217, 1110-1114.

Messmer, U.K., Ankarcrona, M., Nicotera, P., and Brune, B. (1994). p53 expression in nitric oxide-induced apoptosis. FEBS letters 355, 23-26.

Messmer, U.K., and Brune, B. (1996). Nitric oxide (NO) in apoptotic versus necrotic RAW 264.7 macrophage cell death: the role of NO-donor exposure, NAD+ content, and p53 accumulation. Archives of biochemistry and biophysics 327, 1-10.

Michael, D., and Oren, M. (2003). The p53-Mdm2 module and the ubiquitin system. Semin Cancer Biol 13, 49-58.

Michishita E, P.J., Burneskis JM, Barrett JC, Horikawa I (2005). Evolutionarily conserved and nonconserved cellular localizations and functions of human SIRT proteins. Mol Biol Cell 16, 4623-4635.

Midgley, C.A., Fisher, C.J., Bartek, J., Vojtesek, B., Lane, D., and Barnes, D.M. (1992). Analysis of p53 expression in human tumours: an antibody raised against human p53 expressed in Escherichia coli. J Cell Sci 101, 183-189.

Midgley, C.A., and Lane, D.P. (1997). p53 protein stability in tumour cells is not determined by mutation but is dependent on Mdm2 binding. Oncogene 15, 1179-1189.

Mihara, M., Shintani, S., Nakashiro, K., and Hamakawa, H. (2003). Flavopiridol, a cyclin dependent kinase (CDK) inhibitor, induces apoptosis by regulating Bcl-x in oral cancer cells. Oral oncology 39, 49-55.

Miller, C.W., Aslo, A., Tsay, C., Slamon, D., Ishizaki, K., Toguchida, J., Yamamuro, T., Lampkin, B., and Koeffler, H.P. (1990). Frequency and structure of p53 rearrangements in human osteosarcoma. Cancer Res 50, 7950-7954.

Mills, A.A., Zheng, B., Wang, X.J., Vogel, H., Roop, D.R., and Bradley, A. (1999). p63 is a p53 homologue required for limb and epidermal morphogenesis. Nature 398, 708-713.

Milne, D.M., Campbell, D.G., Caudwell, F.B., and Meek, D.W. (1994). Phosphorylation of the tumor suppressor protein p53 by mitogen- activated protein kinases. J Biol Chem 269, 9253-9260.

Milne, D.M., Campbell, L.E., Campbell, D.G., and Meek, D.W. (1995). p53 is phosphorylated in vitro and in vivo by an ultraviolet radiation- induced protein kinase characteristic of the c-Jun kinase, JNK1. J Biol Chem 270, 5511-5518.

Milne, D.M., McKendrick, L., Jardine, L.J., Deacon, E., Lord, J.M., and Meek, D.W. (1996). Murine p53 is phosphorylated within the PAb421 epitope by protein kinase C in vitro, but not in vivo, even after stimulation with the phorbol ester o-tetradecanoylphorbol 13-acetate. Oncogene 13, 205-211.

Milne, D.M., Palmer, R.H., Campbell, D.G., and Meek, D.W. (1992). Phosphorylation of the p53 tumour-suppressor protein at three N- terminal sites by a novel casein kinase I-like enzyme. Oncogene 7, 1361-1369.

Milner, J., Medcalf, E.A., and Cook, A.C. (1991). Tumor suppressor p53: analysis of wild-type and mutant p53 complexes. Mol Cell Biol 11, 12-19.

Miyashita, T., Krajewski, S., Krajewska, M., Wang, H.G., Lin, H.K., Liebermann, D.A., Hoffman, B., and Reed, J.C. (1994). Tumor suppressor p53 is a regulator of bcl-2 and bax gene expression in vitro and in vivo. Oncogene 9, 1799-1805.

Miyashita, T., and Reed, J.C. (1995). Tumor suppressor p53 is a direct transcriptional activator of the human bax gene. Cell 80, 293-299.

Mohr, S., Hallak, H., de Boitte, A., Lapetina, E.G., and Brune, B. (1999). Nitric oxide-induced S-glutathionylation and inactivation of glyceraldehyde-3-phosphate dehydrogenase. J Biol Chem 1 274, 9427-9430.

Moll, U.M., and Petrenko, O. (2003). The MDM2-p53 interaction. Molecular cancer research : MCR 1, 1001-1008.

Momand, J., Jung, D., Wilczynski, S., and Niland, J. (1998). The MDM2 gene amplification database. Nucleic Acids Res 26, 3453-3459.

Momand, J., Zambetti, G.P., Olson, D.C., George, D., and Levine, A.J. (1992). The mdm-2 oncogene product forms a complex with the p53 protein and inhibits p53-mediated transactivation. Cell 69, 1237-1245.

Moncada, S., Palmer, R.M., and Higgs, E.A. (1991). Nitric oxide: physiology, pathophysiology, and pharmacology. Pharmacol Rev 43, 109-142.

Mondoro, T.H., Shafer, B.C., and Vostal, J.G. (1997). Peroxynitrite-induced tyrosine nitration and phosphorylation in human platelets. Free radical biology & medicine 22, 1055-1063.

Moro, M.A., Darley-Usmar, V.M., Goodwin, D.A., Read, N.G., Zamora-Pino, R., Feelisch, M., Radomski, M.W., and Moncada, S. (1994). Paradoxical fate and biological action of peroxynitrite on human platelets. Proc Natl Acad Sci U S A 91, 6702-6706.

Muller, P.A., Caswell, P.T., Doyle, B., Iwanicki, M.P., Tan, E.H., Karim, S., Lukashchuk, N., Gillespie, D.A., Ludwig, R.L., Gosselin, P., et al. (2009). Mutant p53 drives invasion by promoting integrin recycling. Cell 2009 Dec 24;139(7):1327-41.

Muller, P.A., and Vousden, K.H. (2013). p53 mutations in cancer. Nat Cell Biol 15, 2-8.

Muller, P.A., Vousden, K.H., and Norman, J.C. (2011). p53 and its mutants in tumor cell migration and invasion. J Cell Biol 192, 209-218.

Muller, S., Berger, M., Lehembre, F., Seeler, J.S., Haupt, Y., and Dejean, A. (2000). c-Jun and p53 activity is modulated by SUMO-1 modification. J Biol Chem 275, 13321-13329.

Muntane, J., and la Mata, M.D. (2010). Nitric oxide and cancer. World J Hepatol 2, 337-344.

Murray-Zmijewski, F., Lane, D.P., and Bourdon, J.C. (2006). p53/p63/p73 isoforms: an orchestra of isoforms to harmonise cell differentiation and response to stress. Cell death and differentiation 13, 962-972.

Naik, E., Michalak, E.M., Villunger, A., Adams, J.M., and Strasser, A. (2007). Ultraviolet radiation triggers apoptosis of fibroblasts and skin keratinocytes mainly via the BH3-only protein Noxa. J Cell Biol 2007 Feb 12;176(4):415-24 Epub 2007 Feb 5.

Nakamura, K., Pirtle, R.M., Pirtle, I.L., Takeishi, K., and Inouye, M. (1980). Messenger ribonucleic acid of the lipoprotein of the Escherichia coli outer membrane. II. The complete nucleotide sequence. J Biol Chem 255, 210-216.

Nakano, K., and Vousden, K.H. (2001). PUMA, a novel proapoptotic gene, is induced by p53. Molecular cell 7, 683-694.

Naseem KM, B.K. (1995). Hydrogen peroxide at low concentrations strongly enhances the inhibitory effect of nitric oxide on platelets. Biochem J 310, 149-153.

Naseem KM, R.R., Troxler M. (2004). Evaluation of nitrotyrosine-containing proteins in blood platelets. Methods Mol Biol 273, 301-312.

Natal, C., Modol, T., Oses-Prieto, J.A., Lopez-Moratalla, N., Iraburu, M.J., and Lopez-Zabalza, M.J. (2008). Specific protein nitration in nitric oxide-induced apoptosis of human monocytes. Apoptosis : an international journal on programmed cell death 13, 1356-1367.

Nathan, C., and Xie, Q.W. (1994). Nitric oxide synthases: roles, tolls, and controls. Cell 78, 915-918.

Neilsen, P.M., Noll, J.E., Mattiske, S., Bracken, C.P., Gregory, P.A., Schulz, R.B., Lim, S.P., Kumar, R., Suetani, R.J., Goodall, G.J., et al. (2013). Mutant p53 drives invasion in breast tumors through up-regulation of miR-155. Oncogene 2013 Jun 13;32(24):2992-3000.

Nelson, W.G., and Kastan, M.B. (1994). DNA strand breaks: the DNA template alterations that trigger p53- dependent DNA damage response pathways. Mol Cell Biol 14, 1815-1823.

Nguyen, T.A., Menendez, D., Resnick, M.A., and Anderson, C.W. (2014). Mutant TP53 posttranslational modifications: challenges and opportunities. Hum Mutat 35, 738-755.

Nichols, B.P., and Yanofsky, C. (1979). Nucleotide sequences of trpA of Salmonella typhimurium and Escherichia coli: an evolutionary comparison. Proc Natl Acad Sci U S A 76, 5244-5248.

Niles, J.C., Wishnok, J.S., and Tannenbaum, S.R. (2006). Peroxynitrite-induced oxidation and nitration products of guanine and 8-oxoguanine: structures and mechanisms of product formation. Nitric oxide : biology and chemistry / official journal of the Nitric Oxide Society 14, 109-121.

Oda, E., Ohki, R., Murasawa, H., Nemoto, J., Shibue, T., Yamashita, T., Tokino, T., Taniguchi, T., and Tanaka, N. (2000). Noxa, a BH3-only member of the Bcl-2 family and candidate mediator of p53-induced apoptosis. Science 288, 1053-1058.

O'Farrell, T.J., Ghosh, P., Dobashi, N., Sasaki, C.Y., and Longo, D.L. (2004). Comparison of the effect of mutant and wild-type p53 on global gene expression. Cancer Res 64, 8199-8207.

Ogawara, Y., Kishishita, S., Obata, T., Isazawa, Y., Suzuki, T., Tanaka, K., Masuyama, N., and Gotoh, Y. (2002). Akt enhances Mdm2-mediated ubiquitination and degradation of p53. The Journal of biological chemistry 277, 21843-21850.

Ohki, R., Nemoto, J., Murasawa, H., Oda, E., Inazawa, J., Tanaka, N., and Taniguchi, T. (2000). Reprimo, a new candidate mediator of the p53-mediated cell cycle arrest at the G2 phase. The Journal of biological chemistry 275, 22627-22630.

Ohshima, H., and Bartsch, H. (1994). Chronic infections and inflammatory processes as cancer risk factors: possible role of nitric oxide in carcinogenesis. Mutat Res 305, 253-264.

Okorokov, A.L., and Orlova, E.V. (2009). Structural biology of the p53 tumour suppressor. Current opinion in structural biology 19, 197-202.

Oliner, J.D., Kinzler, K.W., Meltzer, P.S., George, D.L., and Vogelstein, B. (1992). Amplification of a gene encoding a p53-associated protein in human sarcomas. Nature 358, 80-83.

Oliner, J.D., Pietenpol, J.A., Thiagalingam, S., Gyuris, J., Kinzler, K.W., and Vogelstein, B. (1993). Oncoprotein MDM2 conceals the activation domain of tumour suppressor p53. Nature 362, 857-860.

Olive KP, T.D., Ruhe ZC, Yin B, Willis NA, Bronson RT, Crowley D, Jacks T. (2004). Mutant p53 gain of function in two mouse models of Li-Fraumeni syndrome. Cell 119, 847-860.

Olson, D.C., Marechal, V., Momand, J., Chen, J., Romocki, C., and Levine, A.J. (1993). Identification and characterization of multiple mdm-2 proteins and mdm-2-p53 protein complexes. Oncogene 8, 2353-2360.

Oren, M. (1985). The p53 cellular tumor antigen: gene structure, expression and protein properties. Biochim Biophys Acta 823, 67-78.

Oren, M., and Rotter, V. (2010). Mutant p53 gain-of-function in cancer. Cold Spring Harb Perspect Biol 2010 Feb;2(2).

Osada, M., Ohba, M., Kawahara, C., Ishioka, C., Kanamaru, R., Katoh, I., Ikawa, Y., Nimura, Y., Nakagawara, A., Obinata, M., et al. (1998). Cloning and functional analysis of human p51, which structurally and functionally resembles p53. Nature medicine 4, 839-843.

Ozaki, M., Kawashima, S., Hirase, T., Yamashita, T., Namiki, M., Inoue, N., Hirata Ki, K., and Yokoyama, M. (2002). Overexpression of endothelial nitric oxide synthase in endothelial cells is protective against ischemia-reperfusion injury in mouse skeletal muscle. The American journal of pathology 160, 1335-1344.

Ozaki, T., and Nakagawara, A. (2011). p53: the attractive tumor suppressor in the cancer research field. Journal of biomedicine & biotechnology 2011, 603925.

Pacher, P., Beckman, J.S., and Liaudet, L. (2007). Nitric oxide and peroxynitrite in health and disease. Physiological reviews 87, 315-424.

Padmaja, S., and Huie, R.E. (1993). The reaction of nitric oxide with organic peroxyl radicals. Biochemical and biophysical research communications 195, 539-544.

Palmer, R.M., Ferrige, A.G., and Moncada, S. (1987). Nitric oxide release accounts for the biological activity of endothelium-derived relaxing factor. Nature 327, 524-526.

Pan, Y., and Haines, D.S. (2000). Identification of a tumor-derived p53 mutant with novel transactivating selectivity. Oncogene 19, 3095-3100.

Parant, J., Chavez-Reyes, A., Little, N.A., Yan, W., Reinke, V., Jochemsen, A.G., and Lozano, G. (2001). Rescue of embryonic lethality in Mdm4-null mice by loss of Trp53 suggests a nonoverlapping pathway with MDM2 to regulate p53. Nat Genet 29, 92-95.

Pearson, M., Carbone, R., Sebastiani, C., Cioce, M., Fagioli, M., Saito, S., Higashimoto, Y., Appella, E., Minucci, S., Pandolfi, P.P., et al. (2000). PML regulates p53 acetylation and premature senescence induced by oncogenic Ras. Nature 406, 207-210.

Pei, D., Zhang, Y., and Zheng, J. (2012). Regulation of p53: a collaboration between Mdm2 and Mdmx. Oncotarget 3, 228-235.

Perfettini, J.L., Castedo, M., Nardacci, R., Ciccosanti, F., Boya, P., Roumier, T., Larochette, N., Piacentini, M., and Kroemer, G. (2005). Essential role of p53 phosphorylation by p38 MAPK in apoptosis induction by the HIV-1 envelope. The Journal of experimental medicine 201, 279-289.

Picksley, S.M., Dart, D.A., Mansoor, M.S., and Loadman, P.M. (2001). Current advances in the inhibition of the auto-regulatory interaction between the p53 tumour suppressor protein and MDM2 protein. Expert Opin Ther Patents 11, 1825-1835.

Picksley, S.M., Vojtesek, B., Sparks, A., and Lane, D.P. (1994). Immunochemical analysis of the interaction of p53 with MDM2;--fine mapping of the MDM2 binding site on p53 using synthetic peptides. Oncogene 9, 2523-2529.

Pietenpol, J.A., Tokino, T., Thiagalingam, S., el-Deiry, W.S., Kinzler, K.W., and Vogelstein, B. (1994). Sequence-specific transcriptional activation is essential for growth suppression by p53. Proc Natl Acad Sci U S A 91, 1998-2002.

Ploner, C., Kofler, R., and Villunger, A. (2008). Noxa: at the tip of the balance between life and death. Oncogene 2008 Dec;27 Suppl 1:S84-92.

Post, L.E., Strycharz, G.D., Nomura, M., Lewis, H., and Dennis, P.P. (1979). Nucleotide sequence of the ribosomal protein gene cluster adjacent to the gene for RNA polymerase subunit beta in Escherichia coli. Proc Natl Acad Sci U S A 76, 1697-1701.

Price, B.D., and Calderwood, S.K. (1993). Increased sequence-specific p53-DNA binding activity after DNA damage is attenuated by phorbol esters. Oncogene 8, 3055-3062.

Prives, C., and Hall, P.A. (1999). The p53 pathway. J Pathol 187, 112-126.

Pryor, W.A., and Squadrito, G.L. (1995). The chemistry of peroxynitrite: a product from the reaction of nitric oxide with superoxide. Am J Physiol 268, L699-722.

Quitana-Lopez L, B.-R.M., Perez-Arana G, Cebada-Aleu A, Lechuga-Sancho A, Aquilar-Diosdado M, Sequndo C (2013). Nitric oxide is a mediator of antiproliferative effects induced by proinflammatory cytokines on pancreatic beta cells. Mediators Inflamm 2013, 10.

Radi, R., Cassina, A., and Hodara, R. (2002). Nitric oxide and peroxynitrite interactions with mitochondria. Biological chemistry 383, 401-409.

Radi, R., Cassina, A., Hodara, R., Quijano, C., and Castro, L. (2002). Peroxynitrite reactions and formation in mitochondria. Free radical biology & medicine 33, 1451-1464.

Radi R, R.M., Castro L, Telleri R. (1994). Inhibition of mitochondrial electron transport by peroxynitrite. Arch Biochem Biophys 308, 89-95.

Ramos, Y.F., Stad, R., Attema, J., Peltenburg, L.T., van der Eb, A.J., and Jochemsen, A.G. (2001). Aberrant expression of HDMX proteins in tumor cells correlates with wild-type p53. Cancer Res 61, 1839-1842.

Ravni, A., Tissir, F., and Goffinet, A.M. (2010). DeltaNp73 transcription factors modulate cell survival and tumor development. Cell Cycle 2010 Apr 15;9(8):1523-7 Epub 2010 Apr 15.

Reference, C.a.T. (2013-2014). New England Biolabs.

Reuter, S., Gupta, S.C., Chaturvedi, M.M., and Aggarwal, B.B. (2010). Oxidative stress, inflammation, and cancer: how are they linked? Free radical biology & medicine 49, 1603-1616.

Riley, T., Sontag, E., Chen, P., and Levine, A. (2008). Transcriptional control of human p53-regulated genes. Nature reviews Molecular cell biology 9, 402-412.

Robertson, F.M., Long, B.W., Tober, K.L., Ross, M.S., and Oberyszyn, T.M. (1996). Gene expression and cellular sources of inducible nitric oxide synthase during tumor promotion. Carcinogenesis 17, 2053-2059.

Robinson, K.M., and Beckman, J.S. (2005). Synthesis of peroxynitrite from nitrite and hydrogen peroxide. Methods Enzymol 396, 207-214.

Rodriguez, M.S., Desterro, J.M., Lain, S., Lane, D.P., and Hay, R.T. (2000). Multiple C-terminal lysine residues target p53 for ubiquitin-proteasome-mediated degradation. Molecular and cellular biology 20, 8458-8467.

Rodriguez, M.S., Desterro, J.M., Lain, S., Midgley, C.A., Lane, D.P., and Hay, R.T. (1999). SUMO-1 modification activates the transcriptional response of p53. Embo J 18, 6455-6461.

Romagosa, C., Simonetti, S., Lopez-Vicente, L., Mazo, A., Lleonart, M.E., Castellvi, J., and Ramon y Cajal, S. (2011). p16(Ink4a) overexpression in cancer: a tumor suppressor gene associated with senescence and high-grade tumors. Oncogene 30, 2087-2097.

Ronson, R.S., Nakamura, M., and Vinten-Johansen, J. (1999). The cardiovascular effects and implications of peroxynitrite. Cardiovascular research 44, 47-59.

Roth, J., Dobbelstein, M., Freedman, D.A., Shenk, T., and Levine, A.J. (1998). Nucleo-cytoplasmic shuttling of the hdm2 oncoprotein regulates the levels of the p53 protein via a pathway used by the human immunodeficiency virus rev protein. Embo J 17, 554-564.

Rufini, A., Tucci, P., Celardo, I., and Melino, G. (2013). Senescence and aging: the critical roles of p53. Oncogene 32, 5129-5143.

Saha, A., Goldstein, S., Cabelli, D., and Czapski, G. (1998). Determination of optimal conditions for synthesis of peroxynitrite by mixing acidified hydrogen peroxide with nitrite. Free Radic Biol Med 24, 653-659.

Saha, T., Kar, R.K., and Sa, G. (2015). Structural and sequential context of p53: A review of experimental and theoretical evidence (Prog Biophys Mol Biol), 1-14.

Saito, S., Goodarzi, A.A., Higashimoto, Y., Noda, Y., Lees-Miller, S.P., Appella, E., and Anderson, C.W. (2002). ATM mediates phosphorylation at multiple p53 sites, including Ser(46), in response to ionizing radiation. J Biol Chem 277, 12491-12494.

Sakaguchi, K., Herrera, J.E., Saito, S., Miki, T., Bustin, M., Vassilev, A., Anderson, C.W., and Appella, E. (1998). DNA damage activates p53 through a phosphorylation-acetylation cascade. Genes & development 12, 2831-2841.

Sakaguchi, K., Saito, S., Higashimoto, Y., Roy, S., Anderson, C.W., and Appella, E. (2000). Damage-mediated phosphorylation of human p53 threonine 18 through a cascade mediated by a casein 1-like kinase. Effect on Mdm2 binding. The Journal of biological chemistry 275, 9278-9283.

Sakaguchi, K., Sakamoto, H., Xie, D., Erickson, J.W., Lewis, M.S., Anderson, C.W., and Appella, E. (1997). Effect of phosphorylation on tetramerization of the tumor suppressor protein p53. J Protein Chem 16, 553-556.

Sakahira, H., Enari, M., and Nagata, S. (1998). Cleavage of CAD inhibitor in CAD activation and DNA degradation during apoptosis. Nature 391, 96-99.

Sakamuro, D., Sabbatini, P., White, E., and Prendergast, G.C. (1997). The polyproline region of p53 is required to activate apoptosis but not growth arrest. Oncogene 15, 887-898.

Salem, M.M., Shalbaf, M., Gibbons, N.C., Chavan, B., Thornton, J.M., and Schallreuter, K.U. (2009). Enhanced DNA binding capacity on up-regulated epidermal wild-type p53 in vitiligo by H2O2-mediated oxidation: a possible repair mechanism for DNA damage. FASEB journal : official publication of the Federation of American Societies for Experimental Biology 23, 3790-3807.

Salgo, M.G., Stone, K., Squadrito, G.L., Battista, J.R., and Pryor, W.A. (1995). Peroxynitrite causes DNA nicks in plasmid pBR322. Biochem Biophys Res Commun 210, 1025-1030.

Sambrook, Fritsh, and Maniatis (1989). Molecular Cloning: A Laboratory Manual. Second Edition, 18.48 and 18.52.

Sata, M., Kakoki, M., Nagata, D., Nishimatsu, H., Suzuki, E., Aoyagi, T., Sugiura, S., Kojima, H., Nagano, T., Kangawa, K., et al. (2000). Adrenomedullin and nitric oxide inhibit human endothelial cell apoptosis via a cyclic GMP-independent mechanism. Hypertension 36, 83-88.

Sax, J.K., Fei, P., Murphy, M.E., Bernhard, E., Korsmeyer, S.J., and El-Deiry, W.S. (2002). BID regulation by p53 contributes to chemosensitivity. Nature cell biology 4, 842-849.

Scherz-Shouval, R., Weidberg, H., Gonen, C., Wilder, S., Elazar, Z., and Oren, M. (2010). p53-dependent regulation of autophagy protein LC3 supports cancer cell survival under prolonged starvation. Proc Natl Acad Sci U S A 107, 18511-18516.

Schilling, T., Kairat, A., Melino, G., Krammer, P.H., Stremmel, W., Oren, M., and Muller, M. (2010). Interference with the p53 family network contributes to the gain of oncogenic function of mutant p53 in hepatocellular carcinoma. Biochem Biophys Res Commun 2010 Apr 9;394(3):817-23.

Schmale, H., and Bamberger, C. (1997). A novel protein with strong homology to the tumor suppressor p53. Oncogene 15, 1363-1367.

Schmidt, H.H., and Walter, U. (1994). NO at work. Cell 78, 919-925.

Schmidt, H.H., Warner, T.D., and Murad, F. (1992). Double-edged role of endogenous nitric oxide. Lancet 339, 986.

Schmitt, C.A., and Lowe, S.W. (2002). Apoptosis and chemoresistance in transgenic cancer models. Journal of molecular medicine 80, 137-146.

Schneiderhan, N., Budde, A., Zhang, Y., and Brune, B. (2003). Nitric oxide induces phosphorylation of p53 and impairs nuclear export. Oncogene 22, 2857-2868.

Schon, O., Friedler, A., Bycroft, M., Freund, S.M., and Fersht, A.R. (2002). Molecular mechanism of the interaction between MDM2 and p53. Journal of molecular biology 323, 491-501.

Schroeder, P., Klotz, L.O., Buchczyk, D.P., Sadik, C.D., Schewe, T., and Sies, H. (2001). Epicatechin selectively prevents nitration but not oxidation reactions of peroxynitrite. Biochemical and biophysical research communications 285, 782-787.

Schwartzenberg-Bar-Yoseph, F., Armoni, M., and Karnieli, E. (2004). The tumor suppressor p53 down-regulates glucose transporters GLUT1 and GLUT4 gene expression. Cancer Res 2004 Apr 1;64(7):2627-33.

Scian, M.J., Stagliano, K.E., Ellis, M.A., Hassan, S., Bowman, M., Miles, M.F., Deb, S.P., and Deb, S. (2004). Modulation of gene expression by tumor-derived p53 mutants. Cancer Res 64, 7447-7454.

Scopes, R. (1982). Protein purification: principles and practice (New York, Springer-Verlag).

Scoumanne, A., and Chen, X. (2008). Protein methylation: a new mechanism of p53 tumor suppressor regulation. Histology and histopathology 23, 1143-1149.

Scoumanne, A., Harms, K.L., and Chen, X. (2005). Structural basis for gene activation by p53 family members. Cancer Biol Ther 4, 1178-1185.

Selvakumaran, M., Lin, H.K., Miyashita ,T. et al. (1994). Immediate early up-regulation of bax expression by p53 but not TGF*β*1: a paradigm for distinct apoptotic pathways. Oncogene
9, 1791–1798.

Shacka, J.J., Sahawneh, M.A., Gonzalez, J.D., Ye, Y.Z., D'Alessandro, T.L., and Estevez, A.G. (2006). Two distinct signaling pathways regulate peroxynitrite-induced apoptosis in PC12 cells. Cell death and differentiation 13, 1506-1514.

Shadfan, M., Lopez-Pajares, V., and Yuan, Z.M. (2012). MDM2 and MDMX: Alone and together in regulation of p53. Transl Cancer Res 1, 88-89.

Shangary, S., Qin, D., McEachern, D., Liu, M., Miller, R.S., Qiu, S., Nikolovska-Coleska, Z., Ding, K., Wang, G., Chen, J., et al. (2008). Temporal activation of p53 by a specific MDM2 inhibitor is selectively toxic to tumors and leads to complete tumor growth inhibition. Proc Natl Acad Sci U S A 105, 3933-3938.

Sharp, D.A., Kratowicz, S.A., Sank, M.J., and George, D.L. (1999). Stabilization of the MDM2 oncoprotein by interaction with the structurally related MDMX protein. J Biol Chem 274, 38189-38196.

Shatzman, A.R. (1990). Gene expression using gram-negative bacteria. Curr Opin Biotechnol 1, 5-11.

Shaulsky, G., Goldfinger, N., Ben-Ze'ev, A., and Rotter, V. (1990). Nuclear accumulation of p53 protein is mediated by several nuclear localization signals and plays a role in tumorigenesis. Mol Cell Biol 10, 6565-6577.

Shaw, P., Freeman, J., Bovey, R., and Iggo, R. (1996). Regulation of specific DNA binding by p53: evidence for a role for O-glycosylation and charged residues at the carboxy-terminus. Oncogene 12, 921-930.

Sherr, C.J. (1998). Tumor surveillance via the ARF-p53 pathway. Genes Dev 12, 2984-2991.

Shi, W.Q., Cai, H., Xu, D.D., Su, X.Y., Lei, P., Zhao, Y.F., and Li, Y.M. (2007). Tyrosine phosphorylation/dephosphorylation regulates peroxynitrite-mediated peptide nitration. Regul Pept 144, 1-5.

Shi, X., Kachirskaia, I., Yamaguchi, H., West, L.E., Wen, H., Wang, E.W., Dutta, S., Appella, E., and Gozani, O. (2007). Modulation of p53 function by SET8-mediated methylation at lysine 382. Molecular cell 27, 636-646.

Shieh, S.Y., Ikeda, M., Taya, Y., and Prives, C. (1997). DNA damage-induced phosphorylation of p53 alleviates inhibition by MDM2. Cell 91, 325-334.

Shiota, M., Izumi, H., Onitsuka, T., Miyamoto, N., Kashiwagi, E., Kidani, A., Hirano, G., Takahashi, M., Naito, S., and Kohno, K. (2008). Twist and p53

reciprocally regulate target genes via direct interaction. Oncogene 27, 5543-5553.

Shvarts, A., Steegenga, W.T., Riteco, N., van Laar, T., Dekker, P., Bazuine, M., van Ham, R.C., van der Houven van Oordt, W., Hateboer, G., van der Eb, A.J., et al. (1996). MDMX: a novel p53-binding protein with some functional properties of MDM2. EMBO Journal 15, 5349-5357.

Sieber, O.M., Heinimann, K., and Tomlinson, I.P. (2003). Genomic instability--the engine of tumorigenesis? Nat Rev Cancer 3, 701-708.

Sigal, A., and Rotter, V. (2000). Oncogenic mutations of the p53 tumor suppressor: the demons of the guardian of the genome. Cancer Res 2000 Dec 15;60(24):6788-93.

Simbulan-Rosenthal, C.M., Rosenthal, D.S., Luo, R., and Smulson, M.E. (1999). Poly(ADP-ribosyl)ation of p53 during apoptosis in human osteosarcoma cells. Cancer Res 59, 2190-2194.

Singer, II, Kawka, D.W., Scott, S., Weidner, J.R., Mumford, R.A., Riehl, T.E., and Stenson, W.F. (1996). Expression of inducible nitric oxide synthase and nitrotyrosine in colonic epithelium in inflammatory bowel disease. Gastroenterology 111, 871-885.

Singh, S., and Gupta, A.K. (2011). Nitric oxide: role in tumour biology and iNOS/NO-based anticancer therapies. Cancer Chemother Pharmacol 67, 1211-1224.

Smith, M.L., Chen, I.T., Zhan, Q., Bae, I., Chen, C.Y., Gilmer, T.M., Kastan, M.B., O'Connor, P.M., and Fornace, A.J., Jr. (1994). Interaction of the p53-regulated protein Gadd45 with proliferating cell nuclear antigen. Science 266, 1376-1380.

Smith, M.M. (2002). Histone variants and nucleosome deposition pathways. Mol Cell 9, 1158-1160.

Soussi, T., Caron de Fromentel, C., and May, P. (1990). Structural aspects of the p53 protein in relation to gene evolution. Oncogene 5, 945-952.

Soussi, T., Caron de Fromentel, C., Mechali, M., May, P., and Kress, M. (1987). Cloning and characterization of a cDNA from Xenopus laevis coding for a protein homologous to human and murine p53. Oncogene 1, 71-78.

Soussi, T., and May, P. (1996). Structural aspects of the p53 protein in relation to gene evolution: a second look. J Mol Biol 260, 623-637.

Souza, J.M., Daikhin, E., Yudkoff, M., Raman, C.S., and Ischiropoulos, H. (1999). Factors determining the selectivity of protein tyrosine nitration. Archives of biochemistry and biophysics 371, 169-178.

Stad, R., Little, N.A., Xirodimas, D.P., Frenk, R., van der Eb, A.J., Lane, D.P., Saville, M.K., and Jochemsen, A.G. (2001). Mdmx stabilizes p53 and Mdm2 via two distinct mechanisms. EMBO reports 2, 1029-1034.

Stad, R., Ramos, Y.F., Little, N., Grivell, S., Attema, J., van Der Eb, A.J., and Jochemsen, A.G. (2000). Hdmx stabilizes Mdm2 and p53. J Biol Chem 275, 28039-28044.

Stephen, C.W., and Lane, D.P. (1992). Mutant conformation of p53. Precise epitope mapping using a filamentous phage epitope library. Journal of molecular biology 225, 577-583.

Stiewe, T. (2007). The p53 family in differentiation and tumorigenesis. Nature reviews Cancer 7, 165-168.

Stommel, J. M., Marchenko, N. D., Jimenez, G. S., Moll, U. M., Hope, T. J., and Wahl, G. M. (1999). A leucine-rich nuclear export signal in the p53 tetramerization domain: regulation
of subcellular localization and p53 activity by NES masking. EMBO Journal 18, 1660–1672.

Strano, S., and Blandino, G. (2003). p73-mediated chemosensitivity: a preferential target of oncogenic mutant p53. Cell Cycle 2, 348-349.

Strano, S., Dell'Orso, S., Mongiovi, A.M., Monti, O., Lapi, E., Di Agostino, S., Fontemaggi, G., and Blandino, G. (2007). Mutant p53 proteins: between loss and gain of function. Head Neck 29, 488-496.

Strano, S., Fontemaggi, G., Costanzo, A., Rizzo, M.G., Monti, O., Baccarini, A., Del Sal, G., Levrero, M., Sacchi, A., Oren, M., et al. (2002). Physical interaction with human tumor-derived p53 mutants inhibits p63 activities. J Biol Chem 277, 18817-18826.

Strano, S., Munarriz, E., Rossi, M., Cristofanelli, B., Shaul, Y., Castagnoli, L., Levine, A.J., Sacchi, A., Cesareni, G., Oren, M., et al. (2000). Physical and functional interaction between p53 mutants and different isoforms of p73. The Journal of biological chemistry 275, 29503-29512.

Studier, F.W., and Moffatt, B.A. (1986). Use of bacteriophage T7 RNA polymerase to direct selective high-level expression of cloned genes. J Mol Biol 189, 113-130.

Studier, F.W., Rosenberg, A.H., Dunn, J.J., and Dubendorff, J.W. (1990). Use of T7 RNA polymerase to direct expression of cloned genes. Methods Enzymol 185, 60-89.

Su, X., Chakravarti, D., Cho, M.S., Liu, L., Gi, Y.J., Lin, Y.L., Leung, M.L., El-Naggar, A., Creighton, C.J., Suraokar, M.B., et al. (2010). TAp63 suppresses

metastasis through coordinate regulation of Dicer and miRNAs. Nature 467, 986-990.

Sugars, K.L., Budhram-Mahadeo, V., Packham, G., and Latchman, D.S. (2001). A minimal Bcl-x promoter is activated by Brn-3a and repressed by p53. Nucleic acids research 29, 4530-4540.

Suzuki, K., and Matsubara, H. (2011). Recent advances in p53 research and cancer treatment. J Biomed Biotechnol 978312, 16.

Sykes, S.M., Mellert, H.S., Holbert, M.A., Li, K., Marmorstein, R., Lane, W.S., and McMahon, S.B. (2006). Acetylation of the p53 DNA-binding domain regulates apoptosis induction. Molecular cell 24, 841-851.

Sykes, S.M., Stanek, T.J., Frank, A., Murphy, M.E., and McMahon, S.B. (2009). Acetylation of the DNA binding domain regulates transcription-independent apoptosis by p53. The Journal of biological chemistry 284, 20197-20205.

Symonds, H., Krall, L., Remington, L., Saenz-Robles, M., Lowe, S., Jacks, T., and Van Dyke, T. (1994). p53-dependent apoptosis suppresses tumor growth and progression in vivo. Cell 78, 703-711.

Szabó C, I.H., Radi R. (2007). Peroxynitrite: biochemistry, pathophysiology and development of therapeutics. Nat Rev Drug Discov 6, 662-680.

Tabor, S., and Richardson, C.C. (1985). A bacteriophage T7 RNA polymerase/promoter system for controlled exclusive expression of specific genes. Proceedings of the National Academy of Sciences of the United States of America 82, 1074-1078.

Tafvizi, A., Huang, F., Leith, J.S., Fersht, A.R., Mirny, L.A., and van Oijen, A.M. (2008). Tumor suppressor p53 slides on DNA with low friction and high stability. Biophys J 2008 Jul;95(1):L01-3.

Taira, N., Nihira, K., Yamaguchi, T., Miki, Y., and Yoshida, K. (2007). DYRK2 is targeted to the nucleus and controls p53 via Ser46 phosphorylation in the apoptotic response to DNA damage. Molecular cell 25, 725-738.

Tamir, S., and Tannenbaum, S.R. (1996). The role of nitric oxide (NO.) in the carcinogenic process. Biochim Biophys Acta 1288, F31-36.

Tan, M., Li, S., Swaroop, M., Guan, K., Oberley, L.W., and Sun, Y. (1999). Transcriptional activation of the human glutathione peroxidase promoter by p53. J Biol Chem 274, 12061-12066.

Tanaka, H., Arakawa, H., Yamaguchi, T., Shiraishi, K., Fukuda, S., Matsui, K., Takei, Y., and Nakamura, Y. (2000). A ribonucleotide reductase gene involved in a p53-dependent cell-cycle checkpoint for DNA damage. Nature 404, 42-49.

Tang, Y., Luo, J., Zhang, W., and Gu, W. (2006). Tip60-dependent acetylation of p53 modulates the decision between cell-cycle arrest and apoptosis. Molecular cell 24, 827-839.

Tang, Y., Zhao, W., Chen, Y., Zhao, Y., and Gu, W. (2008). Acetylation is indispensable for p53 activation. Cell 133, 612-626.

Tanimura, S., Ohtsuka, S., Mitsui, K., Shirouzu, K., Yoshimura, A., and Ohtsubo, M. (1999). MDM2 interacts with MDMX through their RING finger domains. FEBS letters 447, 5-9.

Tao, W., and Levine, A.J. (1999). P19(ARF) stabilizes p53 by blocking nucleo-cytoplasmic shuttling of mdm2. Proc Natl Acad Sci U S A 96, 6937-6941.

Tasdemir, E., Maiuri, M.C., Galluzzi, L., Vitale, I., Djavaheri-Mergny, M., D'Amelio, M., Criollo, A., Morselli, E., Zhu, C., Harper, F., et al. (2008). Regulation of autophagy by cytoplasmic p53. Nat Cell Biol 2008 Jun;10(6):676-87.

Taylor, B.F., McNeely, S.C., Miller, H.L., and States, J.C. (2008). Arsenite-induced mitotic death involves stress response and is independent of tubulin polymerization. Toxicology and applied pharmacology 230, 235-246.

Taylor, W.R., and Stark, G.R. (2001). Regulation of the G2/M transition by p53. Oncogene 20, 1803-1815.

Teufel, D.P., Bycroft, M., and Fersht, A.R. (2009). Regulation by phosphorylation of the relative affinities of the N-terminal transactivation domains of p53 for p300 domains and Mdm2. Oncogene 28, 2112-2118.

Thomas, D.D., Ridnour, L.A., Isenberg, J.S., Flores-Santana, W., Switzer, C.H., Donzelli, S., Hussain, P., Vecoli, C., Paolocci, N., Ambs, S., et al. (2008). The chemical biology of nitric oxide: implications in cellular signaling. Free radical biology & medicine 45, 18-31.

Thut, C.J., Chen, J.L., Klemm, R., and Tjian, R. (1995). p53 transcriptional activation mediated by coactivators TAFII40 and TAFII60. Science 267, 100-104.

Tian B, L.J., Bitterman PB, Bache RJ. (2002). Mechanisms of cytokine induced NO-mediated cardiac fibroblast apoptosis. Am J Physiol Heart Circ Physiol 283, H1958-1967.

Tibbetts, R.S., Brumbaugh, K.M., Williams, J.M., Sarkaria, J.N., Cliby, W.A., Shieh, S.Y., Taya, Y., Prives, C., and Abraham, R.T. (1999). A role for ATR in the DNA damage-induced phosphorylation of p53. Genes & development 13, 152-157.

Toledo, F., and Wahl, G.M. (2006). Regulating the p53 pathway: in vitro hypotheses, in vivo veritas. Nature reviews Cancer 6, 909-923.

Tovar, C., Graves, B., Packman, K., Filipovic, Z., Higgins, B., Xia, M., Tardell, C., Garrido, R., Lee, E., Kolinsky, K., et al. (2013). MDM2 small-molecule antagonist RG7112 activates p53 signaling and regresses human tumors in preclinical cancer models. Cancer Res 73, 2587-2597.

Tucci, P., Agostini, M., Grespi, F., Markert, E.K., Terrinoni, A., Vousden, K.H., Muller, P.A., Dotsch, V., Kehrloesser, S., Sayan, B.S., et al. (2012). Loss of p63 and its microRNA-205 target results in enhanced cell migration and metastasis in prostate cancer. Proc Natl Acad Sci U S A 2012 Sep 18;109(38):15312-7 Epub 2012 Sep 4.

Unger, T., JuvenGershon, T., Moallem, E., Berger, M., Sionov, R.V., Lozano, G., Oren, M., and Haupt, Y. (1999). Critical role for Ser20 of human p53 in the negative regulation of p53 by Mdm2. Embo Journal 18, 1805-1814.

Vander Heiden, M.G., Cantley, L.C., and Thompson, C.B. (2009). Understanding the Warburg effect: the metabolic requirements of cell proliferation. Science 324, 1029-1033.

Vassilev, L.T., Binh, T.V., Graves, B., Carvajal, D., Podlaski, F., Filipovic, Z., Kong, N., Kammlott, U., Lukacs, C., Klein, C., Fotouhi, N., and Liu, E. (2004). In vivo activation of the p53 pathway by small-molecule antagonists of MDM2. Science 303, 844-848.

Vaziri, H., West, M.D., Allsopp, R.C., Davison, T.S., Wu, Y.S., Arrowsmith, C.H., Poirier, G.G., and Benchimol, S. (1997). ATM-dependent telomere loss in aging human diploid fibroblasts and DNA damage lead to the post-translational activation of p53 protein involving poly(ADP-ribose) polymerase. Embo J 16, 6018-6033.

Venot, C., Maratrat, M., Dureuil, C., Conseiller, E., Bracco, L., and Debussche, L. (1998). The requirement for the p53 proline-rich functional domain for mediation of apoptosis is correlated with specific PIG3 gene transactivation and with transcriptional repression. Embo J 17, 4668-4679.

Vikhanskaya, F., Lee, M.K., Mazzoletti, M., Broggini, M., and Sabapathy, K. (2007). Cancer-derived p53 mutants suppress p53-target gene expression--potential mechanism for gain of function of mutant p53. Nucleic Acids Res 35, 2093-2104.

Villunger, A., Michalak, E.M., Coultas, L., Mullauer, F., Bock, G., Ausserlechner, M.J., Adams, J.M., and Strasser, A. (2003). p53- and drug-induced apoptotic responses mediated by BH3-only proteins puma and noxa. Science 302, 1036-1038.

Vinten-Johansen, J. (2000). Physiological effects of peroxynitrite: potential products of the environment. Circ Res 87, 170-172.

Visconti, R., and Grieco, D. (2009). New insights on oxidative stress in cancer. Current opinion in drug discovery & development 12, 240-245.

Vojtesek, B., Bartek, J., Midgley, C.A., and Lane, D.P. (1992). An immunochemical analysis of the human nuclear phosphoprotein p53. New monoclonal antibodies and epitope mapping using recombinant p53. J Immunol Methods 151, 237-244.

Vousden, K.H.,and Lu, X. (2002). Live or let die: the cell's response to p53. Nature Reviews Cancer 2, 594-604.

Vousden, K.H., and Ryan, K.M. (2009). p53 and metabolism. Nat Rev Cancer 9, 691-700.

Wade, M., Wang, Y.V., and Wahl, G.M. (2010). The p53 orchestra: Mdm2 and Mdmx set the tone. Trends in cell biology 20, 299-309.

Waga, S., Hannon, G.J., Beach, D., and Stillman, B. (1994). The p21 inhibitor of cyclin-dependent kinases controls DNA replication by interaction with PCNA. Nature 369, 574-578.

Wahl G.M., S.J.M., Krummel K.A., Wade M (2005). Gatekeepers of the guardian: p53 regulation by post-translational modification, Mdm2 and Mdmx. "25 Years of p53 Research". Publisher: Springer Chapter 4, 73-113.

Walker, K.K., and Levine, A.J. (1996). Identification of a novel p53 functional domain that is necessary for efficient growth suppression. Proc Natl Acad Sci U S A 1996 Dec 24;93(26):15335-40.

Wang, J.B., Erickson, J.W., Fuji, R., Ramachandran, S., Gao, P., Dinavahi, R., Wilson, K.F., Ambrosio, A.L., Dias, S.M., Dang, C.V., et al. (2010). Targeting mitochondrial glutaminase activity inhibits oncogenic transformation. Cancer Cell 18, 207-219.

Wang, P., Reed, M., Wang, Y., Mayr, G., Stenger, J.E., Anderson, M.E., Schwedes, J.F., and Tegtmeyer, P. (1994). p53 domains: structure, oligomerization, and transformation. Molecular and cellular biology 14, 5182-5191.

Wang, S.P., Wang, W.L., Chang, Y.L., Wu, C.T., Chao, Y.C., Kao, S.H., Yuan, A., Lin, C.W., Yang, S.C., Chan, W.K., et al. (2009). p53 controls cancer cell invasion by inducing the MDM2-mediated degradation of Slug. Nat Cell Biol 11, 694-704.

Wang, W., Chen, X., Xu, H., and Lufkin, T. (1996). Msx3: a novel murine homologue of the Drosophila msh homeobox gene restricted to the dorsal embryonic central nervous system. Mechanisms of development 58, 203-215.

Wang, X., and Jiang, X. (2012). Mdm2 and MdmX partner to regulate p53. FEBS Lett 586, 1390-1396.

Wang, X., Michael, D., de Murcia, G., and Oren, M. (2002). p53 Activation by nitric oxide involves down-regulation of Mdm2. The Journal of biological chemistry 277, 15697-15702.

Wang, X., Ohnishi, K., Takahashi, A., and Ohnishi, T. (1998). Poly(ADP-ribosyl)ation is required for p53-dependent signal transduction induced by radiation. Oncogene 17, 2819-2825.

Wang, X., Zalcenstein, A., and Oren, M. (2003). Nitric oxide promotes p53 nuclear retention and sensitizes neuroblastoma cells to apoptosis by ionizing radiation. Cell Death Differ 10, 468-476.

Wang, X.W., Forrester, K., Yeh, H., Feitelson, M.A., Gu, J.R., and Harris, C.C. (1994). Hepatitis B virus X protein inhibits p53 sequence-specific DNA binding, transcriptional activity, and association with transcription factor ERCC3. Proc Natl Acad Sci U S A 91, 2230-2234.

Wang, X.W., Vermeulen, W., Coursen, J.D., Gibson, M., Lupold, S.E., Forrester, K., Xu, G., Elmore, L., Yeh, H., Hoeijmakers, J.H., et al. (1996). The XPB and XPD DNA helicases are components of the p53-mediated apoptosis pathway. Genes Dev 10, 1219-1232.

Wang, X.W., Yeh, H., Schaeffer, L., Roy, R., Moncollin, V., Egly, J.M., Wang, Z., Freidberg, E.C., Evans, M.K., Taffe, B.G., et al. (1995). p53 modulation of TFIIH-associated nucleotide excision repair activity. Nat Genet 10, 188-195.

Wang, Y., and Prives, C. (1995). Increased and altered DNA binding of human p53 by S and G2/M but not G1 cyclin-dependent kinases. Nature 376, 88-91.

Waning, D.L., Lehman, J.A., Batuello, C.N., and Mayo, L.D. (2010). Controlling the Mdm2-Mdmx-p53 Circuit. Pharmaceuticals 3, 1576-1593.

Warburg, O. (1956). On the origin of cancer cells. Science 123, 309-314.

Waterman, M.J., Stavridi, E.S., Waterman, J.L., and Halazonetis, T.D. (1998). ATM-dependent activation of p53 involves dephosphorylation and association with 14-3-3 proteins. Nat Genet 19, 175-178.

Weber, J.D., Taylor, L.J., Roussel, M.F., Sherr, C.J., and Bar-Sagi, D. (1999). Nucleolar Arf sequesters Mdm2 and activates p53. Nature Cell Biology 1, 20-26.

Weinberg, R.A. (2014). The Biology of Cancer. Garland Science.

Whibley, C., Pharoah, P.D., and Hollstein, M. (2009). p53 polymorphisms: cancer implications. Nature reviews Cancer 9, 95-107.

White, E. (1996). Life, death, and the pursuit of apoptosis. Genes Dev 10, 1-15.

Wilhelm, M.T., Rufini, A., Wetzel, M.K., Tsuchihara, K., Inoue, S., Tomasini, R., Itie-Youten, A., Wakeham, A., Arsenian-Henriksson, M., Melino, G., et al. (2010). Isoform-specific p73 knockout mice reveal a novel role for delta Np73 in the DNA damage response pathway. Genes Dev 2010 Mar 15;24(6):549-60.

Wink, D.A., Cook, J.A., Pacelli, R., DeGraff, W., Gamson, J., Liebmann, J., Krishna, M.C., and Mitchell, J.B. (1996). The effect of various nitric oxide-donor agents on hydrogen peroxide-mediated toxicity: a direct correlation between nitric oxide formation and protection. Arch Biochem Biophys 331, 241-248.

Wink DA, K.K., Maragos CM, Elespuru RK, Misra M, Dunams TM, Cebula TA, Koch WH, Andrews AW, Allen JS, et al. (1991). DNA deaminating ability and genotoxicity of nitric oxide and its progenitors. Science 254, 1001-1003.

Wise, D.R., DeBerardinis, R.J., Mancuso, A., Sayed, N., Zhang, X.Y., Pfeiffer, H.K., Nissim, I., Daikhin, E., Yudkoff, M., McMahon, S.B., et al. (2008). Myc regulates a transcriptional program that stimulates mitochondrial glutaminolysis and leads to glutamine addiction. Proc Natl Acad Sci U S A 105, 18782-18787.

Wiseman, H., and Halliwell, B. (1996). Damage to DNA by reactive oxygen and nitrogen species: role in inflammatory disease and progression to cancer. Biochem J 313, 17-29.

Wu, G.S., and El-Diery, W.S. (1996). p53 and chemosensitivity. Nature medicine 2, 255-256.

Wurl, P., Meye, A., Schmidt, H., Lautenschlager, C., Kalthoff, H., Rath, F.W., and Taubert, H. (1998). High prognostic significance of Mdm2/p53 co-overexpression in soft tissue sarcomas of the extremities. Oncogene 16, 1183-1185.

Xie, S., Wu, H., Wang, Q., Cogswell, J.P., Husain, I., Conn, C., Stambrook, P., Jhanwar-Uniyal, M., and Dai, W. (2001). Plk3 functionally links DNA damage to cell cycle arrest and apoptosis at least in part via the p53 pathway. The Journal of biological chemistry 276, 43305-43312.

Xirodimas, D.P., Saville, M.K., Bourdon, J.C., Hay, R.T., and Lane, D.P. (2004). Mdm2-mediated NEDD8 conjugation of p53 inhibits its transcriptional activity. Cell 118, 83-97.

Xirodimas DP, C.J., Desterro JM, Lane DP, Hay RT (2002). P14ARF promotes accumulation of SUMO-1 conjugated (H)Mdm2. FEBS letters 528, 207-211.

Xu, W., Liu, L.Z., Loizidou, M., Ahmed, M., and Charles, I.G. (2002). The role of nitric oxide in cancer. Cell research 12, 311-320.

Yakovlev, V.A., Bayden, A.S., Graves, P.R., Kellogg, G.E., and Mikkelsen, R.B. (2010). Nitration of the tumor suppressor protein p53 at tyrosine 327 promotes p53 oligomerization and activation. Biochemistry 49, 5331-5339.

Yang, A., Kaghad, M., Wang, Y., Gillett, E., Fleming, M.D., Dotsch, V., Andrews, N.C., Caput, D., and McKeon, F. (1998). p63, a p53 homolog at 3q27-29, encodes multiple products with transactivating, death-inducing, and dominant-negative activities. Molecular cell 2, 305-316.

Yang, A., and McKeon, F. (2000). P63 and P73: P53 mimics, menaces and more. Nature reviews Molecular cell biology 1, 199-207.

Yang, A., Schweitzer, R., Sun, D., Kaghad, M., Walker, N., Bronson, R.T., Tabin, C., Sharpe, A., Caput, D., Crum, C., et al. (1999). p63 is essential for regenerative proliferation in limb, craniofacial and epithelial development. Nature 398, 714-718.

Yang, H.Y., Wen, Y.Y., Chen, C.H., Lozano, G., and Lee, M.H. (2003). 14-3-3 sigma positively regulates p53 and suppresses tumor growth. Molecular and cellular biology 23, 7096-7107.

Yee, K.S., Wilkinson, S., James, J., Ryan, K.M., and Vousden, K.H. (2009). PUMA- and Bax-induced autophagy contributes to apoptosis. Cell Death Differ 2009 Aug;16(8):1135-45.

Yew, P.R., and Berk, A.J. (1992). Inhibition of p53 transactivation required for transformation by adenovirus early 1B protein. Nature 357, 82-85.

Ying, L., and Hofseth, L.J. (2007). An emerging role for endothelial nitric oxide synthase in chronic inflammation and cancer. Cancer research 67, 1407-1410.

Yokota, T., Sugisaki, H., Takanami, M., and Kaziro, Y. (1980). The nucleotide sequence of the cloned tufA gene of Escherichia coli. Gene 12, 25-31.

Yonish-Rouach, E., Resnitzky, D., Lotem, J., Sachs, L., Kimchi, A., and Oren, M. (1991). Wild-type p53 induces apoptosis of myeloid leukaemic cells that is inhibited by interleukin-6. Nature 352, 345-347.

Yoon, K.A., Nakamura, Y., and Arakawa, H. (2004). Identification of ALDH4 as a p53-inducible gene and its protective role in cellular stresses. J Hum Genet 49, 134-140.

Yoshida, K., Liu, H., and Miki, Y. (2006). Protein kinase C delta regulates Ser46 phosphorylation of p53 tumor suppressor in the apoptotic response to DNA damage. The Journal of biological chemistry 281, 5734-5740.

Young, C.L., Britton, Z.T., and Robinson, A.S. (2012). Recombinant protein expression and purification: a comprehensive review of affinity tags and microbial applications. Biotechnol J 7, 620-634.

Yu, J., and Zhang, L. (2003). No PUMA, no death: implications for p53-dependent apoptosis. Cancer cell 4, 248-249.

Yu, J., Zhang, L., Hwang, P.M., Kinzler, K.W., and Vogelstein, B. (2001). PUMA induces the rapid apoptosis of colorectal cancer cells. Molecular cell 7, 673-682.

Yuan, J., Luo, K., Zhang, L., Cheville, J.C., and Lou, Z. (2010). USP10 regulates p53 localization and stability by deubiquitinating p53. Cell 140, 384-396.

Z, R. (2000). The 10th p53 Workshop, California USA.

Zacchi, P., Gostissa, M., Uchida, T., Salvagno, C., Avolio, F., Volinia, S., Ronai, Z., Blandino, G., Schneider, C., and Del Sal, G. (2002). The prolyl isomerase Pin1 reveals a mechanism to control p53 functions after genotoxic insults. Nature 419, 853-857.

Zakut-Houri, R., Bienz-Tadmor, B., Givol, D., and Oren, M. (1985). Human p53 cellular tumor antigen: cDNA sequence and expression in COS cells. Embo J 4, 1251-1255.

Zhan, Q., Bae, I., Kastan, M.B., and Fornace, A.J., Jr. (1994). The p53-dependent gamma-ray response of GADD45. Cancer Res 54, 2755-2760.

Zhan, Q., Carrier, F., and Fornace, A.J., Jr. (1993). Induction of cellular p53 activity by DNA-damaging agents and growth arrest. Mol Cell Biol 13, 4242-4250.

Zhang, C., Lin, M., Wu, R., Wang, X., Yang, B., Levine, A.J., Hu, W., and Feng, Z. (2011). Parkin, a p53 target gene, mediates the role of p53 in glucose metabolism and the Warburg effect. Proc Natl Acad Sci U S A 108, 16259-16264.

Zhang, T., and Prives, C. (2001). Cyclin a-CDK phosphorylation regulates MDM2 protein interactions. J Biol Chem 276, 29702-29710.

Zhang, W., McClain, C., Gau, J.P., Guo, X.Y., and Deisseroth, A.B. (1994). Hyperphosphorylation of p53 induced by okadaic acid attenuates its transcriptional activation function. Cancer Res 54, 4448-4453.

Zhang, W.H. (2000). MDM2 oncogene as a novel target for human cancer therapy. Curr Pharm Des 6, 393-416.

Zhang, X., Lin, L., Guo, H., Yang, J., Jones, S.N., Jochemsen, A., and Lu, X. (2009). Phosphorylation and degradation of MdmX is inhibited by Wip1 phosphatase in the DNA damage response. Cancer Res 69, 7960-7968.

Zhang, Y., and Xiong, Y. (2001). A p53 amino-terminal nuclear export signal inhibited by DNA damage-induced phosphorylation. Science 2001 Jun 8;292(5523):1910-5.

Zhao, J., Lu, Y., and Shen, H.M. (2012). Targeting p53 as a therapeutic strategy in sensitizing TRAIL-induced apoptosis in cancer cells. Cancer Lett 314, 8-23.

Zhao, Y., Yu, S., Sun, W., Liu, L., Lu, J., McEachern, D., Shargary, S., Bernard, D., Li, X., Zhao, T., et al. (2013). A potent small-molecule inhibitor of the MDM2-p53 interaction (MI-888) achieved complete and durable tumor regression in mice. J Med Chem 56, 5553-5561.

Zheng, H., You, H., Zhou, X.Z., Murray, S.A., Uchida, T., Wulf, G., Gu, L., Tang, X., Lu, K.P., and Xiao, Z.X. (2002). The prolyl isomerase Pin1 is a regulator of p53 in genotoxic response. Nature 419, 849-853.

Zhivotovsky, B., and Kroemer, G. (2004). Apoptosis and genomic instability. Nature reviews Molecular cell biology 5, 752-762.

Zhou, B.P., Liao, Y., Xia, W., Zou, Y., Spohn, B., and Hung, M.C. (2001). HER-2/neu induces p53 ubiquitination via Akt-mediated MDM2 phosphorylation. Nature cell biology 3, 973-982.

Zhou, G., Wang, J., Zhao, M., Xie, T.X., Tanaka, N., Sano, D., Patel, A.A., Ward, A.M., Sandulache, V.C., Jasser, S.A., et al. (2014). Gain-of-function mutant p53 promotes cell growth and cancer cell metabolism via inhibition of AMPK activation. Mol Cell 54, 960-974.

Zhu, L., Gunn, C., and Beckman, J.S. (1992). Bactericidal activity of peroxynitrite. Arch Biochem Biophys 298, 452-457.

Zhu, Y., Mao, X.O., Sun, Y., Xia, Z., and Greenberg, D.A. (2002). p38 Mitogen-activated protein kinase mediates hypoxic regulation of Mdm2 and p53 in neurons. J Biol Chem 277, 22909-22914.

Zilfou, J.T., and Lowe, S.W. (2009). Tumor suppressive functions of p53. Cold Spring Harbor perspectives in biology 1.

APPENDIX I

PUBLICATIONS AND POSTERS/CONFERENCES

PUBLICATIONS

Roslina Husaini, Munirah Ahmad, Alan Soo-Beng Khoo. Epstein-Barr virus Latent Membrane Protein LMP1 reduces p53 protein levels independent of the PI3K-Akt pathway. BMC Research Notes 2011, 4:551.

Current research project undertaken as a principal investigator (January 2012 – present) titled “Gene Silencing of Multidrug Resistant Genes in Leukaemia Cells” (Manuscript in preparation).

POSTERS/CONFERENCES

Roslina Husaini, Khalid M. Naseem, Martin H. Brinkworth, Zubaidah Zakaria, Steven M. Picksley. (2015) Expression and Purification of Recombinant Human p53 Tumour Suppressor Protein in the BL21(DE3) Bacterial Expression System. *6th Regional Conference on Molecular Medicine (RCMM) 2015 in Conjunction with 2nd National Conference for Cancer, Kuala Lumpur, Malaysia.*

Roslina Husaini, Munirah Ahmad, Zubaidah Zakaria. (2014) Silencing of Multidrug Resistant Genes in Chronic Myeloid Leukaemia Cells and its Effects on the *in vitro* Chemotherapeutic Treatments. *19th National Conference on Medical and Health Sciences, Kelantan, Malaysia.*

R. Husaini, M. Ahmad, A.S.B. Khoo. (2011) The Reduction of p53 Tumour Suppressor Protein Levels by Epstein-Barr Virus Latent Membrane LMP1 is Independent of the PI3K-Akt Pathway. *5th International Symposium on Nasopharyngeal Carcinoma, Pulau Pinang, Malaysia*.

R. Husaini, M. Ahmad, A.S.B. Khoo. (2011) Nutlin-3 Synergises with Cisplatin in Effectively Killing Nasopharyngeal Carcinoma (NPC) Cells. *5th International Symposium on Nasopharyngeal Carcinoma, Pulau Pinang, Malaysia.*

R. Husaini, M. Ahmad, A.S.B. Khoo. (2007) Nasopharyngeal Carcinoma – Preliminary Studies on Mechanisms of Inactivation of the p53 Pathway. *MOH-AMM Conference, Pulau Pinang, Malaysia.*

R. Husaini, A.S.B. Khoo. (2006) Cancer Research – Application of Biotechnology to Study the Molecular and Cell Biology of Cancer. *BioMalaysia Conference, Kuala Lumpur, Malaysia*.

R. Husaini, K.M. Naseem, M.H. Brinkworth, S.M. Picksley. (2005) Investigation of the Effects of Nitration on the Functions of the p53 Tumour Suppressor Protein. *1st National Cancer Research Institute (NCRI) Conference, Birmingham, United Kingdom.*